

AN APPROACH TO THE QUANTIFICATION OF THE  
BENEFITS OF DISTRIBUTED GENERATION

By

PATHOMTHAT CHIRADEJA

Bachelor of Engineering  
Kasetsart University  
Bangkok, Thailand  
1991

Master of Science  
Oklahoma State University  
Stillwater, Oklahoma  
1994

Submitted to the Faculty of the  
Graduate College of the  
Oklahoma State University  
in partial fulfillment of  
the requirements for  
the degree of  
DOCTOR OF PHILOSOPHY  
May, 2003

COPYRIGHT

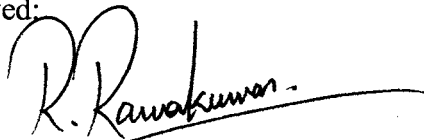
By

Pathomthat Chiradeja

May, 2003

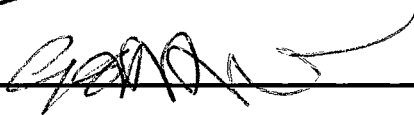
AN APPROACH TO THE QUANTIFICATION OF THE  
BENEFITS OF DISTRIBUTED GENERATION

Thesis Approved:



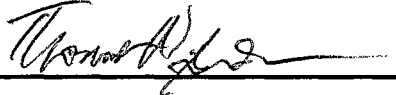
---

Thesis Adviser



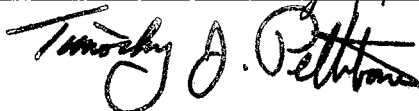
---

J Chandler



---

Ashwini Kumbh



---

Dean of the Graduate College

## PREFACE

The quantification of the technical benefits of distributed generation (DG) has been considered in this work. The objective of this study is to propose an approach to quantify the benefits of DG when introduced into existing utility distribution networks. A set of indices, namely, voltage profile improvement index (VPPI), line loss reduction index (LLRI), environmental impact reduction index (EIRI), and distributed generation benefit index (BI) are developed and proposed to quantify the benefits of DG.

Among the many DG technologies, wind turbine generation (WTG), microturbine systems, photovoltaic systems (PV), and fuel cell systems are considered. The power output of WTG and PV systems are modeled in terms of probability density functions while the power outputs of microturbines and fuel cells are schedulable and are expressed in terms of fuel flow rates. To evaluate and quantify the benefits of DG, suitable mathematical models for DG technologies are employed along with distribution system models and power flow calculations to arrive at a set of indices to quantify the benefits. The basic concept behind the proposed VPPI, LLRI, and EIRI is to compare and calculate the ratio of a measure of the attribute in question with and without the employment of DG for the same loads at the different buses.

With the employment of DG, the simulation results clearly show that voltage profile is improved and line losses and pollutant emissions are reduced. VPPI, LLRI, and

EIRI are sensitive to the ratings of DG as expected. Generally, VPII goes up and EIRI goes down as DG rating goes up. However, this trend is not always applicable to line loss reduction because the amount of reduction can decrease as DG rating goes up in some cases. The location of DG is also significant to both voltage profile improvement and line loss reduction. The operating power factor of DG also plays a major role in determining the benefits of DG. The benefit indices proposed in this work can assist in identifying the best locations and ratings for DG installations to maximize the technical benefits.

## ACKNOWLEDGEMENTS

I would like to express my sincere appreciation to my major advisor, Professor R. Ramakumar for his intelligent supervision, encouragement, guidance, and support during my study at Oklahoma State University. Without his support and guidance, this research would not have been completed. I will always consider the high academic and professional standards that I learned from him.

I wish to thank the other members of my doctoral committee, Dr. T. W. Gedra, Dr. G. Yen, Dr. K. Ashenayi, and Dr. J. P. Chandler for their assistance and suggestions throughout this research.

I would like to take this opportunity to thank my parents, Pravit and Paitoontong, and my brother, Dr. Chatdanai, for their enduring understanding, support, and encouragement.

To my girlfriend, Chussanida Kulachote, I really appreciate all the enduring love, understanding, and support throughout my study at Oklahoma State University.

I would like to express my special appreciation to Dr. Boonpruk Chaygate, Secretary-General of the Office of the Civil Service Commission, Office of the Prime Minister, Bangkok, Thailand, and Dr. Napawan Nopparatnaraporn, Vice-President for Research, Kasetsart University, Bangkok, Thailand for their support, encouragement, and arrangement of my scholarship.

Finally, I would like to thank all of my friends, especially Songklod Phongphonkit, Eriya Limpadanai, Pongchit Chitapong, and Prach Apiratikul, at Stillwater for their helps, encouragement and make my stay at OSU a memorable experience.

## TABLE OF CONTENTS

Chapter	Page
I. INTRODUCTION.....	1
1.1 Emergence of Distributed Generation.....	1
1.2 Technologies and Benefits of Distributed Generation.....	5
1.3 Background of Promising DG Technologies.....	7
1.3.1 Wind Turbine Generation.....	7
1.3.2 Microturbine Systems.....	11
1.3.3 Photovoltaic Systems.....	13
1.3.4 Fuel Cell Systems.....	16
1.3.5 Gas Turbines.....	18
1.4 Distributed Generation Systems Planning.....	22
1.5 Problem Statement.....	24
1.6 Method of Study.....	25
1.7 Organization of Thesis.....	26
II. REVIEW OF RELATED LITERATURE.....	28
2.1 DG Technologies Modeling.....	28
2.1.1 Wind Turbine Generation Model.....	29
2.1.2 Microturbine Model.....	31
2.1.3 Photovoltaic Systems Model.....	31
2.1.4 Fuel Cell Systems Model.....	33
2.2 Literature Review on the Quantification of Benefits of DG.....	35
2.2.1 Benefits of DG in terms of Capacity Credit and Energy Value.....	36
2.2.2 Benefits of DG in terms of Voltage Support and Line Loss Reduction.....	38
2.2.3 Benefits of DG in terms of System Reliability Improvement.....	41
2.3 Literature Review on Economic Considerations.....	44
III. DISTRIBUTED GENERATION AND LOAD MODELS.....	48
3.1 Wind Turbine Generation.....	48
3.1.1 Description of Technology.....	48
3.1.2 Wind Speed Model.....	52



Chapter	Page
3.1.3 Wind Turbine Generation Power Output Model.....	54
3.2 Microturbine Systems.....	58
3.2.1 Description of Technology.....	58
3.2.2 Microturbine Power Output Model.....	59
3.3 Photovoltaic Systems.....	61
3.3.1 Description of Technology.....	61
3.3.2 Insolation Model.....	63
3.3.3 PV Power Output Model.....	66
3.4 Fuel Cells.....	70
3.4.1 Description of Technology.....	70
3.4.2 Fuel Cell Power Output Model.....	73
3.4.2.1 Chemical Reaction.....	73
3.4.2.2 Fuel Utilization.....	74
3.4.2.3 Cell Voltage and Current Output.....	76
3.4.2.4 Electrical Power Output.....	80
3.5 Load Model.....	80
3.6 Summary.....	81
IV. VOLTAGE PROFILE IMPROVEMENT WITH DISTRIBUTED WIND TURBINE GENERATION.....	84
4.1 Introduction.....	84
4.2 System Description.....	85
4.3 Probabilistic Voltage Profile Analysis.....	88
4.3.1 Probabilistic Voltage Profile for System without WTG.....	88
4.3.2 Probabilistic Voltage Profile for System with WTG.....	90
4.4 Simulation Results.....	91
4.4.1 Required Input Data for Simulation.....	91
4.4.2 Impact of WTG Location.....	92
4.4.3 Impact of WTG Rating.....	93
4.4.4 Impact of Load Power Factor.....	94
4.5 Non-Probabilistic Voltage Profile Analysis.....	95
4.5.1 Non-Probabilistic Approach.....	95
4.5.1.1 Calculating the Average Wind Power Output.....	95
4.5.1.2 Calculating Average Load.....	103
4.5.1.3 Calculating the Average RMS Voltage at Load Point.....	103
4.5.2 Simulation Results.....	103
4.5.2.1 Case Study A: Medium Wind Regime with Constant WTG Rating.....	103

Chapter	Page
4.5.2.2 Case Study B: High Wind Regime with Constant WTG Rating.....	104
4.5.2.3 Case Study C: High Wind Regime with Constant Load Power Factor.....	104
4.6 Comparison of Probabilistic Approach and Non-Probabilistic Approach.....	104
4.7 Summary.....	105
 V. QUANTIFICATION OF THE BENEFITS OF DISTRIBUTED GENERATION.....	 108
5.1 The Approach.....	108
5.2 Voltage Profile Improvement.....	111
5.2.1 Introduction.....	111
5.2.2 Voltage Profile Improvement.....	112
5.2.3 Voltage Profile Improvement Index.....	113
5.3 Line Loss Reduction.....	115
5.3.1 Introduction.....	115
5.3.2 Line Loss reduction.....	116
5.3.3 Line Loss Reduction Index.....	117
5.4 Environmental Impact Reduction.....	118
5.4.1 Introduction.....	119
5.4.2 Environmental Impact Reduction.....	120
5.4.3 Environmental Impact Reduction Index.....	121
5.5 Distributed Generation Benefit Index.....	125
5.6 Analysis under Varying Load Conditions.....	126
5.7 Summary.....	129
 VI. NUMERICAL EXAMPLES AND SIMULATION RESULTS.....	 130
6.1 Description of System under Study.....	130
6.2 Study Procedure.....	131
6.3 Case studies and Simulation Results.....	131
6.4 Discussion of Results.....	137
6.4.1 Voltage Profile Improve Results.....	137
6.4.2 Line Loss Reduction Results.....	138
6.4.3 Environmental Impact Reduction Results.....	139
6.4.4 Distributed Generation Benefit Results.....	165
6.5 Summary.....	189
 VII. SUMMARY AND CONCLUDING REMARKS.....	 190
7.1 Summary.....	190

Chapter .....	Page
7.2 Areas for Further Work.....	195
REFERENCES.....	197
APPENDIXES.....	208
APPENDIX A- THERMODYNAMIC CHARACTERISTICS AND VOLTAGE OF FUEL CELL REACTION AT 650 °C.....	209
APPENDIX B- SOLUTIONS FOR EQUATION (4.3.1.5).....	210
APPENDIX C- CLOSED FORM SOLUTION FOR PROBABILITY DENSITY FUNCTION OF C.....	211
APPENDIX D- LOAD FLOW CALCULATION BY NEWTON- RAPHSON METHOD.....	215

## LIST OF TABLES

Table	Page
1. Variation of Voltage at Load Point with Load Power Factor under Medium Wind Speed Condition [Non-Probabilistic Approach].....	106
2. Variation of Voltage at Load Point with Load Power Factor in a High Wind Speed Regime [Non-Probabilistic Approach].....	106
3. Variation of Voltage at Load Point with WTG Rating in a High Wind Speed Regime [Non-Probabilistic Approach].....	106
4. A Comparison of Expected Load Voltage Obtained using Probabilistic and Non-Probabilistic Approaches.....	107
5. A Comparison of Pollutant Emissions from Various Generation Technologies.....	122
6. Conventional Generator Information .....	132
7. Important Pollutant Emissions of Conventional Generator Employed.....	132
8. Load Data for System under Study.....	133
9. Distribution Line Length Data .....	134
10. Assumed Bus Weighting Factor Sets .....	135
11. Simulated Results of Voltage Profile Improvement Index (VPPI), Line Loss Reduction Index (LLRI), and Environmental Impact Reduction Index (EIRI).....	167
12. Tabulation of Selected Cases of Distributed Generation Benefit Results.....	176
13. Distributed Generation Benefit Index (BI) for $BW_{VPI}=1$ , $BW_{LLR}=0$ , and $BW_{EIR}=0$ .....	177
14. Distributed Generation Benefit Index (BI) for $BW_{VPI}=0$ , $BW_{LLR}=1$ , and $BW_{EIR}=0$ .....	180

Table	Page
15. Distributed Generation Benefit Index (BI) for $BW_{VPI}=0$ , $BW_{LLR}=0$ , and $BW_{EIR}=1$ .....	183
16. Distributed Generation Benefit Index (BI) for $BW_{VPI}=0.33$ , $BW_{LLR}=0.33$ , and $BW_{EIR}=0.33$ .....	186
17. Thermodynamic Characteristics and Ideal Voltages of Fuel Cell Reactions at 650 °C.....	209
18. Bus Data.....	224
19. Transformer Data.....	226
20. Line Data.....	226
21. Bus Output Data.....	231

## LIST OF FIGURES

Figure		Page
1.	A Block Diagram of Traditional Power Systems.....	3
2.	Distributed Generation Integrated into an Existing Network.....	4
3.	A 25.2 MW Wind Turbine Installation in Pecos County, Texas.....	10
4.	Capstone C-30 Natural Gas Microturbine System (30 kW/unit).....	12
5.	Solar Power Plant in Europe with a Rating of 1 MW <sub>p</sub> .....	14
6.	A UTC 200 kW Fuel Cell Power Plant in Alaska.....	19
7.	LM 2500+ Gas Turbine.....	21
8.	A Typical Schematic of Wind Turbine Generation System.....	49
9.	Major Components of Wind Turbine Generation.....	51
10.	A Typical WTG Output vs Wind Speed Characteristic.....	55
11.	A Typical Microturbine Cycle.....	60
12.	Typical Schematic of a PV System.....	64
13.	An Equivalent Circuit for Photovoltaic Cell.....	67
14.	A Typical Schematic of an Individual Fuel Cell.....	71
15.	A Typical Schematic for Fuel Cell System.....	75
16.	A Typical Fuel Cell Voltage/Current Characteristic.....	82
17.	Assumed Probability Density Function for Load.....	83
18.	Cumulative Distribution Function for Load.....	83

Figure	Page
19. A Simple Radial Distribution System without WTG.....	86
20. Schematic of a Radial Distribution System with WTG.....	87
21. Variation of Expected Value of Load Voltage with WTG Location.....	96
22. Variation of Variance of Load Voltage with WTG Location.....	97
23. Variation of Expected Value of Load Voltage with WTG Rating.....	98
24. Variation of Variance of Load Voltage with WTG Rating.....	99
25. Variation of Expected Value of Load Voltage with Different Load Power Factors.....	100
26. Variation of Variance of Load Voltage with Different Load Power Factors.....	101
27. A Single Line Diagram of the System under Study.....	136
28. Variation of Voltage Profile Improvement Index with DG Rating for Different Sets of Bus Weighting Factors (case 3 with DG operating at 0.9 pf lag).....	140
29. Variation of Voltage Profile Improvement Index with Different DG Ratings (DG Operating at 0.9 pf lag and Weighting Factor Set#5 used).....	141
30. Impact of DG Operating Power Factor on Voltage Profile Improvement Index (DG Rating is 0.1 pu and Weighted Factor Set#5 used).....	142
31. Impact of DG Operating Power Factor on Voltage Profile Improvement Index (DG Rating is 0.2 pu and Weighted Factor Set#5 used).....	143
32. Impact of DG Operating Power Factor on Voltage Profile Improvement Index (DG Rating is 0.3 pu and Weighted Factor Set#5 used).....	144
33. Variation of Line Loss Reduction Index with DG Rating (DG Operating at 0.9 pf lag).....	145
34. Impact of DG Operating Power Factor on Line Loss Reduction Index (DG Rating is 0.1 pu).....	146
35. Impact of DG Operating Power Factor on Line Loss Reduction Index (DG Rating is 0.2 pu).....	147

Figure	Page
36. Impact of DG Operating Power Factor on Line Loss Reduction Index (DG Rating is 0.3 pu).....	148
37. Variation of Environmental Impact Reduction Index for Carbon Dioxide for Different DG Ratings (DG operating at 0.9 pf lag).....	149
38. Variation of Environmental Impact Reduction Index for Sulfur Dioxide for Different DG Ratings (DG operating at 0.9 pf lag).....	150
39. Variation of Environmental Impact Reduction Index for Nitrogen Oxides for Different DG Ratings (DG operating at 0.9 pf lag).....	151
40. Variation of the overall Environmental Impact Reduction Index for Different DG Ratings (DG Operating at 0.9 pf lag).....	152
41. Impact of DG Operating Power Factor on Environmental Impact Reduction Index for Carbon Dioxide (DG Rating is 0.1 pu).....	153
42. Impact of DG Operating Power Factor on Environmental Impact Reduction Index for Sulfur Dioxide (DG Rating is 0.1 pu).....	154
43. Impact of DG Operating Power Factor on Environmental Impact Reduction Index for Nitrogen Oxides (DG Rating is 0.1 pu).....	155
44. Impact of DG Operating Power Factor on the overall Environmental Impact Reduction Index (DG Rating is 0.1 pu).....	156
45. Impact of DG Operating Power Factor on Environmental Impact Reduction Index for Carbon Dioxide (DG Rating is 0.2 pu).....	157
46. Impact of DG Operating Power Factor on Environmental Impact Reduction Index for Sulfur Dioxide (DG Rating is 0.2 pu).....	158
47. Impact of DG Operating Power Factor on Environmental Impact Reduction Index for Nitrogen Oxides (DG Rating is 0.2 pu).....	159
48. Impact of DG Operating Power Factor on the overall Environmental Impact Reduction Index (DG Rating is 0.2 pu).....	160
49. Impact of DG Operating Power Factor on Environmental Impact Reduction Index for Carbon Dioxide (DG Rating is 0.3 pu).....	161
50. Impact of DG Operating Power Factor on Environmental Impact Reduction Index for Sulfur Dioxide (DG Rating is 0.3 pu).....	162



Figure	Page
51. Impact of DG Operating Power Factor on Environmental Impact Reduction Index for Nitrogen Oxides (DG Rating is 0.3 pu).....	163
52. Impact of DG Operating Power Factor on the overall Environmental Impact Reduction Index (DG Rating is 0.3 pu).....	164
53. Variation of Distributed Generation Benefit Index (BI) with Weighting Factors (case 1 with 0.3 pu rating and 0.8 pf lag).....	170
54. Variation of Distributed Generation Benefit Index (BI) with Weighting Factors (case 2 with 0.2 pu rating and unity pf).....	171
55. Variation of Distributed Generation Benefit Index (BI) with Weighting Factors (case 3 with 0.2 pu rating and 0.9 pf lag).....	172
56. Variation of Distributed Generation Benefit Index (BI) with Weighting Factors (case 4 with 0.1 pu rating and 0.9 pf lag).....	173
57. Variation of Distributed Generation Benefit Index (BI) with Weighting Factors (case 1 with 0.1 pu rating and 0.8 pf lead).....	174
58. Variation of Distributed Generation Benefit Index (BI) with Weighting Factors (case 4 with 0.2 pu rating and 0.9 pf lead).....	175
59. A General Power System Bus.....	219
60. A Single Line Diagram of Test System.....	225

## NOMENCLATURE

a	Fraction of distance of WTG location to the total distribution line distance
$A_{FU}$	Effective area of fuel cell, $\text{cm}^2$
$A_{PV}$	The effective area of PV module, $\text{m}^2$
$A_w$	Rotor area of wind turbine, $\text{m}^2$
$AE_{ij}$	Amount of emission of $i^{\text{th}}$ pollutant for $j^{\text{th}}$ conventional plant, $\text{kg/MWh}$
$AE_{ik}$	Amount of emission of $i^{\text{th}}$ pollutant for $k^{\text{th}}$ DG plant, $\text{kg/MWh}$
B	Total number of conventional generators in the system
BI	Distributed generation benefit index
$BW_i$	Benefit weighting factor for $i^{\text{th}}$ attribute
$BW_j$	Benefit weighting factor for $j^{\text{th}}$ attribute
$BW_{EIR}$	Benefit weighting factor for environmental impact reduction
$BW_{LLR}$	Benefit weighting factor for line loss reduction
$BW_{VPI}$	Benefit weighting factor for voltage profile improvement
$BW_{Eh}$	Hourly weighting factor for environmental impact reduction for the $h^{\text{th}}$ hour
$BW_{LLh}$	Hourly weighting factor for line loss reduction for the $h^{\text{th}}$ hour
$BW_{VPh}$	Hourly weighting factor for voltage profile improvement for the $h^{\text{th}}$ hour
$C_p$	Performance coefficient of wind turbine
D	Distance from the infinite bus to the WEG location, km

$D_i$	Line length for distribution line $i$ , km
$D_H$	Number of daytime intervals during the study period
$EDG_k$	Amount of energy generated by $k^{\text{th}}$ DG plant, MWh
EIRI	Environmental impact reduction index
$EG_j$	Amount of electrical energy generated from $j^{\text{th}}$ conventional power plant, MWh
$EG_{Aj}$	Amount of electrical energy generated from $j^{\text{th}}$ conventional power plant with the employment of DG, MWh
$EI_i$	Weighting factor for $i^{\text{th}}$ pollutant
$EIRI_i$	Environmental impact reduction index for the $i^{\text{th}}$ pollutant
$EIRI_h$	Environmental impact reduction index for the $k^{\text{th}}$ hour
$E[L]$	Expected value of load, pu
$E[P_w]$	Expected value of wind power output, pu
$E[V_L]$	Expected value of load voltage, pu
$E_o$	Standard reversible cell potential, volt
$f_C(c)$	Probability density function for $C$
$f_{I_C}(i_c)$	Probability density function for $I_C$
$f_L(l)$	Probability density function for $L$
$f_{P_s}(p_s)$	Probability density function for $P_s$
$f_{P_A}(p_s)$	Probability density function of PV output (including $p_s=0$ )
$f_{P_w}(p_w)$	Probability density function for $P_w$
$f_T(t)$	Probability density function for $T$
$f_U(u)$	Probability density function for $U$
$f_{V_L}(v_L)$	Probability density function for $V_L$

$F$	Faraday's constant (96,485.3415 C/mol)
$F_1$	Fraction of daytime interval during the study period
$F_{in}$	Total molar flow rate (lb mol/hr)
$F_L(l)$	Cumulative density function for $L$
$F_{P_s}(p_s)$	Cumulative density for $p_s$
$F_{P_A}(p_s)$	Cumulative density function of PV output (including $p_s=0$ )
$F_{P_w}(p_w)$	Cumulative density function for $P_w$
$F_U(u)$	Cumulative density function for $U$
$F_U(u_o)$	Cumulative density function for $U_o$
$F_U(u_c)$	Cumulative density function for $U_c$
$F_U(u_r)$	Cumulative density function for $U_r$
$H$	Total number of DG plants in the system
$HV$	Heating value of fuel, Btu/lb
$HV_s$	Heating value of fuel at standard pressure and temperature, Btu/ft <sup>3</sup>
$H_{2, consumed}$	Consumption rate of hydrogen in electrochemical reaction (lb mol/hr)
$H_{2, in}$	Molar flow rate of hydrogen at the inlet of the fuel cells (lb mol/hr)
$H_{2, out}$	Molar flow rate of hydrogen at the outlet of the fuel cells (lb mol/hr)
$i_{FU}$	Operating output current density of individual fuel cell, A
$i_{L, conc}$	Limiting current density output of fuel cell, A/cm <sup>2</sup>
$I$	Global insolation on a surface, kW/m <sup>2</sup>
$I_{A, i}$	Line current in distribution line $i$ with employment of DG, pu
$I_C$	Global insolation on a surface under cloud cover condition, kW/m <sup>2</sup>
$I_{FU}$	Operating output current of individual fuel cell, A

$I_j$	Total current due to both electron and hole flow across junction of PV equivalent circuit, A
$I_{DG,i}$	Line current provided by DG in distribution line i, pu
$I_{L,i}$	Line current in distribution line i without DG, pu
$I_{L,PV}$	Load current for equivalent circuit of PV cell, A
$I_{o,PV}$	Dark or Saturation current for equivalent circuit of PV cell, A
$I_{S,PV}$	Constant-current source for equivalent circuit of PV cell, A
$I_{max}$	Maximum global insolation on a surface under clear sky condition, kW/m <sup>2</sup>
$I_{sys,FU}$	Fuel cell system output current, A
$II_i$	Improvement index for i <sup>th</sup> attribute
$k$	Boltzmann constant ( $1.38 \times 10^{-23}$ J/°K)
$k_i$	Weighting factor for bus i
$K_p$	Photovoltaic array packing factor
$L$	Load, pu
$L_i$	Load at bus i, pu
$L_{max}$	Maximum load, pu
$L_{min}$	Minimum load, pu
$LL_{w/DG}$	Total line losses in the system with employment of DG, pu
$LL_{wo/DG}$	Total line losses in the system without DG, pu
$LLRI$	Line loss reduction index
$LLRI_h$	Line loss reduction index for the k <sup>th</sup> hour
$M$	Total number of lines in the distribution system
$m$	Order of power output characteristic curve
$m_f^*$	Fuel mass flow rate, lb/hr

$N$	Total number of busses in distribution system
$N_{\text{cell}}$	Number of cells per stack
$N_{\text{H}}$	Number of night-time intervals during the study period
$N_{\text{P}}$	Number of string in the fuel cell system
$N_{\text{S}}$	Number of stacks in the fuel cell system (series configuration)
$NP$	Total number of pollutants under consideration
$P_i$	Real power measured at bus $i$ , pu
$P_{\text{FU}}$	Fuel cell system power output, kW
$P_{\text{L}}$	Load real power, pu
$P_{\text{m}}$	Mechanical power output of wind turbine, kW
$P_{\text{mi}}$	Power output of microturbine, Btu/hr
$P_{\text{CO}_2,a}$	Partial pressure of carbon dioxide at the anode
$P_{\text{CO}_2,c}$	Partial pressure of carbon dioxide at the cathode
$P_{\text{H}_2,a}$	Partial pressure of hydrogen at the anode
$P_{\text{H}_2\text{O},a}$	Partial pressure of water at the anode
$P_{\text{O}_2,c}$	Partial pressure of oxygen at the anode
$P_{\text{out, mi}}$	Power output of microturbine, kW
$P_{\text{R}}$	Wind generation rated power, pu
$P_{\text{S}}$	Random variable of power output of the PV array, kW
$P_{\text{Smax}}$	Maximum power output of the PV array, kW
$P_{\text{w}}$	Wind power output, pu
$P_{\text{w}}(u)$	Wind power output as function of wind speed, pu
$PE_{i \text{ w/DG}}$	Amount of emissions for $i^{\text{th}}$ pollutant with DG, kg

$PE_{i \text{ wo/DG}}$	Amount of emissions for $i^{\text{th}}$ pollutant without DG, kg
$PF_L$	Power factor of load
$PS$	Fuel pressure, psi
$PS_s$	Standard pressure, psi
$Q_f$	Fuel volume flow rate, $\text{ft}^3/\text{hr}$
$Q_i$	Reactive power measured at bus $i$ , pu
$Q_L$	Load reactive power, pu
$R_i$	Line resistance for line $i$ , pu/km
$R_{FU}$	Total cell resistance, $\Omega$
$R_g$	Universal gas constant ( $8.345\text{J/mol} \cdot ^\circ\text{K}$ )
$R_j$	Junction impedance for equivalent circuit of PV cell, $\Omega$
$R_o$	Load impedance for equivalent circuit of PV cell, $\Omega$
$R_w$	Radius of the rotor of wind turbine, m
$RI_j$	Reduction index for $j^{\text{th}}$ attribute
$S_L$	Load complex power, pu
$S_L^*$	Conjugate load complex power, pu
$t$	Random variable represented cloud cover
$T_{mi}$	Microturbine fuel temperature, $^\circ\text{K}$
$T_{PV}$	Photovoltaic array temperature, $^\circ\text{K}$
$T_s$	Standard temperature, $^\circ\text{K}$
$u$	Wind speed, m/s
$U_f$	Fuel utilization
$U_C$	Cut-in speed, m/s

$U_O$	Cut-out speed, m/s
$U_R$	Rated speed, m/s
$\text{Var}(V_L)$	Variance of load voltage
$V_i$	Voltage magnitude at bus $i$ , pu
$V_{FU}$	Individual cell voltage of fuel cell, volt
$V_L$	RMS phase voltage at the load point, pu
$V_O$	Open-circuit reversible cell potential, volt
$V_{PV}$	Voltage across the junction for equivalent circuit of PV cell, volt
$V_s$	RMS phase voltage at the infinite bus, pu
$V_{\text{sys, FU}}$	Fuel cell system output voltage, volt
$VP_{w/DG}$	Voltage profile of the system with DG, pu
$VP_{wo/DG}$	Voltage profile of the system without DG, pu
VPII	Voltage profile improvement index
$VPII_h$	Voltage profile improvement index for the $k^{\text{th}}$ hour
WTG	Wind Turbine Generation
$x$	Reactance per phase per unit length, pu/km
$x_{FU}$	Molar fraction for gas $i$ of fuel cell reaction
$X$	Total reactance per phase, pu
$Y$	Total length of distribution line, km
$\alpha_s$	Scale parameter of beta distribution, assumed constant over the study period
$\beta_s$	Shape parameter of beta distribution, assumed constant over the study period
$\alpha_w$	Scale parameter of wind speed, m/s



$\beta_w$	Shape parameter of wind speed
$\mu_s$	Mean of cloud cover, assumed constant over the study period
$\mu_w$	Mean wind speed, m/s
$\sigma_s$	Standard deviation of the cloud cover, assumed constant over the study period
$\sigma_w$	Standard deviation of wind speed, m/s
$\sigma_s^2$	Variance of the cloud cover, assumed constant over the study period
$\sigma_w^2$	Variance of wind speed, m <sup>2</sup> /s <sup>2</sup>
$\eta_{act}$	Activation polarization, volt
$\eta_{conc}$	Concentration polarization, volt
$\eta_{ohm}$	Ohmic polarization, volt
$\eta_{PV}$	Conversion efficiency of the PV module
$\eta_t$	Overall efficiency of microturbine
$\rho$	Density of the air, kg/m <sup>3</sup>
$\lambda$	Tip speed ratio of wind turbine
$\gamma$	Pitch angle of wind turbine, degree
$\omega$	Mechanical angular speed of blades of wind turbine, rad/s

## CHAPTER I

### INTRODUCTION

#### 1.1 Emergence of Distributed Generation

Electrical energy continues to play a vital role in modern life. The idea to install and operate a power system was introduced in 1880 by Thomas Alva Edison. The earliest power systems were small and local, with generation close to the load, and with distribution lines spread over the area being served. As loads grew and the inhabited areas spread, economy of scale dictated large central-station power plants located far away from load centers. High voltage transmission lines, sub-transmission lines, and distribution lines were used to transmit and deliver electrical energy to customers as shown in Figure 1. Interconnection of neighboring systems enabled large-scale power exchanges to decrease peak loads and to maintain power supply reliability during emergencies. This arrangement led to the concept of a “vertically integrated” electric utility.

Several recent happenings have created a new environment for the electric power infrastructure. They are listed below:

- a. Deregulation of the electric utility industry and the ensuing break up of the vertically integrated utility structure.

- b. Public opposition to building new transmission lines on environmental grounds.
- c. Keen public awareness of the environmental impacts of electric power generation.
- d. Rapid increases in electric power demand in certain regions of the country.
- e. Significant advances in several generation technologies that are much more environmentally benign (wind-electric generation, microturbines, fuel cells, and photovoltaics) than conventional coal, oil, and gas-fired plants.
- f. Increasing public desire to promote “green” technologies based on renewable energy sources.
- g. Awareness of the potential of distributed generation to enhance the security of electric power supply, especially to critical loads, by creating mini- and micro-grids in the case of emergencies and/or terrorist acts, and/or embargoes of energy supplies.

All the factors listed above have led to an upsurge in interest in the development and utilization of distributed generation (DG) [1]. As a result, a new era of power generation and utilization as shown in Figure 2 has become increasingly attractive to the power industry. The key element of this new environment is to build and operate several distributed generation units near load centers instead of expanding the central-station power plants located far away from the customers to meet increasing load demands. DG promises to produce electricity as efficiently as large power plants and at a cost competitive with centralized generation for certain applications. Recently, technological developments have dramatically improved the efficiency and lowered the

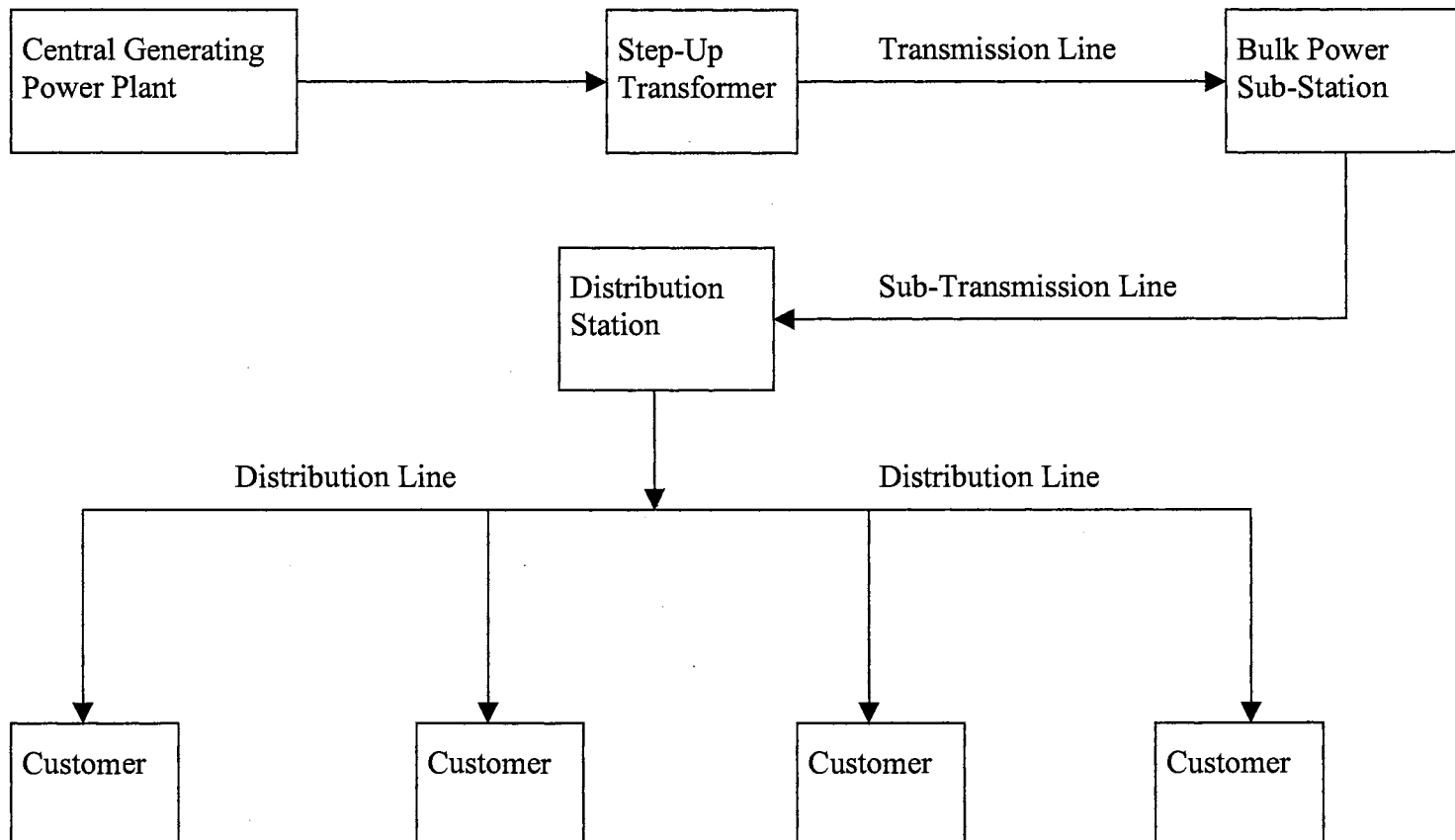


Figure1. A Block Diagram of Traditional Power System

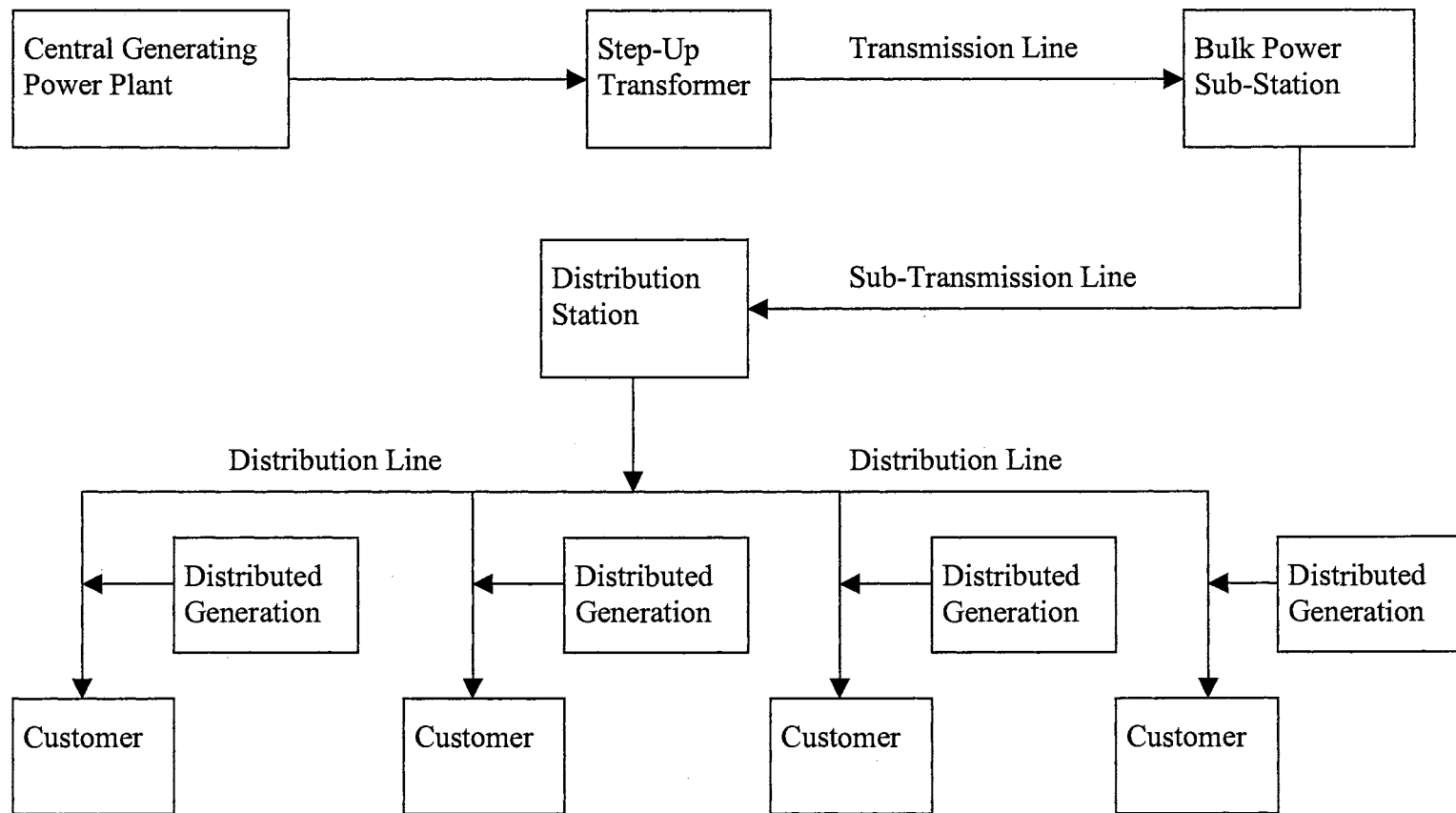


Figure 2. Distributed Generation Integrated into an Existing Utility Network

cost of several DG technologies. Introduction of DG into an existing system offers several benefits to utilities, customers, and society. Details of potential benefits and some of the promising DG technologies will be discussed later.

The slight drawback for some of DG technologies, especially the ones based on renewable resources, is high capital cost. However, surveys have shown that cost is not the only and primary reason to choose the source of power generation. For example, according to a survey, photovoltaic technology has received the highest ranking among various power generation options such as utilization of natural gas, crude oil, gasoline, hydro-electric, nuclear, and coal, in terms of being best for environment, safety, best for US economy, most positive to customers, and the ability to play a significant role in the 21<sup>st</sup> century [2].

Therefore, DG is a promising alternative for utilities seeking new technologies to provide premium power quality and reliability to their customers. With continuing developments to bring the capital costs down, several compact DG technologies are fast becoming economically viable and the pace of DG deployment is accelerating throughout the world.

## 1.2 Technologies and Benefits of Distributed Generation

Distributed Generation (DG) can be considered as “taking power to the load”. This is due to the fact that DG can be installed very near to or on a customer’s site [3]. DG can be used to match increased customer demand where the upgrade or installation of new distribution lines are not available for one reason or another. The size of DG ranges

from a few kilowatts up to 100 MW [4-5]. DG can be powered by both conventional and renewable energy resources. Technologies that utilize conventional energy resources are:

- Gas turbines
- Microturbines
- IC engines
- Fuel cells

These can be considered as “energy transformers” that couple gas and electric systems, possibly involving hydrogen. There are many new technologies that utilize renewable energy sources. However, at the present time, the ones that show promise for DG applications are:

- Wind-Electric Conversion Systems (also known as Wind Turbine Generation, WTG)
- Solar-Thermal-Electric Systems
- Geothermal Systems
- Photovoltaic Systems
- Biomass Systems

Tidal power, ocean thermal electric conversion, and wave energy are not yet fully developed for serious consideration at the present time. Historical backgrounds for some of the most promising DG technologies are outlined in section 1.3.

The deployment of DG in existing distribution networks offers many benefits to utilities, customers, and society [6-9]. Some of the potential benefits to utilities are:

- Reduced line and transformer losses
- Increased overall energy efficiency

- Reduced central generating station reserve requirements
- Increased system reliability and power quality
- Reduced environmental impacts
- Relieving transmission and distribution congestion
- Deferring investments to upgrade or install additional generation, transmission and distribution facilities
- Reduced operation and maintenance cost (O&M) due to the absence of moving parts in the case of some DG technologies
- Peak shaving

Customers receive benefits from the introduction of DG by having a more reliable and better quality of energy at a lower cost and with less environmental impacts.

Society on the whole can receive benefits by the deployment of DG in terms of:

- Improved environment
- Efficient use of energy resources
- Enhanced productivity
- Growing and healthy economy

### 1.3 Historical Background of Promising DG Technologies

#### 1.3.1 Wind Turbine Generation

Wind is a free, clean, and inexhaustible energy source. It has served humanity well for many centuries by propelling ships and driving windmills to grind grains and pump water. In the seventeenth century B.C., the Babylonian emperor Hammurabi planned to use windmills for irrigation [10]. By the middle of the seventh century A.D.,



the Persians were using wind energy extensively. Their machines had vertical-axis with a number of radially mounted sails. The early machines were mechanically inefficient but they served well for many centuries. The first wind turbine used for generating electricity was developed in Denmark around 1890. By 1910, several hundred units were operating in Denmark with capacities ranging from 5 to 25 kW. In the US, the introduction of commercial wind-electric plants using two and three blades propellers, with capacities of 0.2 to 3 kW, appeared in 1925. They were used in remote areas to supply small appliances and charge storage batteries. In order to reduce the cost of electricity, Putnam introduced the largest wind turbine of that time with a capacity of 1250 kW and two blades in 1941 [11]. His machine had a tower 34 m high and a rotor 53 m in diameter. The blade pitch was adjustable to maintain a constant rotor speed of 28.7 rpm. At higher wind speeds, the blades were feathered and the machine was stopped. This machine produced 1250 kW of electrical power at wind speeds above 13 m/s. The important result from this system was the realization that even larger wind turbines were necessary for economic viability.

The U. S. federal wind energy program began in 1972 with a joint effort by the National Aeronautics and Space Administration (NASA) and National Science Foundation (NSF) [12]. In 1974, NSF funded NASA to design, build, and operate a wind turbine for research purposes. As a result, the wind turbine, code named MOD-0, was built and operated in 1975. This machine was rated at 100 kW and had a 38 m diameter rotor with two down-wind blades. The MOD-0 was designed to maintain a constant rotor speed of 40 rpm. Due to the fact that the MOD-0 performed reasonably well, another wind turbine, MOD-0A was built in 1977 with the same size of tower and rotor but the

generator size was doubled to 200 kW. Following MOD-0 and MOD-0A, a series of other wind turbines: MOD-1, MOD-2, MOD-3, and so on were built and tested. The MOD-1 had a rating of 2000 kW with a rotor diameter of 61 m but results from the field showed that the MOD-1 could not lead to a cost competitive production unit. Therefore, the MOD-2 was introduced in 1981. The experimental results were good and this turbine was able to represent a truly cost competitive wind turbine. However, these units operated at constant speeds, resulting in very high mechanical stresses on blades, tower, etc., and all of them failed prematurely.

Although, capital costs of wind turbines were trimmed down from early figures, this technology still required financial support from the government. Thus, in the early 1980s, several countries including the USA and Denmark stimulated the industry and built a large number of wind turbines through tax credits and subsidies programs. As a result, more than 2000 MW of wind turbines were installed between 1982 and 1990. By the end of year 2000, the total worldwide wind capacity rose to nearly 18,000 MW, with Germany, United States, Spain, and Denmark still dominating wind energy production in the world [see reference 3]. In addition, nearly 4000 MW of wind turbines were installed worldwide in the year 2000 alone. A Typical modern wind turbine installation is shown in Figure 3. It must be pointed out that almost all the modern WTGs operate at variable speed to reduce mechanical stresses, and sophisticated power generation and power electronics processing systems are employed to obtain utility-grade constant-voltage constant –frequency output.



Figure. 3 A 25.2 MW Wind Turbine Installation in Pecos County, Texas  
[Source: [www.gepower.com](http://www.gepower.com), June 2002]

### 1.3.2 Microrurbine Systems

The concept of microturbine technology is not new. Microturbine was developed for electric utilities more than 25 years ago. In the 1960s, Allison Energy began to develop microturbines to power engines for a bus company and Allison GT 404 turbines were installed in several buses for the first field trial in 1971 [13]. The engines were the two-stage type with a twin regenerator system that recycles heat from the gas path to heat up the incoming air and cool the exhaust to no higher than 500-600 °F. In 1976, Allison started to develop microturbine driven generators to supply energy for radar sets and control stations. One major goal of this project was to provide energy at a high level of reliability. Such a turbine generator was installed and tested in 1978. The major results from this test included multi-fuel capability, reduction of fuel consumption, and achievement of reliability level. In the early 1990s, the first successful commercial microturbines were produced and made available by JPX of France. During the mid to late 1990s, a number of technical and regulatory events and developments converged to stimulate the development of microturbines. These include the development of compact, low cost, reliable power electronics for power conditioning and frequency conversion. Currently, capital cost of microturbine is still high at about \$800-\$1500/kW, but development efforts are underway to bring it down. In the US, Allison Energy, Allied Signal, Elliott Energy, Northern Research and Engineering, and Capstone are involved in the development and manufacture of microturbines [14]. Currently, both 30 kW and 60 kW microturbine units are being manufactured and marketed by the Capstone Turbine Corporation [15]. A typical array of Capstone microturbine systems is shown in Figure 4.

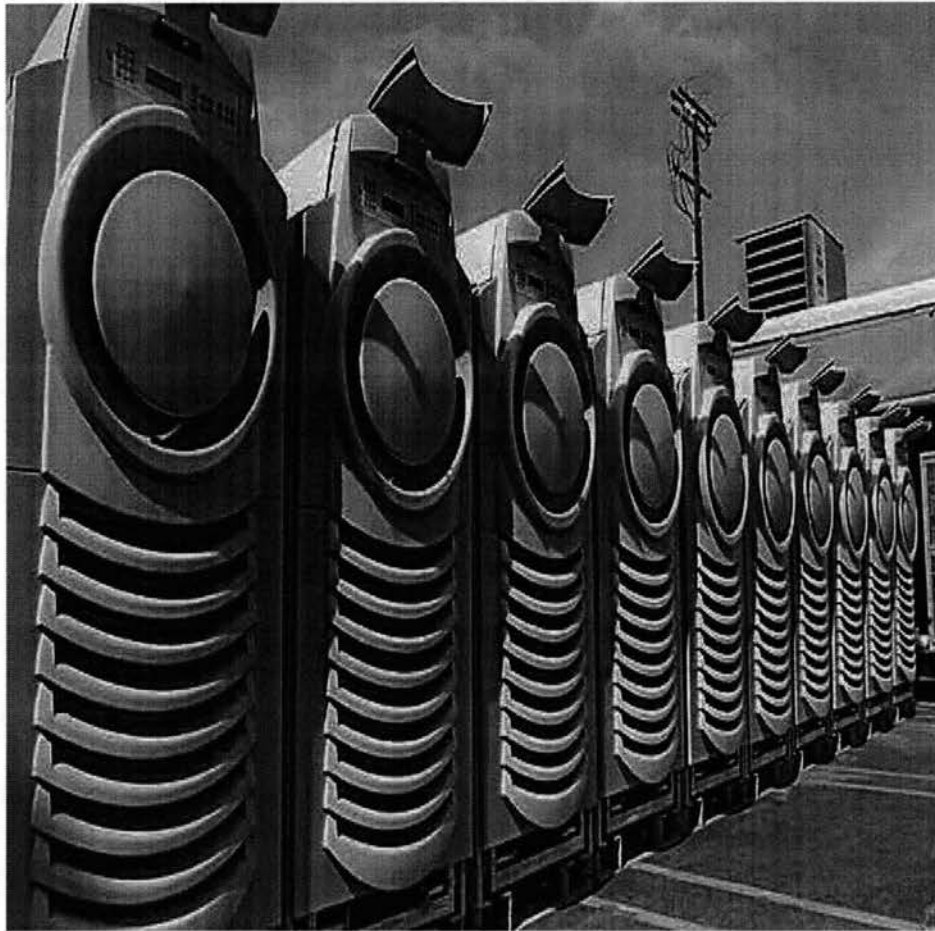


Figure 4. Capstone C-30 Natural Gas Microturbine System (30 kW/unit)  
[See Reference 15]

### 1.3.3 Photovoltaic Systems

Photovoltaic (PV) devices convert incident solar radiation (insolation) directly to electrical energy. The nuclear reaction in the sun yields a huge amount energy [about  $389 \times 10^{24}$  W]. Of this huge amount of emitted energy, only a small fraction is intercepted by the earth's surface, with an average value of  $1370 \text{ W/m}^2$  at the outer atmosphere. Solar energy is clean and renewable. A typical central-station type PV system rated at 1 MWp is shown in Figure 5.

French Scientist Edmund Becquerel discovered the Photovoltaic (PV) effect in 1839 [16-17]. During 1870s, Adams and Day observed the PV effect in selenium. Subsequent work on photovoltaic effects in selenium and cuprous oxide led to the development of the selenium photovoltaic cell widely used for many years. By 1941 conversion efficiencies of about 1% to 2% were achieved with the selenium cell. However, selenium cell was not suitable for power generation because of its high cost. Bell laboratories introduced a practical single crystal silicon PV device in 1954[18]. The modern era of PV began in 1954 with Chapin of Bell Labs reporting a 6% conversion efficiency.

With improved technology, silicon cell efficiency reached 14% by 1958. In 1954 Reynolds reported 6% solar conversion efficiency using cuprous sulfide/cadmium sulfide heterojunction cells. The silicon single-crystal photovoltaic cell has become the prototype of all homojunction cells and has been in focus of research for many years. With the advantage of new technology, the efficiency of gallium arsenide cell has rapidly increased with efficiencies approaching 24% [see reference 17].

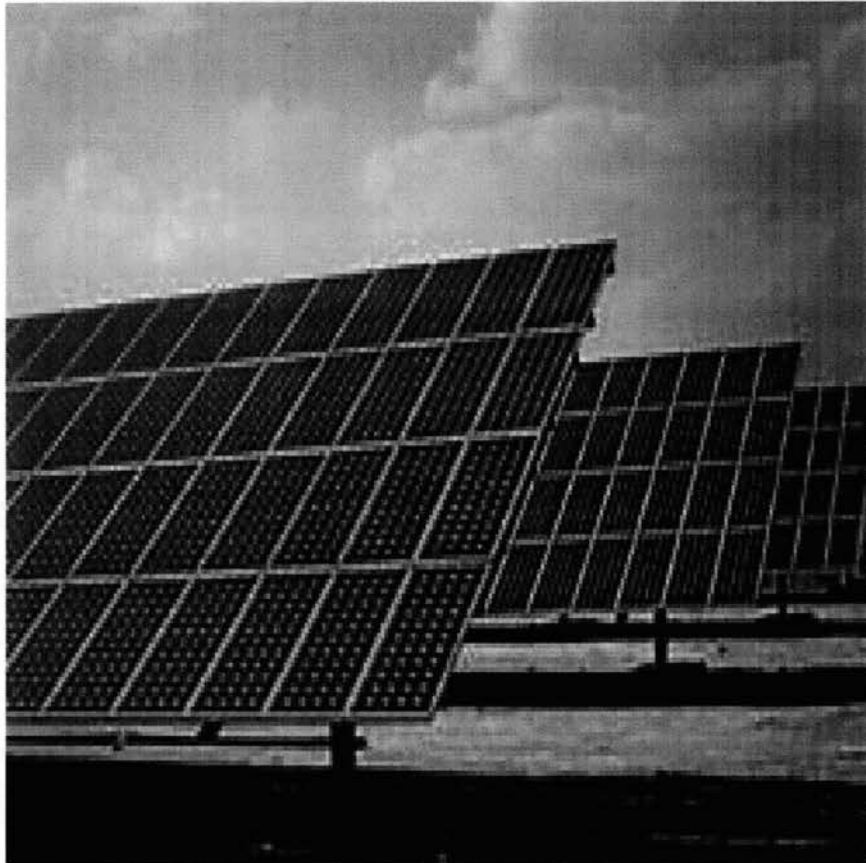


Figure 5. A Solar Power Plant in Europe with a Rating of 1 MWp  
[Source: [www.bpsolar.com](http://www.bpsolar.com), April 2002]

PV found its first significant use in the space program. Vanguard I was the first satellite to generate power from the sun in 1958. However, much interest in PV appeared in the wake of the Arab oil embargo of 1973. As a result, in 1982, a 1 MW single crystal silicon PV power plant was built and operated in southern California. This “Lugo” plant was built by the ARCO solar company. The system required a total array area of 10,275 m<sup>2</sup>. The PV plant had a capacity factor as high as 36% and achieved over 95% availability. Another PV power plant was also installed in California in 1984 with a rating of 6.5 MW. This PV power plant had a capacity factor of nearly 30%. Photovoltaic systems for utility scale applications (PVUSA) project was introduced in the late 1980s. This project was a cooperative effort between government, industry, and utilities and the purpose of this project was to demonstrate PV systems for potential utility applications. In the early 1990, the PV Manufacturing Technology (PVMaT) project was introduced in an effort to improve manufacturing processes, improve commercial product performance, accelerate manufacturing cost reduction for PV modules, and lay the ground work for a substantial scale-up of manufacturing capacity. As a result, the world price of PV modules fell below \$5/W<sub>p</sub> by 1992.

The development of PV systems in the next 10-20 years will be focused on replacing single junction cells with tandem and multiple cell junctions in an effort to increase efficiency [19]. Currently, most of the annual US production of solar cells is for export. PV systems installed in California account for more than 90% of the total PV installations in the USA. With capital costs coming down and improving conversion efficiencies, PV systems have a great potential to compete with other conventional



sources [20]. Recently, new concepts such as building-integrated PV are being actively developed.

#### 1.3.4 Fuel Cell Systems

Fuel cell is a device that converts the chemical energy in a fuel directly and isothermally into electrical energy. The idea of a fuel cell was first suggested by Sir Humphry Davy in 1801. However, Sir William Grove is credited with the building and operation of the first laboratory-scale unit in 1839 [21-22]. His cell electrolyzed water into hydrogen and oxygen, and then combined these gases into water, producing electrical energy. However, the first US patent for fuel cell was assigned to Vergnes in 1860. J. J. Jacques constructed the largest battery that delivered a current density of 100 mA/cm<sup>2</sup> with a rating of 1.5 kW in 1896. His system consisted of large cells with iron vessels serving as cathode and with molten KOH electrolyte at 400-500 °C. A carbon rod served as anode, and air was blown in at the bottom near the wall [see reference 21]. In order to eliminate the use of precious metals and to increase current density, Bacon, in 1939, built a single high pressure reversible cell with 27% KOH electrolyte operating at 100 °C, with gas pressure of 220 bar with a current density of 13 mA/cm<sup>2</sup> at 0.89 V. In 1946, Bacon built a new fuel cell based on feed gases from cylinders, with double-porosity sintered nickel electrodes. In 1954, a six-cell battery was built by Bacon with 12.5 cm diameter electrodes which could generate 150 W at 41 bar and 200 °C. In 1959, with a new sponsor, Bacon built a battery which could deliver 6 kW at a current density of 700 mA/cm<sup>2</sup>. The demonstration of this battery was given in 1959.

The development of Phosphoric Acid Fuel Cell (PAFC) was related to the first fuel cell. In the first cell, sulfuric acid was used as electrolyte. However, this acid was replaced by phosphoric acid, which enabled operation at a temperature of 200 °C. In the late 1960s, Team to Advance Research for Gas Energy Transformation (TARGET) was established for a large scale demonstration of fuel cells by the American Gas Association and United Technology Corporation (UTC), later International Fuel Cell Corporation [23]. During 1967 to 1983, plant size increased from 12.5 kW to 1 MW and finally a 4.8 MW plant was built in New York City in 1983. A similar fuel cell power plant operated reasonably well in Tokyo, Japan. The overall efficiency for the large units is now approaching 45-50%.

The prototype for electrolyte of the Solid Oxide Fuel Cell (SOFC) that used thin rod of a high temperature anion-conducting solid material made from zirconium oxide with 15% yttrium oxide was introduced in 1899. The cell operated at 1050 °C and delivered a current density of 1 mA/cm<sup>2</sup> at 0.65 V. In 1965, Archer introduced a multi-cell SOFC, with calcia-stabilized zirconia as electrolyte and sintered platinum as electrodes. Since 1980, the effort was expanded with new fabrication techniques such as flame spraying the subsequent layers. A SOFC pilot power plant with a rating of 5 kW, employing a 24-cell stack was built in 1986.

Molten Carbonate Fuel Cell (MCFC) was introduced by J. A. A. Ketrlaar and G. H. J. Broers in the 1950s. Their system operated for about 4500 hours on town gas, hydrogen, carbon monoxide, and natural gas. A current density of 50 mA/cm<sup>2</sup> could be achieved with their system. In 1963, some electrolytes were replaced by Al<sub>2</sub>O<sub>3</sub> in an effort to increase current density. The results have shown good performance with a

current density of  $100 \text{ mA/cm}^2$ . The important improvements were made on the anode interface and on the matrix electrolyte, accompanied by increases in size of cell surface area and the construction of cells and stacks. As a result, performance of MCFC improved with current densities approaching  $350 \text{ mA/cm}^2$ .

Proton Exchange Membrane Fuel Cell (PEMFC) was introduced by General Electric (GE) in the 1950s. The first PEMFC with a rating of 1 kW was used to provide primary power for Gemini spacecraft in the early 1960s. PEMFC has also been developed for special space industry and military applications. Five different membranes were developed during 1959 to 1980. The cell performance has increased dramatically since 1959.

A modern fuel cell power plant installed by United Technologies is shown in Figure 6. This fuel cell power plant has a capacity of 200 kW and its output is delivered to an electric utility grid.

### 1.3.5 Gas Turbines

Gas turbines play an important role in distributed generation market. The idea of gas turbine is derived from aircraft engines. The concept employed in a gas turbine is not entirely new. The earliest example of gas turbine can be traced as far back as 150 BC when Egyptians invented an Aeolipile that rotated on top of a boiling pot of water due to reaction effect of hot air or steam exiting several nozzles arranged on wheel. In 1550, Leonardo da Vinci drew a sketch of a device that rotated due to the effect of hot gases flowing up a chimney. The first patent of a basic gas turbine was granted to John Barber in 1791. However, it was not until 1872 that the first true gas turbine engine was

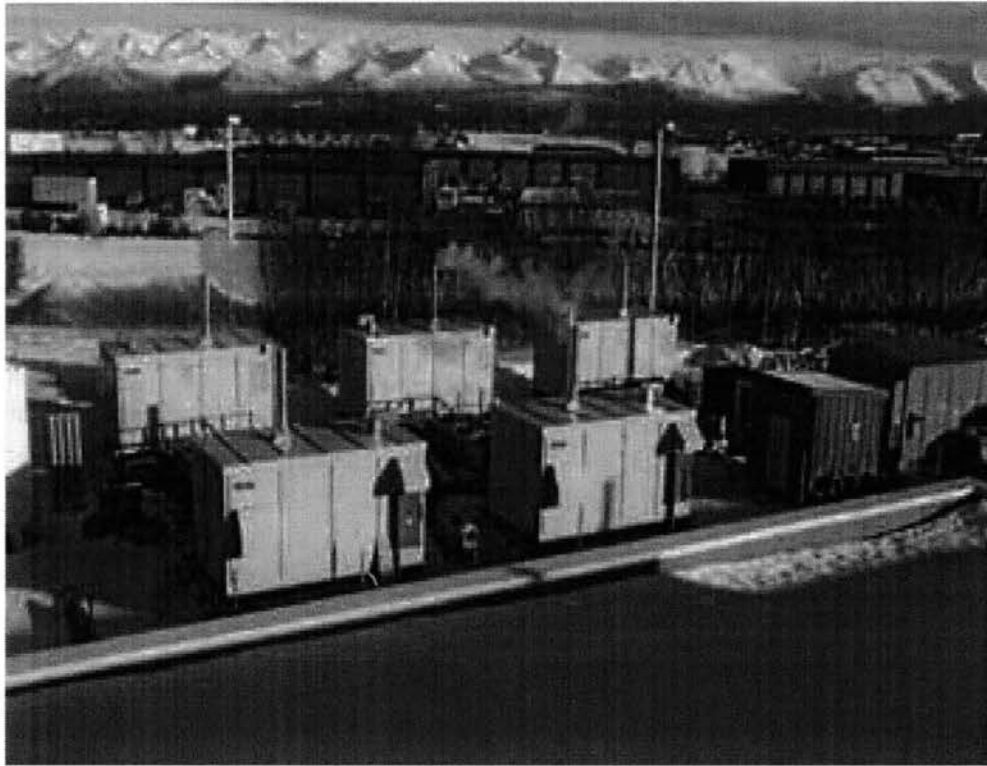


Figure 6. A UTC 200 kW Fuel Cell Power Plant in Alaska [Source: [www.internationalfuelcells.com](http://www.internationalfuelcells.com), April 2002]

designed by Stolze. His system used a multistage turbine section and a multistage axial flow compressor. His invention laid the foundation and basic principles on which gas turbines are based today. The efficiency of his engine was only about 4%. The General Electric Company started a gas turbine division in 1903 and developed the turbo supercharger during World War I. It used hot exhaust gases from a reciprocating engine to drive a turbine wheel that in turn drove a centrifugal compressor used for supercharging. In the late 1920s, Sir Frank Whittle made the first practical proposal for the use of gas engine in an aircraft. However, the potential work of Whittle was not realized until Hans von Ohain made the first gas turbine propelled flight in 1939.

Since then, the attraction of high speed flight has led to extensive research and development on gas turbines. As a result, during 1960s, gas turbine developed into an increasingly efficient and cost effective device for many applications. Higher overall pressure ratio and higher turbine inlet temperature, improvement in materials, and advanced turbine cooling technique were also developed during this period. During 1980s, research work was concentrated in the areas of cost, meeting government regulations, fuel consumption, and the availability of materials [24-27]. At present, gas turbines are commonly used in aircraft as well as electrical power stations.

Currently, General Electric LM-series (LM1600, LM 2500, LM 2500+, and LM 6000] of aeroderivative gas turbines are widely used for many applications including DG. Most of the aeroderivative units use natural gas as the fuel of choice. The ratings of GE units range from about 14 to 44 MW. These units have achieved a high availability (about 97.5%) and high reliability (about 99%) [28]. Cut-away view of a LM 2500 series gas turbine is shown in Figure 7. Pratt&Whitney also introduced aeroderivative gas turbines

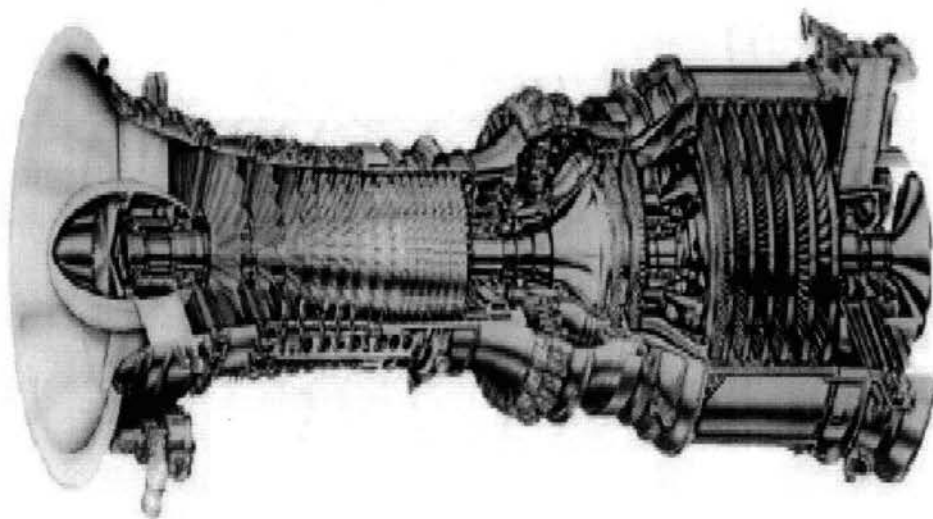


Figure 7. LM 2500+ Gas Turbine [29]

for the commercial market. Their ratings range from 4 to 50 MW. Since 1960, more than 2000 gas turbine units have been placed in commercial operation and achieved excellent record for superior performance, high reliability, high efficiency, and simplicity in maintenance.

#### 1.4 Distributed Generation Systems Planning

DG systems are easy to install with very little maintenance. WTG and PV have been proven to be viable options to produce electrical energy. Both WTG and PV are reasonably mature and are well into the commercial stage. The resource for WTG is abundant (1670 Trillion kWh/year over the land area of earth) but unevenly distributed [30-31]. Several WTGs can be installed in a windfarm and their aggregated electrical output can be injected directly to the utility grid. In terms of economics, wind energy is becoming the most competitive among all the renewable energy technologies. Installed costs at present are about \$1,000/kW. With capacity factors in the 25%-35% range (depending on the wind regime), 5 to 7 cents/kWh electricity costs are being realized. The future of wind energy is very bright with installed cost reductions of 30% or higher and electricity costs of about 3 to 4 cents/kWh for middle-range (5.6 to 6 m/s average wind speed at 10 m height) wind regimes or better.

Similar to WTG, the resource for PV is also unevenly distributed. The average amount of insolation reaching the earth's surface is about one kW/m<sup>2</sup>. The major problems of PV are the high cost of PV modules, low energy conversion efficiency, and the large collection areas required. Currently, cost of energy generated by PV range from 25-75 cents/kWh, still very high compared to other renewable sources. However, it has

been projected that energy costs will come down to about 6-12 cents/kWh by the year 2020 [see reference 3].

Microturbines and fuel cells are beginning to be promising candidates for producing electrical energy. Microturbines are under development to run at very high speeds. The emission levels of microturbines are lower than reciprocating engines. However, the barrier for microturbines is high capital cost. Development work is underway to bring the capital cost down to 250-500 \$/kW.

Presently, fuel cell power plants under development for DG are Phosphoric Acid Fuel Cells (PAFC), Molten Carbonate Fuel Cells (MCFC), Proton Exchange Membrane Fuel Cells (PEMFC), and Solid Oxide Fuel Cells (SOFC) [32-33]. PAFC provides moderate current densities and it is in the early stage of commercial application. MCFC also offers moderate current densities and it is in the field test stage. PEMFC yields high current densities and is in the prototype stage. SOFC operates with high current densities but it is still in laboratory demonstration stage. All fuel cell systems are operated at fairly high efficiencies. Similar to most DG, the primary disadvantage is cost. The current capital cost of PAFC is in the range of 3,450-3,750 \$/kW. It is expected that the capital cost will come down and some of the options will enter commercial stage by the early part of 21<sup>st</sup> century [34].

Several factors have to be considered in the design and application of DG. The most important factor is the availability of resources. The power output of WTG and PV is random and site specific. Therefore, external factors such as wind speed, the amount of solar radiation, cloud cover, and location must be considered very carefully in order to get a desirable performance. Probabilistic models have been used to model and analyze



the power outputs of WTG and PV. Microturbines and fuel cells are fairly new for DG systems. Power outputs of microturbines and fuel cells can be scheduled. Outputs of microturbines and fuel cells mostly depend on the fuel flow rate. Having appropriate models to estimate their outputs are important for planning DG systems. One or more DG systems can be combined together in order to increase output and/or to supply energy when one of the resources is not available to provide electrical energy.

Standardizing interconnection is also another factor to be considered for planning DG. Since most DG will be operated in parallel with distribution systems, it can cause several potential operating conflicts to the system [35-40]. As a result, it is important to develop standards for interconnection. The standards should address the interface between DG devices and a utility system including protection and communication requirements. Therefore, DG planners have to follow the guidelines of the standard to assure an acceptable level of safety and reliability.

### 1.5 Problem Statement

Several benefits accrue by integrating distributed generation with utility networks. These benefits should be clearly understood, analyzed, and quantified in order to increase the potential of DG penetration. The objective of this study is to propose an approach to quantify the technical benefits of DG when introduced into existing utility networks. Among the many benefits, the following three major ones are considered in this study.

- 1) Line loss reduction
- 2) Voltage profile improvement
- 3) Emission reduction

Although several DG technologies are presently available in the market, this study will consider only the four most promising DG technologies:

- 1) Wind Energy Systems
- 2) Photovoltaic Systems
- 3) Microturbine Systems
- 4) Fuel Cell Systems

Since each of the DG technology in this study has its own nature and characteristics, appropriate mathematical models for each DG technology as well as load demand are very important for this research and they will be discussed in Chapter 3.

### 1.6 Method of Study

In order to evaluate and quantify the benefits of distributed generation, several mathematical models have been developed and they are used throughout this research. The steps taken to achieve the objective outlined for this study are enumerated below:

1. Develop appropriate mathematical models to represent wind turbine generation, photovoltaic systems, microturbine systems, fuel cell systems, and load demand. Both wind speed and insolation are random by their nature. Therefore, probabilistic models based on mean and variance of the resources are used in this research. On the other hand, outputs of microturbine systems and fuel cell systems can be modeled as functions of fuel flow rate. In addition, outputs of these two can be scheduled.
2. Quantify the voltage profile improvement in the case of the introduction of wind turbine generation by using a probabilistic approach.

3. Develop a non-probabilistic approach for wind turbine generation and compare the results obtained with the probabilistic approach. The purpose of this step is to investigate whether a non-probabilistic approach is appropriate and sufficient to quantify the benefits.
4. Develop mathematical indices to quantify the benefits of DG in terms of voltage profile improvement index (VPPI), line loss reduction index (LLRI), environmental impact reduction index (EIRI), and distributed generation benefit index (BI).
5. Develop and construct a 12-bus system model. This study system will be used for analyzing and quantifying the benefits of DG under various scenarios.
6. Select suitable case studies and employ the procedures and indices developed to quantify line loss reduction, voltage profile improvement, and emission reduction achieved with the introduction of DG.
7. Arrive at some useful general conclusions and methodologies for the development of DG.

The results of this research will be presented in the form of mathematical models, tables and figures. These results and the associated conclusions should be beneficial to a better understanding of the benefits of distributed generation.

### 1.7 Organization of Thesis

Chapter II presents a review of related literature.

Chapter III discusses the mathematical models used for DG technologies (wind turbine generation, photovoltaic systems, microturbine systems, and fuel cell systems) and load demand.

Chapter IV studies the voltage profile improvement achieved with distributed wind-turbine generation. A comparison of expected value of load voltage obtained using the probabilistic and non-probabilistic approaches employing the average output is presented and discussed.

Chapter V focuses on the quantification of the benefits of DG. Voltage profile improvement index (VPPI), line loss reduction index (LLRI), environmental impact reduction index (EIRI), and an overall distributed generation benefit index (BI) are developed and introduced in an effort to quantify and analyze the benefits of distributed generation.

Chapter VI documents the case studies and simulation results obtained using a 12 bus test system under different scenarios of DG introduction. The indices developed in chapter V are used in this study. The results are analyzed and some general conclusions are drawn to assess the introduction of DG.

Chapter VII summarizes this research, conclusions are drawn, and limitations and drawbacks of this study are identified. Further work needed to improve and advance this research is outlined.

## CHAPTER II

### REVIEW OF RELATED LITERATURE

Distributed generation (DG) is becoming increasingly attractive to the power industry because DG can offer several benefits to both utilities and customers. Analysis and quantification of the benefits of DG are important before large-scale deployment of DG can occur. Most of the major work done earlier by other researchers deals with benefits of wind energy and/or photovoltaic systems in terms of capacity credit and energy cost saving. Only a few attempts have been made to quantify the benefits of DG in terms of voltage profile improvement, electrical line loss reduction, and environmental impact reduction. This chapter focuses on a survey and review of previous work on DG modeling and quantification of the benefits of DG.

#### 2.1 DG Technologies Modeling

To quantify the benefits of DG, suitable mathematical models for DG are required. In addition, wind electric and photovoltaic systems require special models because of the random nature of their output. One method to study the performance of wind energy and photovoltaic systems is to calculate the instantaneous power output and integrate it over the period of interest. However, this method requires hourly meteorological data that are not readily available for long periods of time. Analytical

expressions are available to generate meteorological data, but they are site-specific [41]. Some approaches ignore the stochastic nature of wind speed and insolation and use average values of meteorological data but this may yield inaccurate results [42-43]. As a result, several researchers have developed probabilistic models to include the stochastic nature of the resources.

### 2.1.1 Wind Turbine Generation Model

Billinton and Gan [44] approach wind modeling using statistical techniques. They use time series techniques to model the wind speed. The power output of WTG is treated as a non-linear function of wind speed. Another approach is proposed by Watson, Landberg, and Halliday [45]. They use numerical weather prediction (NWP) model in conjunction with a physical power flow model and a statistical model as a means of predicting wind power output. Their method uses the simple assumption that the wind speed at time  $(t+x)$  is the same as it was at time  $t$ . Therefore, the accuracy of this forecasting method diminishes with increasing  $x$ .

The concept of using a probabilistic approach to model wind power is employed by Abouzahr and Ramakumar [46]. They use the Weibull distribution to model wind speed and using a transformation develop a probability density function of wind power output in terms of cut-in speed, rated speed, cut-out speed, rated power, and scale and shape parameters. Their method is useful because it eliminates the need for a large amount of meteorological data and it can be applied to any site. However, a slight drawback of this work is the fact that a linear relationship is used to represent the power output of WTG between cut-in and rated wind speeds. As a result, Karaki, Chedid, and

Ramadan [47] improve the accuracy of this approach by considering WTG power output as a non-linear function between cut-in and rated wind speeds. A parameter “ $m$ ” is introduced in the power output model to represent the non-linear output characteristic curve when WTG operates between cut-in and rated speeds.

Shuhui, Wunsch, O’Hair, and Giesselmann [48] present a technique to estimate the wind power output. They gather data from two different field tests to develop a neural network based prediction of power produced by wind turbine generation. The inputs used in this work are ten minute average wind velocity and direction from two field tests. The results indicate that neural networks can be used to estimate wind power generation. The results also show that the influence of wind velocity is much higher than the influence of wind direction.

Several approaches have been proposed to develop a dynamic model for wind turbine generation [49]. For example, Usaola and Ledesma [50] study the dynamic incidence of wind turbines in networks with high wind penetration. They study wind turbine generation under low load and high wind penetration conditions in order to ascertain a secure dynamic operation. They develop dynamic equations for the mechanical system by employing classical rotational dynamics. They also discuss a model for fixed speed devices and for doubly fed induction generator. Discussions of the control system in terms of torque control, reactive power control, and control strategy are also mentioned in this work.

International Council on Large Electric Systems (CIGRE) [51] also studied the WTG dynamic model. The purpose of this effort is to study power system dynamics in the transient stability range. They develop rotor dynamic power, mechanical torque, and

generator models to study the dynamic behavior of WTG. They discuss steady state and dynamic models to evaluate the performance and control of WTG. Control of reactive power, pitch regulation, torque control, and control strategy are developed and discussed in this work. This work serves as the first step to develop appropriate models and simulation technique for studying power system dynamics and the effect of the introduction of WTG and other distributed generation technologies.

### 2.1.2 Microturbine Model

Output of a microturbine is not stochastic in nature and it depends on the fuel flow rate. Not much published work is available on this topic.

Etezadi-Amoli and Choma [52] study the performance characteristics of a microturbine driven generator. They develop a model for microturbine power output based on the ideal law gas and the model is expressed in terms of fuel flow rate, fuel pressure, and temperature. Lasseter [53] studies dynamic models for microturbines. He develops dynamic expressions in terms of mechanical output to represent the performance of a microturbine. CIGRE [see reference 51] also investigates the dynamic behavior of microturbines.

### 2.1.3 Photovoltaic Systems Model

Young, Woo and Munro [54] present a method to model solar radiation. Their objective is to develop the radiation model under clear sky condition and then modify the radiation thus obtained through various cloud models. As a result, radiation under clear sky conditions and radiation under cloudy sky conditions were both considered. For



cloudy skies, two sets of radiation models that incorporated the cloud effect were developed: models using total cloud amount and models using a cloud layer approach. The results indicate that incident solar radiation (insolation) can be estimated by a total cloud model and cloud layer model. However, their method involves statistical techniques. Therefore, a large amount of data is required to develop the insolation model and the model can be used only for the Arctic location where the meteorological data are collected in this study.

Yaramanoglu, Brinsfield, and Muller [55] present a technique to estimate insolation by using stochastically generated cloud cover data. They treat cloud cover data as a random variable. The main objective of this work is to find the appropriate probability distribution for representing the cloud cover. Several insolation data sets including cloud cover are observed from two different locations. The result shows that Beta Distribution is the best fit for cloud cover data.

Abouzahr and Ramakumar [56] develop PV model by applying probabilistic techniques. The stochastic nature of insolation is included in their model. The PV power output is expressed in terms of maximum power and a random variable that accounts for cloud cover during that time. The random variable, which accounts for cloud cover is modeled using Beta Distribution. Once again, their work eliminates the need for a large amount of meteorological data.

Jewell and Ramakumar [57] introduce a work related to moving clouds. They investigate the effect of moving clouds on electric utilities with dispersed photovoltaic generation. They develop a cloud pattern and describe it in terms of: size of individual cloud, shape of individual cloud, percent of sky covered by clouds, speed and direction of

cloud movement, optical transmission of clouds, and variation in optical properties from the center to the edge of clouds. Simulation results show that cumulus clouds caused only very small changes in PV generation while squall line or similar pattern caused the largest changes during the summer season. This work can be used to study the actual effect of dispersed photovoltaic generation on utility systems.

Several approaches have been used to develop a dynamic model for PV. For example, CIGRE [see reference 51] develops a PV model for studying the influence of PV under transient stability condition. Ujiie, Izumi, Yokoyama, and Haneyoshi [58] also study the dynamic characteristic of photovoltaic systems. The purpose of this work is to estimate the static characteristics of PV from the dynamic ones. They develop the dynamic characteristics by making a momentary short-circuit of the PV system. Then, the authors propose a new approach, momentarily short calibration method, to obtain the maximum power point. Generally, maximum power point tracking (MPPT) control methods are based on static characteristics. But, this new method is based on dynamic characteristics. Simulation results show that static characteristic can be obtained from dynamic characteristics by momentarily short calibration method.

#### 2.1.4 Fuel Cell Systems Model

Most of the major research work done thus far for study the dynamic behavior of fuel cell systems. For example, Padulles, Ault, and McDonald [59] discuss a dynamic model for fuel cell characteristics. They present an approach to model fuel cell dynamics for DG operation. The purpose of this work is to report on the modeling of the different plant subsystems in order to understand how such a plant will operate in the future. The

approach includes model characteristics, fuel cell stack model, power conditioning unit model, and plant control system model.

Lukas, Lee, and Ghezal-Ayagh [60-65] have presented detailed studies of the performance of molten carbonate fuel cells (MCFC). They also attempt to develop a dynamic model for MCFC. A dynamic model should include representation of all subsystems: direct reforming fuel cell stack, heat recovery including boiler and fuel preheating, cathode gas preparation including anode oxidizer, fuel processing, and power conversion unit (PCU). For each subsystem, an explicit set of differential equations were developed to describe its dynamic behavior. Then, the authors attempt to make the set of differential equations simpler by introducing a reduced-order dynamic model for MCFC. Simulation results suggest that results using the reduced-order model match well with those obtained using the full-order model. They also develop an expression for total system DC current output in terms of fuel utilization, fuel flow rate, and total number of cells. Their work can be used to study and describe the behavior of MCFC under load changes conditions.

Hatziadoniu, Lobo, Pourboghrat, and Daneshdoost [66] also study a dynamic model for fuel cell generator. They propose a reduced-order dynamic model for a grid-connected fuel-cell power plant. The purpose of this work is to investigate the nature and behavior of fuel cell power plants introduced in a utility system. A linearized dynamic model to represent the fuel cell, network, and inverter control are derived in this work. The influences of generation mix, power controller bandwidth, and transient stability are simulated. The results indicate that a simplified dynamic model can be used to obtain a

preliminary assessment of the impact of fuel cell power plants on system dynamic and transient stability.

Several other groups have studied other types of fuel cell systems. For example, Hall and Colclaser [67] discuss a dynamic model for simulating the transient operation of a tubular solid oxide fuel cell (SOFC). Their overall model includes models for electrochemical, thermal, and mass flow that affect SOFC electrical output.

Electrochemical and thermal parts of the model were developed separately before they were combined to form the transient model. Simulation is conducted to study the transient electrical response of the fuel cell to a load change. The results confirm that this model can be used to study the transient behavior of SOFC. Correa, Farret, and Canha [68] present a dynamic model for representation, simulation, and evaluation of the proton exchange membrane fuel cells (PEMFC). Their models can be applied to evaluate the performance of small size generation systems using PEMFC.

For the other applications of fuel cell systems, Turner, Parten, Vines, Jones, and Maxwell [69] study the modeling of fuel cells for use in for electric vehicles. They develop and describe the power output in terms of fuel and oxidant mass flow rates.

## 2.2 Literature Review on the Quantification of Benefits of DG

Quantification of the benefits of DG is still in its early stages. Some of the published results in this area are summarized next.

### 2.2.1 Benefits of DG in terms of Capacity Credit and Energy Value

Capacity credit is an important measure of the performance of wind power plants that can assist utility planners to evaluate this resource. Several techniques have been used to calculate wind capacity credit. Milligan and Graham [70] study the integration of wind power into utility production cost models. Their approach involves probabilistic simulation techniques. It focuses on long-term measures of capacity credit that would help the utility to evaluate a potential future wind power plant. Two techniques are used and applied to arrive at capacity credit. The first technique is an enumerated probabilistic approach (EPA). This technique allows for the creation of an enumerated set of wind power series, each of which can be run in the production cost or reliability model. Another technique is a reduced enumerated probabilistic approach (REPA). This approach is based on a selective reduction in multiple model runs with a minimal loss of accuracy and is carried out in weighted and unweighted variations. The advantage of the REPA technique is that it is not as computationally demanding. However, the results will lack in some accuracy. Two production cost models are applied to simulate and measure wind capacity credit and the results are compared. The first model is the Elfin model. It uses the load-duration curve method for calculating production cost and reliability. This model has several options to include thermal and hydro generation. WTG can be modeled as time varying load-modifiers. The P plus model is another tool proposed for such studies. It allows for several thermal and hydro generator types, and unit commitment and dispatch occur in sequence by type. The results from simulation simply show that REPA method is not as accurate as EPA, but the loss of accuracy is small. However, the difference in results between Elfin and P plus models is slightly high

whereas the difference in loss of load hours (LOLH) is about 12% while expected unserved energy (EUE) difference is about 7%. The results from this work provide useful data such as effective load carrying capability (ELCC) that can be used to determine the wind plant capacity credit. However, the drawback of this research is that it requires long time wind data which is not usually available. Therefore, only a single year of wind data is used to calculate the state transition matrices and that may lead to inaccurate results.

Hoff [71] presents a method to calculate the values of PV to a utility system. He uses the performance data gathered from the PV plant in California for a period of three years. The values are divided into two categories: energy and capacity value. Energy value is calculated incrementally and varies with the load. A load duration curve is used as a tool to assist in the evaluation process. Capacity value is calculated by multiplying shortage value with the load carrying capability (LCC). The shortage value is the dollar value of an increment of perfectly reliable capacity that is obtained by evaluating the generation system reliability without PV. LCC is determined by calculating loss of load probability (LOLP) without PV and then re-calculating LOLP with the load increased until LOLP reaches its previous value. The resulting increase in load is the LCC. The results show that PV plant power output provides a good match with peak load thus giving the plant a high value. However, his method requires data for extended times that may not be available.

Shugar [72] studies the benefits of distributed grid-connected PV generation. His objective is to develop a methodology to evaluate cost saving applications of PV generation strategically sited to offset utility distribution capacity costs. Hourly load and

PV power output are collected from the field and are used to evaluate the benefits of PV. Once again, historical data for long periods of time are required in this study. Transmission and distribution benefits, system energy value, generation capacity value, system transmission capacity value, electrical loss savings, reactive power value, reliability benefits, and environmental benefits are considered as benefits. The results suggest that PV can provide significant benefits to the utility.

### 2.2.2 Benefits of DG in terms of Voltage Support and Line Loss Reduction

Chowdhury and Sawab [73] present the benefits of distributed PV generation in radial distribution networks. Their objective is to examine the value of PV systems in terms of voltage support, loss reduction and reduction in peak demand. Data on outputs of PV power plants and load data are collected from field tests. Therefore, this study requires a large amount of data to evaluate the loss reduction and voltage correction. A voltage index (VI) is used for the purpose of quantifying the effectiveness of voltage correction in the system. As a result, a lower VI implies a better voltage profile along the feeder. The results clearly show that PV can improve voltage index and also reduce line losses. Results from economic evaluations further indicate that PV can provide valuable service to the utility if they are introduced with proper planning.

Hoff and Shugar [74-75] discuss the value of grid-support in reducing distribution system losses. Their objective is to evaluate loss reduction for the entire feeder. Their simple method deals with feeder loss saving, transformer loss saving, and total energy loss saving. They also discuss the determination of optimal plant size, the determination of optimal plant distribution along a feeder, and the determination of optimal feeder

configuration. The results show that total savings is quite attractive for PV plant investment. They also study the economic value to substation transformer. The objective is to determine if PV systems can reduce the transformer temperature. The temperature reduction can be converted to allowable load increase and then to years of deferral of investments. The number of years of deferral is calculated by determining the PV plant's reduction in peak load and dividing it by projected load growth. The authors employ the model to estimate transformer hottest-spot temperature in this study. The results show that PV provides value to substation transformer. However, it should be pointed that PV plant output data, load data, and distribution system characteristics from the field are used for both studies. Therefore, their results are site-specific.

Ijumba, Jimoh, and Nkabinde [76] study the effects of distributed generation on distribution network performance. In their method, DG is compared with the shifting of transformer towards load center for its effectiveness in maintaining voltage levels, reducing losses and improving the system efficiency of a distribution network. The distribution network is simulated by using ERACS computer software. The load is increased from 10% to 200%, and at each loading level, a load flow analysis is carried out to determine voltage levels and line losses. The results show that DG is more effective in improving the overall network performance at increased loadings. The results also show significant line loss reduction as compared to base case and to the case of shifting transformer towards the load center technique.

Chiradeja and Ramakumar [77-78] study the benefits of DG in terms of loss reduction and voltage support. They apply DG along a simple distribution line to evaluate line loss reduction and voltage support. They find that DG can reduce line loss



and improve voltage profile of the system. The results show that loss reduction increases as the DG is installed closer and closer to the load and as the fraction of the load power supplied by DG increases. The amount of voltage support depends on the location of DG with respect to the load, power factor, line impedance, and the fraction of the load supplied by DG. However, their work is limited to a simple case study. In a follow-up work, they present a probabilistic approach based on convolution technique to quantify voltage profile improvement in the case of wind turbine generation used as DG. The influence of varying load power factors, and ratings and locations of WTG are discussed in this work. They quantify this benefit in terms of the mean and variance of the load voltage. The results show that the expected value of load voltage increases with the inclusion of WTG. The amount of this increase goes up as the WTG is moved closer to the load point and as the WTG rating increases. A better wind regime also leads to an improved expected value of load voltage. The variance also shows improvement with the introduction of WTG. This indicates that load voltage has less variability and stays closer to the expected value as compared to the system without distributed WTG.

Caire, Retiere, Martino, Andrieu, and Hadjsaid [79] also present a method to quantify the benefit of DG in terms of voltage profile improvement. They propose an index for voltage profile and then study the variation of voltage profile in medium-voltage (MV) networks when DG is connected to low-voltage (LV) distribution networks. The results show that DG does not have a significant relative impact on MV voltage profile but it could become significant under some operating conditions. They also suggest that if a large amount of DG is connected to a distribution system, new network control strategies have to be designed and implemented to ensure power quality

and a safe, reliable operation of the network. However, the drawback of this work is the fact that their voltage profile index considers only the voltages at each bus and does not consider the amount and importance of different loads. Therefore, their model does not allow the possibility of a low load bus with critical load to have a strong impact on the improvement index.

### 2.2.3 Benefits of DG in terms of System Reliability Improvement

An improvement in overall system reliability is an important potential benefit offered by distributed generation. However, this benefit is not a main focus of this research. Therefore, only some of the system reliability improvement approaches are reviewed in this section.

Deshmukh and Ramakumar [80] study the reliability analysis of combined wind-electric conversion systems (WECS) and conventional generating systems. Their objective is to discuss two probabilistic models for WECS and study the impact of the parameters involved on the overall system reliability when WECS are included in utility grids. The first model is based on a suitable wind speed distribution. The authors use the Weibull distribution to model wind speed. They suggest that the number of capacity states needed in the model depends on the type of wind data available, characteristics of electrical components, the nature of wind regime, and the accuracy desired. The other model is based on the Markov approach. This model is based on hourly integer mean wind speed data collected over a long period of time. The results from this also indicate that the effect of WECS is not significant if the peak load on the system is lower than the conventional generation capacity. On the other hand, if the peak load exceeds the

conventional generation capacity, the expected loss of load sharply increases. This is due to the low confidence one can place on the WECS output.

Billinton and Chowdhury [81] present an energy-based model to study the incorporation of WECS into a conventional generation system. They employ a conventional generation model, load model and WECS model. WECS is represented by a multi-state model where the number of states depends on the accuracy desired, nature of wind, and amount of wind data available. WECS model used in this paper includes the forced outage rate (FOR) of wind energy systems in order to determine the impact of maintenance strategies. The expected energy not served (EENS) is used as the reliability index in this study. The results show that EENS increases slightly as WECS FOR increases and the system EENS decreases as the amount of penetration by WECS increases. However, the margin of reduction in EENS decreases as the WECS penetration into system decreases. In addition, the amount of peak load also impacts system EENS. EENS increases sharply as the peak load approaches and exceed the conventional generation capacity. The effect of WECS on IEEE-RTS (reliability test system) is also considered in this work. The results confirm that system reliability improves slightly for higher penetration and system EENS slightly increases as WECS FOR increases.

Further work on adequacy evaluation of generating systems including wind energy has been undertaken by Billinton, Chen, and Ghajar [82]. They present a sequential Monte Carlo simulation technique for reliability evaluation of generating system containing WECS. An auto-regressive moving average (ARMA) time series analysis based on F-criterion is used to simulate the wind speed. The basic simulation is

started by creating a capacity model for conventional generating facilities by using a chronological simulation technique. Then, a capacity model is constructed by using time series techniques. A combined system capacity model is then obtained. The results from case studies show that WECS improves the overall system reliability. However, WECS does not provide the degree of improvement as the conventional unit additions do.

Ubeda and Rodriguez Garcia [83] evaluate the effect of connecting wind energy generators to the electric supply system and particularly to distribution networks. They use the auto-regressive model to represent wind speed and the exponential distribution is used to describe the time-to-fail of any WTG. The wind energy production and network (WEPN) model is used in simulation studies. WEPN is based on the IEEE RTS-79. The results show a slight increase in system reliability when wind generation is connected into the system. The degree of reliability improvement also depends on the location of wind generators in the system.

Brown and Freeman [84] analyze the reliability impact of distributed generation. They present a reliability modeling technique for DG on distribution systems and discuss backup applications, peak shaving applications, and net metering applications and apply them to both radial and networks models. DG backup generators for radial system can be modeled using a transfer switch and the DG unit can be treated as a voltage source. Since DG unit does not start instantaneously, it can be modeled by setting switching time of the transfer switch equal to the starting time of DG unit. DG online net metering for radial system can be modeled as a negative load that injects real and reactive power into the system independent of system voltage. DG units in networks can be modeled as constant power voltage sources. The results from a utility system show that DG can improve the

system reliability by reducing System Average Interruption Duration Index (SAIDI). It can effectively transfer load to other feeders after a fault occurs, resulting in significant improvement in system reliability.

Reliability cost worth is another approach to evaluate system reliability improvement. Billinton and Wang [85] present an analytical approach and a time sequential Monte Carlo simulation technique for evaluating customer interruption cost in radial distribution networks. The results from both approaches are then compared. Load model, equipment model, and customer sector interruption cost model are required to evaluate customer interruption cost indices. A two-state model is used to represent equipment while the average load at each point is used as load model. The process also recognizes the overlap that can occur in the different equipment failure/repair cycles. Customer surveys are used to estimate the sector damage function (SCDF). Surveys show the cost of an interruption, and magnitude and duration of the interruption. Reliability indices such as expected interruption cost (ECOST), interrupted energy assessment rate (IEAR), and EENS are calculated by computer programs. The results show that the analytical technique is fast and provides results comparable to simulation approach. In addition, the effect of overlapping time is considered and compared and it is found that if the system is small and restoration times are short, the overlapping time could be ignored. However, the overlapping time should be taken into account if the distribution system is large and restoration times are relatively long.

Karki and Billinton [86] discuss the reliability/cost implications of wind energy and PV systems in small isolated power systems (SIPS). Their objective is to help system planners decide on installation sites, operating strategies, and selection of energy

types when wind energy and PV systems are utilized in SIPS. The adequacy assessment of SIPS containing wind energy and/or PV systems is developed in this work. A WATGEN computer program is used to generate hourly weather data from monthly mean values available at a given location. Then, WATSUN-PV decomposes the hourly global radiation data into diffuse, beam, and reflected components and evaluates the total radiation incident on a tilted array surface. PV power output is calculated based on radiation data. Wind speed is modeled by using time series. The electrical output is then calculated by combining the wind speed data and power curve of WTG. A Monte Carlo simulation technique developed for conventional sources, which generates both conventional risk and well-being indices, is modified to include PV and wind energy systems. The generation model created by combining the power available from all the generating units is compared with the hourly load in order to identify the healthy and risk states. The fuel energy saving due to renewable energy sources is also under consideration in this study. Four cases are considered and compared to the base system. The results show that system health increases for each capacity addition. However, the marginal increases in system reliability decreases with further renewable additions. The results also indicate that conventional sources yield higher system reliability than renewable sources. However, renewable sources play an important role in reducing the fuel cost. The results further suggest that the desired system reliability may not be achieved if only renewable energy is added to the base system to meet the growth in load demand.

### 2.3 Literature Review on Economic Considerations

Generally, capital investment for DG is relatively high as compared to conventional technologies. Therefore, analysis of the economics of DG is crucial to increase the potential of DG penetration. Some of the efforts involved in this area are summarized next.

Karagiannis [87] studies an economic approach for wind energy system investments. The objective is to evaluate the potential of investments in wind energy. The net present value (NPV), internal rate of return (IRR), discounted payback period (DPB), and benefit-to-cost ratio (BCR) are used as the economic indicators in this approach. The parameters required for economic analysis are the investment cost, O&M cost, sales price of the produced electrical energy, and economic lifecycle of the investment. The results indicate that wind energy offers a very high value for the return-on-equity (ROE) and a DPB of less than 5 years if wind farm is connected to the medium-voltage grid. However, if a wind farm is connected to HV grid, it requires high subsidies to be economically viable.

Ramakumar, Butler, Rodriguez, and Venkata [88] study the economics of advanced energy technologies. They present economic considerations for a wide variety of resources with particular emphasis on renewable technologies including PV, solar-thermal, WECS, biomass, hydro, tidal, and wave energy. The models to calculate cost of energy and reliability indices are also discussed in this paper. For each of the technologies, energy cost is calculated based on total capital cost, amortization period, capacity factor, interest rate, and operation and maintenance cost (O&M). They also discuss integrated renewable energy systems (IRES). They define IRES as a system that

utilizes two or more renewable energy resources and energy conversion/utilization technologies to supply a variety of energy and other needs. They have developed a knowledge-based approach to design IRES. Some case studies are also presented in this paper.

Lamberth and Lepley [89] study the value of PV systems in terms of economics. They gather solar radiation from the field and use PVFORM computer program to develop a PV model. Their results confirm that there is a value to distributed PV generation throughout the utility distribution system. They also find that PV systems would usually have more value if distributed throughout the system rather than installed at a central site.

At the present time, there is very little literature on approaches to quantify the benefits of distributed generation in terms of voltage profile improvement, electrical line loss reduction, and environmental impact reduction taken together, including the development of a set of benefit indices. A systematic approach is needed to analyze different scenarios and arrive at best locations and ratings of DG for inclusion in a distribution system. This is the focus and motivation for the research work documented in this dissertation.



## CHAPTER III

### DISTRIBUTED GENERATION AND LOAD MODELS

This chapter describes models appropriate for some of the distributed generation technologies and the load model used in this research. They include models for wind turbine generators, microturbine systems, photovoltaic systems, fuel cell systems, and load demand. The associated mathematical expressions are documented to represent the nature and characteristics of DG and load. Basic descriptions of the technologies involved in WTG, microturbines, PV, and fuel cells are also included in this chapter.

#### 3.1 Wind Turbine Generation

##### 3.1.1 Description of the Technology

Wind energy system is a very good candidate for distributed generation. In fact, in terms of economics, wind energy is rapidly becoming the most competitive among all the renewable energy technologies [see reference 15]. Wind turbine generators (WTG) generate electrical energy by converting the energy in moving air (wind) into mechanical energy first and then to AC electrical energy. The output of a WTG will be fed to the utility grid at the subtransmission or distribution level. A general scheme of a WTG system is shown in Figure 8. In a typical unit, the blades are attached to an axle

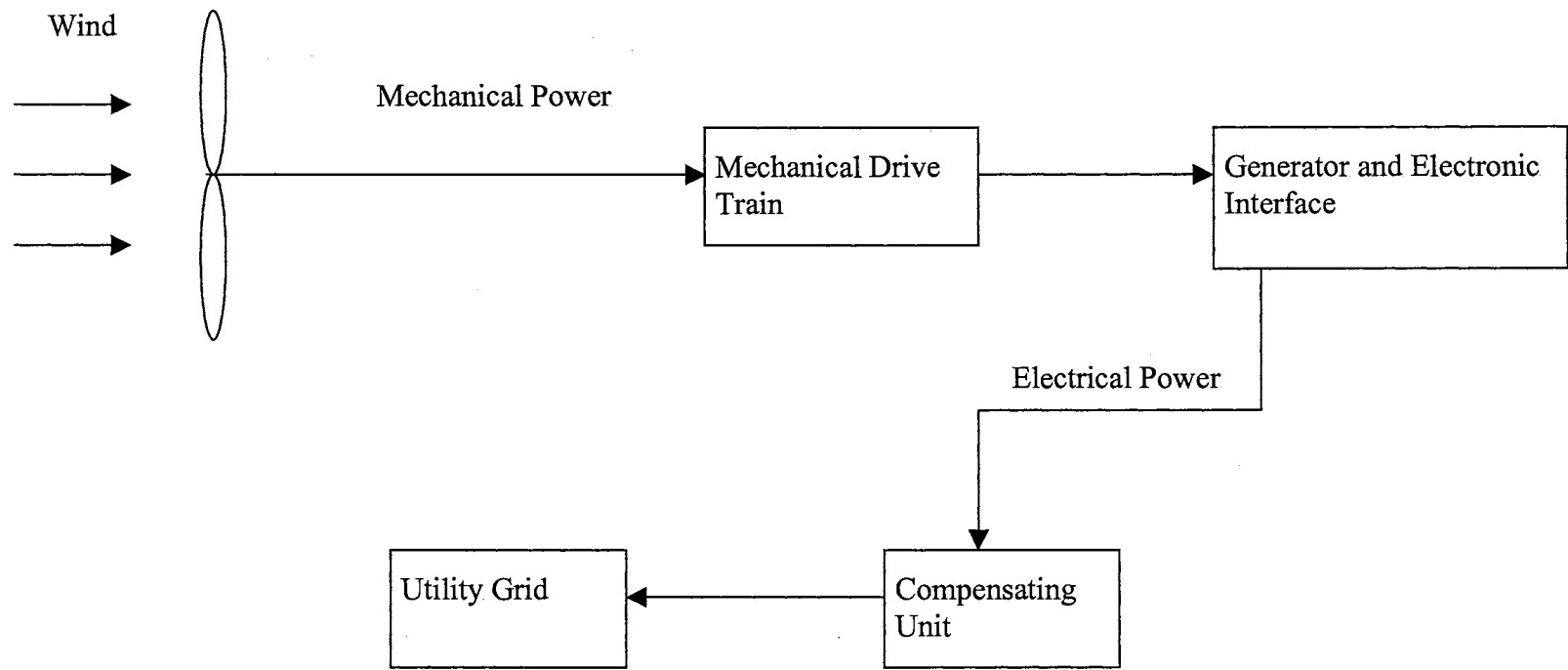
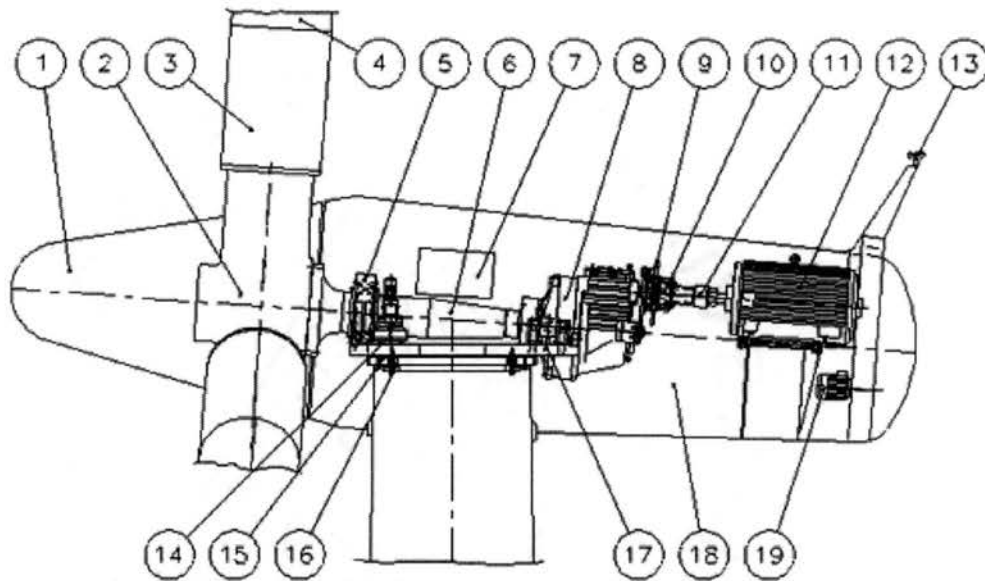


Figure 8. A Typical Schematic of Wind Turbine Generation System

that is coupled to a mechanical drive train. The mechanical drive train usually includes a gear box that couples the low speed turbine to a generator operating at a higher speed. The electrical generator converts mechanical energy into electrical energy. The generator can operate at a constant-speed or a nearly-constant-speed or variable-speed. An associated compensating unit generally includes power factor correction devices.

Typical, large wind turbine units employ 120 to 200 feet tall towers. The diameter of the rotor and blades can reach more than 200 feet. In general, wind turbine units consist of three main parts: the tower, the blades, and the nacelle. The nacelle is a box behind the blades where the mechanical energy is converted to electricity. The major components of a WTG are shown in Figure 9.

Typically, two basic types of aeroturbines are in use for WTG: Horizontal-Axis Wind Turbine (HAWT) and Vertical-Axis Wind Turbine (VAWT) [90-91]. The HAWT requires a yaw drive mechanism to direct it into the wind. The symmetry of vertical-axis allows VAWT to catch wind from any directions. Thus, VAWT requires no yaw control. Depending on the electrical generation technology employed, the turbines are operated in one of three modes: constant-speed with pitch control, nearly constant-speed, and variable-speed. The nearly constant-speed is commonly used because of its simplicity. However, the many disadvantages of this operating mode include lower aerodynamic efficiencies without pitch control, low power factor, and excessive reactive power demands from the grid. As a result, after years of operation and gathering data, the variable-speed mode is preferred at present. The primary goals of the variable speed operating mode are to maximize wind energy capture and reduce stresses on the blades, tower, and other components [see reference 11].



- |                   |                            |
|-------------------|----------------------------|
| 1. Spinner        | 11. Coupling               |
| 2. Rotor hub      | 12. Generator              |
| 3. Blade Extender | 13. Meteorological sensors |
| 4. Blade          | 14. Yaw gearbox            |
| 5. Main bearing   | 15. Yaw ring               |
| 6. Main shaft     | 16. Yaw bearing            |
| 7. Top controller | 17. Nacelle bedplate       |
| 8. Gear box       | 18. Canopy                 |
| 9. Brake disc     | 19. Generator fan          |
| 10. Brake caliper |                            |

Figure 9. Major Components of Wind Turbine Generation [Source: [www.bonus.dk](http://www.bonus.dk), April 2002]

By its nature, wind is highly variable and site-specific. The geographical site location is very important because the power output is highly dependent on the prevailing wind regime. The ideal site for WTG is high, clear, and wide area in order to avoid any obstructions such as trees. Before determining the type of WTG to be installed, many factors from a site have to be considered very carefully. These factors include mean wind speed, variance, gusting pattern, and directional characteristics.

### 3.1.2 Wind Speed Model

As discussed earlier, wind is highly variable and site-specific. Wind speed has instantaneous, hourly, daily, yearly, and seasonal variations. Thus, wind speed can be considered as a continuous random variable, with an appropriate statistical distribution. Several statistical distributions have been used to model wind speed. However, the Weibull distribution is widely accepted for wind speed modeling [see reference 46]. In order to adjust its shape to fit the data, two parameters- scale parameter ( $\alpha_w$ ) and shape parameter ( $\beta_w$ ) are employed. The corresponding probability density function (pdf) is expressed as follows [92].

$$f_U(u) = \frac{\beta_w}{\alpha_w \beta_w} u^{\beta_w-1} \exp \left[ - \left( \frac{u}{\alpha_w} \right)^{\beta_w} \right] \quad 3.1.2.1$$

where  $u$  is the wind speed. The corresponding cumulative distribution function (cdf) is given by:

$$F_U(u) = 1 - \exp\left[-\left(\frac{u}{\alpha_w}\right)^{\beta_w}\right] \quad 3.1.2.2$$

The scale and shape parameters are related to mean ( $\mu_w$ ) and variance ( $\sigma_w^2$ ) of wind speed as shown below:

$$\mu_w = \alpha_w \Gamma\left(1 + \frac{1}{\beta_w}\right) \quad 3.1.2.3$$

$$\sigma_w^2 = \alpha_w^2 \left[ \Gamma\left(1 + \frac{2}{\beta_w}\right) - \Gamma^2\left(1 + \frac{1}{\beta_w}\right) \right] \quad 3.1.2.4$$

where  $\Gamma$  is the gamma function and is given by:

$$\Gamma(x) = \int_0^{\infty} t^{x-1} e^{-t} dt \quad , x > 0 \quad 3.1.2.5$$

For integer value of  $x$ , equation (3.1.2.5) becomes:

$$\Gamma(x) = (x-1)! \quad 3.1.2.6$$

and

$$\Gamma(x+1) = x\Gamma(x) \quad 3.1.2.7$$

### 3.1.3 Wind Turbine Generator Power Output Model

The rotor aerodynamic power output of wind turbine, under smooth wind flow condition is given as [93-94]:

$$P_m = 0.5\rho A_w u^3 C_P(\lambda, \gamma) \quad 3.1.3.1$$

where  $P_m$  is mechanical power output of wind turbine,  $\rho$  is density of air,  $A_w$  is rotor area,  $u$  is wind speed,  $C_P$  is performance coefficient which is a function of,  $\lambda$ , tip speed ratio and,  $\gamma$ , pitch angle.

The tip speed ratio is defined as:

$$\lambda = \frac{\omega R_w}{u} \quad 3.1.3.2$$

where  $\omega$  is the rotational angular speed of blades and  $R_w$  is the radius of the rotor.

The performance coefficient, which depends on tip speed ratio and pitch angle, is different for each wind turbine. Usually, it can be obtained experimentally from the field. However, some analytical approximate models have been developed. Ultimately, the electrical power output obtained can be expressed as a function of wind speed. The power output varies in a non-linear fashion with the wind speed for turbine operation between cut-in and rated wind speeds. The relationship between electrical power output and wind speed is shown graphically in Figure 10 and is expressed by equation (3.1.3.3).

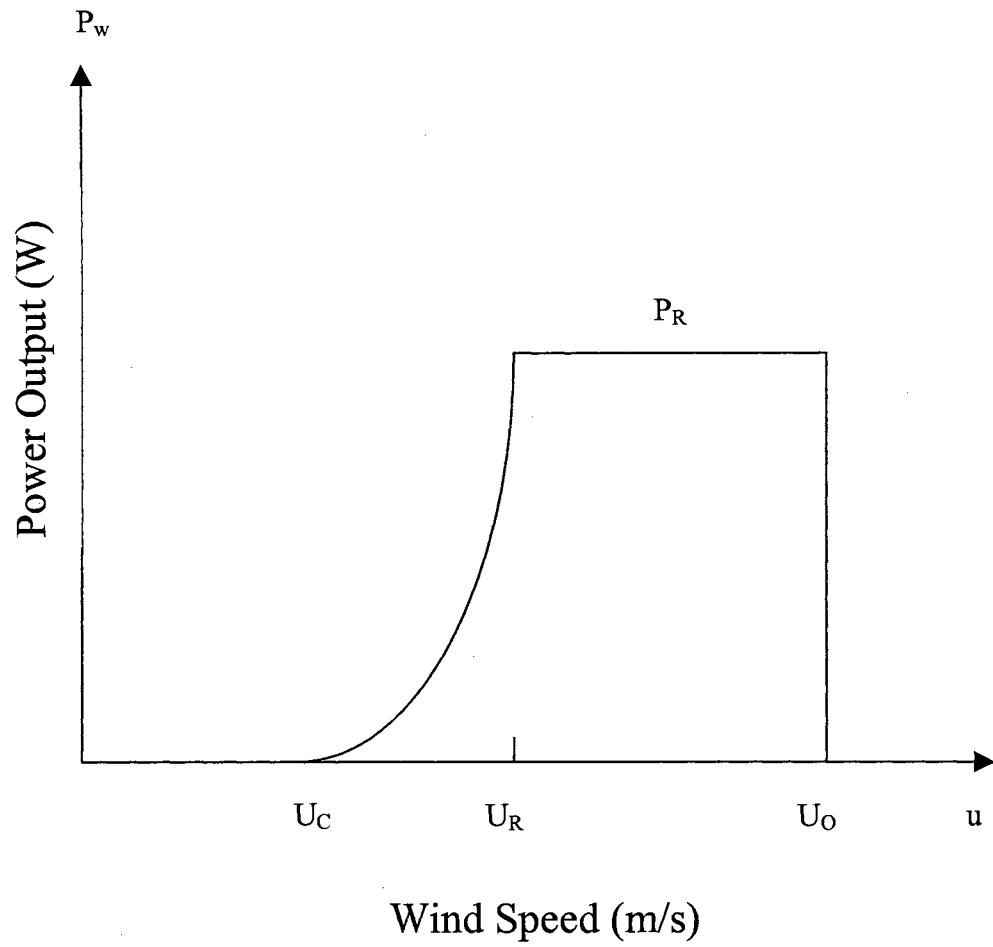


Figure 10. A Typical WTG Output vs. Wind Speed Characteristic



$$P_w(u) = \begin{cases} 0 & 0 \leq u \leq U_C \\ a + bu^m & U_C \leq u \leq U_R \\ P_R & U_R \leq u \leq U_O \\ 0 & u > U_O \end{cases} \quad 3.1.3.3$$

where  $P_w$  is the electrical power output,  $U_C$  is the cut-in speed,  $U_R$  is the rated speed,  $U_O$  is the cut-off speed,  $m$  is the order of power output characteristic curve, and  $P_R$  is the rated power of WTG.

The most representative value for  $m$  has been found to be 2.28 and this value will be used throughout this analysis. The constants  $a$  and  $b$  can be expressed in terms of other parameters as follows.

$$a = \frac{P_R U_C^{2.28}}{U_C^{2.28} - U_R^{2.28}} \quad 3.1.3.4$$

$$b = \frac{P_R}{U_R^{2.28} - U_C^{2.28}} \quad 3.1.3.5$$

Equation (3.1.3.3) can be rewritten in terms of cut-in speed, rated speed, cut-off speed, rated power, and  $m$  (equal to 2.28) as:

$$p_w(u) = \begin{cases} 0 & 0 \leq u \leq U_c \\ \frac{P_R(u^{2.28} - U_c^{2.28})}{U_R^{2.28} - U_c^{2.28}} & U_c \leq u \leq U_R \\ P_R & U_R \leq u \leq U_o \\ 0 & u > U_o \end{cases} \quad 3.1.3.6$$

The probability density function (pdf) for the electrical power output ( $P_w$ ) can be derived using equations (3.1.2.1) and (3.1.3.6) by the application of the transformation theorem and the result leads to [95-96]:

$$f_{P_w}(p_w) = \begin{cases} (1 - F_U(u_o) + F_U(u_c))\delta(p_w) & p_w = 0 \\ \left( \frac{\beta_w}{\alpha_w \beta_w} \right) \left( \frac{U_R^{2.28} - U_c^{2.28}}{2.28 P_R} \right) \left( \frac{p_w}{P_R} (U_R^{2.28} - U_c^{2.28}) + U_c^{2.28} \right)^{\frac{\beta_w - 2.28}{2.28}} \times \\ \exp \left( - \left( \frac{\left( \frac{p_w}{P_R} (U_R^{2.28} - U_c^{2.28}) + U_c^{2.28} \right)^{\frac{1}{2.28}} \beta_w}{\alpha_w} \right) \right) & 0 < p_w < P_R \\ (F_U(u_o) - F_U(u_R))\delta(p_w - P_R) & p_w = P_R \end{cases}$$

3.1.3.7

## 3.2 Microturbine Systems

### 3.2.1 Description of the Technology

Microturbine is another promising candidate for distributed generation. The systems under development for DG run at very high speeds (80,000 rpm or higher) on air bearings and have multi-fuel capability (natural gas, propane, diesel, kerosene, CNG/LNG, methane, ethanol, and alcohol) [see reference 3]. Their size and weight are smaller and lighter as compared to diesel units. Because of their modular nature, higher output capacities can be easily achieved with multiple installations via a single control point. Additional benefits of microturbines include long mean time between overhauls, short lead-time, and near-zero maintenance due to very few moving parts, and near-zero emissions (nitrogen oxide is less than 9 ppm, carbon monoxide and hydrocarbon are 40 ppm and 9 ppm respectively). Waste heat recovery can be used in combined heat and power system to achieve overall efficiencies as high as 60-80%.

A microturbine is composed of compressor, recuperator, combustor, turbine, generator, and inverter. Block diagram of a typical microturbine cycle is illustrated in Figure 11. Basically, microturbine operation starts with air brought in through the air inlet, heated through a heat exchanger called recuperator, compressed by a compressor and fed into a combustion chamber. The recuperator is a ceramic disk with holes that rotates slowly in front of the exhaust and the inlet to the combustion chamber. The exhaust gases heat the disk and in turn heats the compressed inlet air which increases the efficiency of combustion of fuel. The exhaust gases are then discharged to the environment or can be used to provide space heating and hot water cogeneration. In the

combustion chamber, air is mixed with fuel and burned in a continuous process. The high temperature gases are expanded in the turbine. The shaft turns at approximately 80,000 rpm and is coupled to a generator that provides a high frequency ac power output. A power electronic converter is used to convert the high frequency output into the required utility-grade 60 or 50 Hz AC using an intermediate dc link [see references 13 and 52].

### 3.2.2. Microturbine Power Output Model

Unlike wind and solar systems, the power output of microturbines can be scheduled. Typically, the power output depends on the fuel mass flow. As more fuel flows through the combustor, more heat and power are generated [see references 52 and 53]. Thus, the microturbine power output can be modeled in terms of fuel mass flow rate as shown below.

$$P_{mi} = (HV)\eta_t m_f \quad 3.2.2.1$$

where  $P_{mi}$  is microturbine power output (Btu/hr),  $HV$  is heating value of fuel (Btu/lb),  $\eta_t$  is the overall efficiency, and  $m_f$  is fuel mass flow rate (lb/hr).

By applying the ideal gas law to the equation (3.2.2.1), the power output can be expressed in terms of fuel volume flow rate, fuel pressure, and temperature as follows.

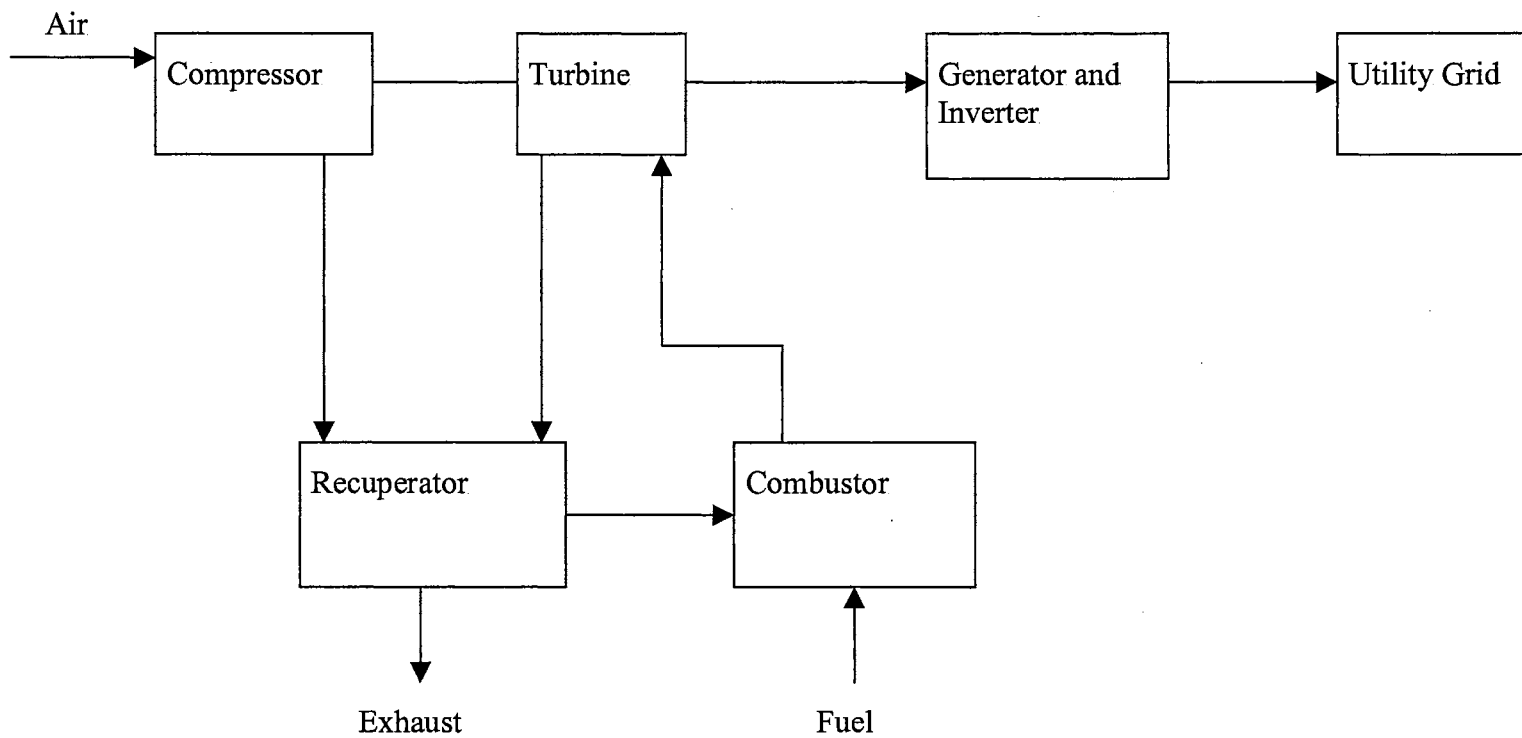


Figure 11. A Typical Microturbine Cycle

$$P_{mi} = Q_f (HV)_s \eta_t \left( \frac{PS}{PS_s} \right) \left( \frac{T_s}{T} \right) \quad 3.2.2.2$$

where  $Q_f$  is fuel volume flow rate ( $\text{ft}^3/\text{hr}$ ),  $(HV)_s$  is heating value of the fuel at standard pressure and temperature ( $\text{Btu}/\text{ft}^3$ ),  $PS$  is fuel pressure (psi),  $T$  is fuel temperature ( $^\circ\text{K}$ ),  $PS_s$  is standard pressure (psi), and  $T_s$  is the standard temperature ( $^\circ\text{K}$ ).

Expressing the power output of microturbines in kilowatts, equation (3.2.2.2) becomes [97]:

$$P_{out,mi} = (0.000293) Q_f (HV)_s \eta_t \left( \frac{PS}{PS_s} \right) \left( \frac{T_s}{T} \right) \quad 3.2.2.3$$

where  $P_{out,mi}$  is the microturbine output in kilowatts.

### 3.3 Photovoltaic Systems

#### 3.3.1 Description of the Technology

Photovoltaic (PV) systems convert incident solar radiation (insolation) directly to electricity. The advantages of PV include clean energy, absence of recurring fuel costs, high modularity, short lead time to design and install, and low operation and maintenance (O&M) cost due to absence of moving parts. These advantages make PV another ideally suited technology for distributed generation. PV ratings can range from a few watts to Megawatts and systems can be located and operated as central station power plants or as distributed generators throughout a large geographical area. As discussed earlier, PV

systems require large collection areas. In general, a land area of one hectare is required for an electrical output of 1 MW. In addition, the land area required will be even larger if the effect of inter-array shadowing is taken into account. However, technology development to increase PV efficiency is underway which will help to reduce the land area required in the future.

A solar cell is a well designed large- area p-n junction semiconductor diode with a solid metal contact in the bottom and a grid-type contact on the top [98-99]. It has an inherent built-in potential barrier that is capable of separating the electrons and holes that are generated by the absorption of light (photons) within the semiconductor. Incident photons having energies equal to or greater than the energy gap of the semiconductor material are absorbed to generate electron-hole pairs. The transport of minority charge carriers across the junction and through the external circuit provides the electrical output.

The output of a PV system strongly depends on external factors such as cloud cover, location, the amount of insolation, and season. Since the output of each PV cell is quite small, several cells have to be connected together in a series-parallel configuration in order to get the desired voltage and power outputs. A power electronic converter is required to convert its dc output to ac output. Typical schematic of a PV system is illustrated in Figure 12.

There are two basic types of PV systems: flat plate and concentrating [see reference 18]. Simplest flat plate systems are stationary with fixed tilt. However, tilt can be periodically adjusted to capture more energy. Concentrating systems could have either point focus or line focus. Point focus systems require two-axis tracking while line focus requires only one-axis tracking. Concentrating systems are ideal for locations with

mostly clear skies throughout the year. However, they require larger land areas (2 to 2.5 times) in order to avoid the shadow of adjacent modules as compared to flat plate systems.

### 3.3.2 Insolation Model

As mentioned earlier, power output of a PV system depends on insolation. Therefore, an insolation model is required in order to evaluate the performance of a PV system. Several insolation models have been developed in the past. They include cloud model, probabilistic model, time-series model, and spectral model. However, cloud model has been widely accepted as a simple model to use. Beta distribution has been successfully used to model cloud cover [100]. The available insolation is expressed as a product of the maximum insolation and a random variable representing cloud cover as follows:

$$I_C = I_{\max} (1-t) \quad 3.3.2.1$$

where  $I_C$  is the insolation under cloud cover conditions,  $I_{\max}$  is the clear sky insolation, and  $t$  is a random variable representing the cloud cover. The corresponding probability density function (pdf) is given in terms of a scale parameter ( $\alpha_s$ ) and a shape parameter ( $\beta_s$ ) as follows.



Insolation

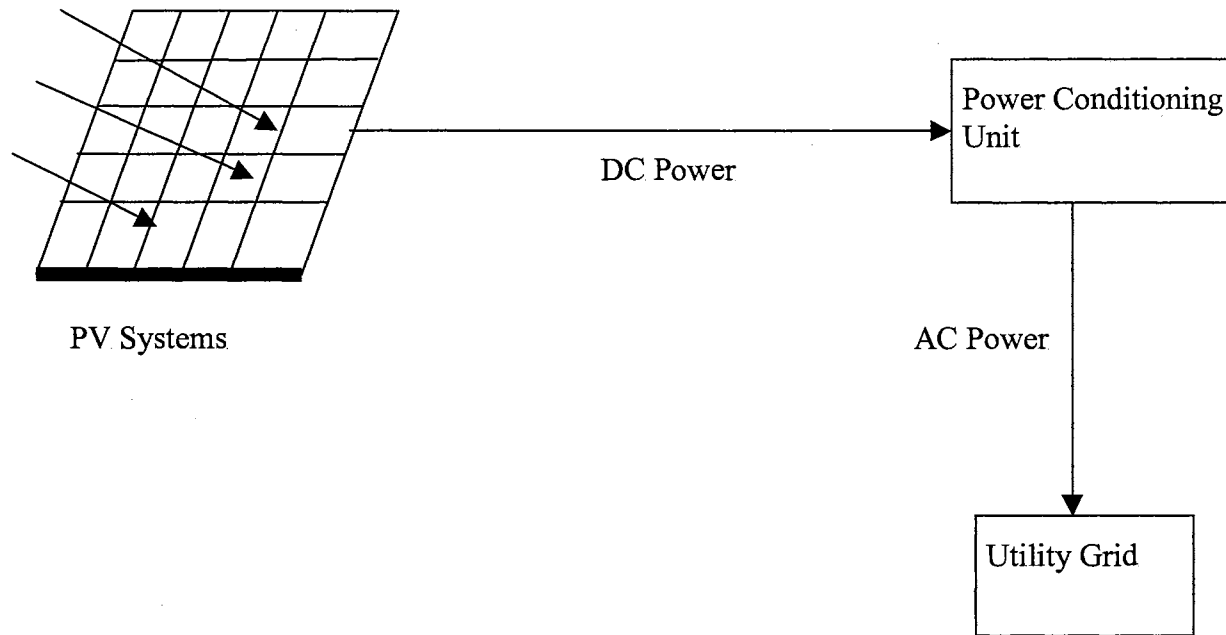


Figure 12. Typical Schematic of a PV System

$$f_T(t) = \begin{cases} \frac{t^{\alpha_s-1}(1-t)^{\beta_s-1}\Gamma(\alpha_s + \beta_s)}{\Gamma(\alpha_s)\Gamma(\beta_s)} & 0 \leq t \leq 1 \\ 0 & \text{Otherwise} \end{cases} \quad 3.3.2.2$$

where  $\alpha_s > 0$ ,  $\beta_s > 0$ , and  $\Gamma(x)$  is the gamma function given by equation (3.1.2.5) The scale and shape parameters can be obtained in terms of mean ( $\mu_s$ ) and variance ( $\sigma_s^2$ ) as shown below.

$$\alpha_s = \mu_s \left( \frac{\mu_s(1-\mu_s)}{\sigma_s^2} - 1 \right) - 1 \quad 3.3.2.3$$

$$\beta_s = (1-\mu_s) \left( \frac{\mu_s(1-\mu_s)}{\sigma_s^2} - 1 \right) - 1 \quad 3.3.2.4$$

By applying the transformation theorem in conjunction with equations (3.3.2.1) and (3.3.2.2), probability density function for available insolation can be expressed as follows.

$$f_{I_c}(ic) = \begin{cases} \left( \frac{1}{I_{\max}} \right) \left( 1 - \frac{ic}{I_{\max}} \right)^{\alpha_s-1} \left( \frac{ic}{I_{\max}} \right)^{\beta_s-1} \frac{\Gamma(\alpha_s + \beta_s)}{\Gamma(\alpha_s)\Gamma(\beta_s)} & 0 \leq ic \leq I_{\max} \\ 0 & \text{Otherwise} \end{cases} \quad 3.3.2.5$$

### 3.3.3 PV Power Output Model

A PV cell can be modeled in terms of a current source, a non-linear impedance representing the junction, and load resistance. Its equivalent circuit in its simplest form is shown in Figure 13. This simplified circuit model is derived from a more realistic model by making two key assumptions: (i) the intrinsic series resistance is ignored as small, and (ii) the intrinsic shunt resistance is ignored as very large. By applying Kirchhoff's laws to the equivalent circuit, the output (load) current can be expressed as:

$$I_{L,PV} = I_{S,PV} - I_{O,PV} \left( \exp\left(\frac{eV_{PV}}{kT}\right) - 1 \right) \quad 3.3.3.1$$

where  $I_{L,PV}$  is the load (output) current,  $I_{S,PV}$  is a constant-current source that depends on insolation,  $I_{O,PV}$  is the dark or saturation current,  $V_{PV}$  is the voltage across the junction,  $k$  is the Boltzmann constant, and  $T$  is the temperature in Kelvin.

The factors that influence PV power output are effective area of cell modules, insolation, cell conversion efficiency, and cell temperature. Typically, average efficiency is used and it is assumed to be constant. Neglecting temperature effect, the PV power output can be calculated using equation (3.3.3.2).

$$P_S = A_{PV} K_P I_C \eta_{PV} \quad 3.3.3.2$$

where  $A_{PV}$  is the effective area of cell module,  $K_P$  is the packing factor,  $\eta_{PV}$  is the average cell conversion efficiency.

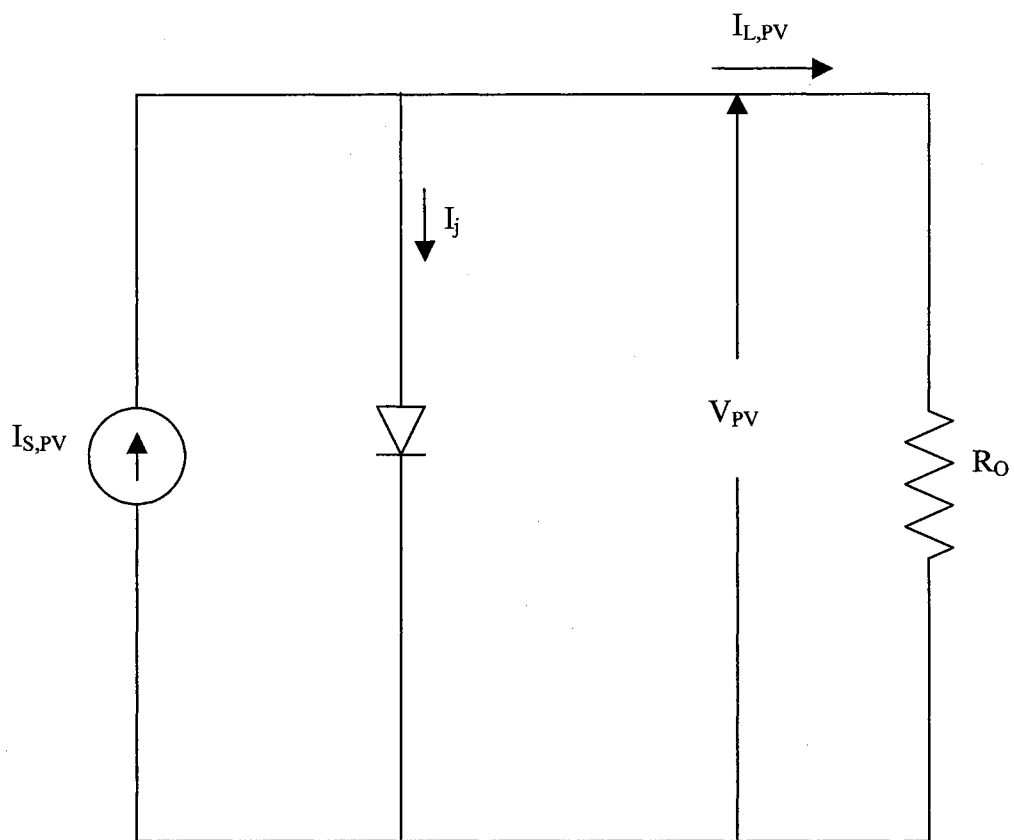


Figure 12. An Equivalent Circuit for Photovoltaic Cell

By substituting equation (3.3.2.1) into equation (3.3.3.2), the new expression for PV power output becomes:

$$\begin{aligned} P_S &= A_{PV} K_P I_{\max} (1-t) \eta_{PV} \\ &= P_{s\max} (1-t) \end{aligned} \quad 3.3.3.3$$

where  $P_{s\max}$  is the maximum power output under clear sky conditions and is given by:

$$P_{s\max} = A_{PV} K_P I_{\max} \eta_{PV} \quad 3.3.3.4$$

Since PV power output will be zero during night-time, it is important to consider the entire range of possible outputs including zero output. Considering only the daytime interval, the probability density function for the PV power output in terms of  $P_{s\max}$ , shape parameter, and scale parameter is obtained by applying the transformation theorem in conjunction with equations (3.3.2.2) and (3.3.3.3) as follows.

$$f_{P_s}(p_s) = \begin{cases} \frac{\Gamma(\alpha_s + \beta_s)}{\Gamma(\alpha_s) + \Gamma(\beta_s)} \left( \frac{1}{P_{s\max}} \right) \left( \frac{p_s}{P_{s\max}} \right)^{\beta_s - 1} \times & 0 < p_s \leq P_{s\max} \\ \left( 1 - \frac{p_s}{P_{s\max}} \right) & \\ 0 & \text{Otherwise} \end{cases}$$

3.3.3.5

During night-time, the probability density function for the PV power output can be expressed as impulse function at zero ( $p_s=0$ ) as follows.

$$f_{P_s}(p_s) = (1 - F_1) \times \delta(p_s) \quad , p_s = 0 \quad 3.3.3.6$$

Let  $F_1$  be the fraction of daytime interval during the study period and its expression can be derived as:

$$F_1 = \frac{D_H}{D_H + N_H} \quad 3.3.3.7$$

where  $D_H$  and  $N_H$  are the number of daytime and night-time hours during the study period respectively.

It should be noted that all the time intervals in equation (3.3.3.7) are assumed to have the same duration during the study period. Corresponding to equation (3.3.3.7), the distribution function of the PV power output including zero output,  $F_{PA}(p_s)$ , can be expressed as follows.

$$F_{PA}(p_s) = F_1 \times F_{P_s}(p_s) + (1 - F_1) \quad 3.3.3.8$$

where  $F_{P_s}(p_s)$  is the distribution function corresponding to the density function  $f_{P_s}(p_s)$  and  $(1-F_1)$  is the fraction of night-time interval during the study period.

Equation (3.3.3.8) contains a non-zero value with the magnitude of  $(1-F_1)$  when  $p_s=0$ . Therefore, the density function,  $f_{p_A}(p_s)$ , includes the impulse function with the magnitude of  $(1-F_1)$  at  $p_s=0$ .

### 3.4 Fuel Cell Systems

#### 3.4.1. Description of the Technology

Fuel cell is a simple static device that converts the chemical energy in a fuel directly and isothermally into electrical energy. Fuel cell offers high conversion efficiency, modularity, reasonably long lifetime, minimal environmental impacts, and quick start up. Externally, fuel cell produces power similar to a battery system as long as fuel and oxidant are continuously fed. Fuel cell can use a variety of fuels such as natural gas, coal-bed methane, and landfill gas. Basically, fuel cell consists of two porous electrodes: anode and cathode, separated by an electrolyte region. The input fuel should be processed chemically into hydrogen or hydrogen-rich gas, no matter what the fuel used, because hydrogen-oxygen reaction releasing electrical power and producing water/steam is the basis of all fuel cell systems [see reference 3].

In a typical fuel cell, fuel is fed continuously to the anode and air is fed continuously to the cathode. Electrochemical reactions take place at the solid-liquid-gas interface in the pores of the electrodes to release electrons (produce electricity). A typical schematic of an individual fuel cell is illustrated in Figure 14. Several types of fuel cells are in different stage of development. They include phosphoric acid fuel cell (PAFC), solid oxide fuel cell (SOFC), molten carbonate fuel cell (MCFC), and proton exchange membrane fuel cell (PEMFC) [101].

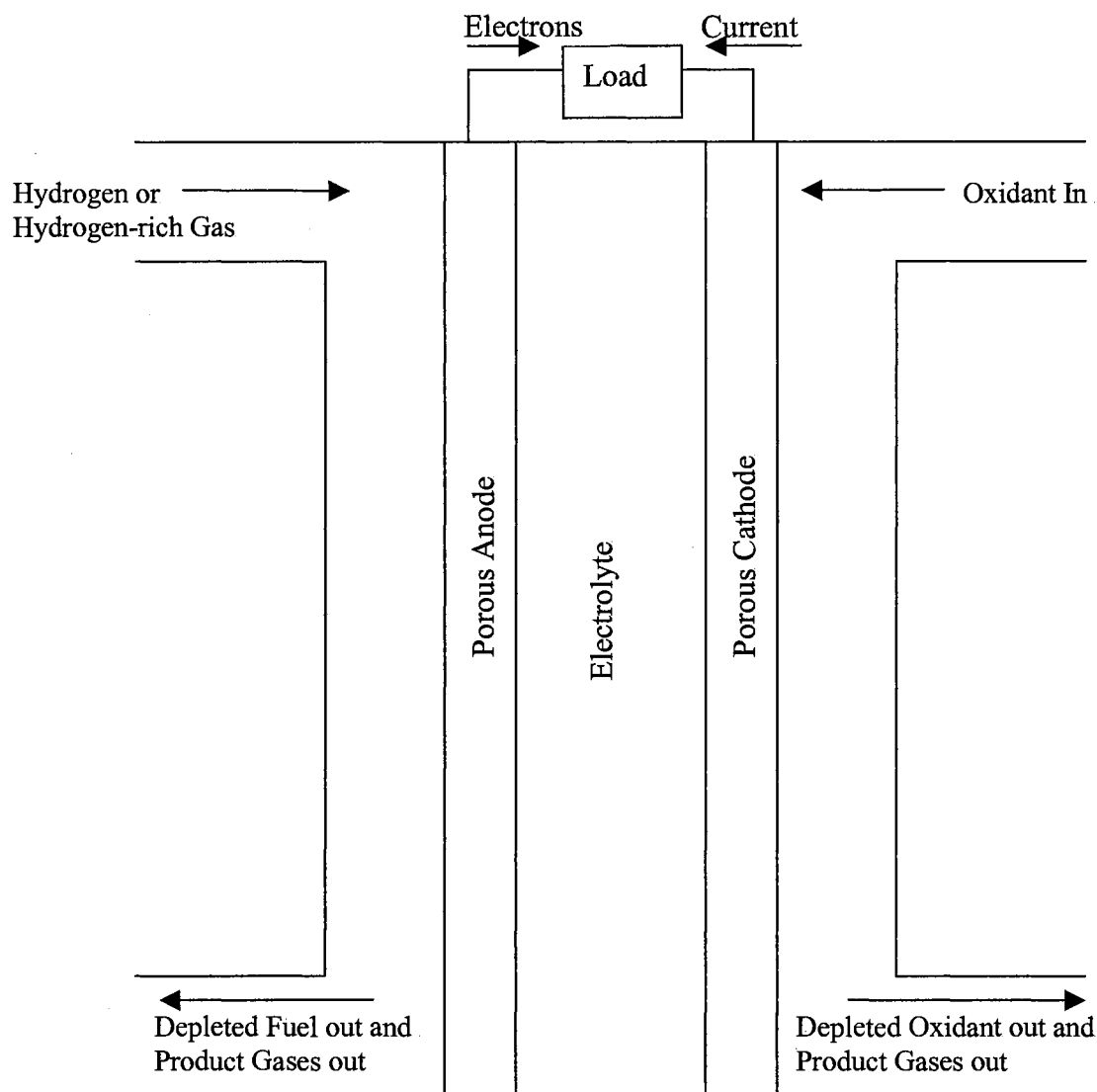


Figure 14. A Typical Schematic of an Individual Fuel Cell



Each type of fuel has its own operating temperature. The operating temperature plays a vital role in dictating the type of fuel that can be used in the fuel cell. High temperature fuel cells can use CO or CH<sub>4</sub> because of the inherently rapid electrode kinetics and the lesser need for high catalytic activity at high temperature. In low temperature fuel cells, the fuel is restricted to hydrogen.

A brief description of the most promising fuel cell technologies is given next [102-105]. PAFC uses phosphoric acid concentrated for the electrolyte in this fuel cell. PAFC operates in the 200-220 °C range with moderate current densities. PAFC systems have currently achieved efficiencies of 37 to 42%. The waste heat from PAFC is available for co-generation applications. PEMFC has a solid electrolyte. The electrolyte in this fuel cell is an ion exchange membrane (fluorinated sulfonic acid polymer). PEMFC operates in the 70-80 °C range with high current densities. However, the exhaust heat from PEMFC cannot be used for co-generation due to low operating temperature. MCFC generally uses a combination of alkali carbonate for the electrolyte. MCFC operates in the 600-650 °C range with moderate current densities at efficiencies of around 50%. The exhaust heat from MCFC is at a sufficiently high temperature to produce high pressure steam for use in a steam turbine or in co-generation applications. SOFC operates in the 600-1000 °C range with high current densities and high efficiencies. A solid polymeric membrane acts as electrolyte for this fuel cell. This fuel cell has, however, a lower cell performance than MCFC due to the high electrical resistivity of the electrolyte.

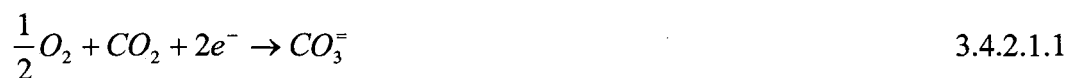
A typical fuel cell consists of three main sections: fuel processor (reformer), energy conversion section, and power conditioning unit. Figure 15 presents a typical

block diagram for fuel cell systems. The fuel processor (reformer) is used to convert the input fuel into hydrogen-rich gas. The energy conversion section is used to produce electrical energy (dc current) by electrochemical reaction. The dc output is converted to ac power at a suitable voltage by the power conditioning unit. Typically, a single fuel cell generates a very low power output. Therefore, several cells are connected in a series-parallel configuration in order to get the desired voltage, current and power outputs.

### 3.4.2 Fuel Cell Power Output Model

The power output model of a fuel cell can be constructed in terms of fuel flow rate and mole fraction of gas flow into reformer unit. Similar to microturbines, the output increases as fuel flow rate increases. Molten carbonate fuel cell (MCFC) is used to represent fuel cell power output in this research because it operates at a high efficiency. In addition, MCFC is currently considered to be the most promising fuel cell technology in terms of potential for large scale fuel cell systems. Therefore, the power output model of MCFC is considered in some detail as an example.

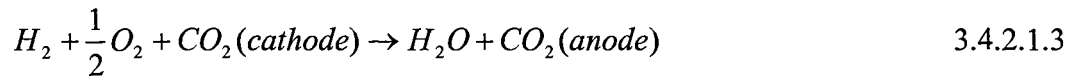
3.4.2.1 Chemical Reaction. The cathode electrochemical reaction in MCFC can be described as:



where carbonate ions migrate to the anode through the electrolyte. The electrochemical reaction at anode can be expressed as:



The overall reaction in MCFC can be expressed as:



3.4.2.2 Fuel Utilization. The performance of a single fuel cell is characterized by its V-I characteristics, under specified conditions. These conditions include the temperature and pressure of the operation and the inlet composition of the fuel and oxidant gases. In addition, the utilization of fuel and that of the oxidant are the key parameters. Fuel utilization ( $U_f$ ) is defined as the fraction of the fuel that reacts electrochemically in the fuel cell.  $U_f$  can be expressed as follows [see reference 60].

$$U_f = \frac{H_{2,in} - H_{2,out}}{H_{2,in}} \quad 3.4.2.2.1$$

$$= \frac{H_{2,consumed}}{H_{2,in}} \quad 3.4.2.2.2$$

where  $H_{2,in}$  and  $H_{2,out}$  are the molar flow rates of hydrogen at the inlet and outlet of the fuel cells respectively, and  $H_{2,consumed}$  is the consumption rate of hydrogen in electrochemical reaction.

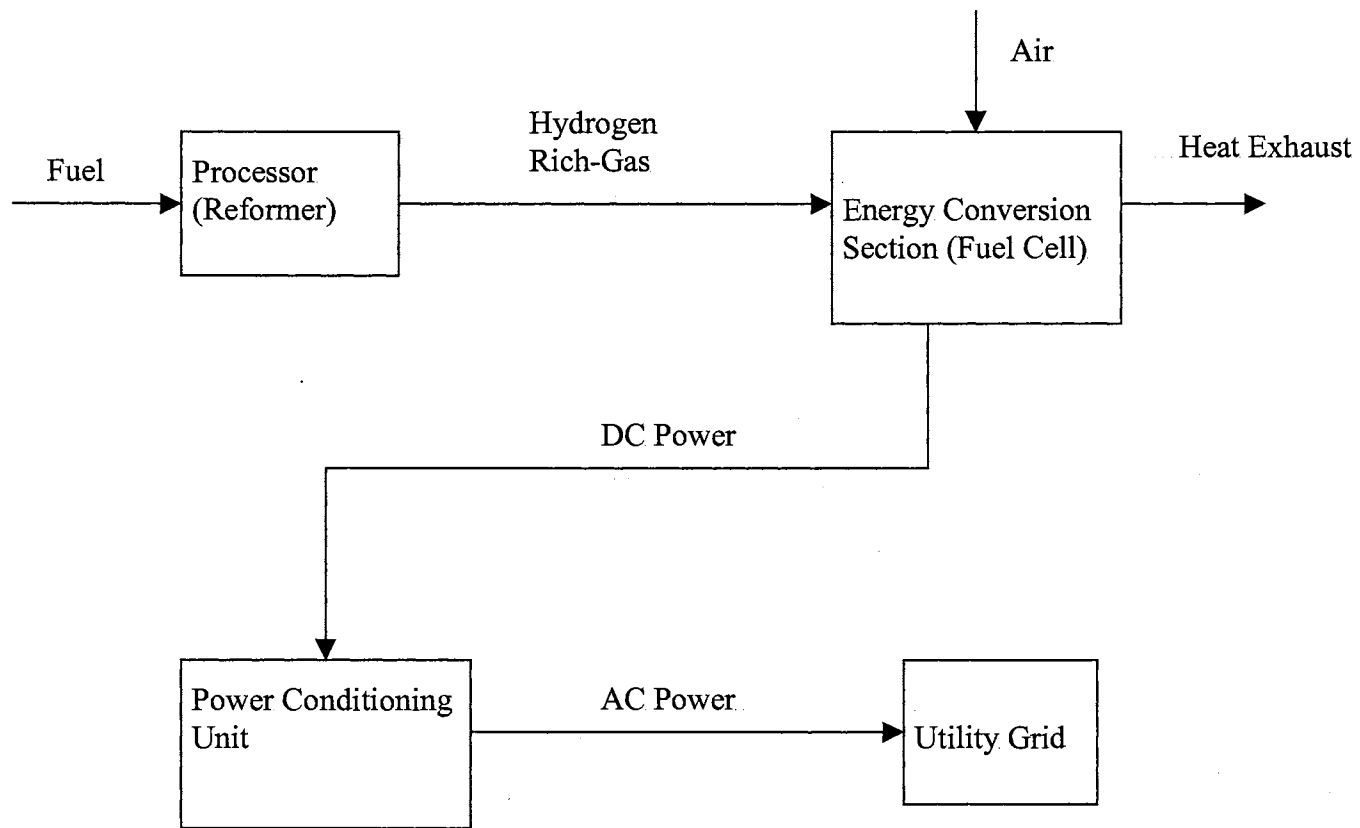


Figure 15. A Typical Schematic for Fuel Cell System

The molar flow rate of hydrogen at the inlet of fuel cell can be expressed in terms of total molar flow rate of gas mixture and gas mole fraction as follows.

$$H_{2,in} = F_{in} \left( x_{H_{2,in}} + x_{CO_{in}} + x_{CH_{4,in}} \right) \quad 3.4.2.2.3$$

where  $F_{in}$  is the total molar flow rate and  $x_{H_{2,in}}$ ,  $x_{CO_{in}}$ , and  $x_{CH_{4,in}}$  are the molar fraction of  $H_2$ ,  $CO$ , and  $CH_4$  respectively. Typically, gas composition is a function of fuel utilization. Therefore, if the utilization of fuel at that point is specified, the gas composition can be established.

3.4.2.3 Cell Voltage and Current Output. A stack output current of fuel cell system,  $I_{FU}$ , can be found by applying the Faraday's law and it can be expressed in terms of fuel utilization as follows.

$$I_{FU} = \frac{2FU_f H_{2,in}}{N_{cell} N_s} \quad 3.4.2.3.1$$

where  $F$  is the Faraday constant,  $N_{cell}$  is the number of cells per stack (series connection), and  $N_s$  is the number of stacks in the system (series connection).

By substituting equation (3.4.2.2) into equation (3.4.2.3.1), the output current can be defined in terms of the amount of hydrogen consumed by fuel cell as follows.

$$I_{FU} = \frac{2FH_{2,consumed}}{N_{cell}N_s} \quad 3.4.2.3.2$$

Then, the output current density of a stack fuel cell system,  $i_{FU}$ , can be found by dividing equation (3.4.2.3.2) by the effective area of fuel cell,  $A_{FU}$ .

$$i_{FU} = \frac{I_{FU}}{A_{FU}} \quad 3.4.2.3.3$$

The open-circuit voltage of fuel cell will be close to the reversible cell potential. The reversible potential of MCFC depends on the three gases at anode side and two gases on the cathode side. The Nernst equation can be expressed as follows [106-107].

$$V_o = E_o + \frac{R_g T}{2F} \ln \left\{ \left[ \frac{(P_{H_2,a})(P_{O_2,c})^{0.5}}{(P_{H_2O,a})} \right] \left[ \frac{P_{CO_2,c}}{P_{CO_2,a}} \right] \right\} \quad 3.4.2.3.4$$

where  $V_o$  is the open circuit reversible cell potential,  $E_o$  is standard reversible cell potential [see appendix A],  $R_g$  is universal gas constant,  $F$  is Faraday's constant,  $P_{CO_2,a}$  and  $P_{CO_2,c}$  are the partial pressure of carbon dioxide at the anode and cathode respectively,  $P_{O_2,c}$  is the partial pressure of oxygen at the cathode,  $P_{H_2,a}$  is the partial pressure of hydrogen at the anode, and  $P_{H_2O,a}$  is the partial pressure of water at the anode.

The partial pressures depend on the anode and cathode gas compositions and pressures. Their values are normalized to atmospheric pressure. The appropriate mole

fraction can be used to replace the anode and cathode partial pressure. Thus, the equation for the equilibrium in terms of mole fraction can be expressed as:

$$V_O = E_o + \frac{R_g T}{2F} \ln \left\{ \left[ \frac{(x_{FU} H_2)(x_{FU} O_2)^{0.5}}{(x_{FU} H_2 O)} \right] \left[ \frac{x_{FU} CO_{2,c}}{x_{FU} CO_{2,a}} \right] \right\} \quad 3.4.2.3.5$$

The output voltage is affected by ohmic polarization, activation polarization, and concentration polarization. Fuel cell polarizations are usually dependent on partial pressures, temperature, and current density. Ohmic losses occur as the current flows through the total internal resistance of the fuel cell. Activation polarization is caused by electrode kinetics while concentration polarization is caused by concentration gradients in the electrode. Therefore, the expression for individual cell voltage,  $V_{FU}$ , can be found by equation (3.4.2.3.6).

$$V_{FU} = V_O - \eta_{ohm} - \eta_{act} - \eta_{conc} \quad 3.4.2.3.6$$

where:

$$\eta_{ohm} = I_{FU} R_{FU} \quad 3.4.2.3.7$$

and

$$\eta_{act} = \frac{R_g T}{2F} \left( a_0 + a_1 \ln P_{H_2,a} + a_3 \ln P_{CO_2,a} + a_4 \ln P_{H_2O,a} + a_5 \ln P_{CO_2,c} \right. \\ \left. + a_6 \ln P_{CO_2,c} + \frac{a_7}{T} + a_8 \ln i_{FU} \right) \quad 3.4.2.3.8$$

and

$$\eta_{conc} = \frac{RT}{2F} \ln \left( 1 - \frac{i_{FU}}{i_{L,conc}} \right) \quad 3.4.2.3.9$$

where  $\eta_{act}$  is the activation polarization,  $\eta_{conc}$  is the concentration polarization,  $\eta_{ohm}$  is the ohmic polarization,  $R_{FU}$  is the total cell resistance, and  $i_{L,conc}$  is the limiting current density. The limiting current density is a measure of the maximum rate at which a reactant can be supplied to an electrode. In general, the parameter  $a_1$  to  $a_8$  can be found by suitable experimentation.

By substituting equations (3.4.2.3.7), (3.4.2.3.8), and (3.4.2.3.9) into equation (3.4.2.3.6), it can be seen that the cell voltage decreases as the current density increases. As mentioned earlier, the performance of fuel cell is characterized by V-I plane as shown in Figure 16. It can be seen that any number of operating points can be selected for fuel cell application in a particular system. Typically, it would be practical to operate the cell at the maximum power output.

3.4.2.4 Electrical Power Output. The practical fuel cell power output is typically described in terms of cell terminal voltage and current output. As mentioned earlier, fuel cell systems are connected in a series-parallel in order to obtain a desirable voltage,



current, and power output. Therefore, the system voltage and current are expressed as below.

$$V_{sys,FU} = N_{cell} N_s V_{FU} \quad 3.4.2.4.1$$

$$I_{sys,FU} = N_P I_{FU} \quad 3.4.2.4.2$$

where  $N_P$  is the number of strings in the system.

Therefore, the total power output of fuel cell system,  $P_{FU}$ , can be obtained by combining equations (3.4.2.4.1) and (3.4.2.4.2) and the result leads to:

$$P_{FU} = V_{sys,FU} I_{sys,FU} \quad 3.4.2.4.3$$

### 3.5 Load Model

Electricity demands usually have a variation between a maximum value ( $S_{Lmax}$ ) and a minimum value ( $S_{Lmin}$ ). In general, it can be considered as a continuous random variable. A simple load model with a uniform distribution is used in this study. Consequently, the probability density function for the load can be expressed as:

$$f_{|S_L|}(|s_L|) = \begin{cases} \frac{1}{|S_{Lmax}| - |S_{Lmin}|} & |S_{Lmin}| \leq |s_L| \leq |S_{Lmax}| \\ 0 & \text{Otherwise} \end{cases} \quad 3.5.1$$

The probability density function and the cumulative distribution function for the load model used in this study are illustrated in Figures 17 and 18 respectively.

### 3.6 Summary

This chapter has presented a collection of models for the most promising distributed generation technologies and a simple load model used in this research. Basic descriptions of technologies and mathematical models for some of the DG technologies and load are derived and discussed in this chapter. Weibull distribution is used to study and analyze the wind resource while cloud cover is modeled using a Beta distribution. The power output of a fuel cell is expressed in terms of fuel mass flow rate, fuel utilization, and mole fraction. Microturbine system is modeled in terms of fuel flow rate, and fuel pressure and temperature. Finally, a simple uniform distribution is used to model the electricity demand.

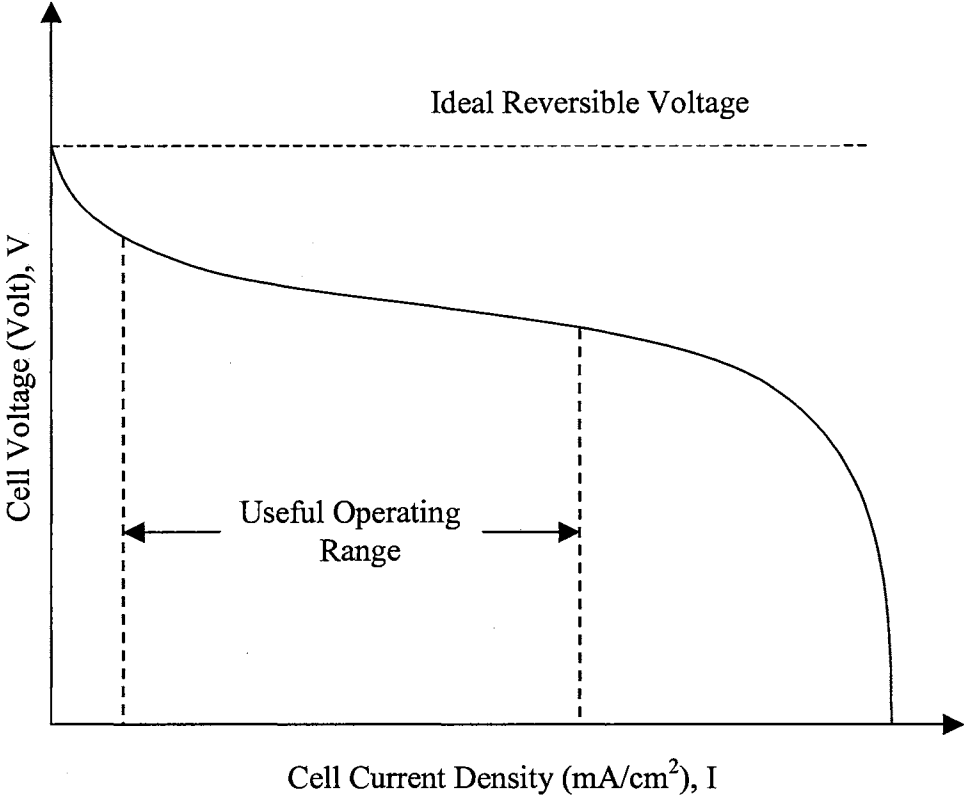


Figure 16. A Typical Fuel Cell Voltage/Current Characteristic

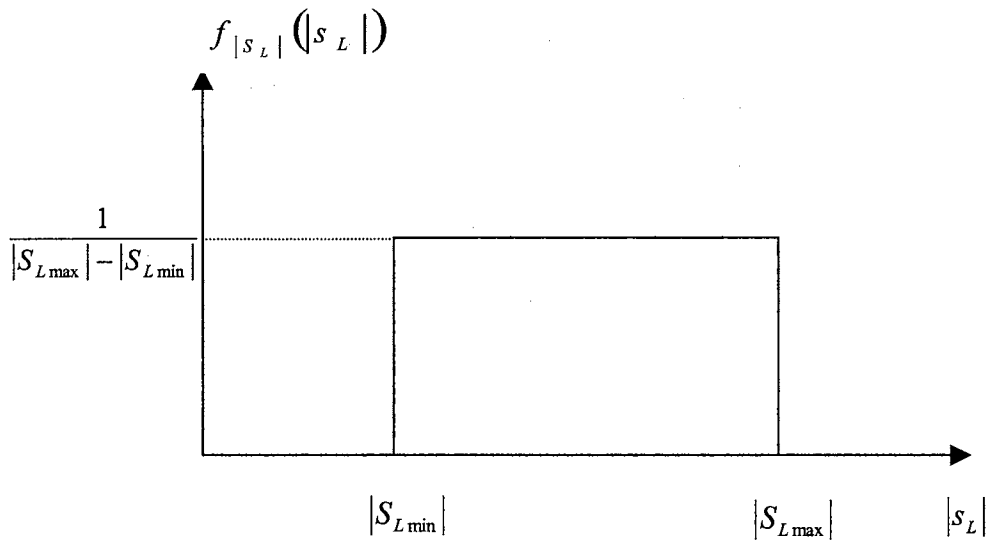


Figure 17. Assumed Probability Density Function for Load

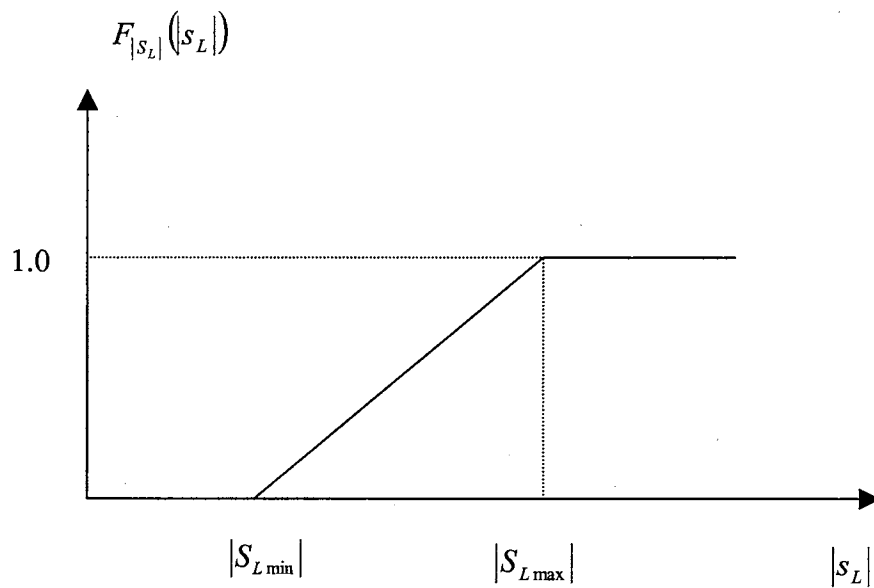


Figure 18. Cumulative Distribution Function for Load

## CHAPTER IV

### VOLTAGE PROFILE IMPROVEMENT WITH DISTRIBUTED WIND-TURBINE GENERATION

This chapter deals with the analysis of a benefit of distributed generation with the introduction of wind-turbine generation. Among the several benefits of distributed generation is voltage profile improvement. A probabilistic approach based on convolution technique to quantify this benefit in the case of wind turbine generation (WTG) is presented. A simple radial system with WTG and a uniformly distributed load are considered. Mathematical expressions for the probability density function, expected value, and variance of load voltage are developed in order to analyze this benefit. Typical simulation results are also given in this chapter. A comparison of the results of expected value of load voltage obtained using the probabilistic approach and a non-probabilistic approach employing the average output is presented. It is shown that there is only a slight difference in the expected value of load voltage between these two approaches.

#### 4.1 Introduction

In the past, chronological simulation techniques have been used to evaluate the performance of WTG. However, that approach requires a large amount of time series

data on wind speed, which may not always be available. This chapter employs a probabilistic approach to model the output of a WTG and load by considering wind speed and load as random variables. By applying convolution technique, these models can be combined to evaluate the voltage profile at the location of load. The quantification of voltage profile improvement is discussed in terms of expected value and variance of load voltage. With the introduction of wind turbine generation, voltage profile at a load point can be significantly improved.

## 4.2 System Description

A simple radial distribution system is considered in this chapter. The total length of the distribution line is assumed to be  $Y$  km. Schematics of the system considered are shown in Figures 19 and 20.

The following assumptions are made in this study:

- 1) Load absorbs real power at some specified power factor.
- 2) Load is Y-connected; therefore line current is the same as phase current.
- 3) WTG injects power at unity power factor.
- 4) Line resistance is ignored, only line reactance is considered in line model.
- 5)  $V_S$  is the RMS phase voltage at the infinite bus;  $V_S$  is the reference phasor,  $V_S \angle 0^\circ$ .
- 6) WTG is assumed to be located at  $D$  km from the infinite bus.

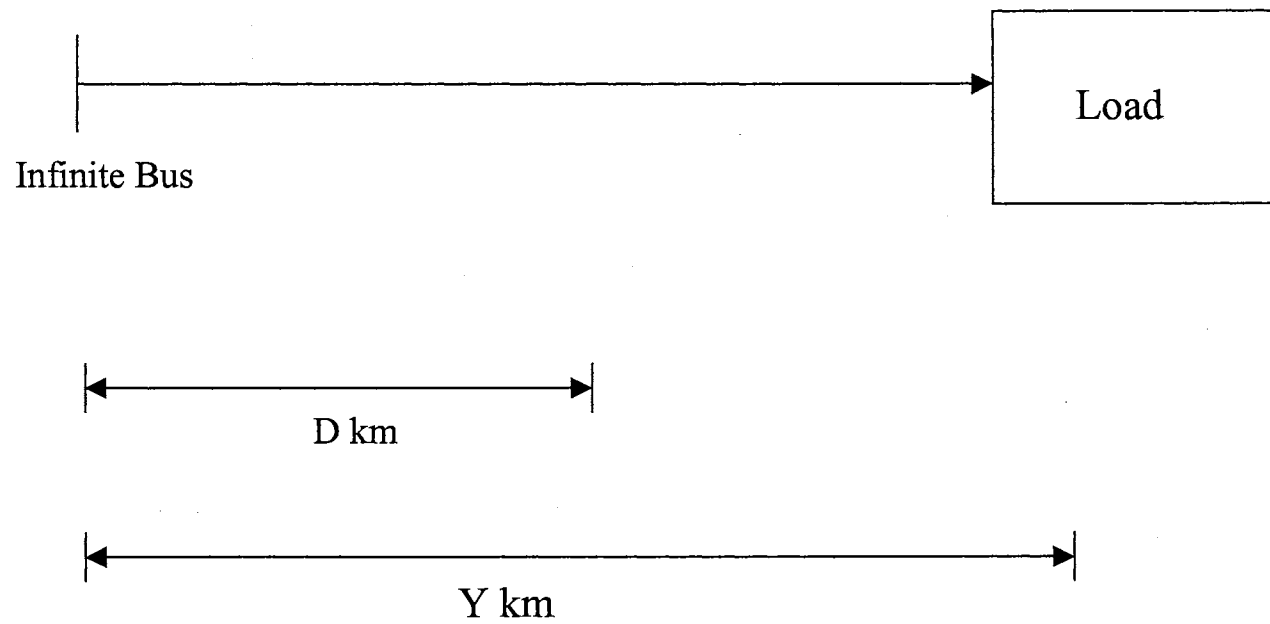


Figure 19. A simple radial distribution system without WTG

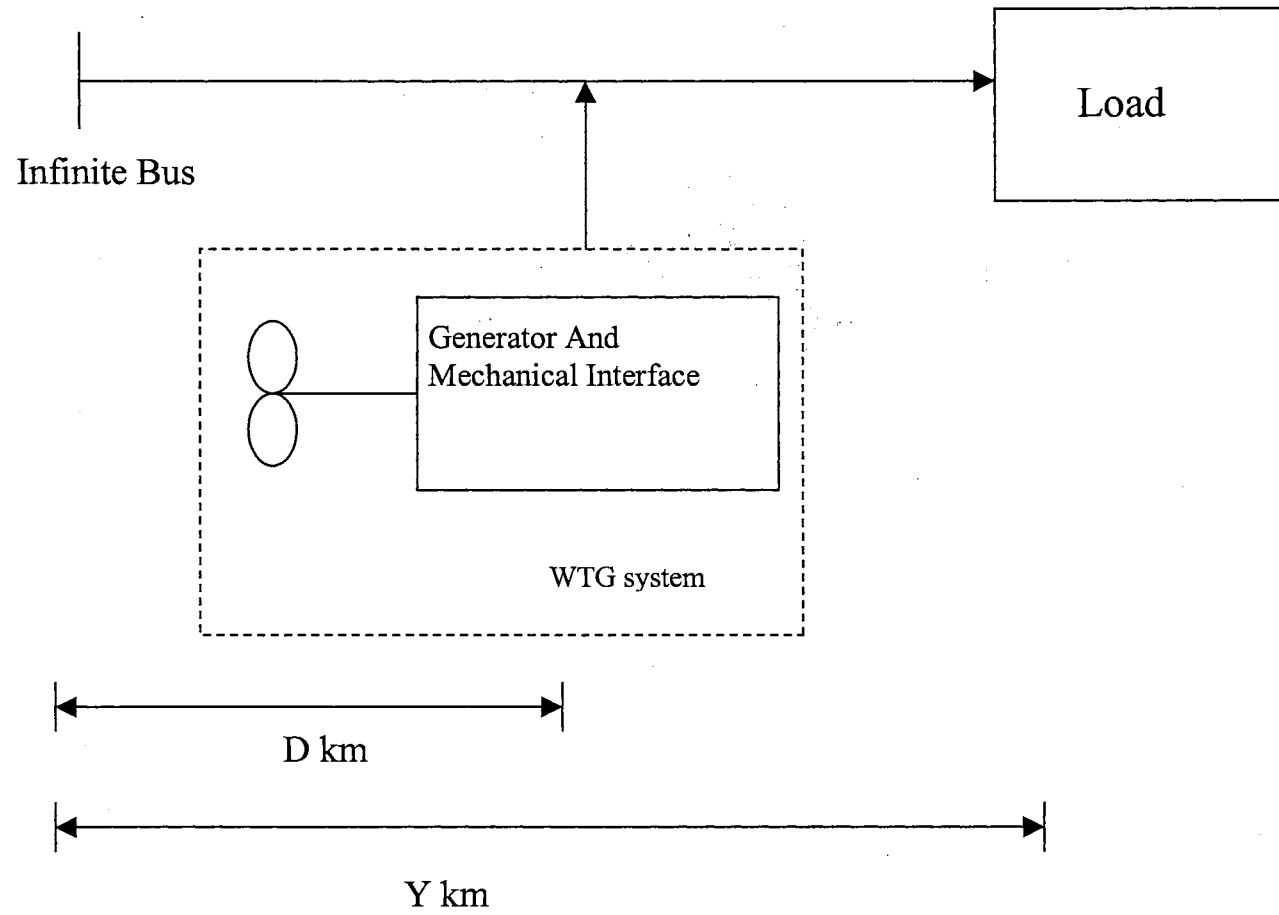


Figure 20. Schematic of a radial distribution system with WTG



### 4.3 Probabilistic Voltage Profile Analysis

In this section, expressions for the probabilistic voltage profile at the load point are developed. For the case with WTG, the complex power supplied by the infinite bus is reduced due to the injection of power from the WTG, thus helping to decrease current along a portion of the distribution line. Analyses of the base case system and the case with WTG are also given in this section.

#### 4.3.1 Probabilistic Voltage Profile for System without WTG

Schematic of the system for this analysis is illustrated in Figure 19. Obviously, the voltage at load is equal to voltage at source,  $V_s$ , minus voltage drop over line reactance. By applying the basic circuit laws, the magnitude of the RMS load phase voltage,  $|V_L|$ , can be expressed as a function of the infinite bus voltage, load complex power, total line reactance, and power factor as:

$$|V_L| = \sqrt{\frac{(3V_s^2 - 2XB|S_L|) + \sqrt{9V_s^4 - 12XB|S_L|V_s^2 + 4X^2(B^2 - 1)|S_L|^2}}{6}} \quad 4.3.1.1$$

where  $V_s$  is the infinite bus voltage,  $|S_L|$  is the absolute value of load complex power,  $X$  is the total line reactance,

$B$  in equation (4.3.1.1) is given by

$$B = (-1)^{n_L} \sqrt{1 - (PF_L)^2} \quad 4.3.1.2$$

and  $PF_L$  is load power factor with  $n_L$  defined as

$$n_L = \begin{cases} 1 & \text{for leading power factor load} \\ 2 & \text{for lagging power factor load} \end{cases} \quad 4.3.1.3$$

In order to find the probability density function of RMS load phase voltage,  $f_{|V_L|}(|v_L|)$ , the application of transformation theorem leads to:

$$f_{|V_L|}(|v_L|) = \frac{f_{|S_L|}(|S_L|)}{|V'_L(|S_L|)|} \quad 4.3.1.4$$

where  $f_{|S_L|}(|s_L|)$  is the probability density function of load and it is given by equation (3.5.1)

By taking the first derivative of equation (4.3.1.1) with respect to  $|S_L|$  and then substituting it into equation (4.3.1.4), the probability density function for RMS load phase voltage can be expressed as follows:

$$f_{|V_L|}(|v_L|) = \frac{2\sqrt{6}}{(|S_{L\max}| - |S_{L\min}|)} \left( \frac{\sqrt{G + \sqrt{K}}}{\frac{Q}{2\sqrt{K}} - E} \right) \quad 4.3.1.5$$

where E, G, K, and Q are given in appendix B.

### 4.3.2 Probabilistic Voltage Profile for System with WTG

In this analysis, WTG is assumed to be located at  $D$  km from the infinite bus as shown in Figure 20. The magnitude of the RMS phase load voltage for a specified location of WTG can be expressed as follows:

$$|V_L| = \sqrt{\frac{3V_s^2 + \sqrt{9V_s^4 - 4X^2 C^2}}{6}} \quad 4.3.2.1$$

where  $C$  is given by

$$C = |S_L^* - aP_w| \quad 4.3.2.2$$

and  $a$  is the fraction of distance from the infinite bus where WTG is located with reference to the total line length.

Once again, by the application of the transformation theorem, the probability density function for RMS load phase voltage can be expressed as follows:

$$f_{|v_L|}(|v_L|) = \frac{X \times v_L}{3(V_s^2 - 2v_L^2)} f_C(c) \quad 4.3.2.3$$

The probability density function  $f_C(c)$  can be obtained by convolving the probability density functions of wind turbine power output equation (3.1.3.7) and the load. The closed form solution for the probability density function of  $C$  is given in appendix C.

The expected value and variance of the load voltage can be used to assess and quantify voltage profile improvement and they can be expressed as:

$$E[|V_L|] = \int_{|V_{L,\min}|}^{|V_{L,\max}|} |v_L| f_{|v_L|}(|v_L|) d|v_L| \quad 4.3.2.4$$

$$\text{Var}(|V_L|) = E(|V_L|^2) - [E(|V_L|)]^2 \quad 4.3.2.5$$

Since the infinite bus voltage is taken as reference in this analysis, the closer the expected value of load voltage is to the infinite bus voltage and smaller the variance, the better the voltage profile at the load point.

#### 4.4 Simulation Results

In this section, equations (4.3.2.4) and (4.3.2.5) are used to study the variation of load voltage under different conditions to assess the voltage profile improvement at the customer location. The effects of varying load power factor, WTG location, and rating of WTG are analyzed and discussed.

##### 4.4.1 Required Input Data for Simulation

The following parameter values are used throughout this simulation.

##### a) WTG characteristics:

Cut-in speed ( $U_C$ )	4 m/s
Rated speed ( $U_R$ )	16 m/s
Cut-out speed ( $U_O$ )	25 m/s

b) Wind speed data:

Wind speeds are assumed to be Weibull distributed with a shape parameter  $\beta_w$  and a scale parameter  $\alpha_w$ . The influence of wind regime is investigated for low, medium, and high wind regimes.

Low: mean = 4m/s, standard deviation = 2m/s,  $\alpha_w = 4.52$  m/s,  $\beta_w = 2.10$

Medium: mean = 6 m/s, standard deviation = 2.5 m/s,  $\alpha_w = 6.76$ m/s,  $\beta_w = 2.57$

High: mean = 8 m/s, standard deviation = 2.93 m/s,  $\alpha_w = 8.96$  m/s,  $\beta_w = 2.97$

c) Load:

Load is assumed to be a uniformly distributed with:

$$|S_{L_{\max}}| = 0.8 \text{ pu}$$

$$|S_{L_{\min}}| = 0.4 \text{ pu}$$

d) Distribution line:

Reactance = 0.00375 pu/km

Total line distance = 80 km

e) Base Value:

All per-unit quantities used in this analysis are on 100 MVA base.

4.4.2 Impact of WTG Location

The location of WTG plays a vital role in improving the voltage profile at the load. To study the influence of WTG location, the location of WTG is varied from 20% to 100% of the total length of the distribution line measured from the infinite bus while

the load power factor and WTG rating are set at 0.8 lagging and 0.08 pu respectively. The results are presented in Figures 21 and 22.

It can be seen from Figure 21 that the expected value of load voltage increases as WTG location is moved closer to the load as expected. The impact of WTG is relatively small if it is installed very far away from the load, see for example the case  $a=0.2$ . As a result, WTG should be installed as close to the load as possible in order to capture the full benefit. Wind regime has a significant impact on the voltage profile. As expected, better wind regimes lead to improved expected values. This is due to the fact that WTG produces more energy with better wind regimes, thus helping to improve voltage profile at the customer location. Variance of the load voltage decreases with the introduction of WTG as compared to the system without WTG as shown in Figure 22. Once again, the decrease is more significant as the WTG is located closer to the load. This implies that the load voltage has less variability and stays closer to the expected value as compared to the base case. However, the variance exhibits slightly higher values at high wind speeds because the power output of WTG is more volatile at high wind regimes.

#### 4.4.3 Impact of WTG Rating

The WTG rating is also an important factor in determining voltage profile improvement. To illustrate this, the rating of WTG is varied from 0.04 pu to 0.32 pu with the location of WTG set at 70% ( $a = 0.7$ ) from the infinite bus and the load power factor set at 0.8 lagging for this case study. The load is set at the same level as before. Figures 23 and 24 show the impact of WTG rating on load voltage profile improvement.

As the rating of WTG increases, the expected value of load voltage increases in a nonlinear fashion. The increase is very pronounced at high penetration levels. However, the voltage at the load point does not improve as much as 8 times when the rating of WTG is increased from 0.04 pu to 0.32 pu. Thus, this factor should be considered in determining the rating of WTG used in distributed generation. The WTG rating impacts variance as illustrated in Figure 24. It is clear that the variance decreases with the inclusion of WTG and more so as its rating increases. The degree of decrease is more significant at high penetration levels.

#### 4.4.4 Impact of Load Power Factor

Load power factor is another parameter that can significantly influence the extent of voltage profile improvement that can be expected. To study this impact, four different load power factors were considered: unity power factor, 0.9 lagging, 0.8 lagging, and 0.8 leading. The location of WTG is set at 70% from the infinite bus and its rating is varied from 0.04 to 0.32 pu and it is assumed to inject power at unity power factor as before. With the medium wind regime, the results of the effect of load power factor on voltage profile improvement are shown in Figures 25 and 26.

It can be seen from Figure 25 that the expected value of load voltage exhibits the highest value under leading power factor load conditions. This is due to the fact that load itself provides a portion of reactive power requirements of the system, thus helping to support the system voltage. With lagging power factor loads, the expected value decreases as power factor decreases because load consumes more reactive power, causing increased voltage drop at the customer location. Power factor of load impacts the

variance of load voltage also and the nature of this variation is shown in Figure 26. It can be seen that with unity power factor load, variance of load voltage has the lowest value. In general, variance increases under non-unity load power factors, with largest values occurring under leading power factor conditions.

#### 4.5 Non-Probabilistic Voltage Profile Analysis

In this section, the analysis of voltage profile improvement is performed by using a non-probabilistic approach instead of the probabilistic approach discussed earlier. Non-probabilistic approach is an alternative simpler method to quantify the benefits of WTG. The advantage of this approach is the avoidance of the application of convolution between wind power output and load thus helping to reduce the amount of calculations required.

##### 4.5.1 Non-Probabilistic Approach

Three steps are involved in the proposed non-probabilistic approach. The steps include calculating the average wind power output, average load, and RMS voltage at load point. The procedures of each step are described below.

4.5.1.1 Calculating the Average Wind Power Output. Since wind power output is highly variable and site-specific, the probability density function of wind power output is a good means to represent wind power output as discussed in chapter 3. Since wind power output can be considered as a random variable, the average wind power output can be found by calculating the expected value using the probability density function of wind power output equation (3.1.3.7) which can be expressed as follows:



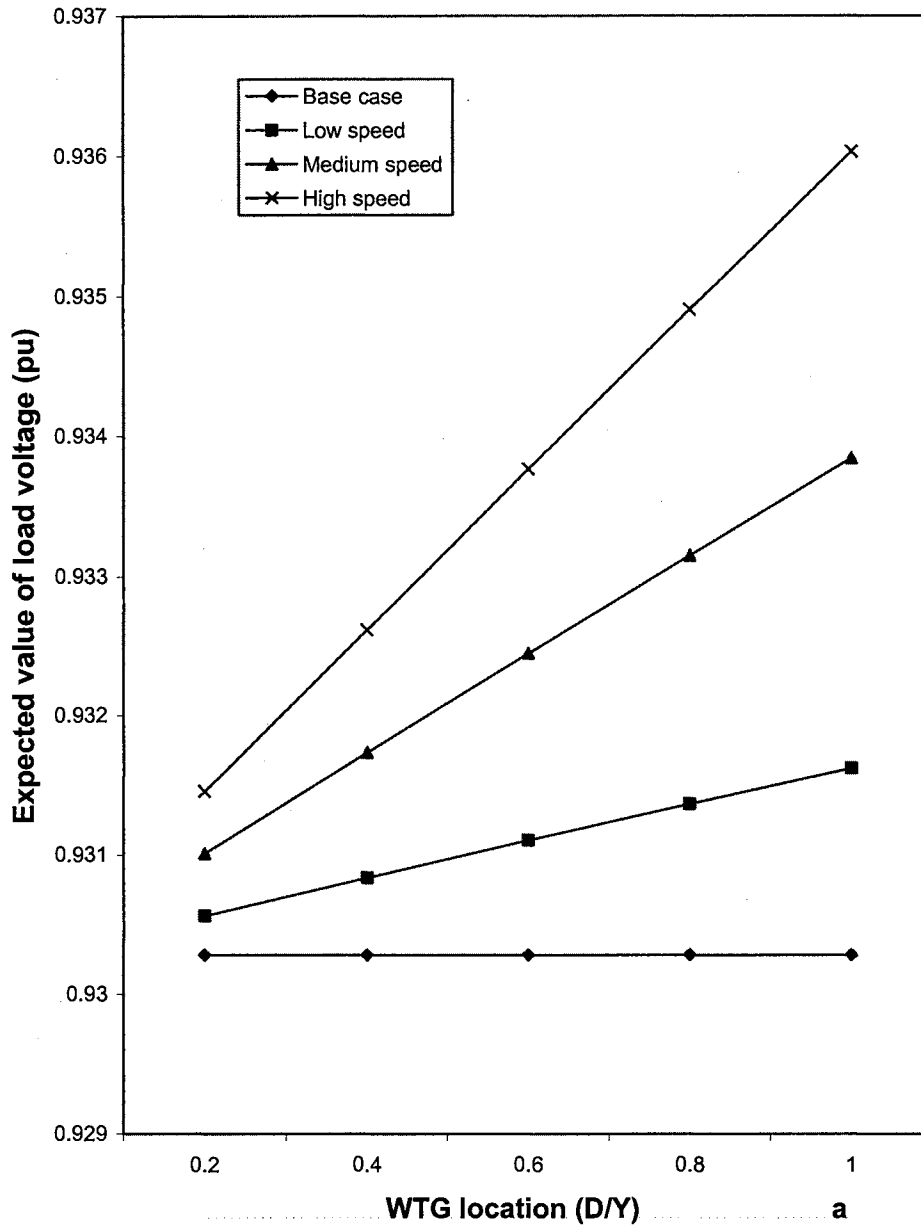


Figure 21. Variation of Expected Value of Load Voltage with WTG Location

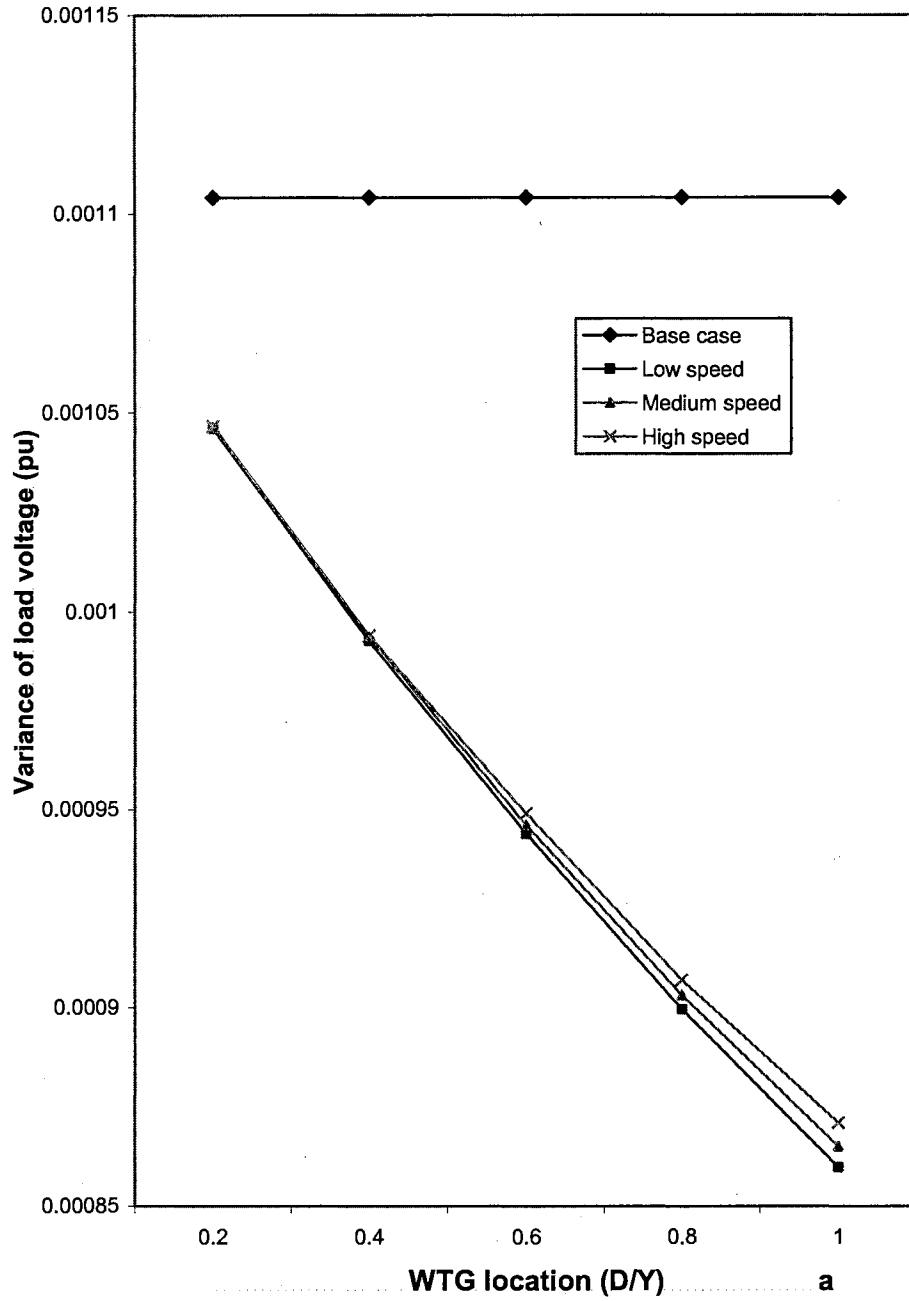


Figure 22. Variation of Variance of Load Voltage with WTG Location

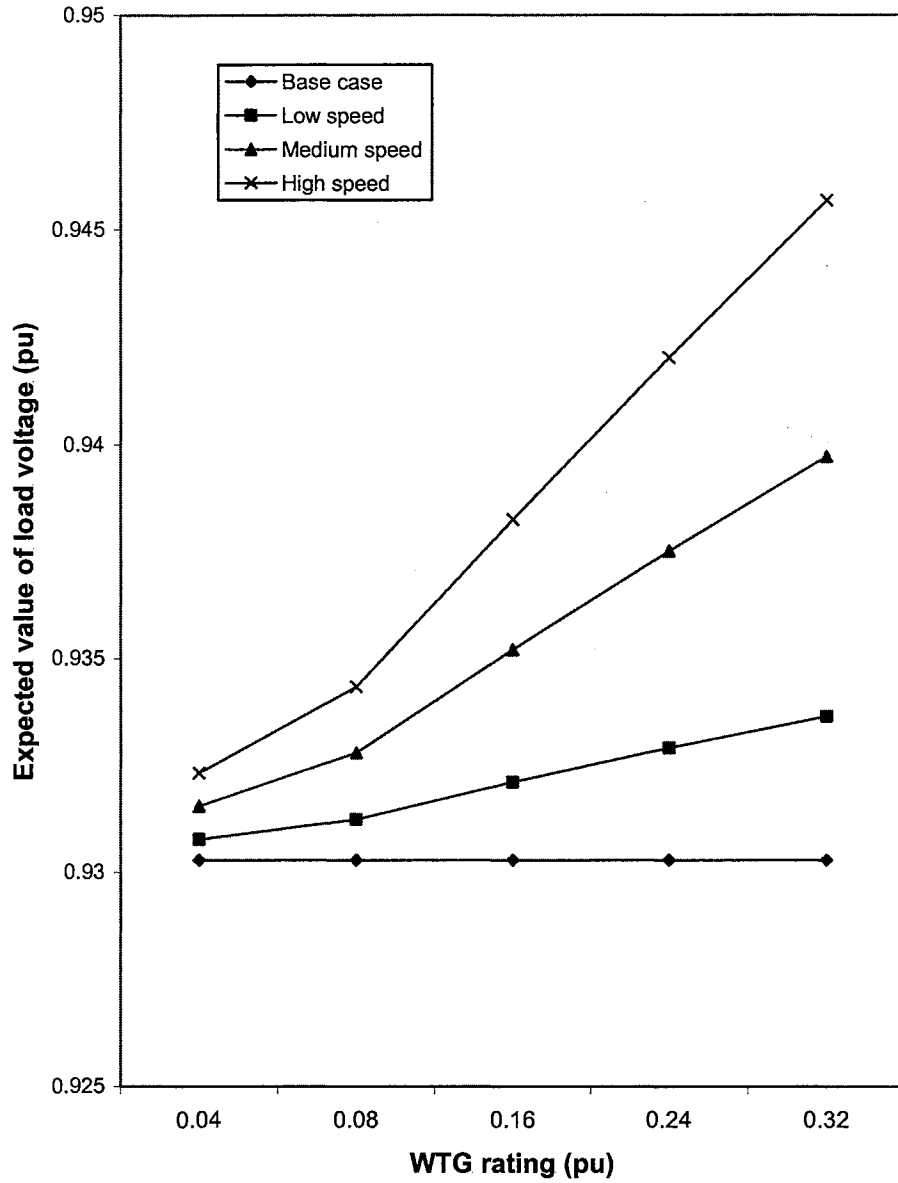


Figure 23. Variation of Expected Value of Load Voltage with WTG Rating

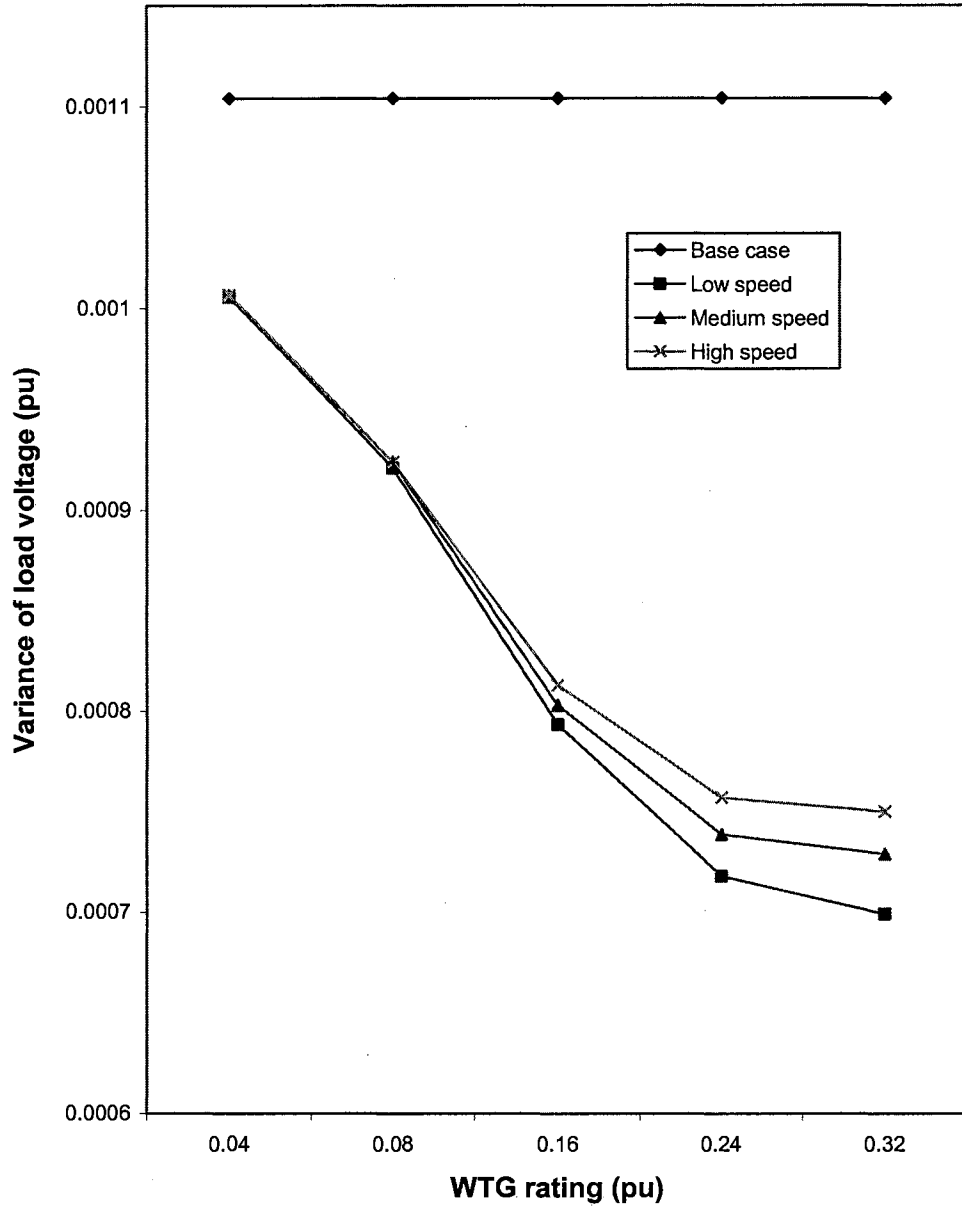


Figure 24. Variation of Variance of Load Voltage with WTG Rating

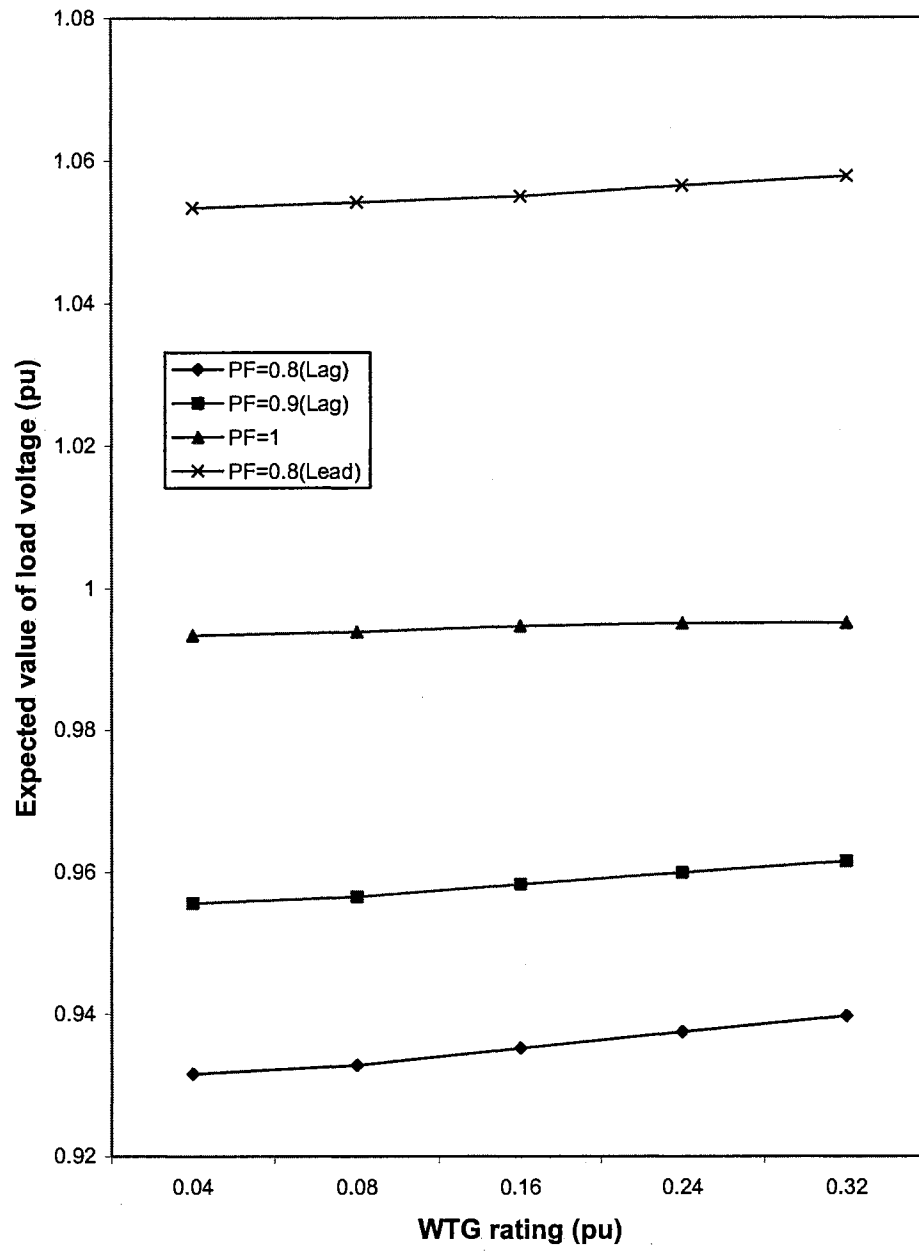


Figure 25. Variation of Expected Value of Load Voltage with Different Load Power Factors

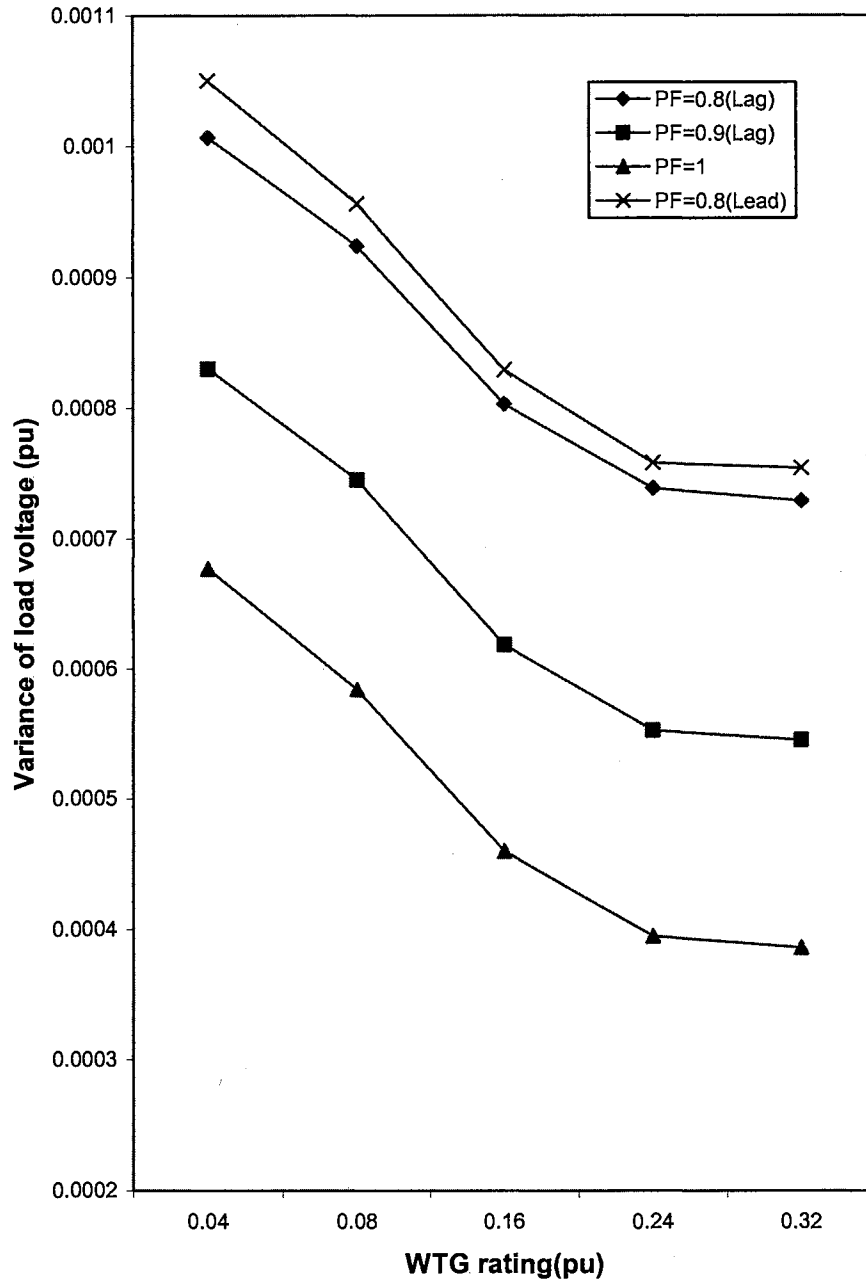


Figure 26. Variation of Variance of Load Voltage with Different Load Power Factors

$$E[P_w]_{p_w=0} = 0 \times \{(1 - F_U(u_o) + F_U(u_c))\delta(p_w)\} \quad \text{for } p_w=0 \quad 4.5.1.1.1$$

$$E[P_w]_{0 < p_w < P_R} = \int_{0.001}^{P_R - 0.001} p_w \times \left\{ \left( \frac{\beta_w}{\alpha_w \beta_w} \right) \left( \frac{U_R^{2.28} - U_C^{2.28}}{2.28 P_R} \right) \left( \frac{p_w (U_R^{2.28} - U_C^{2.28})}{P_R} + U_C^{2.28} \right)^{\frac{\beta_w - 2.28}{2.28}} \times \right. \\ \left. \exp \left[ - \left( \frac{\left( \frac{p_w (U_R^{2.28} - U_C^{2.28})}{P_R} + U_C^{2.28} \right)^{\frac{1}{2.28}} \beta_w}{\alpha_w} \right) \right] \right\} dp_w \quad \text{for } 0 < p_w < P_R \quad 4.5.1.1.2$$

$$E[P_w]_{p_w=P_R} = P_R \times \{(F_U(u_o) - F_U(u_r))\delta(p_w - P_R)\} \quad \text{for } p_w = P_R \quad 4.5.1.1.3$$

It should be noted that the equation (4.5.1.1.2) is integrated from 0.001 to (P<sub>R</sub>-0.001) because this equation is used to evaluate the expected value of wind power output when output is greater than zero but less than rated power output. Therefore, the range of integration should be as close to 0 and P<sub>R</sub> as possible. The value of 0.001 is justified as an appropriate value to cover the range of wind power outputs from 0 and P<sub>R</sub>. As a result, the equation (4.5.1.1.2) is considered from 0.001 to (P<sub>R</sub>-0.001).

The total expected value of wind power output can be obtained by combining equations (4.5.1.1.1), (4.5.1.1.2), and (4.5.1.1.3) together and the result leads to:

$$E[P_w] = E[P_w]_{0 < p_w < P_R} + E[P_w]_{p_w=P_R} \quad 4.5.1.1.4$$

4.5.1.2 Calculating Average Load. With the assumption of a uniformly distributed load model, the average load is simply obtained as follows:

$$E[L] = \frac{|S_{L \max}| + |S_{L \min}|}{2} \quad 4.5.1.2.1$$

4.5.1.3 Calculating the Average Value of RMS Voltage at Load Point. After the average wind power output and the average load have been obtained, the RMS phase load voltage can be calculated by substituting equations (4.5.1.1.4) and (4.5.1.2.1) into equation (4.3.2.2) and then back into equation (4.3.2.1).

## 4.5.2 Simulation Results

As mentioned earlier, the purpose of this section is to consider an alternative method to quantify the voltage profile improvement at load point. Therefore, only a few cases and only the expected values of load voltage are considered and the results will then be compared with those obtained by the probabilistic approach. The required simulation data for this analysis are obtained from section 4.4.1 and the WTG is assumed to be located at 70% of the total distribution line distance from the infinite bus in this analysis.

4.5.2.1 Case Study A: Medium Wind Regime with Constant WTG Rating. This case studies the influence of load power factor under medium wind regime conditions by considering load power factors of 0.8 and 0.9 lagging and by keeping  $P_R$  constant at 0.2 pu. The results are shown in Table 1.



4.5.2.2 Case Study B: High Wind Regime with Constant WTG Rating. This case also studies the effect of load power factor but under high wind regime conditions.

Similar to case A, load power factors of 0.8 and 0.9 lagging are considered while WTG rating is maintained at 0.2 pu. The results from this case study are presented in Table 2.

4.5.2.3 Case Study C: High Wind Regime with Constant Load Power Factor.

This case evaluates the effect of WTG rating under high wind regime condition. WTG ratings are varied from 0.1 to 0.3 pu while the load power factor is kept constant at 0.9 lagging. The results are presented in Table 3.

#### 4.6 Comparison of Results Using Probabilistic and Non-Probabilistic Approaches

In this section, expected values of voltage at load point obtained by simulation using probabilistic and non-probabilistic approaches are compared. In general, probabilistic approach represents the nature of wind turbine output better than non-probabilistic approach. However, non-probabilistic approach offers an alternative method to quantify the voltage profile at load point by reducing calculation time and avoiding the complicated convolution procedure. A comparison of the results obtained by these two approaches is presented in Table 4.

It can be seen from Table 4 that the differences between the expected load voltages obtained by the two approaches for all the cases are very small. The largest difference is less than 0.1%. Therefore, the results suggest that non-probabilistic approach is justified as an alternative method to evaluate voltage profile improvement. As a result, the non-probabilistic approach will be used to quantify the benefits of wind

component of distributed generation in later work. Also, the non-probabilistic approach consistently gives a very slightly higher (optimistic) value for the average load voltage and this point should be kept in mind.

#### 4.7 Summary

In this chapter, voltage profile improvement has been discussed and quantified for the case of distributed wind turbine generation. A probabilistic approach involving the application of convolution technique is developed to quantify this benefit. The impacts of WTG rating, load power factor, and location of WTG are evaluated. Typical numerical examples and simulation results are also given and discussed in this chapter. A non-probabilistic approach is proposed and the associated results are compared with those obtained by the probabilistic approach. The comparison leads to the conclusion that the differences are quite small, justifying the use of the non-probabilistic approach in studies to be presented later.

TABLE 1

VARIATION OF VOLTAGE AT LOAD POINT WITH LOAD POWER FACTOR UNDER MEDIUM WIND SPEED CONDITIONS  
[NON-PROBABILISTIC APPROACH]

Load power factor	Voltage at load point (pu)
PF = 0.9 Lag	0.968799600
PF = 0.8 Lag	0.951688868

TABLE 2

VARIATION OF VOLTAGE AT LOAD POINT WITH LOAD POWER FACTOR IN A HIGH WIND SPEED REGIME  
[NON-PROBABILISTIC APPROACH]

Load power factor	Voltage at load point (pu)
PF = 0.9 Lag	0.969629292
PF = 0.8 Lag	0.952829579

TABLE 3

VARIATION OF VOLTAGE AT LOAD POINT WITH WTG RATING IN A HIGH WIND SPEED REGIME  
[NON-PROBABILISTIC APPROACH]

WTG rating (pu)	Voltage at load point (pu)
$P_R = 0.1$	0.968867370
$P_R = 0.2$	0.969629292
$P_R = 0.3$	0.970472612

TABLE 4

A COMPARISON OF EXPECTED LOAD VOLTAGES  
OBTAINED USING PROBABILISTIC AND  
NON-PROBABILISTIC APPROACHES

Case A)			
Load power factor	Expected load voltage (pu) Non-probabilistic approach	Expected value of load voltage (pu) Probabilistic approach	Percentage difference
PF = 0.8 Lag	0.968799600	0.968274581	0.054
PF = 0.9 Lag	0.951688868	0.951025816	0.070
Case B)			
Load power factor	Expected load voltage (pu) Non-probabilistic approach	Expected value of load voltage (pu) Probabilistic approach	Percentage difference
PF = 0.8 Lag	0.969629292	0.969104391	0.054
PF = 0.9 Lag	0.952829579	0.952168305	0.069
Case C)			
WTG rating (pu)	Expected load voltage (pu) Non-probabilistic approach	Expected value of load voltage (pu) Probabilistic approach	Percentage difference
$P_R = 0.1$	0.968867370	0.968181182	0.071
$P_R = 0.2$	0.969629292	0.969104391	0.054
$P_R = 0.3$	0.970472612	0.96994512	0.054

## CHAPTER V

### QUANTIFICATION OF THE BENEFITS OF DISTRIBUTED GENERATION

This chapter deals with the quantification of some of the technical benefits of distributed generation. The benefits considered include voltage profile improvement, line loss reduction, and environmental impact reduction. A set of indices, namely, voltage profile improvement index (VPPI), line loss reduction index (LLRI), environmental impact reduction index (EIRI), and distributed generation benefit index (BI) are proposed to evaluate and quantify the benefits of distributed generation when they are introduced in an existing power system. Expressions for VPPI, LLRI, EIRI, and BI are developed and discussed.

#### 5.1 The Approach

Most of the benefits of employing distributed generation in existing distribution networks have both economic and technical implications and they are interrelated. While all the benefits can be ultimately valued in terms of money, some of them have a strong technical flavor than others. As such, it is proposed to classify the benefits into two groups--technical and economic.

The major technical benefits are:

- Reduced line losses
- Voltage profile improvement

- Reduced emissions of pollutants
- Increased overall energy efficiency
- Enhanced system reliability and security
- Improved power quality
- Relieved T&D congestion

The major economic benefits are:

- Deferred investments for upgrades of facilities
- Reduced O&M costs of some DG technologies
- Enhanced productivity
- Reduced health care costs due to improved environment
- Reduced fuel costs due to increased overall efficiency
- Reduced reserve requirements and the associated costs
- Lower operating costs due to peak shaving
- Increased security for critical loads

In this thesis, a general approach is presented to quantify the technical benefits of distributed generation. It is then applied to assess three major technical benefits, namely, voltage profile improvement, line loss reduction, and environmental impact reduction.

Technical Benefits of introducing distributed generation can accrue in one of two broad categories:

- (i) Improvement of a certain attribute such as voltage profile, reliability, power quality, etc.
- (ii) Reduction of an attribute such as line losses, emissions, congestion, etc.

By comparing and taking the ratio of a measure of an attribute with and without distributed generation (with the loads served being the same), an index can be derived for each of the attributes. If the introduction of DG is beneficial, indices corresponding to the attributes in Category (i) will be greater than unity and indices corresponding to the attributes in Category (ii) will be less than unity.

Designating the indices as  $II_i$  and  $RI_j$  for the different attributes in categories (i) and (ii) respectively, an overall composite benefit index (BI) can be formulated as:

$$BI = \sum_i BW_i II_i + \sum_j BW_j \frac{1}{RI_j} \quad 5.1.1$$

in which  $BW_i$  and  $BW_j$  are the benefits weighting factors and:

$$\sum_i BW_i + \sum_j BW_j = 1 \quad 5.1.2$$

The use of weighting factors will enable the emphasis of certain critical attributes depending on the location of the DG units, types of loads served by the distribution system and the region involved. With this formulation, the planner can select the locations and ratings of DG that will result in the highest value for BI to maximize the benefits.

## 5.2 Voltage Profile Improvement

One of the justifications for introducing distributed generation is to improve the voltage profile of the system and maintain the voltage at the customer terminals to within an acceptable range. A means to quantify this benefit is proposed for use in evaluating different scenarios of distributed generator installations.

### 5.2.1 Introduction

All electrical devices are designed to operate with the supply of electric power within a specified range of voltage and frequency. While major variations of frequency are not common, voltage variations are very prevalent, depending on the location of the load, location of generators, electrical characteristics of lines, and power factor of the load. Too high or too low a voltage can cause damage to the electric equipment. Therefore, the utility must monitor and control the voltage at the customer end and ensure that it does not fall below a certain specified value under heavy load conditions and not rise above a certain specified value under light load condition.

Generally, as current flows through transmission or distribution lines, voltage drop occurs at the customer site. Voltage drop increases as current increases (under heavier load) or travel farther away from source. Therefore, the customers at the end of a line may receive too low a voltage under heavy load condition. Several techniques can be used to solve voltage drop problems. Some of them are:

- 1) Tap Changers
- 2) Capacitors for voltage regulation
- 3) Varying the generator voltage



- 4) Employing of distributed generation
- 5) Voltage regulating transformers

The introduction of distributed generation into existing systems is the main focus for voltage profile improvement in this research because DG does not only improve voltage profile but it also offers several other benefits to both utilities and customers.

### 5.2.2 Voltage Profile Improvement

By introducing distributed generation into the system, voltage profile can be improved because DG can provide a portion of the real and reactive power to the load, thus helping to decrease current along a section of the transmission/distribution line, which, in turn, will provide a boost in the voltage magnitude at the customer site.

The amount of voltage profile improvement depends on several factors such as locations and ratings of DG. In addition, if wind energy systems and/or photovoltaic systems are used for DG, external factors such as wind regime and solar radiation will play an important role in determining the amount of voltage profile improvement.

Location and rating of DG play a vital role in determining the voltage profile improvement. In general, there will be several scenarios for the locations and ratings of distributed generation. However, it is possible to justify the best scenario to maximize the benefits of DG in terms of voltage profile improvement. One way to address this problem is to propose and develop an index to quantify the amount of voltage profile improvement offered by DG.

### 5.2.3 Voltage Profile Improvement Index (VPII)

A voltage profile improvement index (VPII) is developed and used to quantify the amount of voltage profile improvement. The proposed voltage profile improvement index quantifies the improvement in the voltage profile (VP) in a simple manner with the inclusion of DG. Thus, VPII can be simply described as the ratio of voltage profile index of the system with DG to the voltage profile index of the system without DG (base case system) and it is expressed as:

$$VPII = \frac{VP_{w/DG}}{VP_{wo/DG}} \quad 5.2.3.1$$

where  $VP_{w/DG}$  and  $VP_{wo/DG}$  are measures of the voltage profile of the system with DG and without DG respectively with the same load at the different load buses. The general expression for VP is given as:

$$VP = \sum_{i=1}^N V_i L_i k_i \quad 5.2.3.2$$

with

$$0 \leq k_i \leq 1 \quad 5.2.3.3$$

where  $V_i$  is the voltage magnitude at bus  $i$  in per-unit,  $L_i$  is the load at bus  $i$  in per-unit,  $k_i$  is the weighting factor for bus  $i$ , and  $N$  is the total number of buses in the distribution system.

It should be noted that if all the buses are equally weighted, the value of  $k_i$  is given as:

$$k_1 = k_2 = k_3 = \dots = k_N = \frac{1}{N} \quad 5.2.3.4$$

The voltage profile expression in (5.2.3.2) recognizes the influences of the amount and importance of load at each bus. It allows the possibility of a low load bus with important load to have a strong impact. In general, weighting factors are assigned based on the importance/criticality of load at each bus. Therefore, a higher value of  $k_i$  indicates a higher importance of bus  $i$  to the system.

In this study, a power flow simulation is used to evaluate the magnitude of voltage at each bus. By substituting equation (5.2.3.2) into equation (5.2.3.1),  $VPII$  for an  $N$ -bus system can be expressed as follows:

$$VPII = \frac{\left[ \sum_{i=1}^N V_i L_i k_i \right]_{w/DG}}{\left[ \sum_{i=1}^N V_i L_i k_i \right]_{wo/DG}} \quad 5.2.3.5$$

Based on this definition, one can conclude the following attributes:

$$VP_{II} = \begin{cases} <1 & \text{DG has not been beneficial} \\ =1 & \text{DG has no impact on the system voltage profile} \\ >1 & \text{DG has improved the voltage profile of the system} \end{cases} \quad 5.2.3.6$$

Theoretically, DG can be installed almost anywhere in the system. However,  $VP_{II}$  can be used to select the best locations and ratings for installing DG. In general, the highest value of  $VP_{II}$  implies the best locations and ratings for DG in terms of improving voltage profile only.

### 5.3 Line Loss Reduction

Another major potential benefit offered by DG is the reduction in electrical line losses. The general idea of electrical line losses is briefly discussed. Then, a line loss reduction index is proposed to quantify this benefit.

#### 5.3.1 Introduction

Electrical line losses occur when current flows through transmission and distribution systems. The loss can be significant under the heavy load conditions. The utility is forced to pass the cost of electrical line losses to all customers in terms of higher energy cost. Thus, it would be beneficial to both utilities and customers if electrical line losses are reduced. In general, the magnitude of the electrical line losses depend on the amount of current flow and the line resistance. The magnitude of losses for three-phase system without the employment of DG is expressed as:

$$LL_{wo/DG} = \sum_{i=1}^M I_{L,i}^2 R_i D_i \quad 5.3.1.1$$

where  $I_{L,i}$  is the per-unit line current in distribution line  $i$  without DG,  $R_i$  is the line resistance for line  $i$  (pu/km),  $D_i$  is the  $i^{\text{th}}$  distribution line length (km), and  $M$  is total number of lines in the distribution system.

Therefore, electrical line losses can be decreased by reducing either line current or line resistance or both. To reduce line resistance, the utility needs to significantly increase investment to replace all transmission and distribution lines. The main focus of this study is to reduce line current with the employment of DG. Electrical line losses is the product of line current squared times the line resistance. Therefore, if line current is reduced by 25%, it would reduce the line losses by nearly 50%.

### 5.3.2 Line Loss Reduction

By installing distributed generation, the line current can be reduced because DG can provide both real power and reactive power locally to the load. Therefore, it will help to reduce line current along a portion of the transmission/distribution line, resulting in line loss reduction. The expression for electrical line losses with the inclusion of DG is given as:

$$LL_{w/DG} = \sum_{i=1}^M (I_{L,i} - I_{DG,i})^2 R_i D_i \quad 5.3.2.1$$

where  $LL_{w/DG}$  is the total line losses in the system with the employment of DG,  $I_{DG,i}$  is the per-unit current provided by distributed generation in distribution line  $i$ , and  $M$  is the total number of distribution lines in the system. The subtraction of the two currents are vectorial, not arithmetic.

Expressing the  $(I_{L,i} - I_{DG,i})$  term in equation (5.3.2.1) as:

$$I_{A,i} = I_{L,i} - I_{DG,i} \quad 5.3.2.2$$

Equation (5.3.2.1) becomes:

$$LL_{w/DG} = \sum_{i=1}^M I_{A,i}^2 R_i D_i \quad 5.3.2.3$$

where  $I_{A,i}$  is the per-unit line current in distribution line  $i$  with the deployment of DG. As before, the loads at the different buses are assumed to be the same both with and without DG.

### 5.3.3 Line Loss Reduction Index (LLRI)

Line loss reduction is very sensitive to locations and ratings of DG. If an appropriate index is available to quantify and evaluate the benefit of line loss reduction, it can be used to identify DG scenarios that are preferable. This index is developed by comparing the total electrical line losses in the system with and without DG.

The proposed LLRI is defined as the ratio of the total line losses in the system with DG to the total line losses in the system without DG and it is expressed as:

$$LLRI = \frac{LL_{w/DG}}{LL_{wo/DG}} \quad 5.3.3.1$$

By substituting equations (5.3.1.1) and (5.3.2.3) into equation (5.3.3.1), the result leads to:

$$LLRI = \frac{\sum_{i=1}^M I_{A,i}^2 D_i R_i}{\sum_{i=1}^M I_{L,i}^2 D_i R_i} \quad 5.3.3.2$$

Based on this definition, one can make the following observations:

$$LLRI = \begin{cases} < 1 & \text{DG has reduced electrical line losses} \\ = 1 & \text{DG has no impact on system line losses} \\ > 1 & \text{DG has increased electrical line losses} \end{cases} \quad 5.3.3.3$$

This index can also be used to identify the best locations and ratings for installing DG to maximize line loss reduction (minimize line losses). Clearly, minimum value of LLRI corresponds to the best locations and ratings of DG in terms of line loss reduction only.

#### 5.4 Environmental Impact Reduction

Another great potential benefit of DG is the production of energy with minimal greenhouse gas emissions and other pollutants as compared to conventional technologies. The main focus of this section is to propose the idea of an environmental impact reduction index (EIRI) to quantify this benefit for DG.

### 5.4.1 Introduction

Concerns about greenhouse effect are growing rapidly in the public's view. Greenhouse effect is a result of rising carbon dioxide emissions and other greenhouse gases. It is believed that greenhouse effect will lead to global warming and world-wide climate change. Electricity generation from fossil fuels is the single largest emitter of carbon dioxide. During 1990, it was estimated that the world-wide electricity generation contributed to nearly 35 percent of the world-wide carbon dioxide emissions. Therefore, greenhouse gases should be reduced significantly in order to eliminate the possibility of a world-wide climate change.

As a result, the industrial nations around the globe agreed to cut their greenhouse gas emissions at the conference that was held in Kyoto, Japan in 1997. The Kyoto Protocol plans to reduce emissions by reforming the energy and transportation sector, promoting the usage of renewable energy, improving energy efficiency, and limiting methane emissions from waste management and energy systems. Therefore, this could create a great opportunity for the environmentally friendly generation technologies such as wind and solar systems and fuel cells.

Among the emissions the most damaging ones are carbon dioxide, sulfur dioxide, and nitrogen oxides. Carbon dioxide is believed to be a cause of the greenhouse effect resulting in global warming. Sulfur dioxide is the leading contributor of acid rain. Nitrogen oxides are responsible for smog and also contribute to acid rain. The amount of pollutant emissions from electrical energy production depends on several factors such as the technology employed, fuel used, energy efficiency, and amount of electrical energy produced.



### 5.4.2 Environmental Impact Reduction

Some of the DG technologies have the potential to generate electrical energy with far less environmental impacts. These technologies include wind turbine generation (WTG), solar cells, fuel cells, and microturbines. In general, the amount of pollutant emission is measured in terms of emission produced per unit of energy, such as kilograms per megawatt-hour. Table 5 provides pollutant emissions data for several electricity generation technologies. From Table 5, it is clear that distributed generation technologies lead to significant reductions in emissions as compared to conventional generation technologies such as coal fired power plants.

### 5.4.3 Environmental Impact Reduction Index (EIRI)

It is also useful to develop a suitable index to quantify the benefit of DG in terms of pollutant emission reduction. The basic idea behind the proposed environmental impact reduction index (EIRI) is to compare the emission of a particular pollutant with and without the employment of DG and it can be expressed as:

$$EIRI_i = \frac{PE_{i\ w/DG}}{PE_{i\ wo/DG}} \quad 5.4.3.1$$

for the  $i^{\text{th}}$  pollutant ( $\text{CO}_2$ ,  $\text{SO}_2$ ,  $\text{NO}_x$ , etc.)

where  $PE_{i\ w/DG}$  and  $PE_{i\ wo/DG}$  are the amount of emissions with and without DG respectively.

The amount of emissions of  $i^{\text{th}}$  pollutant without the employment of DG is given as:

$$PE_{i_{\text{wo/DG}}} = \sum_{j=1}^B (EG)_j (AE)_{ij} \quad 5.4.3.2$$

where  $(EG)_j$  is the amount of electrical energy generated by the  $j^{\text{th}}$  conventional power plant (MWh),  $(AE)_{ij}$  is the amount of emissions of  $i^{\text{th}}$  pollutant for  $j^{\text{th}}$  conventional plant per MWh of energy generated, and B is the total number of conventional generators in the system.

With the inclusion of DG, the amount of energy generated by conventional power plants can be reduced. However, the amount of reduction of a particular pollutant will be different for different technologies. Power plant with the highest emission of  $i^{\text{th}}$  pollutant should lower its output to significantly impact  $i^{\text{th}}$  pollutant. The amount of emission of  $i^{\text{th}}$  pollutant with the employment of DG can be expressed as:

$$PE_{i_{\text{w/DG}}} = \sum_{j=1}^B (EG)_{Aj} (AE)_{ij} + \sum_{k=1}^H (EDG)_k (AE)_{ik} \quad 5.4.3.3$$

where  $(EG)_{Aj}$  is the amount of electrical energy generated by the  $j^{\text{th}}$  conventional power plant with the employment of DG (MWh),  $(EDG)_k$  is the amount of energy generated by the  $k^{\text{th}}$  DG plant (MWh),  $(AE)_{ik}$  is the amount of emission of  $i^{\text{th}}$  pollutant for  $k^{\text{th}}$  DG plant per MWh of energy generated, and H is the total number of DG plants in the system.

Once again, the loads supplied at different buses are assumed to be the same both with and without DG.

TABLE 5

A COMPARISON OF POLLUTANT EMISSIONS FROM  
VARIOUS GENERATION TECHNOLOGIES  
[SEE REFERENCES 29 AND 108]

Generation Technologies	CO <sub>2</sub> (kg/MWh, unless indicated otherwise)	SO <sub>2</sub> (kg/MWh, unless indicated otherwise)
Combustion Cycle Gas Turbine	370-420	0.045-0.14
Coal Fired	830-920	0.63-1.37
Wind Turbine (at 5.5m/s)	13-22	0.013-0.02
Micro-Turbine	290-400	Negligible
Fuel Cells:		
Molten Carbonate	350-400	Negligible
Proton Exchange Membrane	500-680	Negligible
Hybrid Solid Oxide	310-350	Negligible
Phosphoric Acid	510-550	Negligible
Photovoltaic:		
Amorphous	Negligible	Negligible
Mono-crystalline	Negligible	Negligible
Multi-crystalline	Negligible	Negligible

TABLE 5 (CONTINUED)  
 A COMPARISON OF POLLUTANT EMISSIONS FROM  
 VARIOUS GENERATION TECHNOLOGIES

Generation Technologies	NO <sub>x</sub> (kg/MWh, unless Indicated otherwise)	CO (kg/MWh, unless indicated otherwise)
Combustion Cycle Gas Turbine	0.65-0.81	N.A.
Coal Fired	0.63-1.56	N.A.
Wind Turbine	0.018-0.027	Negligible
Micro-Turbine	3-50 ppm	3-50 ppm
Fuel Cells:		
Molten Carbonate	Negligible	Negligible
Proton Exchange Membrane	Negligible	Negligible
Hybrid Solid Oxide	Negligible	Negligible
Phosphoric Acid	Negligible	Negligible
Photovoltaic:		
Amorphous	Negligible	Negligible
Mono-crystalline	Negligible	Negligible
Multi-crystalline	Negligible	Negligible

By substituting equations (5.4.3.2) and (5.4.3.3) into equation (5.4.3.1), the result leads to:

$$EIRI_i = \frac{\sum_{j=1}^B (EG)_{Aj} (AE)_{ij} + \sum_{k=1}^H (EDG)_k (AE)_{ik}}{\sum_{j=1}^B (EG)_j (AE)_{ij}} \quad 5.4.3.4$$

Based on this definition, one can conclude that:

$$EIRI_i = \begin{cases} < 1 & \text{DG has decreased impacts due to the } i^{\text{th}} \text{ pollutant} \\ = 1 & \text{DG has no impact} \\ > 1 & \text{DG has increased impacts due to the } i^{\text{th}} \text{ pollutant} \end{cases} \quad 5.4.3.5$$

In reality, power plants emit many pollutants into the atmosphere. Thus, it is useful to define a composite index to include all the major pollutants. This index is given as:

$$EIRI = \sum_{i=1}^{NP} (EI)_i (EIRI)_i \quad 5.4.3.6$$

with

$$0 \leq (EI)_i \leq 1 \quad 5.4.3.7$$

and

$$\sum_{i=1}^{NP} (EI)_i = 1 \quad 5.4.3.8$$

where  $(EI)_i$  is the weighting factor for  $i^{\text{th}}$  pollutant and NP is total number of pollutants under consideration. In general, larger value of  $(EI)_i$  implies a higher impact of  $i^{\text{th}}$  pollutant on the environment.

EIRI can also be used to identify the best locations and ratings for installing DG in the system. The lowest value of EIRI indicates the highest benefit in terms of environmental impact reduction only.

### 5.5 Distributed Generation Benefit Index

Distributed generation benefit index (BI) is a composite index used to measure and quantify the overall benefits of DG. Among the several benefits offered by DG, only three major ones are considered in this work: voltage profile improvement, line loss reduction, and environmental impact reduction. Since, in general, each benefit has different value to the system, a weighting factor for each benefit is included in formulating this index. The expression for BI in equation (5.1.1) becomes:

$$BI = (BW_{VPI})(VPII) + \left( \frac{BW_{LLR}}{LLRI} \right) + \left( \frac{BW_{EIR}}{EIRI} \right) \quad 5.5.1$$

with

$$0 \leq BW_{VPI} \leq 1$$

$$0 \leq BW_{LLR} \leq 1 \quad 5.5.2$$

$$0 \leq BW_{EIR} \leq 1$$

and

$$BW_{VPI} + BW_{LLR} + BW_{EIR} = 1 \quad 5.5.3$$

where  $BW_{VPI}$ ,  $BW_{LLR}$ , and  $BW_{EIR}$  are the benefit weighting factors for voltage profile improvement, line loss reduction, and environmental impact reduction respectively.

Generally, the highest value of VPII implies maximum benefit in terms of voltage profile improvement while the lowest values of LLRI and EIRI imply the highest benefits in terms of line loss reduction and environmental impact reduction respectively.

Therefore, the highest value of BI corresponds to the maximum composite benefit of distributed generation in terms of voltage profile improvement, line loss reduction, and environmental impact reduction. This index can be used to select the best locations and ratings for DG installations to maximize these benefits.

## 5.6 Analysis under Varying Load Conditions

The quantification approach discussed thus far is based on a snapshot of loads at a specific time. However, in practice, loads vary continuously. This implies that all the benefit indices (VPII, LLRI, and EIRI) are functions of time. Moreover, overall benefits of DG will depend on the time of day considered. DG may not be as beneficial under

light load conditions as under heavy load conditions. Therefore, it is useful to modify the indices proposed earlier to include varying load conditions.

One possible approach is to consider loads on an hourly basis and calculate the benefit indices for each hour of the day.

Hour	Results
1	VPII <sub>1</sub> , LLRI <sub>1</sub> , EIRI <sub>1</sub>
2	VPII <sub>2</sub> , LLRI <sub>2</sub> , EIRI <sub>2</sub>
3	VPII <sub>3</sub> , LLRI <sub>3</sub> , EIRI <sub>3</sub>
4	VPII <sub>4</sub> , LLRI <sub>4</sub> , EIRI <sub>4</sub>
:	:
:	:
23	VPII <sub>23</sub> , LLRI <sub>23</sub> , EIRI <sub>23</sub>
24	VPII <sub>24</sub> , LLRI <sub>24</sub> , EIRI <sub>24</sub>

The hourly indices are aggregated to derive weighted values applicable for the whole day. Since, in general, the benefits of DG are less significant under low load conditions as compared to high load conditions, hourly weighting factors are included in the formulation as given below:

$$VPII = \frac{1}{24} \sum_{h=1}^{24} BW_{VPh} \times VPII_h \quad 5.6.1$$



$$LLRI = \frac{1}{24} \sum_{h=1}^{24} BW_{LLh} \times LLRI_h \quad 5.6.2$$

$$EIRI = \frac{1}{24} \sum_{h=1}^{24} BW_{Eih} \times EIRI_h \quad 5.6.3$$

with

$$0 \leq BW_{VP_h} \leq 1$$

$$0 \leq BW_{LLh} \leq 1$$

5.6.4

$$0 \leq BW_{Eih} \leq 1$$

and

$$\sum_{h=1}^{24} BW_{VP_h} = 1$$

$$\sum_{h=1}^{24} BW_{LLh} = 1$$

5.6.5

$$\sum_{h=1}^{24} BW_{Eih} = 1$$

where  $BW_{VP_h}$ ,  $BW_{LL_h}$ , and  $BW_{EI_h}$  are the hourly weighting factors for voltage profile improvement, line loss reduction, and environmental impact reduction respectively for the  $h^{\text{th}}$  hour.  $VPII_h$ ,  $LLRI_h$ , and  $EIRI_h$  are voltage profile improvement index, line loss reduction index, and environmental impact reduction index respectively for the  $h^{\text{th}}$  hour.

The overall distributed generation benefit index under varying load conditions can be calculated by substituting equations (5.6.1), (5.6.2), and (5.6.3) into equation (5.5.1).

### 5.7 Summary

In this chapter, a set of indices is proposed to quantify some of the technical benefits of distributed generation. They are: (i) voltage profile improvement index (VPII), (ii) line loss reduction index (LLRI), (iii) environmental impact reduction index (EIRI), and (iv) distributed generation benefit index (BI). VPII is used to quantify the improvement in the voltage profile (VP) with the inclusion of DG. LLRI deals with line loss reduction that can be achieved with DG. The idea behind the proposed EIRI is to compare the emissions of a particular pollutant with and without the deployment of DG. In addition, an overall benefit index is proposed to integrate all three benefits into one composite index. Both instantaneous loads and time-varying loads are considered. However, it may be sufficient to do the evaluations for just maximum load conditions. The indices proposed in this chapter can assist in identifying the best locations and ratings for DG. This approach is used to evaluate different case study examples in the next chapter.

## CHAPTER VI

### NUMERICAL EXAMPLES AND SIMULATION RESULTS

This chapter presents and discusses simulation results obtained using a simple twelve-bus test system to illustrate the value and use of the proposed indices. In order to evaluate and quantify the benefits of distributed generation, suitable mathematical models for DG systems must be employed along with distribution system models and power flow calculation to arrive at indices of benefits proposed in chapter 5. The results are presented and discussed. The approach to identify best locations and ratings of DG to maximize the overall benefits is illustrated using the examples simulated.

#### 6.1 Description of System under Study

A twelve-bus study system is constructed and used to evaluate the benefits of DG by employing the proposed indices and approach. All per-unit quantities used in this study are on 400 MVA base. This system consists of three conventional generators located at bus 1, bus 5, and bus 12 with ratings of 1.0, 0.75, and 0.625 pu respectively as listed in Table 6. The significant emissions of each of the generators are listed in Table 7. A total load of 2.013 pu located unevenly on every bus is assumed as listed in Table 8. Resistance and reactance of all the distribution lines are assumed to be 0.000625 pu/km and 0.00375 pu/km respectively [109-111]. The lengths of the distribution lines are

listed in Table 9. The sets of weighting factors assumed for each bus are listed in Table 10. Figure 27 shows a one-line diagram of the system under study.

## 6.2 Study Procedure

To evaluate and quantify some of the technical benefits of distributed generation, several steps are required. They are listed below:

1. Appropriate distributed generation models developed in Chapter 3 are employed to determine the power outputs of distributed generators.
2. A twelve-bus system is constructed and used to study voltage profile, line losses, and pollutant emissions of the system for the base case (no DG) and for the cases with the employment of DG.
3. Power flow calculations<sup>1</sup> are performed using PowerWorld simulation computer program<sup>2</sup> for selected cases to arrive at indices of benefits proposed in this work.
4. Simulation results are presented and discussed to arrive at conclusions for the best locations and ratings of DG installations.

## 6.3 Case Studies and Simulation Results

Four cases are simulated and studied for assessing voltage profile improvement, line loss reduction, and environmental impact reduction. For each case, the influence of varying ratings and operating power factors of DG are investigated. DG ratings of 0.1, 0.2, and 0.3 pu and DG power factors of 0.8 (lag), 0.9 (lag), unity, 0.9 (lead), and 0.8

---

<sup>1</sup> An example 5-bus load flow program is presented in Appendix D.

<sup>2</sup> PowerWorld simulator is an interactive power simulation package designed to simulate high voltage power system operation. PowerWorld simulator is developed, produced, and marketed by PowerWorld Corporation ([www.powerworld.com](http://www.powerworld.com)).

(lead) are employed. Emissions from distributed generators are considered to be negligibly small in this study. The cases considered are listed below:

Case 1) DG located at bus 9

Case 2) DG located at bus 10

Case 3) 50% of DG is located at bus 9 and the remaining 50% is located at bus 10

Case 4) 50% of DG is located at bus 9 and the remaining 50% is located at bus 4

TABLE 6  
CONVENTIONAL GENERATOR INFORMATION

Generator Number	Type	Location (Bus Number)	Rating (pu)
1	Coal fired	1	1
2	Combustion Cycle Gas Turbine	5	0.75
3	Coal fired	12	0.675

TABLE 7  
IMPORTANT POLLUTANT EMISSIONS OF CONVENTIONAL GENERATORS EMPLOYED

Generator Number	CO <sub>2</sub> in kg/MWh	SO <sub>2</sub> in kg/MWh	NO <sub>x</sub> in kg/MWh
1	850	1.0	1.2
2	400	0.7	0.8
3	900	1.1	1.4

TABLE 8  
LOAD DATA FOR SYSTEM  
UNDER STUDY

Load Point	Load (pu)	Power Factor (lag)
L1	0.425	0.96
L2	0.125	0.98
L3	0.250	0.96
L4	0.200	0.95
L5	0.175	0.96
L6	0.050	0.97
L7	0.175	0.94
L8	0.050	0.97
L9	0.113	0.97
L10	0.150	0.97
L11	0.075	0.95
L12	0.225	0.93

TABLE 9  
DISTRIBUTION LINE LENGTH DATA

From Bus	To Bus	Length (km)
1	2	30
1	3	50
2	3	40
2	6	10
3	4	20
3	5	30
4	5	40
4	8	30
5	7	30
6	8	20
6	9	10
7	11	20
8	10	10
8	11	30
11	12	20

TABLE 10  
ASSUMED BUS WEIGHTING FACTOR SETS

Bus	Set#1	Set#2	Set#3	Set#4	Set#5
1	0.083	0.211	0.115	0.300	0.200
2	0.083	0.062	0.034	0.036	0.050
3	0.083	0.124	0.068	0.200	0.120
4	0.083	0.099	0.054	0.058	0.070
5	0.083	0.087	0.048	0.050	0.080
6	0.083	0.025	0.150	0.014	0.020
7	0.083	0.087	0.048	0.050	0.070
8	0.083	0.025	0.150	0.014	0.100
9	0.083	0.056	0.031	0.033	0.060
10	0.083	0.075	0.041	0.043	0.070
11	0.083	0.037	0.200	0.022	0.030
12	0.083	0.112	0.061	0.180	0.130



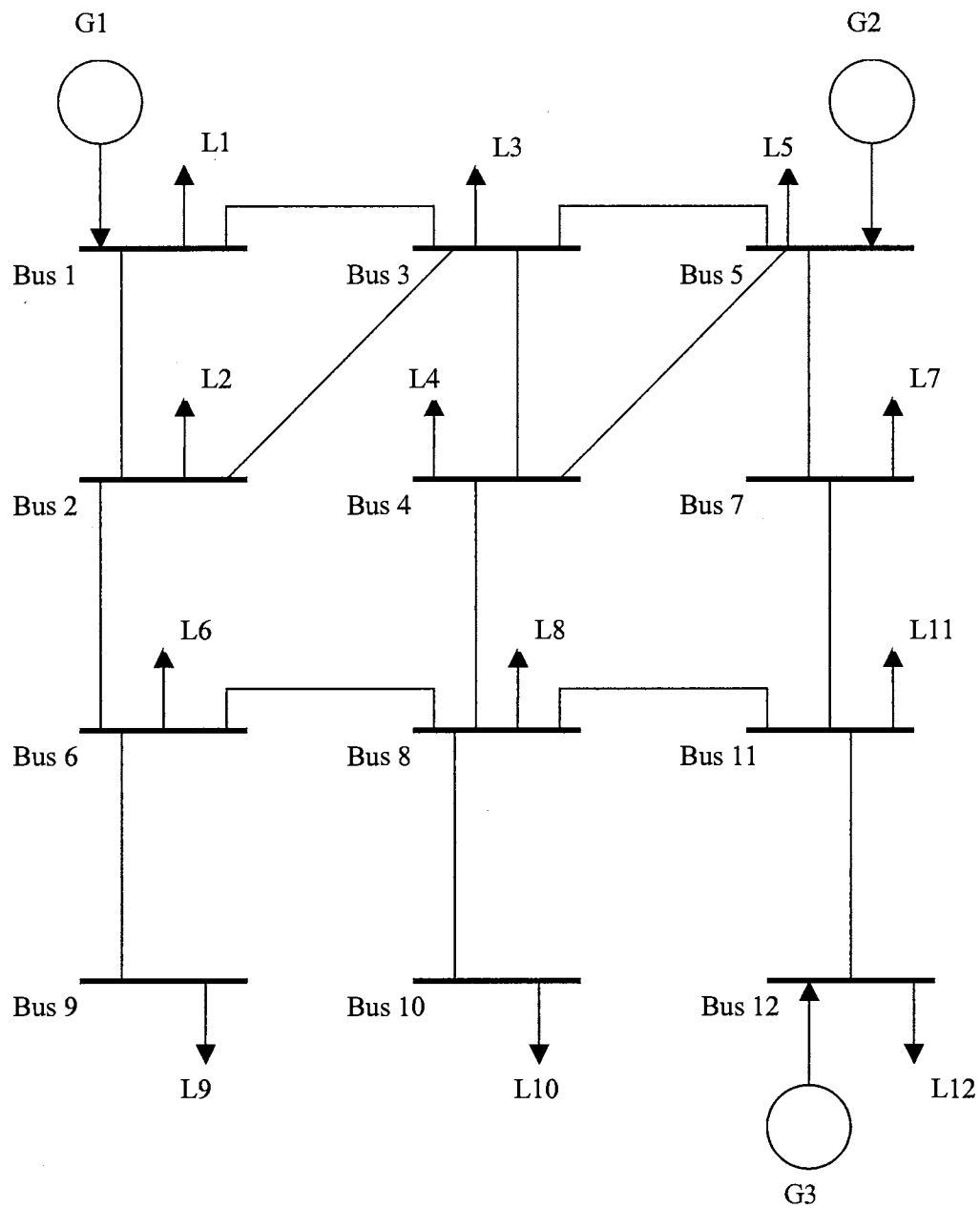


Figure 27. A Single Line Diagram of the System under Study

## 6.4 Discussion of Results

The results clearly indicate that installation of DG can improve the system voltage profile, reduce electrical line losses, and reduce environmental impacts. Simulation results obtained for the cases studied are discussed below.

### 6.4.1 Voltage Profile Improvement Results

Bus weighting factors are significant in determining VP<sub>II</sub>. They should be selected with care. To study their impact, four sets of bus weighting factors (sets 1 through 4) as listed in Table 10 are used to quantify the voltage profile improvement and the results are shown in Figure 28. It can be seen that VP<sub>II</sub> exhibits the highest value under weighting factor set#1 (equal weights). With weighting factor set#4 (importance given to high load buses), the VP<sub>II</sub> has the lowest value. This is due to the fact that voltages at high load buses before employing DG (base case) are relatively high as compared to low load buses. Therefore, the voltage profile improvement at high load buses with the employment of DG is not as significant as the improvement at low load buses. As a result, the VP<sub>II</sub> with bus weighting factor set#3 (importance given to low load bus) is higher than for the case with weighting factor set#4.

DG rating plays a significant role in determining VP<sub>II</sub> as shown in Figure 29. As the DG rating increases, VP<sub>II</sub> also increases. The location and operating power factor of DG are also important factors in improving the voltage profile. Generally, DG can supply reactive power to the system under lagging power factor operating conditions, thus helping to support the system voltage profile. With leading power factor operation, DG draws reactive power from the system, thus causing higher voltage drops in the lines.

It can be seen from Figures 30-32 that VPII decreases as DG operating power factor varies from lagging to unity. In addition, DG has not been beneficial to the system ( $VPII < 1$ ) under leading power factor conditions.

It should be noted that voltages at every bus before employing DG (base case) was maintained within 5% of the reference voltage (1 pu). Therefore, an improvement of about 0.4%-1.5% indicates a reasonably good and significant impact on voltage profile.

#### 6.4.2 Line Loss Reduction Results

Simulation results show that DG significantly reduces electrical line losses in the system. For the cases considered, up to 46% reduction ( $(1-LLRI) \times 100$ ) (case 3 with 0.3 pu rating and 0.8 pf lag) is achieved with the employment of DG. The rating, location, and operating power factor of DG are all very important contributing factors in determining the amount of line loss reduction. Generally, LLRI decreases as DG rating increases. However, higher DG penetration cannot always guarantee lower line losses. For example, as DG rating increases from 0.2 to 0.3 pu in cases 1 and 2, the rate of decrease actually declines as shown in Figure 33. This fact should be taken into account before determining the rating of DG.

The results also indicate that DG operating power factor plays a vital role in line loss reduction. It can be seen from Figures 34-36 that LLRI exhibits the lowest value under lagging power factor conditions and sharply increases (lower line loss reductions) under leading power factor conditions because DG draws reactive power from the system. This increases the current in the lines, resulting in higher electrical line losses.

### 6.4.3 Environmental Impact Reduction Results

Among several pollutant emissions, only three major ones are considered in this study: Carbon Dioxide ( $\text{CO}_2$ ), Sulfur Dioxide ( $\text{SO}_2$ ), and Nitrogen Oxides ( $\text{NO}_x$ ). In general, the weighting factor for each pollutant can be set to emphasize certain pollutants by using equations (5.4.3.7) and (5.4.3.8). However, in this study, it is assumed that all the pollutants are equally weighted. The results clearly indicate that DG significantly reduces emissions of carbon dioxide, sulfur dioxide, and nitrogen oxides. As with other benefits, the amount of pollutant emissions reduction depends on the locations and ratings of DG. As DG rating goes up, the EIRI of  $\text{CO}_2$ ,  $\text{SO}_2$ , and  $\text{NO}_x$  significantly decrease as shown in Figures 37-39. In addition, the overall EIRI encompassing all three pollutant emissions also significantly decreases as DG rating goes up as shown in Figure 40.

Since each conventional generator emits different amounts of pollutants, the locations and operating power factors of DG can influence the amount of emission reductions. Simulation results indicate that EIRI for each pollutant and the overall EIRI exhibit the lowest value under lagging power factor operating conditions and slightly increase under leading power factor conditions as shown in Figures 41-52. However, the impacts of locations and operating power factors of DG are relatively small as compared to the impact of the ratings of DG. This is because the amount of real power generated by DG is the same at all DG operating power factors. As a result, the amount of real power generated by conventional generators with the employment of DG does not change much except for changes in line losses, resulting only in small changes in emissions.

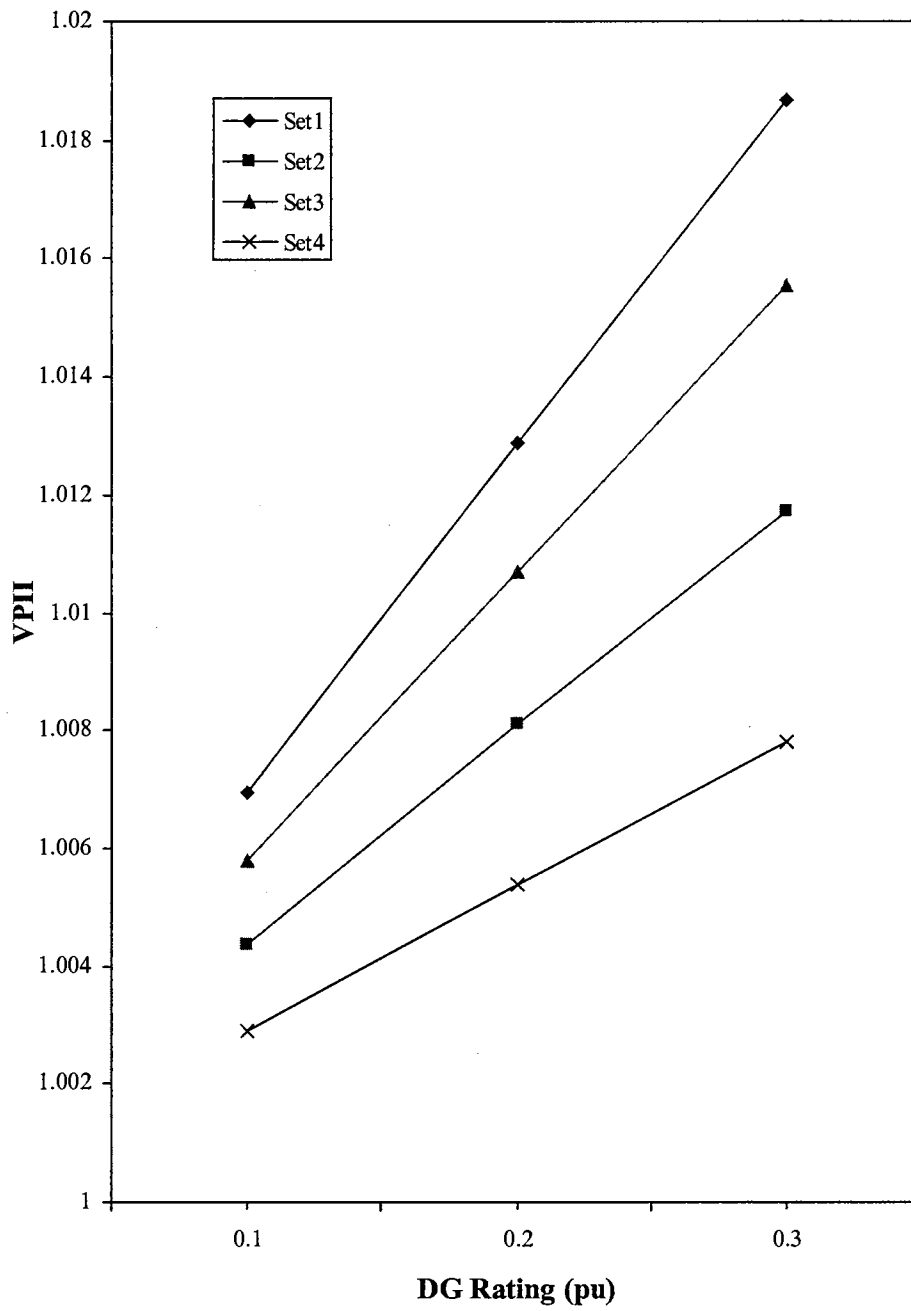


Figure 28. Variation of Voltage Profile Improvement Index with DG Rating for Different Sets of Bus Weighting Factors (case 3 with DG operating at 0.9 pf lag)

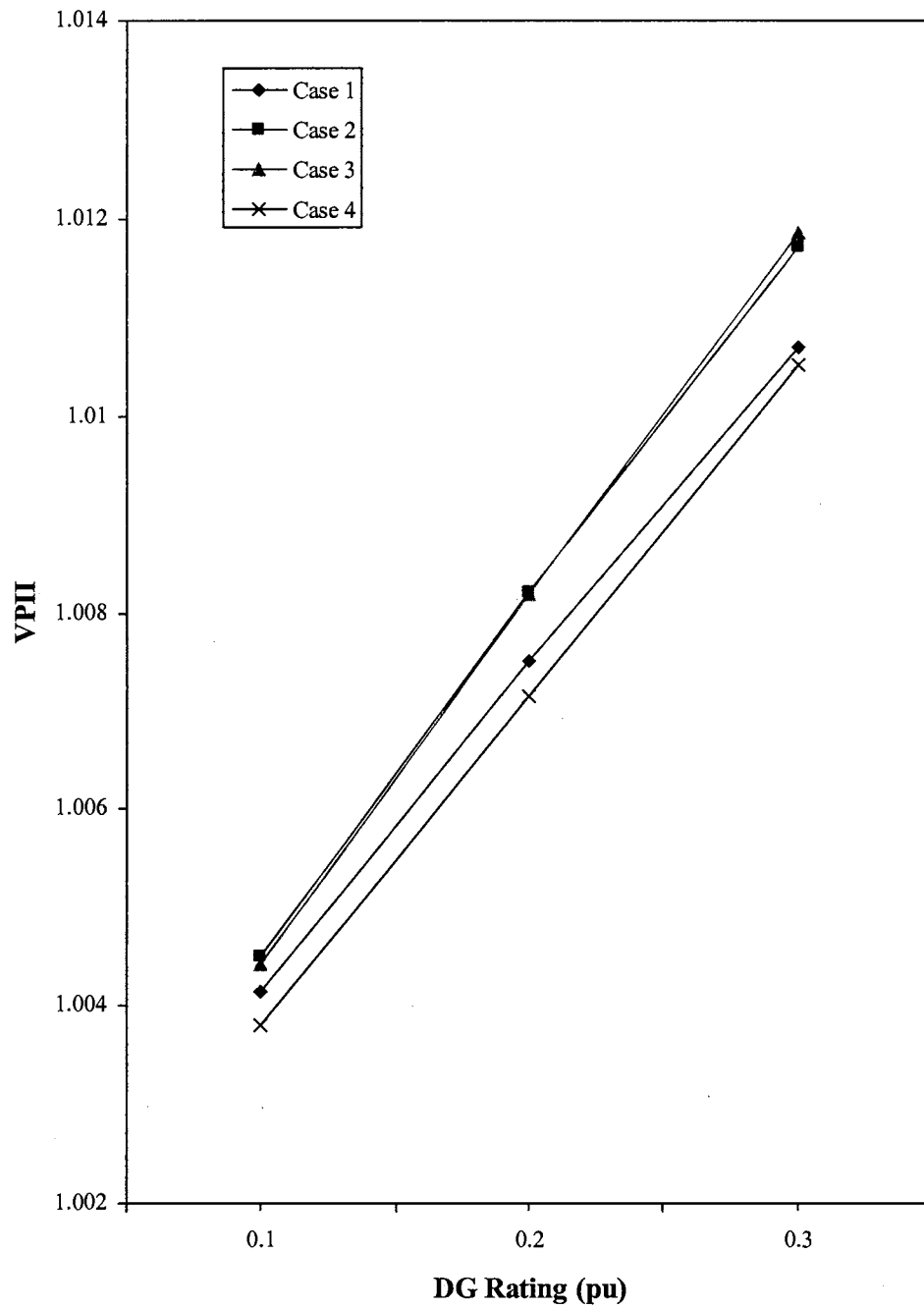


Figure 29. Variation of Voltage Profile Improvement Index with Different DG Ratings (DG Operating at 0.9 pf lag and Weighting Factor Set#5 used)

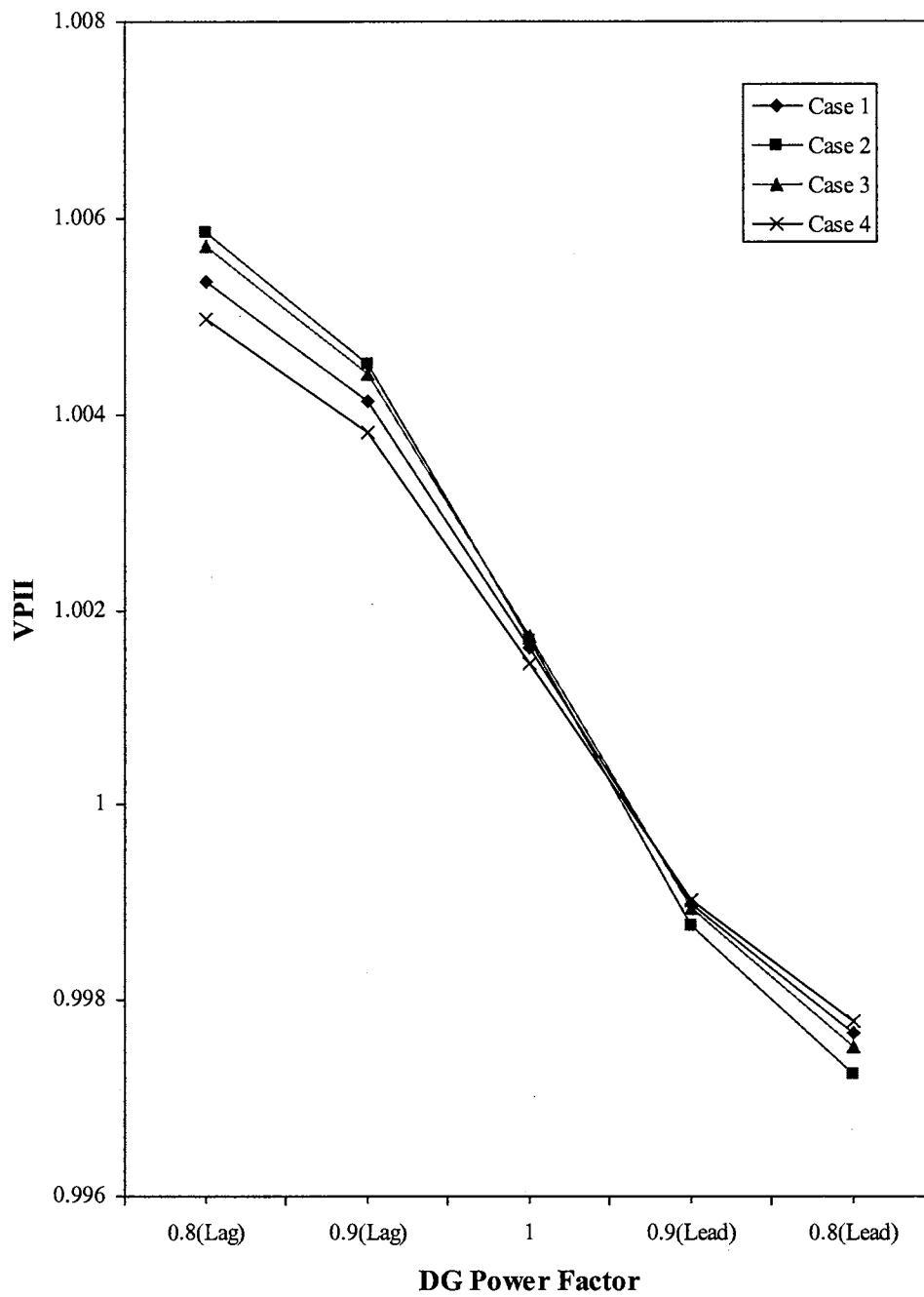


Figure 30. Impact of DG Operating Power Factor on Voltage Profile Improvement Index (DG Rating is 0.1 pu and Weighted Factor Set#5 used)

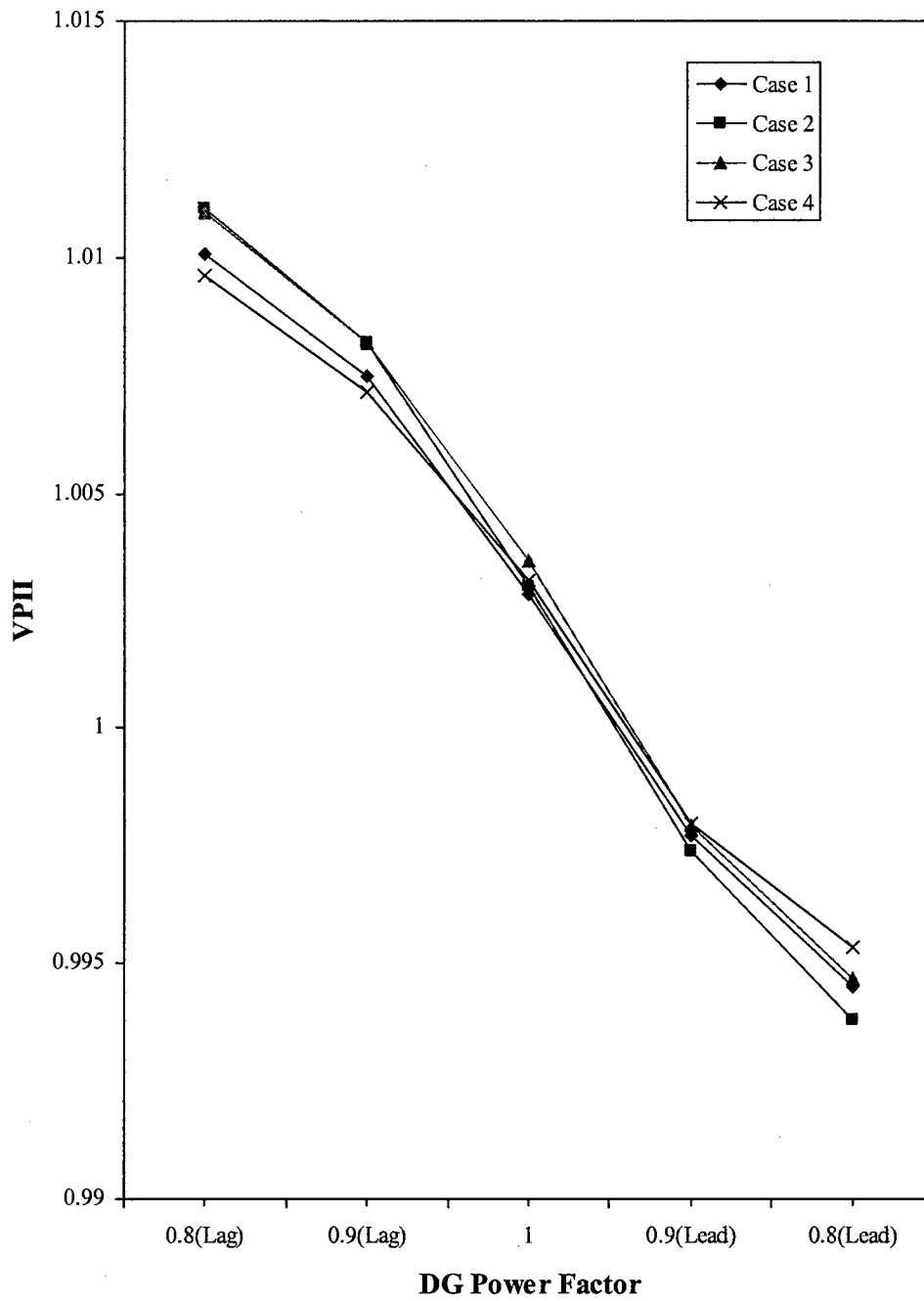


Figure 31. Impact of DG Operating Power Factor on Voltage Profile Improvement Index (DG Rating is 0.2 pu and Weighted Factor Set#5 used)



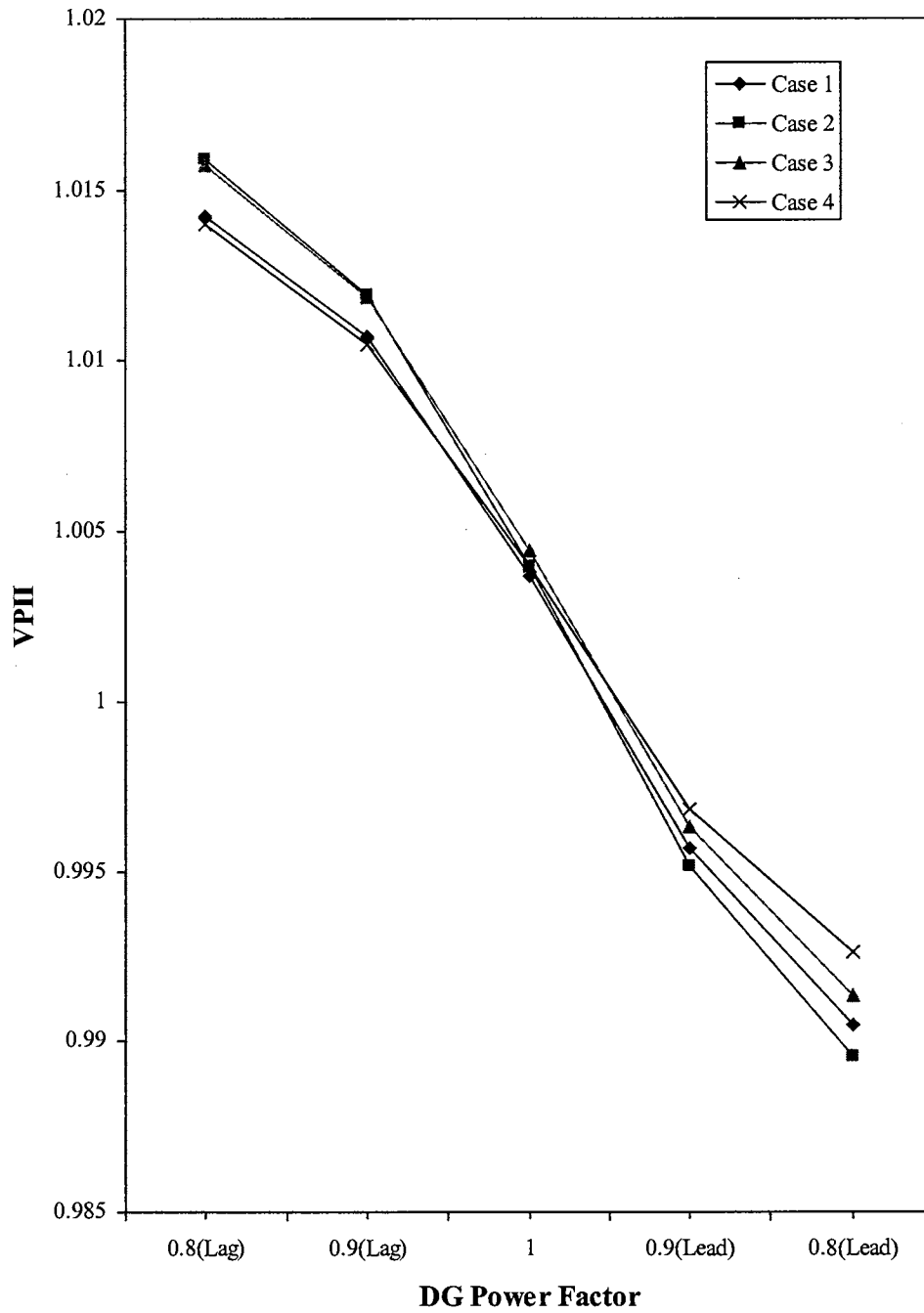


Figure 32. Impact of DG Operating Power Factor on Voltage Profile Improvement Index (DG Rating is 0.3 pu and Weighted Factor Set#5 used)

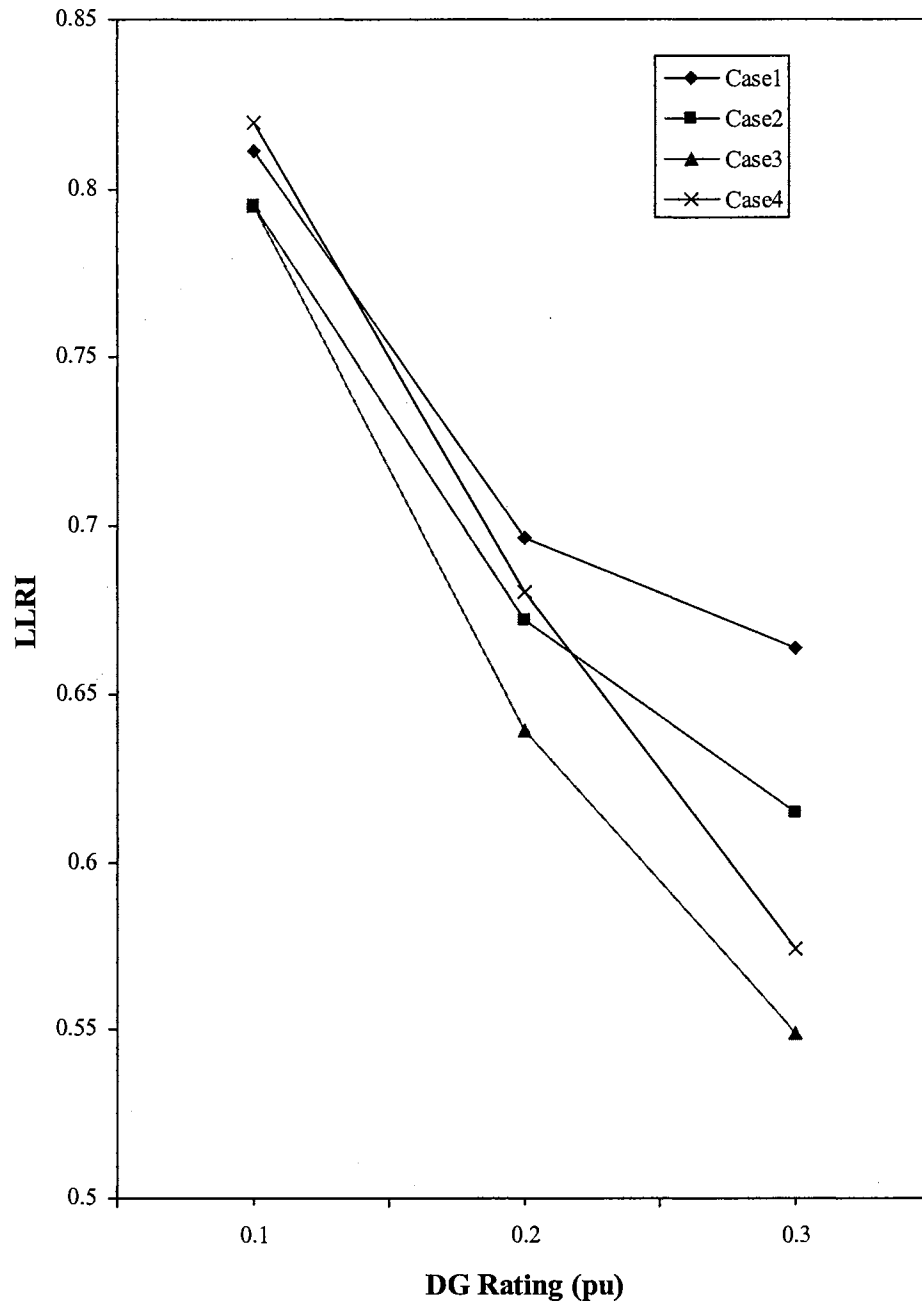


Figure 33. Variation of Line Loss Reduction Index with DG Rating (DG Operating at 0.9 pf lag)

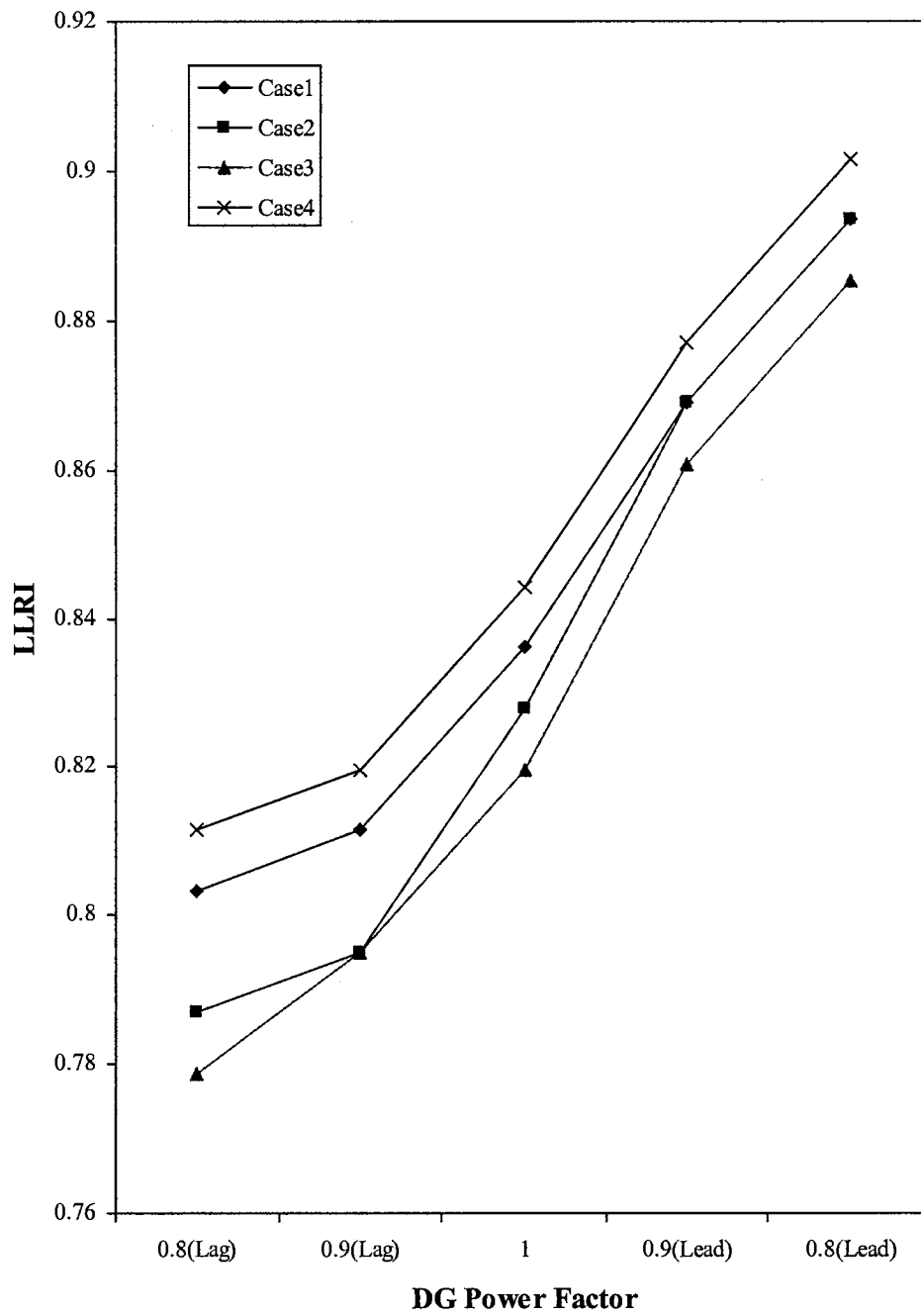


Figure 34. Impact of DG Operating Power Factor on Line Loss Reduction Index (DG Rating is 0.1 pu)

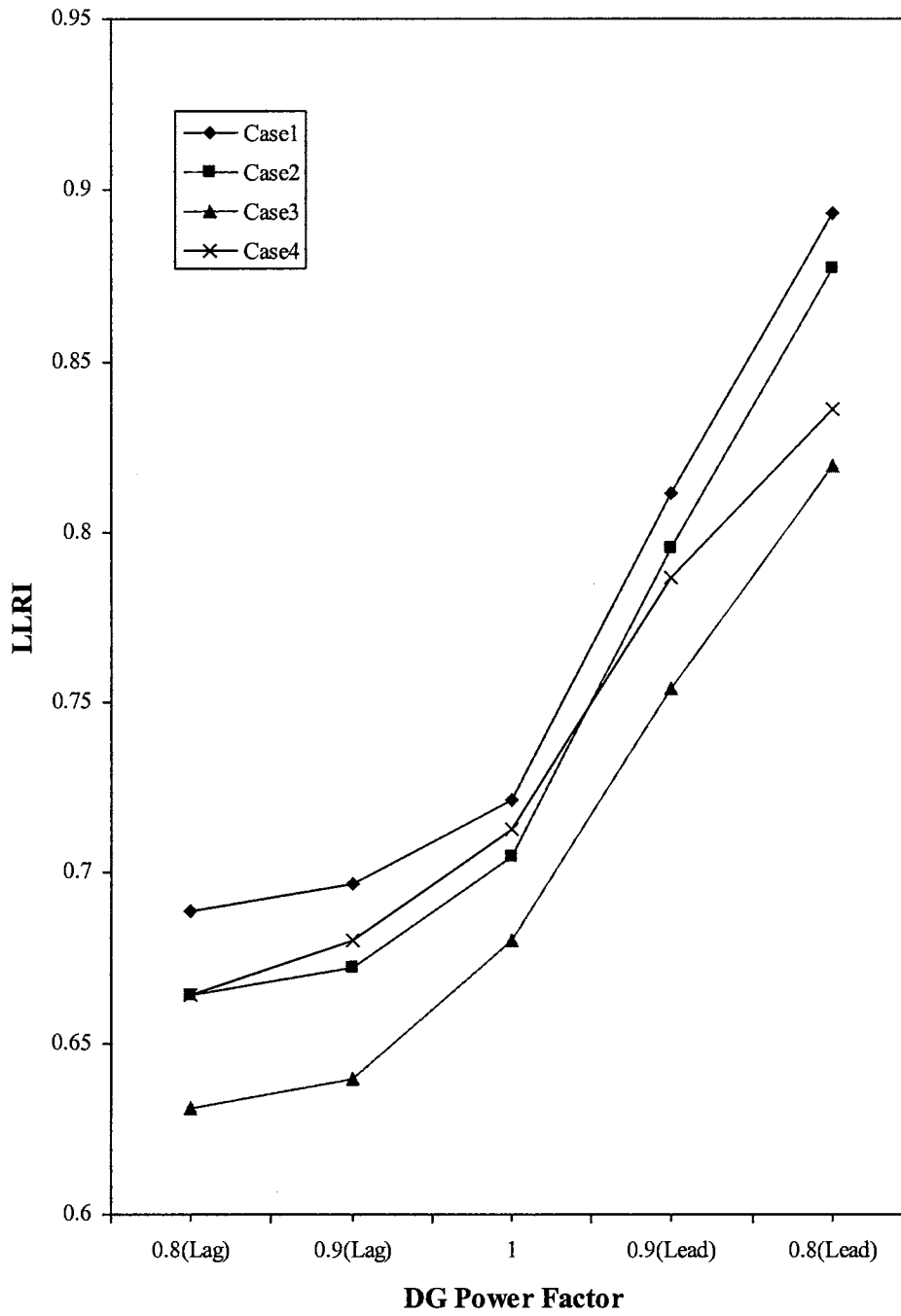


Figure 35. Impact of DG Operating Power Factor on Line Loss Reduction Index (DG Rating is 0.2 pu)

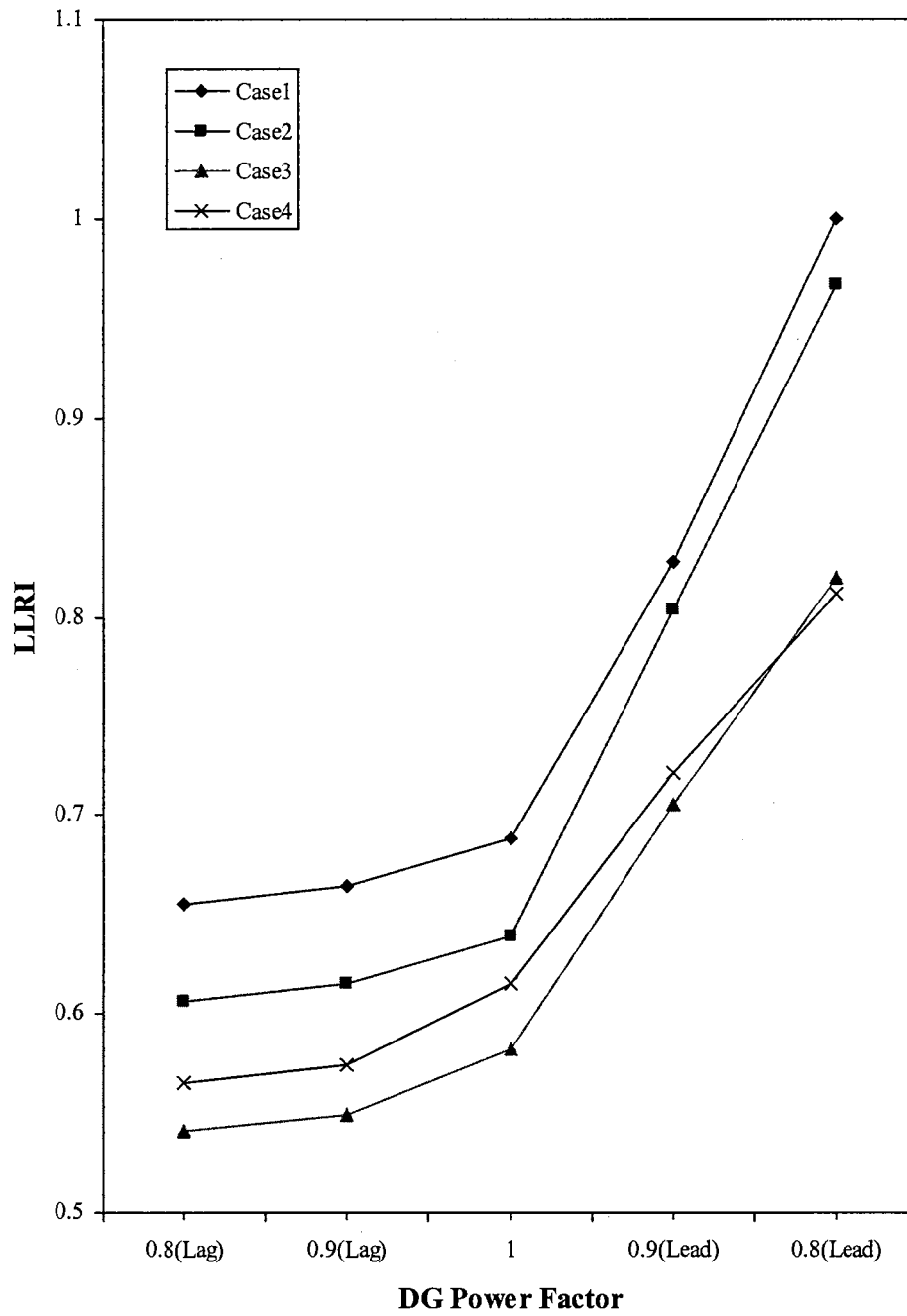


Figure 36. Impact of DG Operating Power Factor on Line Loss Reduction Index (DG Rating is 0.3 pu)

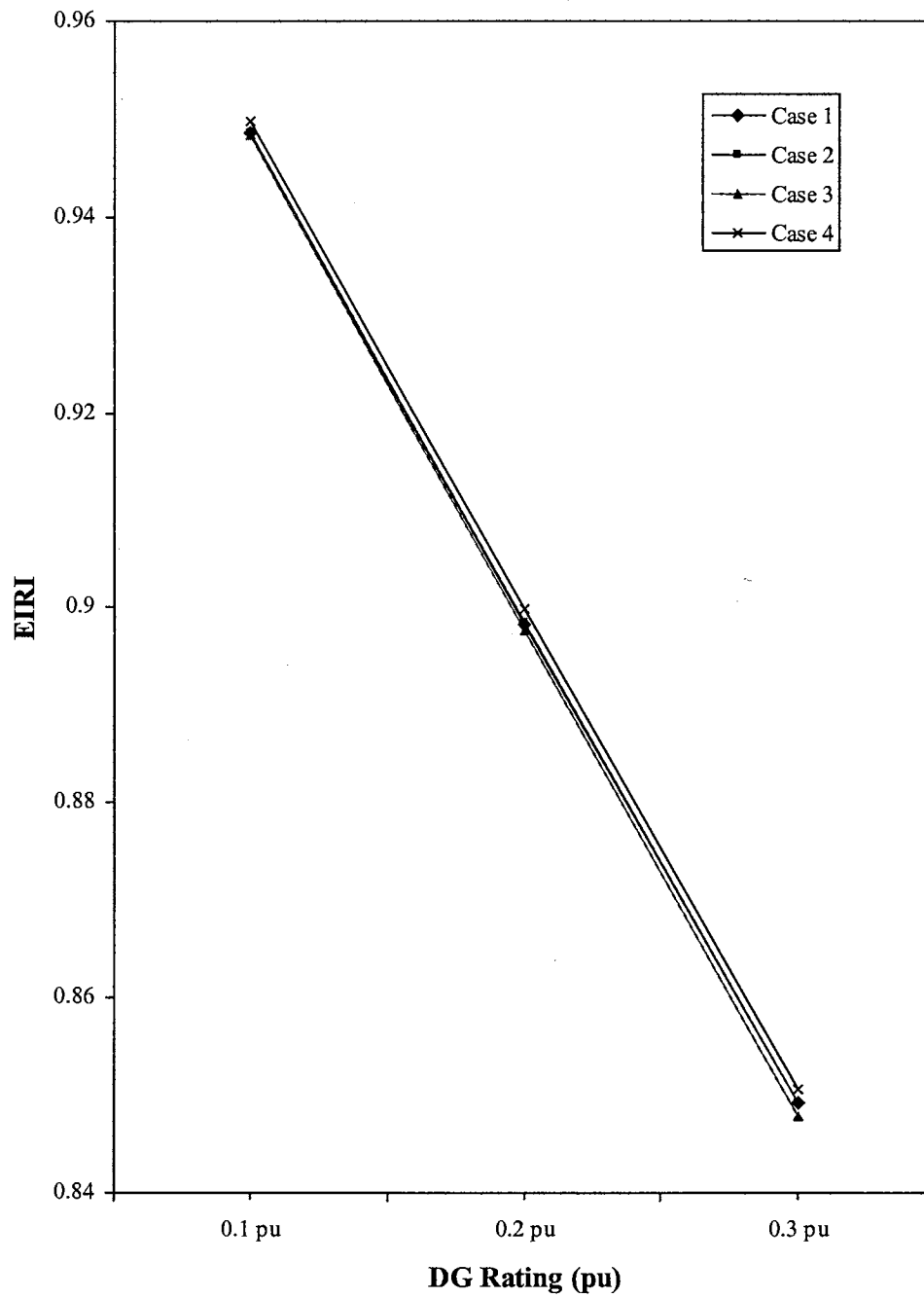


Figure 37. Variation of Environmental Impact Reduction Index for Carbon Dioxide for Different DG Ratings (DG operating at 0.9 pf lag)

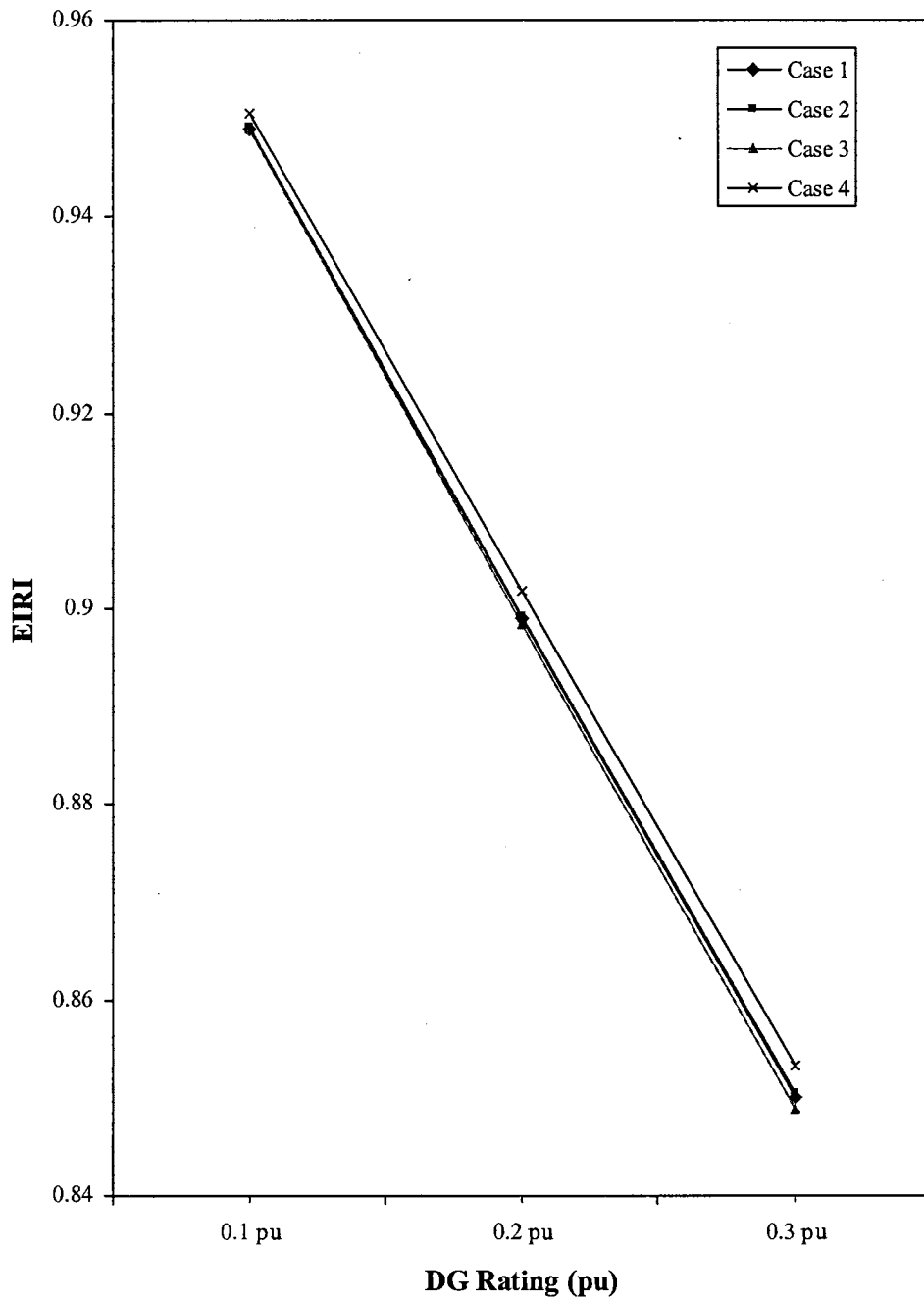


Figure 38. Variation of Environmental Impact Reduction Index for Sulfur Dioxide for Different DG Ratings (DG operating at 0.9 pf lag)

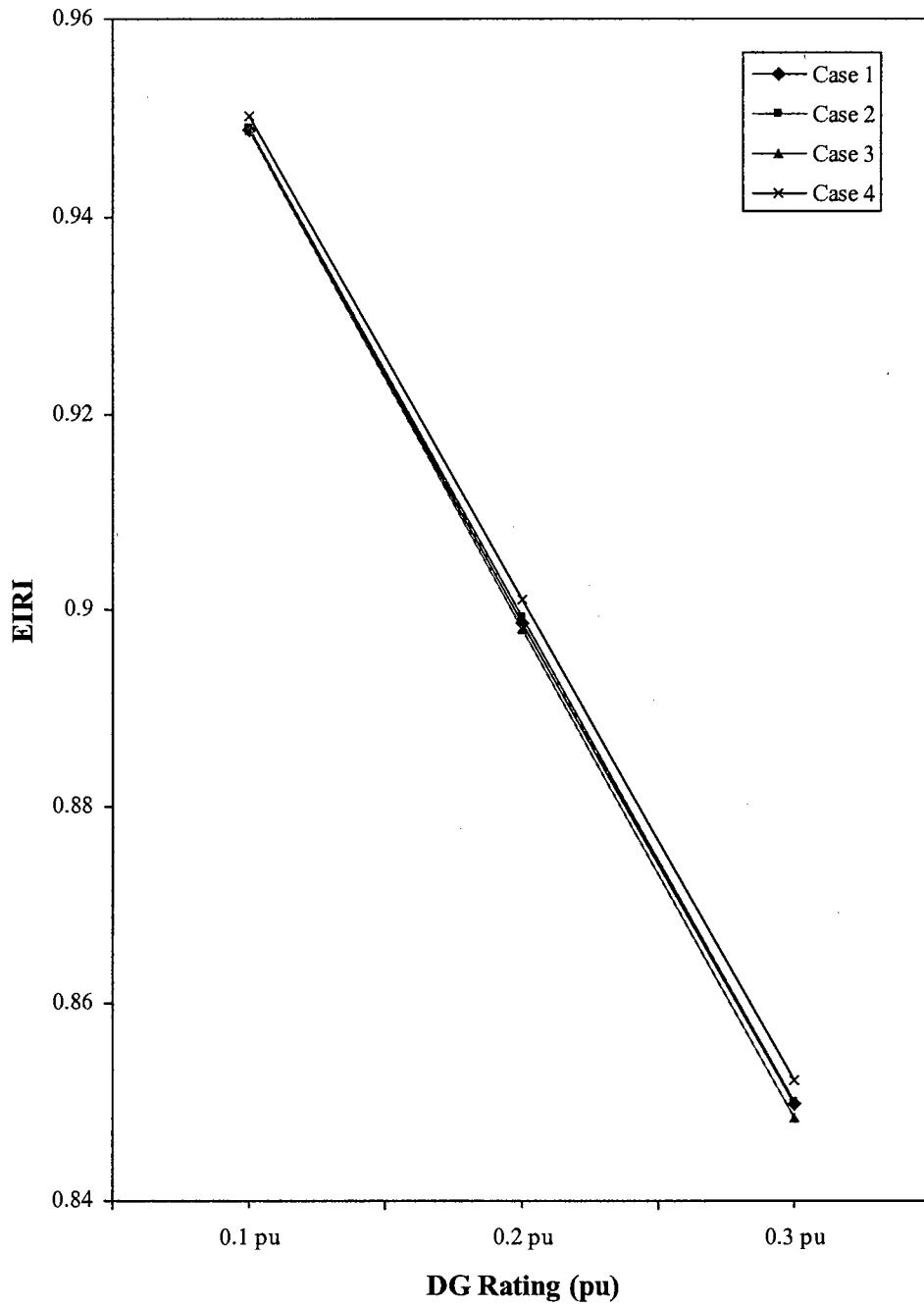


Figure 39. Variation of Environmental Impact Reduction Index for Nitrogen Oxides for Different DG Ratings (DG operating at 0.9 pf lag)



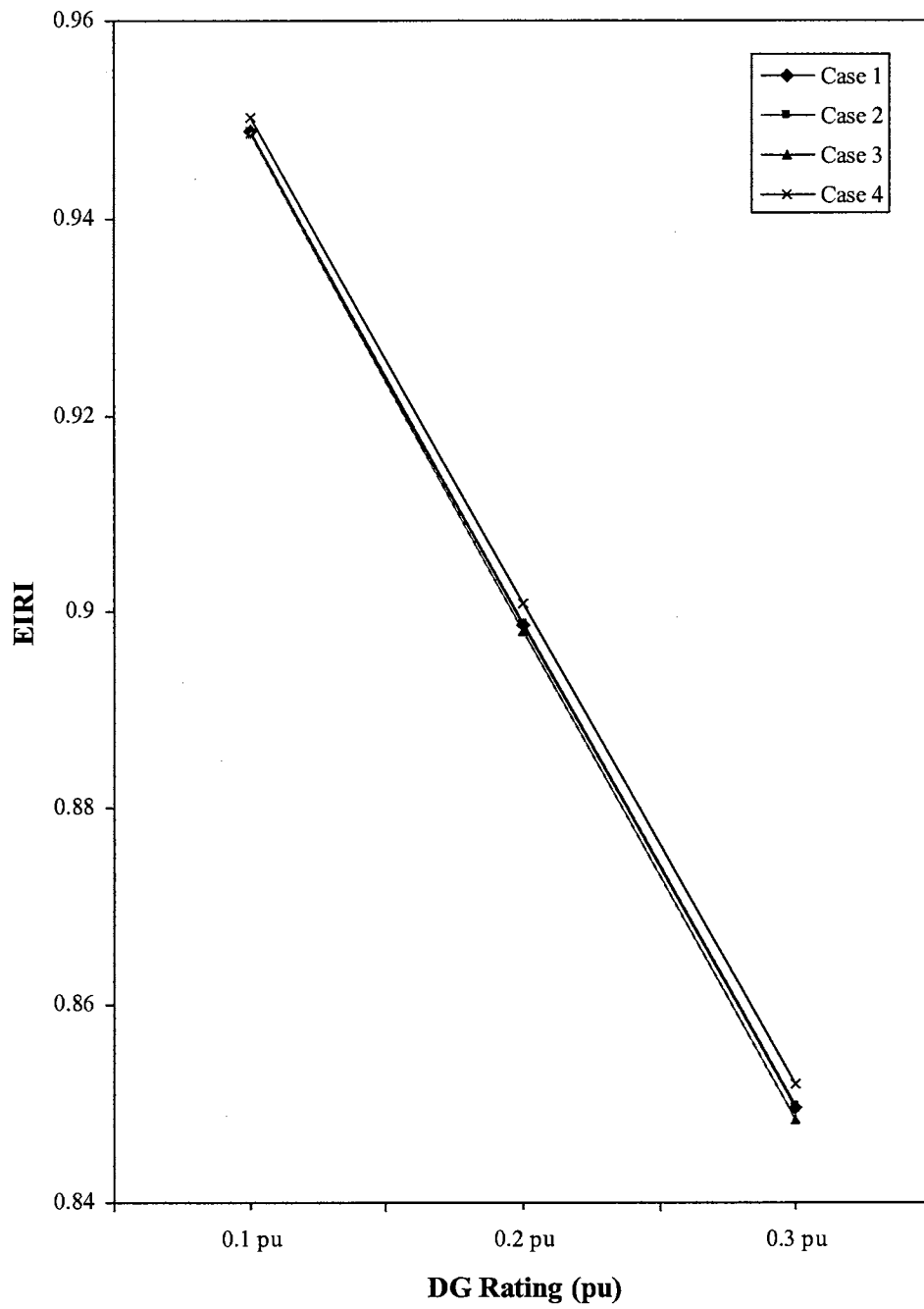


Figure 40. Variation of the Overall Environmental Impact Reduction Index for Different DG Ratings (DG Operating at 0.9 pf lag)

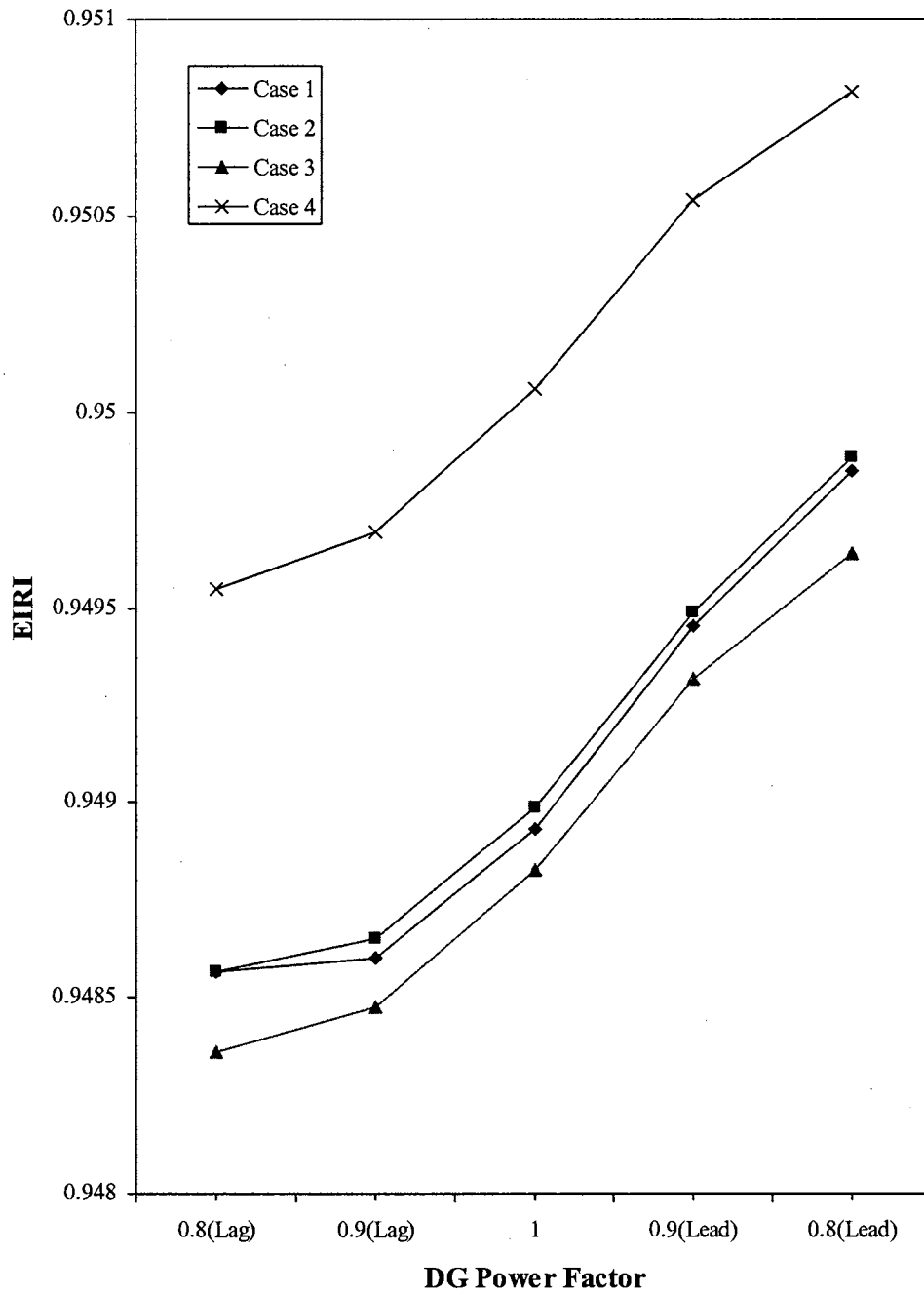


Figure 41. Impact of DG Operating Power Factor on Environmental Impact Reduction Index for Carbon Dioxide (DG Rating is 0.1 pu)

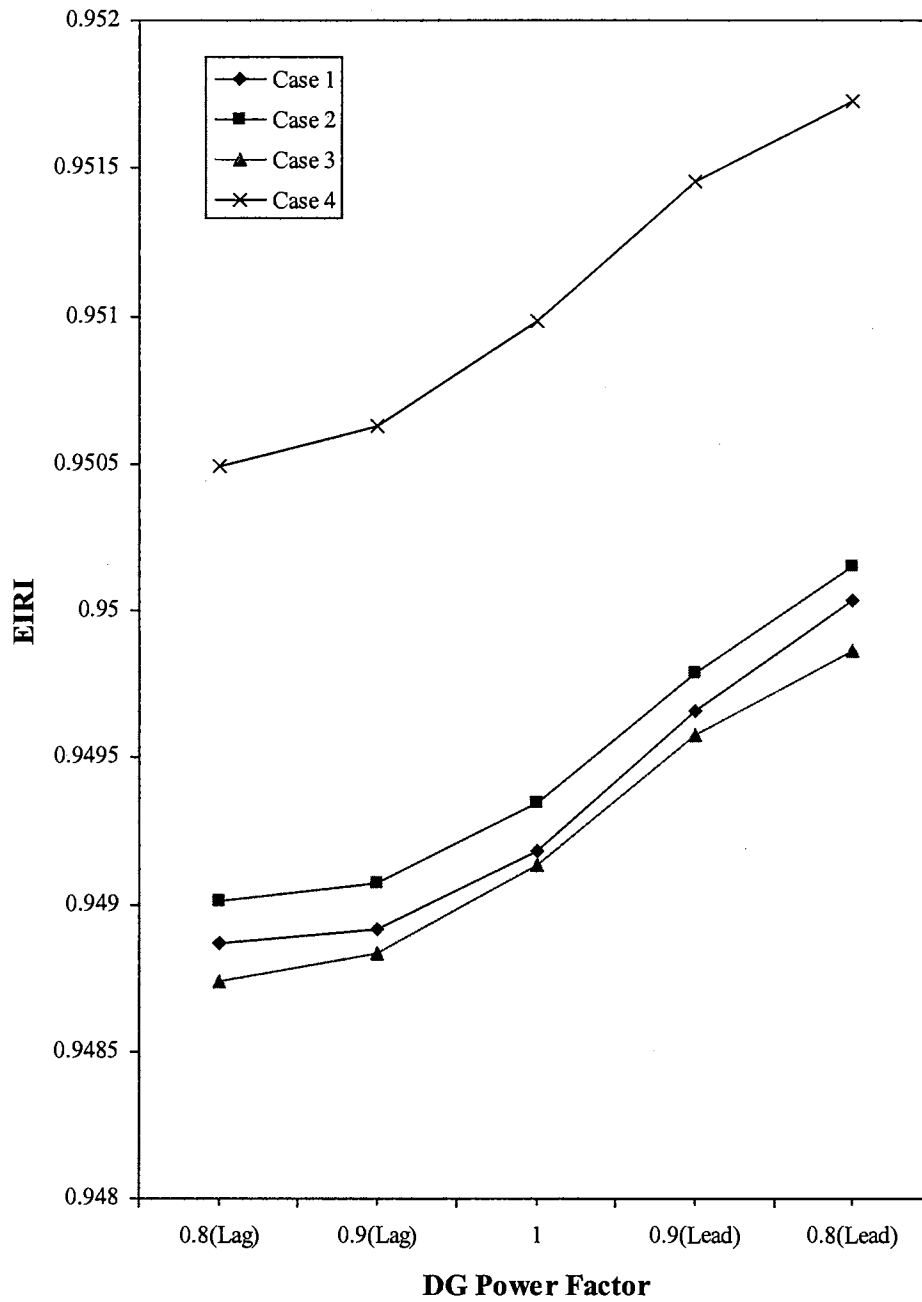


Figure 42. Impact of DG Operating Power Factor on Environmental Impact Reduction Index for Sulfur Dioxide (DG Rating is 0.1 pu)

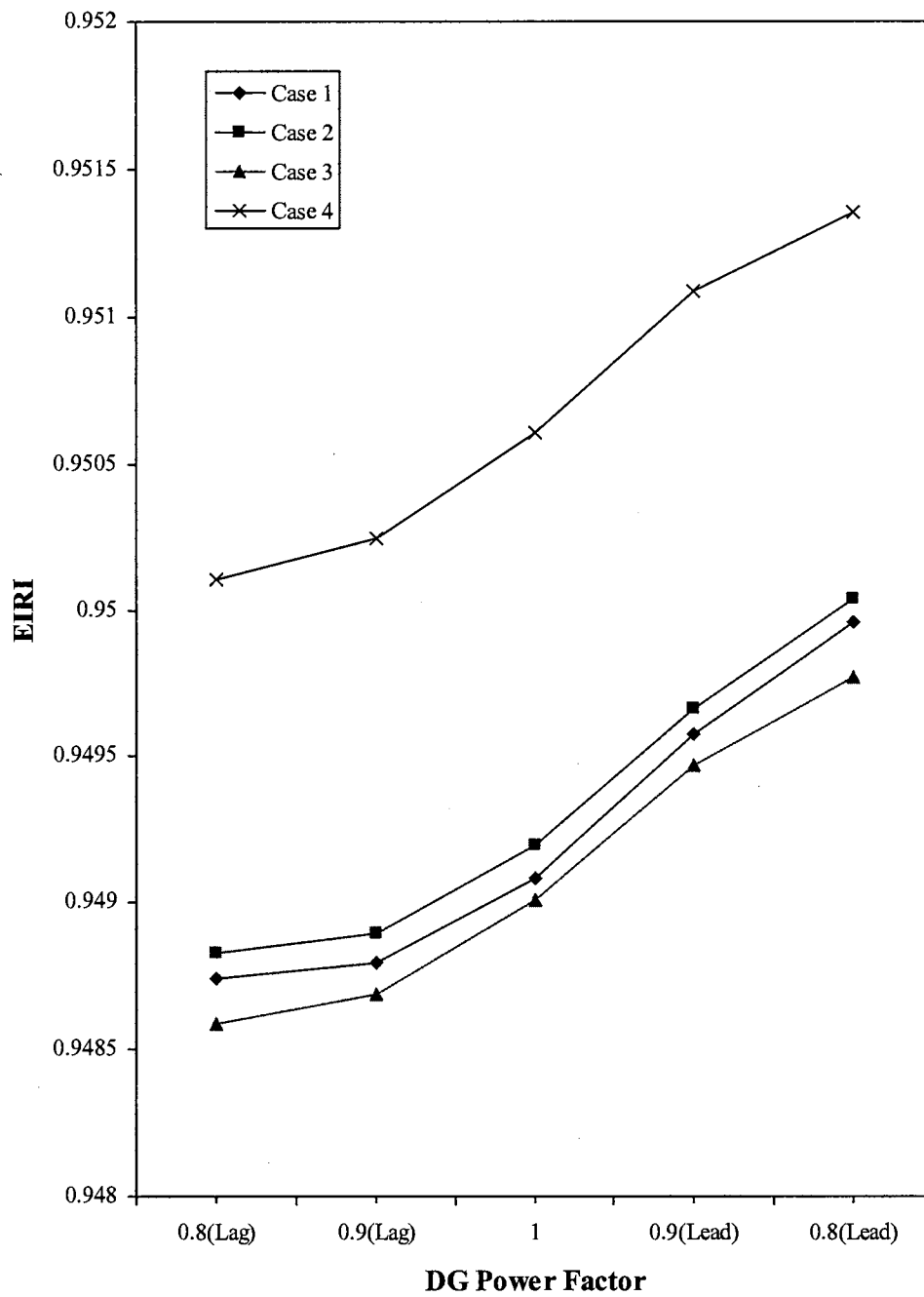


Figure 43. Impact of DG Operating Power Factor on Environmental Impact Reduction Index for Nitrogen Oxides (DG Rating is 0.1 pu)

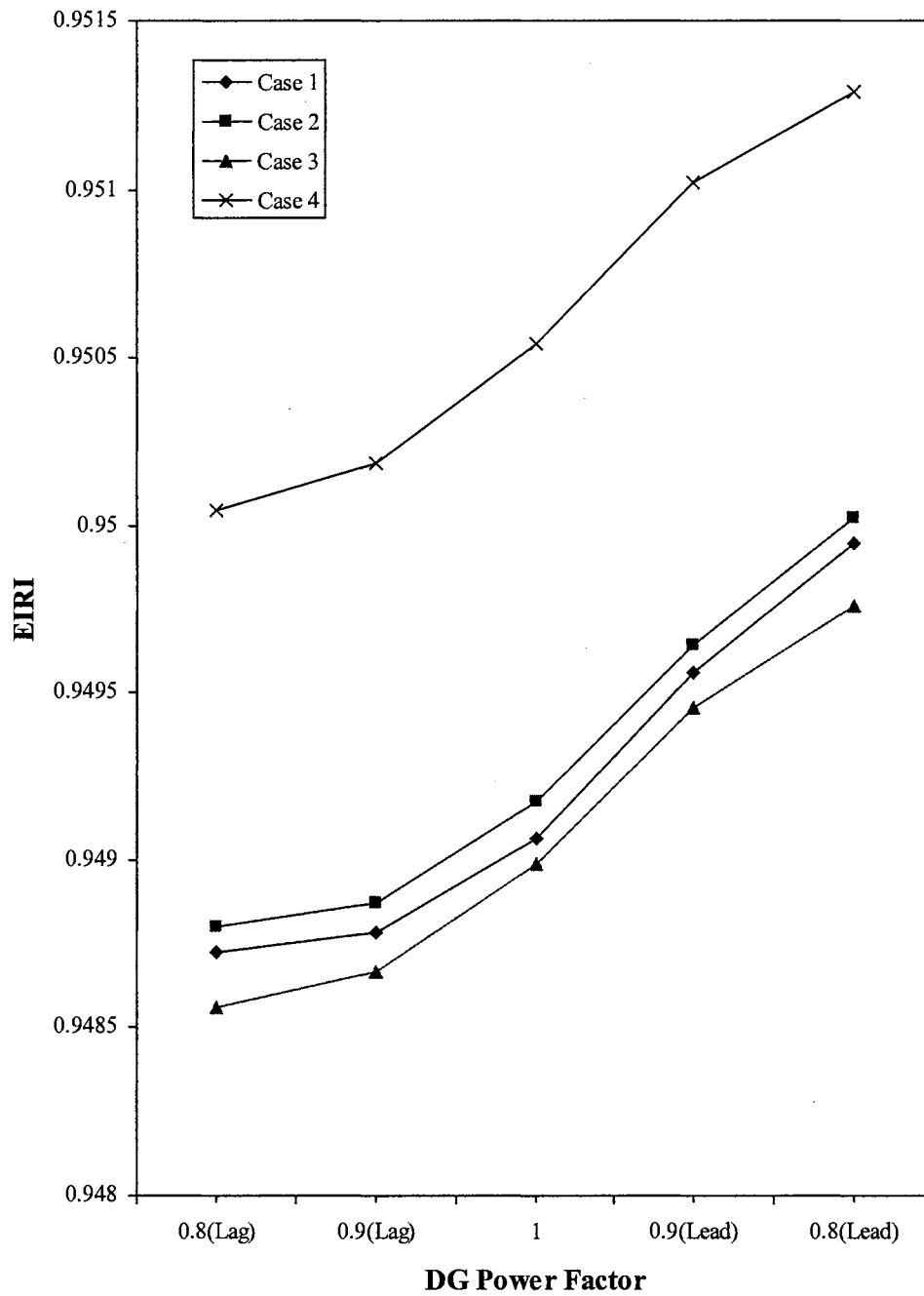


Figure 44. Impact of DG Operating Power Factor on the Overall Environmental Impact Reduction Index (DG Rating is 0.1 pu)

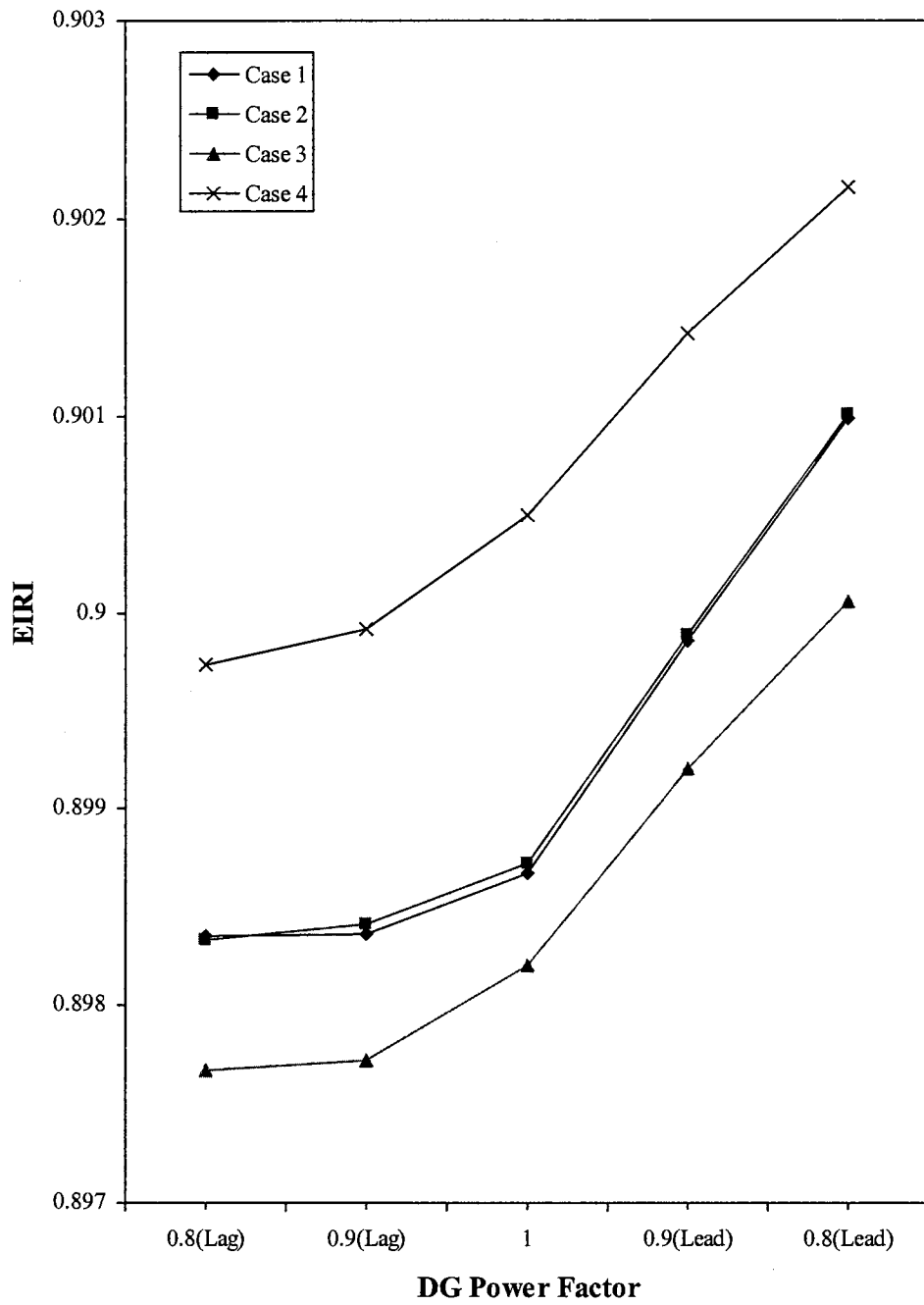


Figure 45. Impact of DG Operating Power Factor on Environmental Impact Reduction Index for Carbon Dioxide (DG Rating is 0.2 pu)

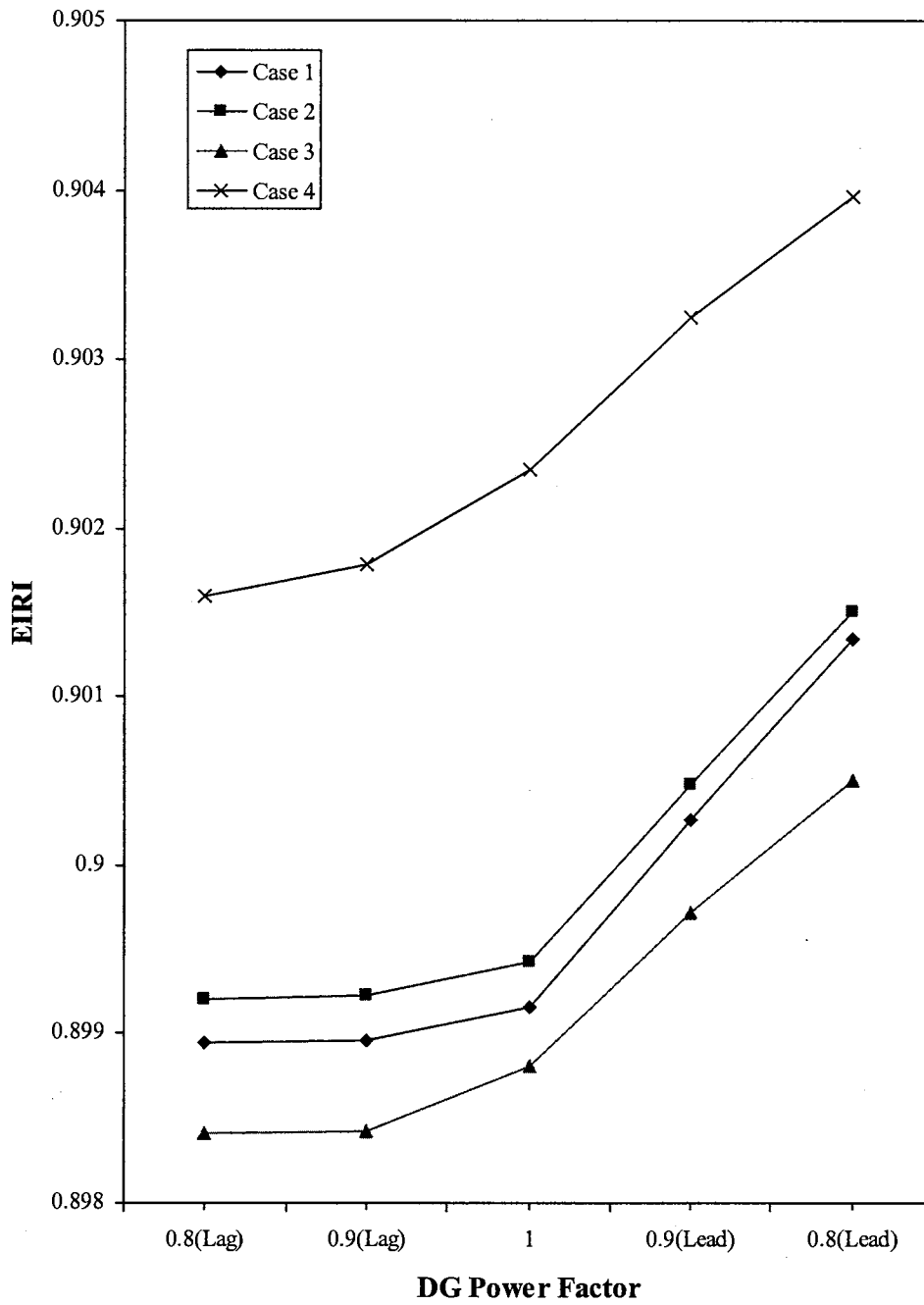


Figure 46. Impact of DG Operating Power Factor on Environmental Impact Reduction Index for Sulfur Dioxide (DG Rating is 0.2 pu)

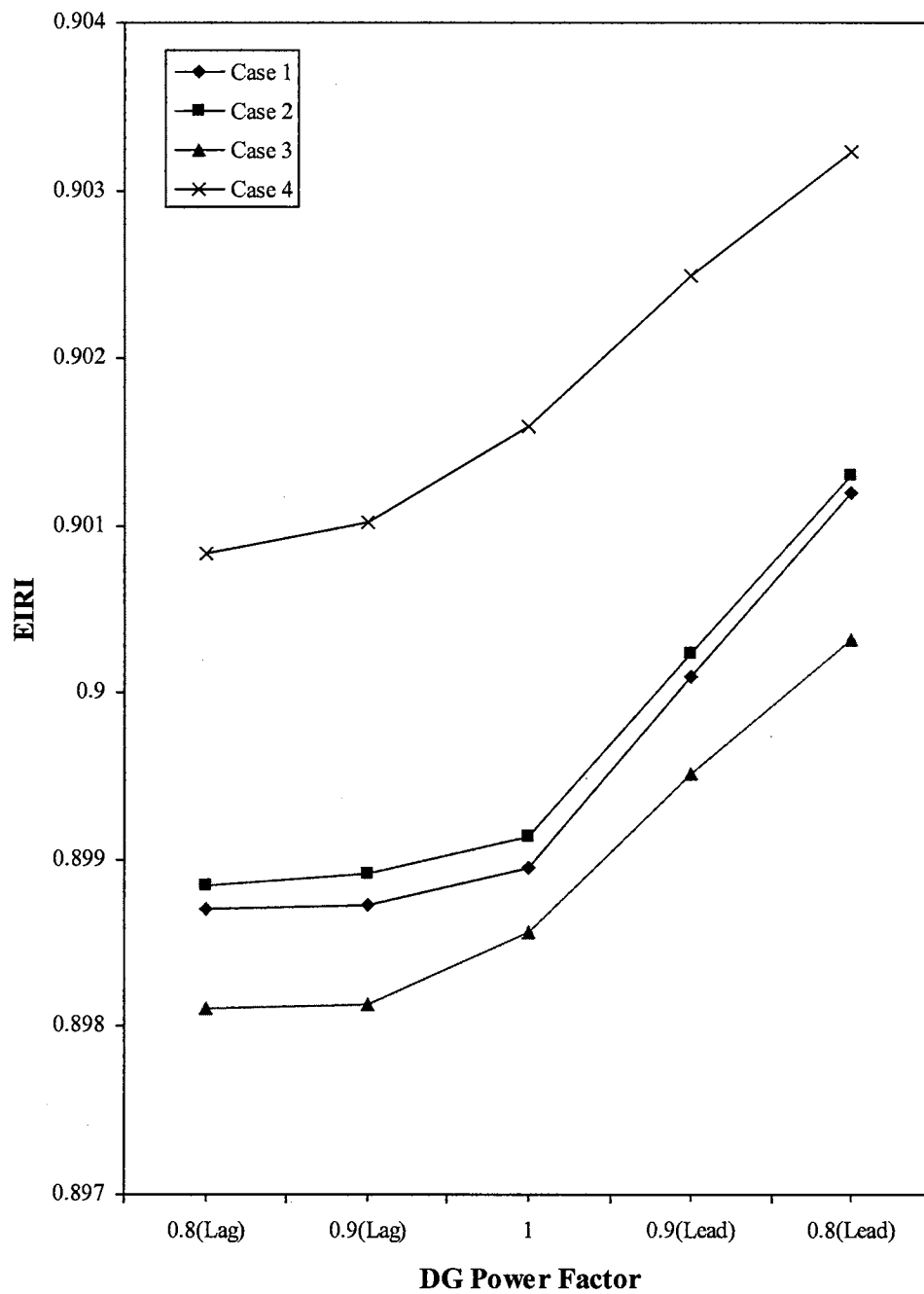


Figure 47. Impact of DG Operating Power Factor on Environmental Impact Reduction Index for Nitrogen Oxides (DG Rating is 0.2 pu)



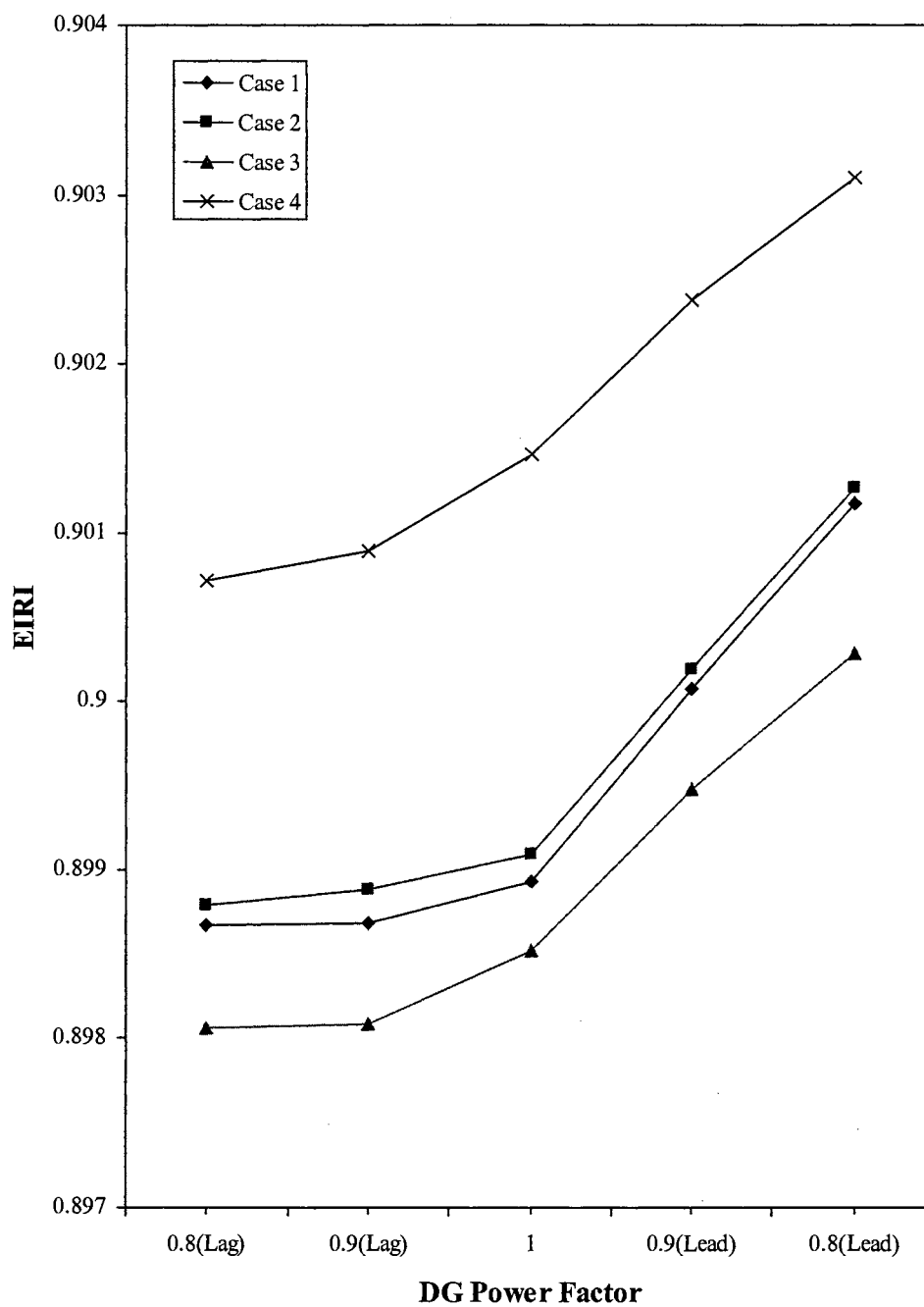


Figure 48. Impact of DG Operating Power Factor on the overall Environmental Impact Reduction Index (DG Rating is 0.2 pu)

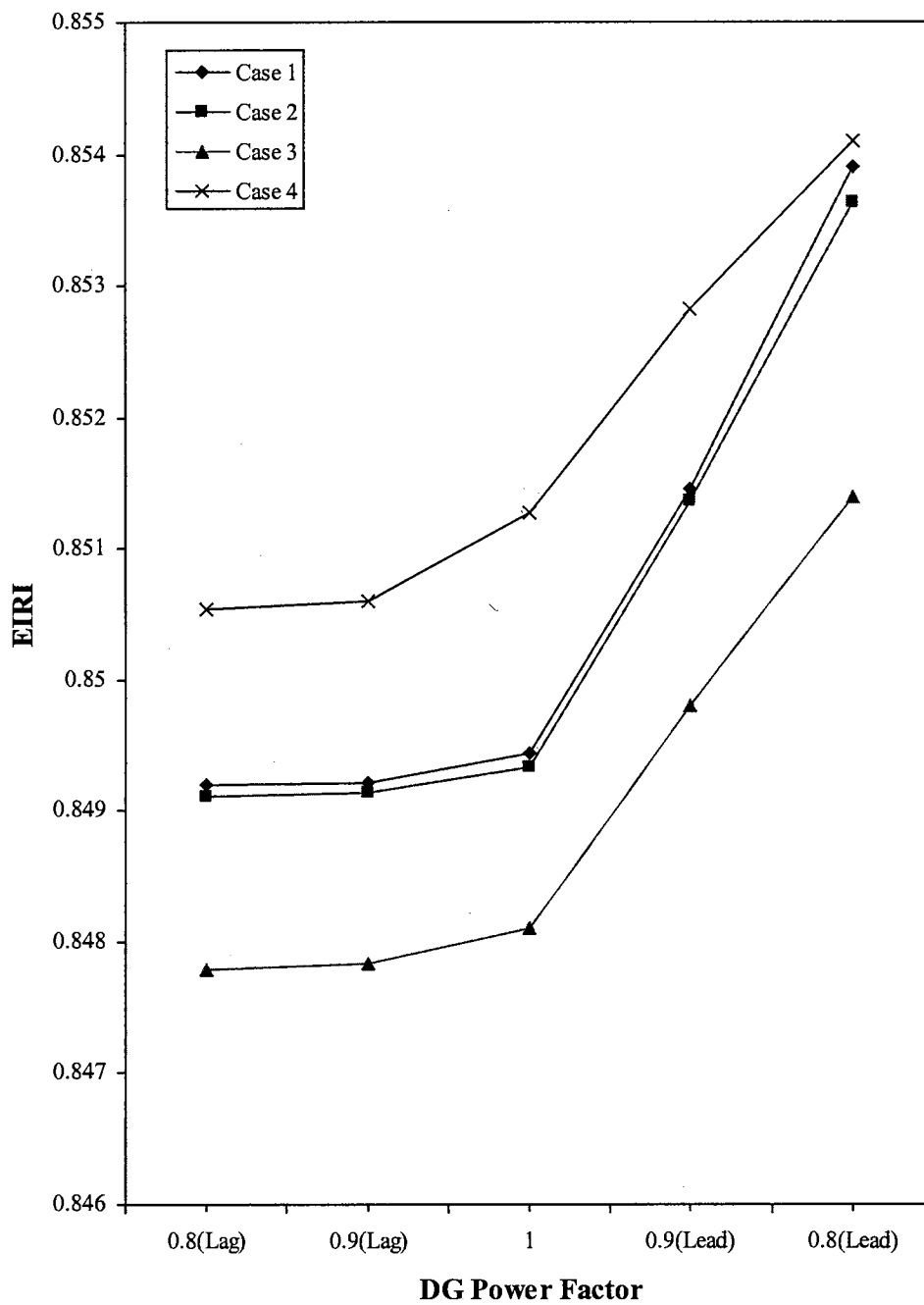


Figure 49. Impact of DG Operating Power Factor on Environmental Impact Reduction Index for Carbon Dioxide (DG Rating is 0.3 pu)

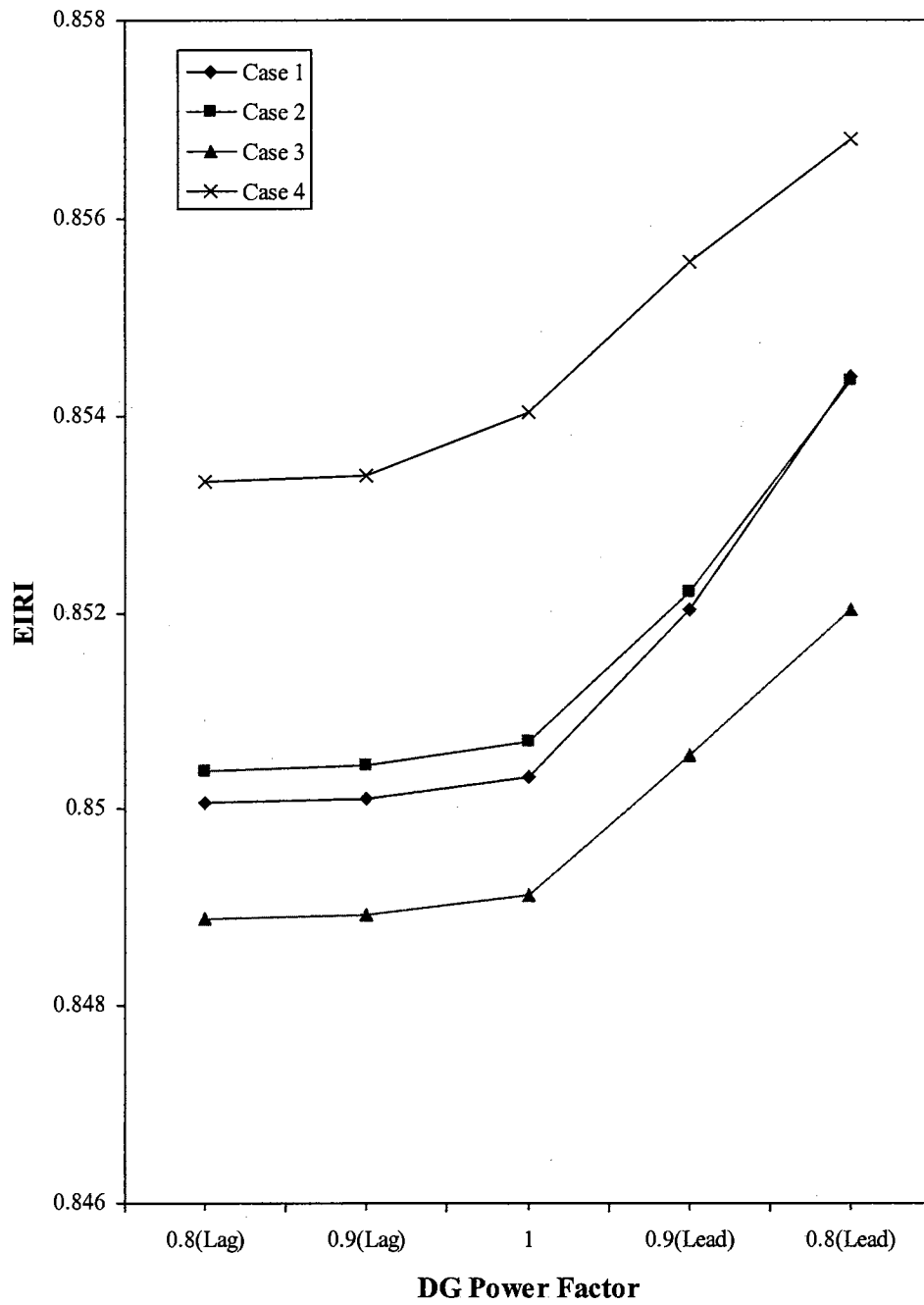


Figure 50. Impact of DG Operating Power Factor on Environmental Impact Reduction Index for Sulfur Dioxide (DG Rating is 0.3 pu)

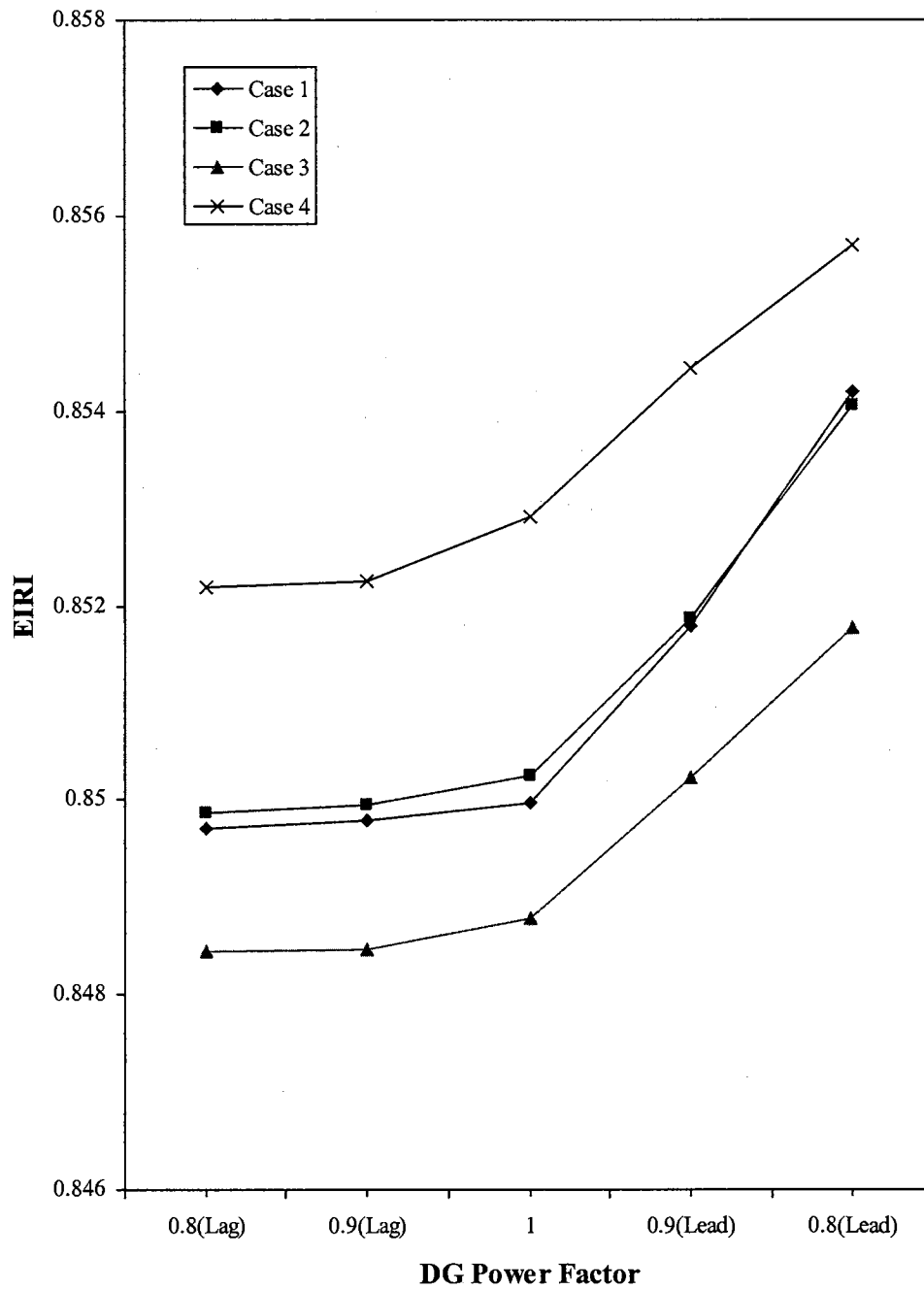


Figure 51. Impact of DG Operating Power Factor on Environmental Impact Reduction Index for Nitrogen Oxides (DG Rating is 0.3 pu)

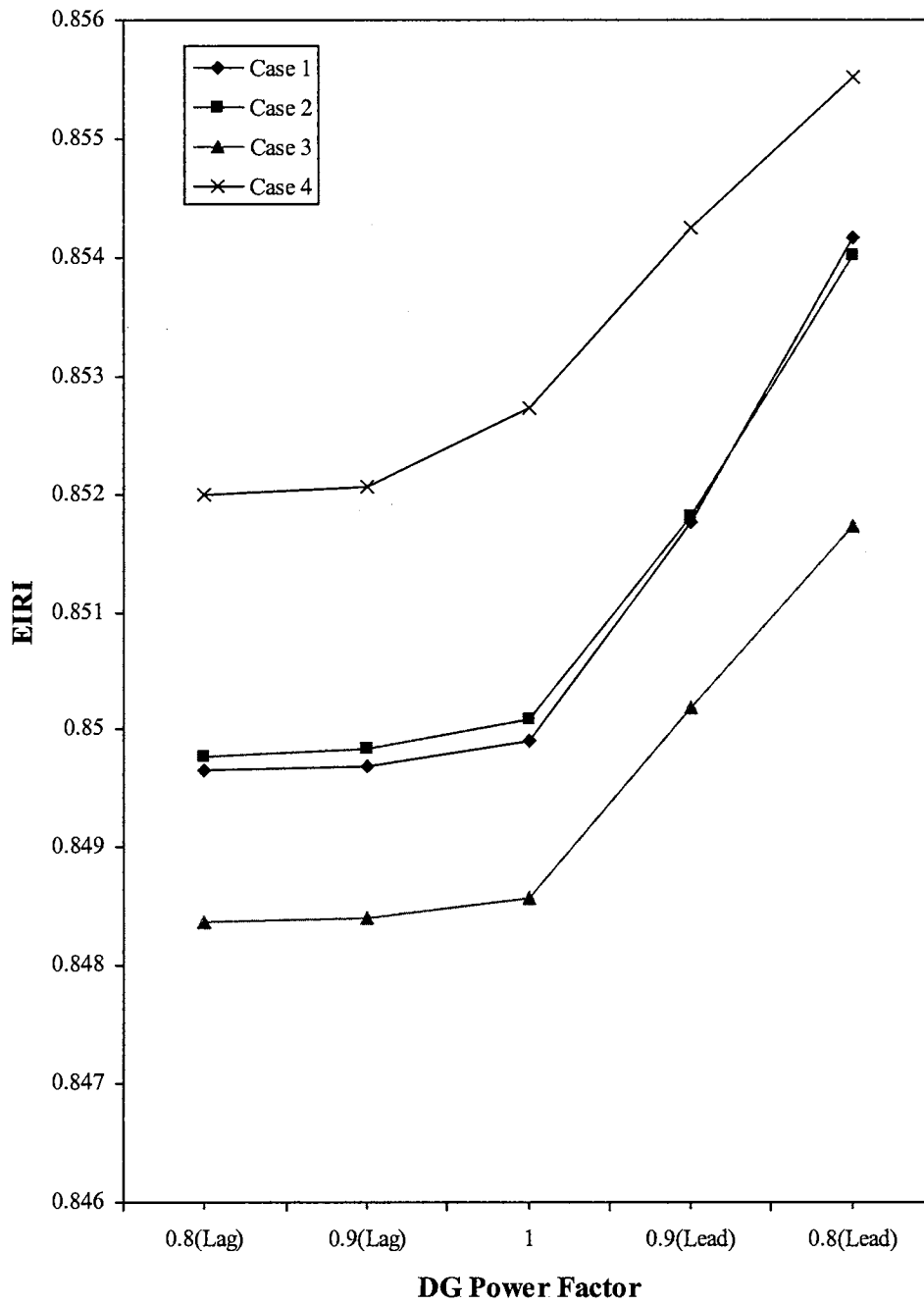


Figure 52. Impact of DG Operating Power Factor on the Overall Environmental Impact Reduction Index (DG Rating is 0.3 pu)

#### 6.4.4 Distributed Generation Benefit Results

The overall combined benefits of DG in terms of voltage profile improvement, line loss reduction, and environmental impact reduction should be considered to arrive at conclusions regarding the best locations and ratings for DG installations. The simulation results for VPRI, LLRI, and EIRI for all the cases studied are presented in Table 11. To calculate the distributed generation benefit index (BI), benefit weighting factors for voltage profile improvement, line loss reduction, and environmental impact reduction are required. To study the influence of these weighting factors on BI, a three-dimensional plot is developed as shown in Figures 53-58. It can be seen that BI increases as  $BW_{LLR}$  increases and BI decreases as  $BW_{VPI}$  increases. This is because line loss reduction dominates among all the benefits as shown in Table 12. The results from all the six study cases confirm that BI attains its maximum value when  $BW_{LLR}$  is set at its maximum value of unity, and  $BW_{VPI}$  and  $BW_{EIR}$  are both set at zero.

To arrive at the best locations and ratings of DG, several sets of benefit weighting factors are employed and the results show that case 2 (with DG rating of 0.3 pu located at bus 10 and 0.8 pf lag) is the best for maximizing the overall benefits when voltage profile improvement is given the maximum importance ( $BW_{VPI}=1$ ,  $BW_{LLR}=0$ , and  $BW_{EIR}=0$ ) as listed in Table 13. However, If line loss reduction is given the maximum importance ( $BW_{VPI}=0$ ,  $BW_{LLR}=1$ , and  $BW_{EIR}=0$ ), the simulation results indicate that case 3 (with DG at buses 9 and 10 and 0.8 pf lag) is the best scenario for employing DG as listed in Table 14. With maximum importance given for environmental impact reduction ( $BW_{VPI}=0$ ,  $BW_{LLR}=0$ , and  $BW_{EIR}=1$ ), case 3 turns out to be the best as documented in Table 15. If all the benefit weighting factors are equally weighted ( $BW_{VPI}=0.33$ ,  $BW_{LLR}=0.33$ , and

$BW_{EIR}=0.33$ ), the results suggest that once again case 3 is the best to maximize the overall benefits as documented in Table 16. However, in practice, the benefit weighting factors can be set to emphasize the desired attributes by using equations (5.1.2), (5.5.2), and (5.5.3).

TABLE 11

SIMULATED RESULTS OF VOLTAGE PROFILE IMPROVEMENT  
INDEX (VPII), LINE LOSS REDUCTION INDEX (LLRI), AND  
ENVIRONMENTAL IMPACT REDUCTION INDEX (EIRI)

Case	VPII	LLRI	EIRI
Case 1 with 0.1 pu rating and 0.8 pf lag	1.0053537	0.8032787	0.9487245
Case 1 with 0.1 pu rating and 0.9 pf lag	1.0041428	0.8114754	0.9487853
Case 1 with 0.1 pu rating and unity pf	1.0016131	0.8360656	0.9490622
Case 1 with 0.1 pu rating and 0.9 pf lead	0.9989763	0.8688525	0.9495608
Case 1 with 0.1 pu rating and 0.8 pf lead	0.9976672	0.8934426	0.9499471
Case 1 with 0.2 pu rating and 0.8 pf lag	1.0100543	0.6885246	0.8986660
Case 1 with 0.2 pu rating and 0.9 pf lag	1.0075030	0.6967210	0.8986801
Case 1 with 0.2 pu rating and unity pf	1.0028462	0.7213115	0.8989244
Case 1 with 0.2 pu rating and 0.9 pf lead	0.9977266	0.8114754	0.9000715
Case 1 with 0.2 pu rating and 0.8 pf lead	0.9944924	0.8934426	0.9011714
Case 1 with 0.3 pu rating and 0.8 pf lag	1.0142115	0.6557377	0.8496498
Case 1 with 0.3 pu rating and 0.9 pf lag	1.0106974	0.6639344	0.8496950
Case 1 with 0.3 pu rating and unity pf	1.0037029	0.6885246	0.8499086
Case 1 with 0.3 pu rating and 0.9 pf lead	0.9956520	0.8278689	0.8517582
Case 1 with 0.3 pu rating and 0.8 pf lead	0.9904965	1.0000000	0.8541640
Case 2 with 0.1 pu rating and 0.8 pf lag	1.0058552	0.7868852	0.9487997
Case 2 with 0.1 pu rating and 0.9 pf lag	1.0045132	0.7950820	0.9488702
Case 2 with 0.1 pu rating and unity pf	1.0016950	0.8278689	0.9491744
Case 2 with 0.1 pu rating and 0.9 pf lead	0.9987644	0.8688525	0.9496437
Case 2 with 0.1 pu rating and 0.8 pf lead	0.9972337	0.8934426	0.9500212



TABLE 11 (CONTINUED)

SIMULATED RESULTS OF VOLTAGE PROFILE IMPROVEMENT  
INDEX (VPII), LINE LOSS REDUCTION INDEX (LLRI), AND  
ENVIRONMENTAL IMPACT REDUCTION INDEX (EIRI)

Case	VPII	LLRI	EIRI
Case 2 with 0.2 pu rating and 0.8 pf lag	1.0110194	0.6639344	0.8987924
Case 2 with 0.2 pu rating and 0.9 pf lag	1.0082055	0.6721311	0.8988849
Case 2 with 0.2 pu rating and unity pf	1.0030170	0.7049180	0.8990930
Case 2 with 0.2 pu rating and 0.9 pf lead	0.9973680	0.7950820	0.9001953
Case 2 with 0.2 pu rating and 0.8 pf lead	0.9938102	0.8770492	0.9012684
Case 2 with 0.3 pu rating and 0.8 pf lag	1.0159112	0.6065574	0.8497771
Case 2 with 0.3 pu rating and 0.9 pf lag	1.0119215	0.6147541	0.8498396
Case 2 with 0.3 pu rating and unity pf	1.0039804	0.6393443	0.8500853
Case 2 with 0.3 pu rating and 0.9 pf lead	0.9951281	0.8032787	0.8518102
Case 2 with 0.3 pu rating and 0.8 pf lead	0.9895404	0.9672131	0.8540137
Case 3 with 0.1 pu rating and 0.8 pf lag	1.0057175	0.7786885	0.9485601
Case 3 with 0.1 pu rating and 0.9 pf lag	1.0044193	0.7950820	0.9486640
Case 3 with 0.1 pu rating and unity pf	1.0017338	0.8196721	0.9489886
Case 3 with 0.1 pu rating and 0.9 pf lead	0.9989539	0.8606557	0.9494530
Case 3 with 0.1 pu rating and 0.8 pf lead	0.9975298	0.8852459	0.9497572
Case 3 with 0.2 pu rating and 0.8 pf lag	1.0109341	0.6311475	0.8980597
Case 3 with 0.2 pu rating and 0.9 pf lag	1.0081834	0.6393443	0.8980894
Case 3 with 0.2 pu rating and unity pf	1.0035484	0.6803279	0.8985223
Case 3 with 0.2 pu rating and 0.9 pf lead	0.9979197	0.7540984	0.8994740
Case 3 with 0.2 pu rating and 0.8 pf lead	0.9946725	0.8196721	0.9002880

TABLE 11 (CONTINUED)

SIMULATED RESULTS OF VOLTAGE PROFILE IMPROVEMENT  
INDEX (VPII), LINE LOSS REDUCTION INDEX (LLRI), AND  
ENVIRONMENTAL IMPACT REDUCTION INDEX (EIRI)

Case	VPII	LLRI	EIRI
Case 3 with 0.3 pu rating and 0.8 pf lag	1.0157211	0.5409836	0.8483650
Case 3 with 0.3 pu rating and 0.9 pf lag	1.0118597	0.5491803	0.8483976
Case 3 with 0.3 pu rating and unity pf	1.0044561	0.5819672	0.8485725
Case 3 with 0.3 pu rating and 0.9 pf lead	0.9962869	0.7049180	0.8501866
Case 3 with 0.3 pu rating and 0.8 pf lead	0.9913688	0.8196721	0.8517302
Case 4 with 0.1 pu rating and 0.8 pf lag	1.0049756	0.8114754	0.9500442
Case 4 with 0.1 pu rating and 0.9 pf lag	1.0038041	0.8196721	0.9501840
Case 4 with 0.1 pu rating and unity pf	1.0014462	0.8442623	0.9505432
Case 4 with 0.1 pu rating and 0.9 pf lead	0.9990271	0.8770492	0.9510219
Case 4 with 0.1 pu rating and 0.8 pf lead	0.9977849	0.9016393	0.9512919
Case 4 with 0.2 pu rating and 0.8 pf lag	1.0096161	0.6639344	0.9007141
Case 4 with 0.2 pu rating and 0.9 pf lag	1.0071547	0.6803279	0.9008964
Case 4 with 0.2 pu rating and unity pf	1.0031411	0.7131148	0.9014653
Case 4 with 0.2 pu rating and 0.9 pf lead	0.9979822	0.7868852	0.9023771
Case 4 with 0.2 pu rating and 0.8 pf lead	0.9953368	0.8360656	0.9031056
Case 4 with 0.3 pu rating and 0.8 pf lag	1.0140030	0.5655738	0.8520001
Case 4 with 0.3 pu rating and 0.9 pf lag	1.0105118	0.5737705	0.8520597
Case 4 with 0.3 pu rating and unity pf	1.0039499	0.6147541	0.8527273
Case 4 with 0.3 pu rating and 0.9 pf lead	0.9967968	0.7213115	0.8542511
Case 4 with 0.3 pu rating and 0.8 pf lead	0.9926263	0.8114754	0.8555110

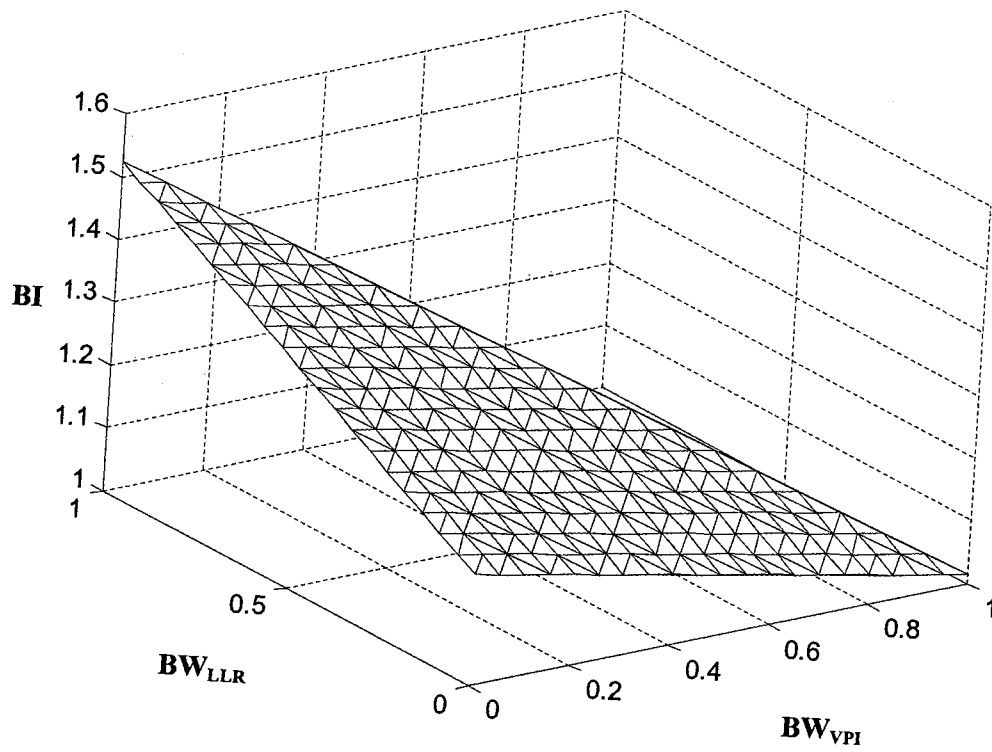


Figure 53. Variation of Distributed Generation Benefit Index (BI) with Weighting Factors (case 1 with 0.3 pu rating and 0.8 pf lag)

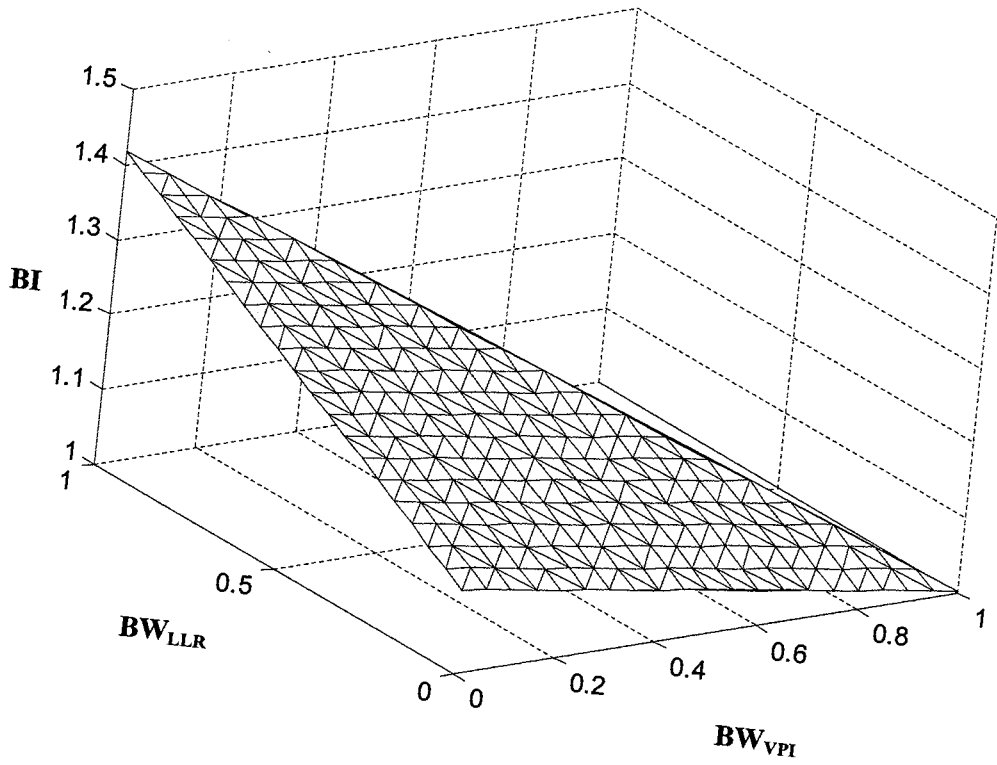


Figure 54. Variation of Distributed Generation Benefit Index (BI) with Weighting Factors (case 2 with 0.2 pu rating and unity pf)

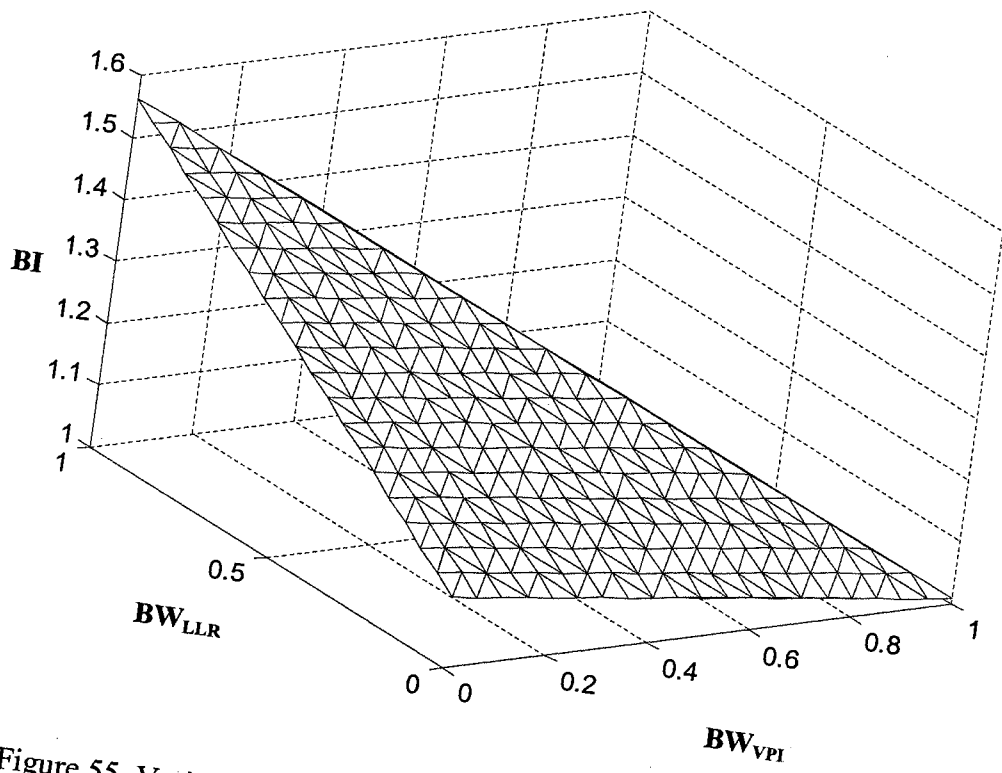


Figure 55. Variation of Distributed Generation Benefit Index (BI) with Weighting Factors (case 3 with 0.2 pu rating and 0.9 pf lag)

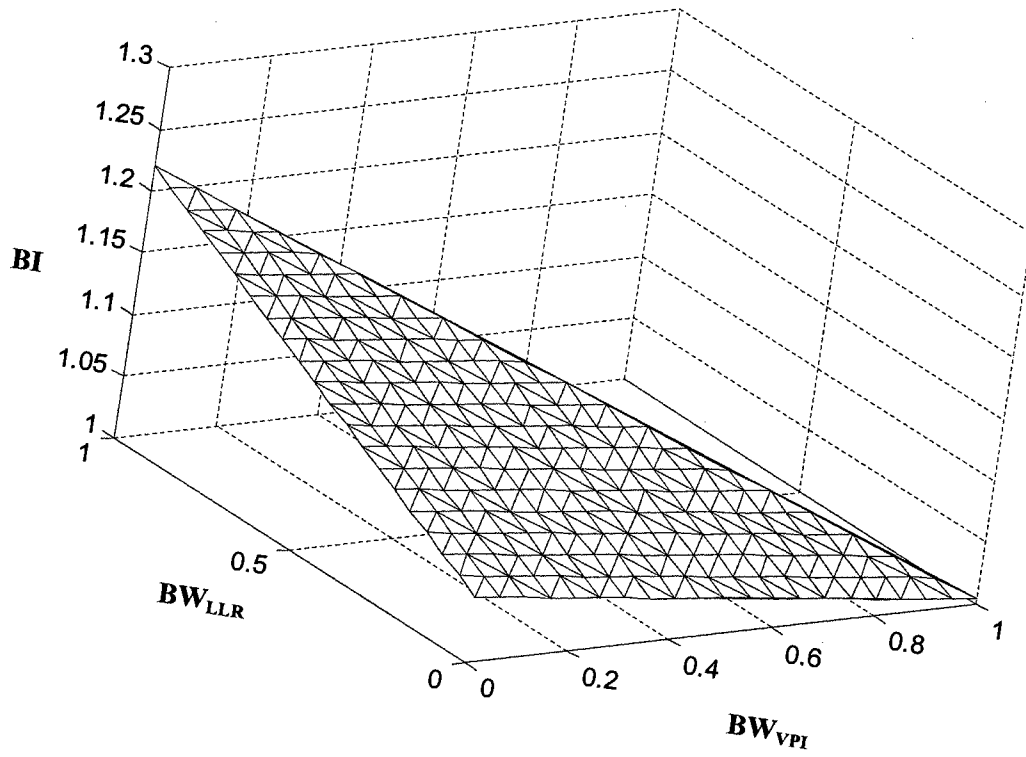


Figure 56. Variation of Distributed Generation Benefit Index (BI) with Weighting Factors (case 4 with 0.1 pu rating and 0.9 pf lag)

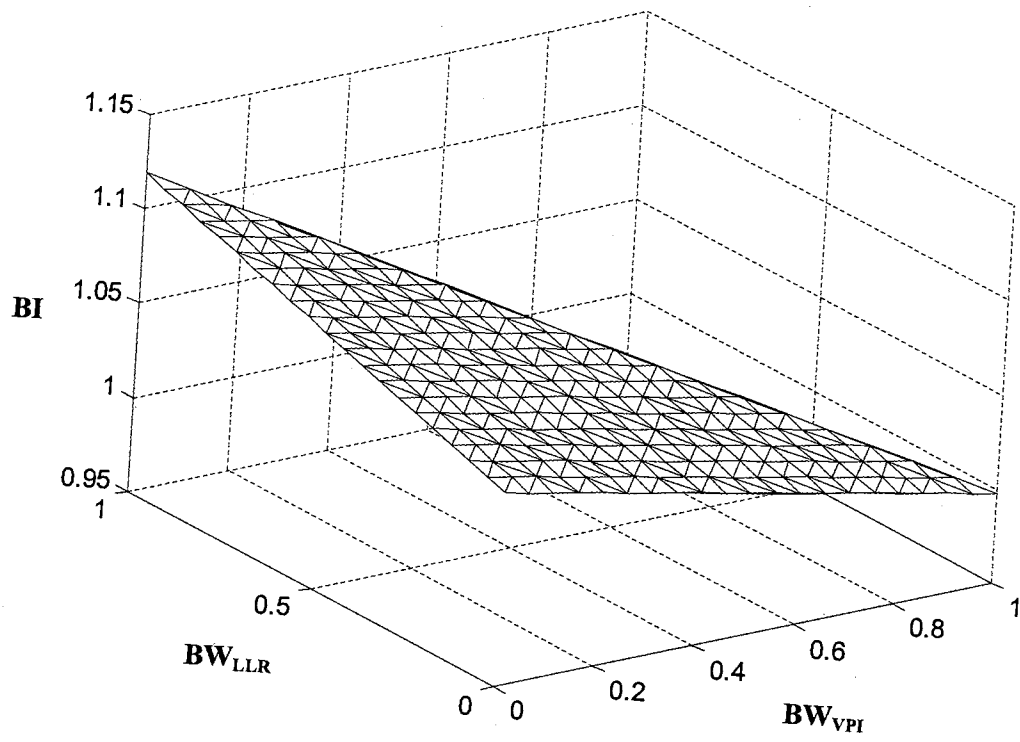


Figure 57. Variation of Distributed Generation Benefit Index (BI) with Weighting Factors (case 1 with 0.1 pu rating and 0.8 pf lead)

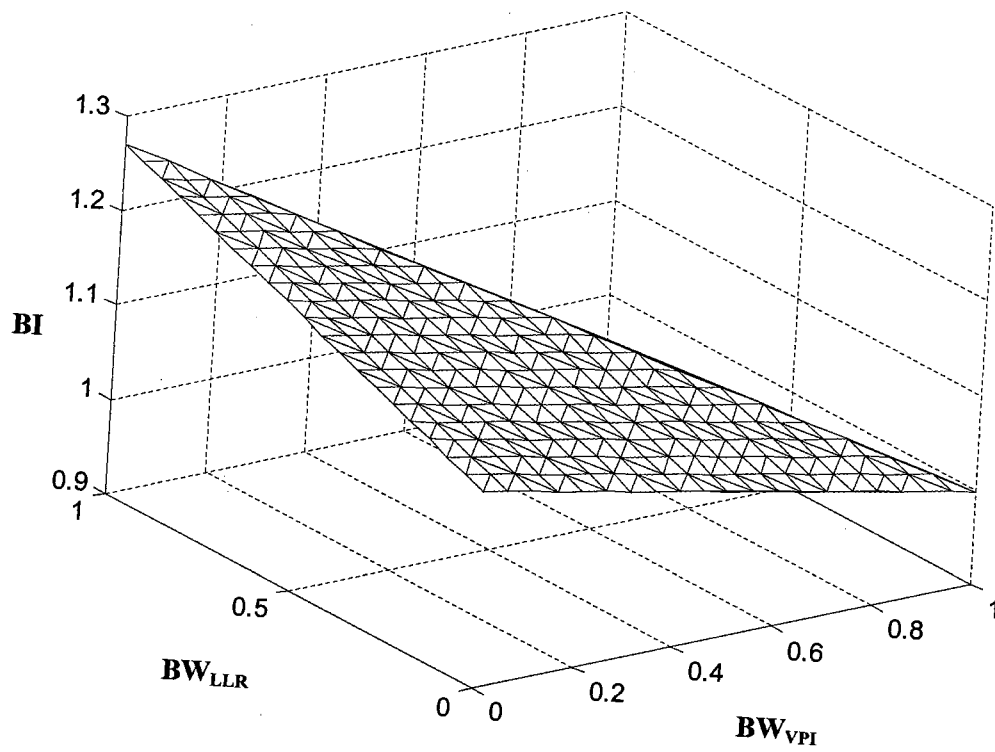


Figure 58. Variation of Distributed Generation Benefit Index (BI) with Weighting Factors (case 4 with 0.2 pu rating and 0.9 pf lead)



TABLE 12

TABULATION OF SELECTED CASES OF DISTRIBUTED  
GENERATION BENEFIT RESULTS

Selected Cases	Percentage of Voltage Profile Improvement	Percentage of Line Loss Reduction	Percentage of Environmental Impact Reduction
Case 1 with 0.3 pu rating and 0.8 pf (lag)	1.42	34.43	15.04
Case 2 with 0.2 pu rating and unity pf	0.30	29.51	10.09
Case 3 with 0.2 pu rating and 0.9 pf (lag)	0.82	36.06	10.19
Case 4 with 0.1 pu rating and 0.9 pf (lag)	0.38	18.03	4.98
Case 1 with 0.1 pu rating and 0.8 pf (lead)	-0.23	10.66	5.01
Case 4 with 0.2 pu rating and 0.9 pf (lead)	-0.20	21.31	9.76

TABLE 13

DISTRIBUTED GENERATION BENEFIT INDEX (BI)  
FOR  $BW_{VPI}=1$ ,  $BW_{LLR}=0$ , AND  $BW_{EIR}=0$

Case	BI
Case 2 with 0.3 pu rating and 0.8 pf lag	1.0159112
Case 3 with 0.3 pu rating and 0.8 pf lag	1.0157211
Case 1 with 0.3 pu rating and 0.8 pf lag	1.0142115
Case 4 with 0.3 pu rating and 0.8 pf lag	1.0140030
Case 2 with 0.3 pu rating and 0.9 pf lag	1.0119215
Case 3 with 0.3 pu rating and 0.9 pf lag	1.0118597
Case 2 with 0.2 pu rating and 0.8 pf lag	1.0110194
Case 3 with 0.2 pu rating and 0.8 pf lag	1.0109341
Case 1 with 0.3 pu rating and 0.9 pf lag	1.0106974
Case 4 with 0.3 pu rating and 0.9 pf lag	1.0105118
Case 1 with 0.2 pu rating and 0.8 pf lag	1.0100543
Case 4 with 0.2 pu rating and 0.8 pf lag	1.0096161
Case 2 with 0.2 pu rating and 0.9 pf lag	1.0082055
Case 3 with 0.2 pu rating and 0.9 pf lag	1.0081834
Case 1 with 0.2 pu rating and 0.9 pf lag	1.0075030
Case 4 with 0.2 pu rating and 0.9 pf lag	1.0071547
Case 2 with 0.1 pu rating and 0.8 pf lag	1.0058552
Case 3 with 0.1 pu rating and 0.8 pf lag	1.0057175
Case 1 with 0.1 pu rating and 0.8 pf lag	1.0053537
Case 4 with 0.1 pu rating and 0.8 pf lag	1.0049756

TABLE 13 (CONTINUED)

DISTRIBUTED GENERATION BENEFIT INDEX (BI)  
FOR  $BW_{VPI}=1$ ,  $BW_{LLR}=0$ , AND  $BW_{EIR}=0$

Case	BI
Case 2 with 0.1 pu rating and 0.9 pf lag	1.0045132
Case 3 with 0.3 pu rating and unity pf	1.0044561
Case 3 with 0.1 pu rating and 0.9 pf lag	1.0044193
Case 1 with 0.1 pu rating and 0.9 pf lag	1.0041428
Case 2 with 0.3 pu rating and unity pf	1.0039804
Case 4 with 0.3 pu rating and unity pf	1.0039499
Case 4 with 0.1 pu rating and 0.9 pf lag	1.0038041
Case 1 with 0.3 pu rating and unity pf	1.0037029
Case 3 with 0.2 pu rating and unity pf	1.0035484
Case 4 with 0.2 pu rating and unity pf	1.0031411
Case 2 with 0.2 pu rating and unity pf	1.0030170
Case 1 with 0.2 pu rating and unity pf	1.0028462
Case 3 with 0.1 pu rating and unity pf	1.0017338
Case 2 with 0.1 pu rating and unity pf	1.0016950
Case 1 with 0.1 pu rating and unity pf	1.0016131
Case 4 with 0.1 pu rating and unity pf	1.0014462
Case 4 with 0.1 pu rating and 0.9 pf lead	0.9990271
Case 1 with 0.1 pu rating and 0.9 pf lead	0.9989763
Case 3 with 0.1 pu rating and 0.9 pf lead	0.9989539
Case 2 with 0.1 pu rating and 0.9 pf lead	0.9987644

TABLE 13 (CONTINUED)

DISTRIBUTED GENERATION BENEFIT INDEX (BI)  
FOR  $BW_{VPI}=1$ ,  $BW_{LLR}=0$ , AND  $BW_{EIR}=0$

Case	BI
Case 4 with 0.2 pu rating and 0.9 pf lead	0.9979822
Case 3 with 0.2 pu rating and 0.9 pf lead	0.9979197
Case 4 with 0.1 pu rating and 0.8 pf lead	0.9977849
Case 1 with 0.2 pu rating and 0.9 pf lead	0.9977266
Case 1 with 0.1 pu rating and 0.8 pf lead	0.9976672
Case 3 with 0.1 pu rating and 0.8 pf lead	0.9975298
Case 2 with 0.2 pu rating and 0.9 pf lead	0.9973680
Case 2 with 0.1 pu rating and 0.8 pf lead	0.9972337
Case 4 with 0.3 pu rating and 0.9 pf lead	0.9967968
Case 3 with 0.3 pu rating and 0.9 pf lead	0.9962869
Case 1 with 0.3 pu rating and 0.9 pf lead	0.9956520
Case 4 with 0.2 pu rating and 0.8 pf lead	0.9953368
Case 2 with 0.3 pu rating and 0.9 pf lead	0.9951281
Case 3 with 0.2 pu rating and 0.8 pf lead	0.9946725
Case 1 with 0.2 pu rating and 0.8 pf lead	0.9944924
Case 2 with 0.2 pu rating and 0.8 pf lead	0.9938102
Case 4 with 0.3 pu rating and 0.8 pf lead	0.9926263
Case 3 with 0.3 pu rating and 0.8 pf lead	0.9913688
Case 1 with 0.3 pu rating and 0.8 pf lead	0.9904965
Case 2 with 0.3 pu rating and 0.8 pf lead	0.9895404

TABLE 14

DISTRIBUTED GENERATION BENEFIT INDEX (BI)  
FOR  $BW_{VPI}=0$ ,  $BW_{LLR}=1$ , AND  $BW_{EIR}=0$

Case	BI
Case 3 with 0.3 pu rating and 0.8 pf lag	1.8484848
Case 3 with 0.3 pu rating and 0.9 pf lag	1.8208955
Case 4 with 0.3 pu rating and 0.8 pf lag	1.7681159
Case 4 with 0.3 pu rating and 0.9 pf lag	1.7428571
Case 3 with 0.3 pu rating and unity pf	1.7183099
Case 2 with 0.3 pu rating and 0.8 pf lag	1.6486486
Case 2 with 0.3 pu rating and 0.9 pf lag	1.6266667
Case 4 with 0.3 pu rating and unity pf	1.6266667
Case 3 with 0.2 pu rating and 0.8 pf lag	1.5844156
Case 2 with 0.3 pu rating and unity pf	1.5641026
Case 3 with 0.2 pu rating and 0.9 pf lag	1.5641026
Case 1 with 0.3 pu rating and 0.8 pf lag	1.5250004
Case 1 with 0.3 pu rating and 0.9 pf lag	1.5061728
Case 2 with 0.2 pu rating and 0.8 pf lag	1.5061728
Case 4 with 0.2 pu rating and 0.8 pf lag	1.5061728
Case 2 with 0.2 pu rating and 0.9 pf lag	1.4878049
Case 3 with 0.2 pu rating and unity pf	1.4698795
Case 4 with 0.2 pu rating and 0.9 pf lag	1.4698795
Case 1 with 0.2 pu rating and 0.8 pf lag	1.4523810
Case 1 with 0.3 pu rating and unity pf	1.4523810

TABLE 14 (CONTINUED)

DISTRIBUTED GENERATION BENEFIT INDEX (BI)  
FOR  $BW_{VPI}=0$ ,  $BW_{LLR}=1$ , AND  $BW_{EIR}=0$

Case	BI
Case 1 with 0.2 pu rating and 0.9 pf lag	1.4352948
Case 2 with 0.2 pu rating and unity pf	1.4186047
Case 3 with 0.3 pu rating and 0.9 pf lead	1.4186047
Case 4 with 0.2 pu rating and unity pf	1.4022989
Case 1 with 0.2 pu rating and unity pf	1.3863636
Case 4 with 0.3 pu rating and 0.9 pf lead	1.3863636
Case 3 with 0.2 pu rating and 0.9 pf lead	1.3260870
Case 3 with 0.1 pu rating and 0.8 pf lag	1.2842105
Case 2 with 0.1 pu rating and 0.8 pf lag	1.2708333
Case 4 with 0.2 pu rating and 0.9 pf lead	1.2708333
Case 2 with 0.1 pu rating and 0.9 pf lag	1.2577320
Case 2 with 0.2 pu rating and 0.9 pf lead	1.2577320
Case 3 with 0.1 pu rating and 0.9 pf lag	1.2577320
Case 1 with 0.1 pu rating and 0.8 pf lag	1.2448980
Case 2 with 0.3 pu rating and 0.9 pf lead	1.2448980
Case 1 with 0.1 pu rating and 0.9 pf lag	1.2323232
Case 1 with 0.2 pu rating and 0.9 pf lead	1.2323232
Case 4 with 0.1 pu rating and 0.8 pf lag	1.2323232
Case 4 with 0.3 pu rating and 0.8 pf lead	1.2323232
Case 3 with 0.1 pu rating and unity pf	1.2200012

TABLE 14 (CONTINUED)

DISTRIBUTED GENERATION BENEFIT INDEX (BI)  
 FOR  $BW_{VPI}=0$ ,  $BW_{LLR}=1$ , AND  $BW_{EIR}=0$

Case	BI
Case 3 with 0.2 pu rating and 0.8 pf lead	1.2200001
Case 3 with 0.3 pu rating and 0.8 pf lead	1.2200001
Case 4 with 0.1 pu rating and 0.9 pf lag	1.2200001
Case 1 with 0.3 pu rating and 0.9 pf lead	1.2079208
Case 2 with 0.1 pu rating and unity pf	1.2079208
Case 1 with 0.1 pu rating and unity pf)	1.1960784
Case 4 with 0.2 pu rating and 0.8 pf lead	1.1960784
Case 4 with 0.1 pu rating and unity pf	1.1844660
Case 3 with 0.1 pu rating and 0.9 pf lead	1.1619048
Case 1 with 0.1 pu rating and 0.9 pf lead	1.1509434
Case 2 with 0.1 pu rating and 0.9 pf lead	1.1509434
Case 2 with 0.2 pu rating and 0.8 pf lead	1.1401869
Case 4 with 0.1 pu rating and 0.9 pf lead	1.1401869
Case 3 with 0.1 pu rating and 0.8 pf lead	1.1296296
Case 1 with 0.1 pu rating and 0.8 pf lead	1.1192661
Case 1 with 0.2 pu rating and 0.8 pf lead	1.1192661
Case 2 with 0.1 pu rating and 0.8 pf lead	1.1192661
Case 4 with 0.1 pu rating and 0.8 pf lead	1.1090909
Case 2 with 0.3 pu rating and 0.8 pf lead	1.0338983
Case 1 with 0.3 pu rating and 0.8 pf lead	1.0000000

TABLE 15

DISTRIBUTED GENERATION BENEFIT INDEX (BI)  
FOR  $BW_{VPI}=0$ ,  $BW_{LLR}=0$ , AND  $BW_{EIR}=1$

Case	BI
Case 3 with 0.3 pu rating and 0.8 pf lag	1.1787379
Case 3 with 0.3 pu rating and 0.9 pf lag	1.1786926
Case 3 with 0.3 pu rating and unity pf	1.1784497
Case 1 with 0.3 pu rating and 0.8 pf lag	1.1769555
Case 1 with 0.3 pu rating and 0.9 pf lag	1.1768929
Case 2 with 0.3 pu rating and 0.8 pf lag	1.1767792
Case 2 with 0.3 pu rating and 0.9 pf lag	1.1766926
Case 1 with 0.3 pu rating and unity pf	1.1765971
Case 2 with 0.3 pu rating and unity pf	1.1763525
Case 3 with 0.3 pu rating and 0.9 pf lead	1.1762124
Case 3 with 0.3 pu rating and 0.8 pf lead	1.1740807
Case 1 with 0.3 pu rating and 0.9 pf lead	1.1740421
Case 2 with 0.3 pu rating and 0.9 pf lead	1.1739704
Case 4 with 0.3 pu rating and 0.8 pf lag	1.1737088
Case 4 with 0.3 pu rating and 0.9 pf lag	1.1736266
Case 4 with 0.3 pu rating and unity pf	1.1727078
Case 2 with 0.3 pu rating and 0.8 pf lead	1.1709415
Case 1 with 0.3 pu rating and 0.8 pf lead	1.1707354
Case 4 with 0.3 pu rating and 0.9 pf lead	1.1706160
Case 4 with 0.3 pu rating and 0.8 pf lead	1.1688921



TABLE 15 (CONTINUED)

DISTRIBUTED GENERATION BENEFIT INDEX (BI)  
 FOR  $BW_{VPI}=0$ ,  $BW_{LLR}=0$ , AND  $BW_{EIR}=1$

Case	BI
Case 3 with 0.2 pu rating and 0.8 pf lag	1.1135117
Case 3 with 0.2 pu rating and 0.9 pf lag	1.1134749
Case 3 with 0.2 pu rating and unity pf	1.1129384
Case 1 with 0.2 pu rating and 0.8 pf lag	1.1127604
Case 1 with 0.2 pu rating and 0.9 pf lag	1.1127430
Case 2 with 0.2 pu rating and 0.8 pf lag	1.1126039
Case 2 with 0.2 pu rating and 0.9 pf lag	1.1124895
Case 1 with 0.2 pu rating and unity pf	1.1124406
Case 2 with 0.2 pu rating and unity pf	1.1122320
Case 3 with 0.2 pu rating and 0.9 pf lead	1.1117608
Case 1 with 0.2 pu rating and 0.9 pf lead	1.1110228
Case 2 with 0.2 pu rating and 0.9 pf lead	1.1108701
Case 3 with 0.2 pu rating and 0.8 pf lead	1.1107557
Case 4 with 0.2 pu rating and 0.8 pf lag	1.1102302
Case 4 with 0.2 pu rating and 0.9 pf lag	1.1100055
Case 1 with 0.2 pu rating and 0.8 pf lead	1.1096668
Case 2 with 0.2 pu rating and 0.8 pf lead	1.1095473
Case 4 with 0.2 pu rating and unity pf	1.1093051
Case 4 with 0.2 pu rating and 0.9 pf lead	1.1081842
Case 4 with 0.2 pu rating and 0.8 pf lead	1.1072903

TABLE 15 (CONTINUED)

DISTRIBUTED GENERATION BENEFIT INDEX (BI)  
FOR  $BW_{VPI}=0$ ,  $BW_{LLR}=0$ , AND  $BW_{EIR}=1$

Case	BI
Case 3 with 0.1 pu rating and 0.8 pf lag	1.0542296
Case 3 with 0.1 pu rating and 0.9 pf lag	1.054114
Case 1 with 0.1 pu rating and 0.8 pf lag	1.0540467
Case 1 with 0.1 pu rating and 0.9 pf lag	1.0539792
Case 2 with 0.1 pu rating and 0.8 pf lag	1.0539633
Case 2 with 0.1 pu rating and 0.9 pf lag	1.0538849
Case 3 with 0.1 pu rating and unity pf	1.0537534
Case 1 with 0.1 pu rating and unity pf	1.0536717
Case 2 with 0.1 pu rating and unity pf	1.0535472
Case 3 with 0.1 pu rating and 0.9 pf lead	1.053238
Case 1 with 0.1 pu rating and 0.9 pf lead	1.0531185
Case 2 with 0.1 pu rating and 0.9 pf lead	1.0530265
Case 3 with 0.1 pu rating and 0.8 pf lead	1.0529007
Case 1 with 0.1 pu rating and 0.8 pf lead	1.0526902
Case 2 with 0.1 pu rating and 0.8 pf lead	1.0526081
Case 4 with 0.1 pu rating and 0.8 pf lag	1.0525826
Case 4 with 0.1 pu rating and 0.9 pf lag	1.0524277
Case 4 with 0.1 pu rating and unity pf	1.0520301
Case 4 with 0.1 pu rating and 0.9 pf lead	1.0515005
Case 4 with 0.1 pu rating and 0.8 pf lead	1.0512021

TABLE 16

DISTRIBUTED GENERATION BENEFIT INDEX (BI)  
 FOR  $BW_{VPI}=0.33$ ,  $BW_{LLR}=0.33$ , AND  $BW_{EIR}=0.33$

Case	BI
Case 3 with 0.3 pu rating and 0.8 pf lag	1.3443287
Case 3 with 0.3 pu rating and 0.9 pf lag	1.3338964
Case 4 with 0.3 pu rating and 0.8 pf lag	1.3155632
Case 4 with 0.3 pu rating and 0.9 pf lag	1.3060137
Case 3 with 0.3 pu rating and unity pf	1.2974457
Case 2 with 0.3 pu rating and 0.8 pf lag	1.2778010
Case 2 with 0.3 pu rating and 0.9 pf lag	1.2691619
Case 4 with 0.3 pu rating and unity pf	1.2651365
Case 2 with 0.3 pu rating and unity pf	1.2457035
Case 1 with 0.3 pu rating and 0.8 pf lag	1.2364773
Case 3 with 0.2 pu rating and 0.8 pf lag	1.2340336
Case 1 with 0.3 pu rating and 0.9 pf lag	1.2290488
Case 3 with 0.2 pu rating and 0.9 pf lag	1.2263829
Case 1 with 0.3 pu rating and unity pf	1.2088218
Case 2 with 0.2 pu rating and 0.8 pf lag	1.2079429
Case 4 with 0.2 pu rating and 0.8 pf lag	1.2066825
Case 2 with 0.2 pu rating and 0.9 pf lag	1.2008870
Case 3 with 0.3 pu rating and 0.9 pf lead	1.1950272
Case 4 with 0.2 pu rating and 0.9 pf lag	1.1937947
Case 3 with 0.2 pu rating and unity pf	1.1935364

TABLE 16 (CONTINUED)

DISTRIBUTED GENERATION BENEFIT INDEX (BI)  
 FOR  $BW_{VPI}=0.33$ ,  $BW_{LLR}=0.33$ , AND  $BW_{EIR}=0.33$

Case	BI
Case 1 with 0.2 pu rating and 0.8 pf lag	1.1899151
Case 1 with 0.2 pu rating and 0.9 pf lag	1.1834035
Case 4 with 0.3 pu rating and 0.9 pf lead	1.1827142
Case 2 with 0.2 pu rating and unity pf	1.1762019
Case 4 with 0.2 pu rating and unity pf	1.1698973
Case 1 with 0.2 pu rating and unity pf	1.1655731
Case 3 with 0.2 pu rating and 0.9 pf lead	1.1437825
Case 2 with 0.3 pu rating and 0.9 pf lead	1.1365701
Case 4 with 0.3 pu rating and 0.8 pf lead	1.1298940
Case 3 with 0.3 pu rating and 0.8 pf lead	1.1271120
Case 1 with 0.3 pu rating and 0.9 pf lead	1.1245694
Case 4 with 0.2 pu rating and 0.9 pf lead	1.1243897
Case 2 with 0.2 pu rating and 0.9 pf lead	1.1207438
Case 3 with 0.1 pu rating and 0.8 pf lag	1.1136292
Case 1 with 0.2 pu rating and 0.9 pf lead	1.1125312
Case 2 with 0.1 pu rating and 0.8 pf lag	1.1091736
Case 3 with 0.2 pu rating and 0.8 pf lead	1.1073380
Case 3 with 0.1 pu rating and 0.9 pf lag	1.1044117
Case 2 with 0.1 pu rating and 0.9 pf lag	1.1043680
Case 1 with 0.1 pu rating and 0.8 pf lag	1.1004720

TABLE 16 (CONTINUED)

DISTRIBUTED GENERATION BENEFIT INDEX (BI)  
 FOR  $BW_{VPI}=0.33$ ,  $BW_{LLR}=0.33$ , AND  $BW_{EIR}=0.33$

Case	BI
Case 4 with 0.2 pu rating and 0.8 pf lead	1.0985262
Case 1 with 0.1 pu rating and 0.9 pf lag	1.0958884
Case 4 with 0.1 pu rating and 0.8 pf lag	1.0957106
Case 4 with 0.1 pu rating and 0.9 pf lag	1.0911945
Case 3 with 0.1 pu rating and unity pf	1.0909281
Case 2 with 0.1 pu rating and unity pf	1.0868607
Case 1 with 0.1 pu rating and unity pf	1.0829660
Case 2 with 0.2 pu rating and 0.8 pf lead	1.0803078
Case 4 with 0.1 pu rating and unity pf	1.0785354
Case 1 with 0.2 pu rating and 0.8 pf lead	1.0736753
Case 3 with 0.1 pu rating and 0.9 pf lead	1.0706414
Case 1 with 0.1 pu rating and 0.9 pf lead	1.0669924
Case 2 with 0.1 pu rating and 0.9 pf lead	1.0668901
Case 2 with 0.3 pu rating and 0.8 pf lead	1.0640408
Case 4 with 0.1 pu rating and 0.9 pf lead	1.0629261
Case 3 with 0.1 pu rating and 0.8 pf lead	1.0593952
Case 1 with 0.1 pu rating and 0.8 pf lead	1.0559524
Case 2 with 0.1 pu rating and 0.8 pf lead	1.0557779
Case 1 with 0.3 pu rating and 0.8 pf lead	1.0531115
Case 4 with 0.1 pu rating and 0.8 pf lead	1.0521436

## 6.5 Summary

Simulation results obtained using a test system clearly show that DG can improve system voltage profile, reduce electrical line losses, and reduce pollutant emissions. DG rating plays a vital role in determining the amount of voltage profile improvement and environmental impact reduction. Typically, VPII goes up and EIRI goes down as DG rating increases. However, this trend may not always be applicable to line loss reduction because the amount of line loss reduction may actually decrease in some cases with increased DG penetration.

The operating power factor of DG is also important in determining the benefits of DG. The results clearly indicate that introduction of DG is not beneficial to the system voltage profile and in lowering LLRI and EIRI when operated under leading power factor conditions.

The location of DG is also significant in determining both voltage profile improvement and line loss reduction. However, it should be noted that location and operating power factor of DG have only a minor impact on environmental impact reduction as compared to the impact of the rating of DG.

The simulation results clearly indicate that line loss reduction benefit dominates all the rest. Therefore, the choice of unity weighting factor ( $BW_{LLR}=1$ ) for line loss reduction yields the highest composite BI in all cases.

## CHAPTER VII

### SUMMARY AND CONCLUDING REMARKS

#### 7.1 Summary

The impending deregulated environment facing the electric utilities in the twenty first century is both a challenge and an opportunity for a variety of technologies and operating scenarios. Electric utilities are seeking new technologies to provide acceptable power quality and reliability to their customers. The option of using distributed generation is rapidly becoming attractive to many utilities across the United States because they generate electrical energy with less environmental impacts, are easy to site, and are highly efficient. One of the key features of this new environment is to build and operate several distributed generation units near load centers instead of expanding the central-station power plants.

Deployment of DG in existing distribution networks offers many benefits to utilities, customers, and society. They are: improved voltage profile, peak shaving, reduced line and transformer losses, reduced environmental impacts, increased overall system reliability and enhanced power quality, relieved transmission and distribution congestion, increased overall energy efficiency, and reduced central generating station reserve requirements.

Although several DG technologies are presently available in the market, only the four most promising ones have been considered in this study. They are:

- (i) Wind turbine generation
- (ii) Microturbine systems
- (iii) Photovoltaic systems
- (iv) Fuel cell systems

Both wind speed and insolation are random by nature. Therefore, probabilistic models based on mean and variance of the resource are used to model WTG and PV systems. Wind is highly variable and site-specific and it is considered as a continuous random variable, with an appropriate statistical distribution. The Weibull distribution is widely accepted for wind speed modeling. For PV systems, cloud model based on Beta distribution has been widely accepted as a simple approach to model insolation. Values for the mean and standard deviation of cloud cover are required to evaluate the parameters of the Beta distribution. The power output of fuel cell systems can be modeled in terms of fuel flow rates and mole fraction of gas flow into the reformer. Microturbine system is modeled in terms of fuel flow rates, and fuel pressure and temperature. Obviously, power outputs of fuel cell system and microturbine system are schedulable.

A comparison of the results obtained using a probabilistic approach and a non-probabilistic approach based on average value of WTG output for voltage profile improvement is made. Simulation results indicate that the differences are small and a non-probabilistic approach is justified to evaluate the benefits of DG.



Among the many benefits offered by DG, only three major ones are considered in this thesis: voltage profile improvement, line loss reduction, and environmental impact reduction. Accordingly, a set of four indices is proposed to quantify the technical benefits of DG. They are:

- (i) Voltage profile improvement index (VPPI)
- (ii) Line loss reduction index (LLRI)
- (iii) Environmental impact reduction index (EIRI)
- (iv) Distributed generation benefit index (BI)

Voltage profile improvement index (VPPI) quantifies the improvement in system voltage profile (VP) with the inclusion of DG. It is defined as the ratio of the voltage profile index of the system with DG to the voltage profile index of the system without DG. The voltage profile expression developed in this work incorporates weighting factors to recognize the influences of the amount and importance of loads. It allows a low load bus with important load to have a strong impact on the system voltage profile index. The case with the highest value of VPPI corresponds to the best locations and ratings for DG in terms of improving voltage profile.

Line loss reduction index (LLRI) is simply defined as the ratio of the total distribution line losses in the system with DG to the total distribution line losses in the system without DG. The minimum value of LLRI implies the best locations and ratings for DG installations to maximize line loss reduction.

The basic idea behind the environmental impact reduction index (EIRI) is to compare the emission of a particular pollutant with and without the employment of DG. A composite index with weighting factors to account for all the major pollutants is also

defined since power plants emit many pollutants into the atmosphere. EIRI can also be used to identify the best locations and ratings for installing DG in the system. The minimum value of EIRI corresponds to the best locations and ratings of DG in terms of environmental impact reduction.

Distributed generation benefit index (BI) is a composite index used to evaluate the overall benefits of DG in terms of voltage profile improvement, line loss reduction, and environmental impact reduction. The highest value of BI indicates the maximum overall benefits of DG and this index can be used to select the best locations and ratings to install DG in the system.

Simulation results clearly show that introduction of DG in existing distribution networks can improve system voltage profile, reduce electrical line losses, and reduce pollutant emissions. Results also indicate that DG rating plays a significant role in determining voltage profile improvement index, line loss reduction index, and environmental impact reduction index. As DG rating increases, VPPI goes up and LLRI and EIRI go down. However, this trend is not always applicable to line loss reduction because the rate of decrease may decline in some cases as DG rating increases.

Results indicate that the impact of location is very significant to both voltage profile improvement and line loss reduction. If DG is placed at the proper location, it can yield the maximum benefits. However, it should be noted that the impact of location on environmental impact reduction is relatively small as compared to the other impacts of DG.

Simulation results show that the operating power factor of DG is also an important factor in determining VPPI, LLRI, and EIRI. It is clear that DG is not

beneficial to the system voltage profile under leading power factor operating conditions. Once again, results show that the impact of operating power factor is relatively small to environmental impact reduction as compared to the impact of the rating of DG.

Simulation results clearly show that line loss reduction benefit dominates all the rest. Therefore, the choice of unity weighting factor ( $BW_{LLR}=1$ ) for line loss reduction yields the highest composite BI in all cases.

The results indicate that case 2 (with DG rating of 0.3 pu located at bus 10 and 0.8 pf lag) is the best scenario for employing DG when voltage profile improvement is given the maximum importance ( $BW_{VPI}=1$ ,  $BW_{LLR}=0$ , and  $BW_{EIR}=0$ ). If line loss reduction is given the maximum importance ( $BW_{VPI}=0$ ,  $BW_{LLR}=1$ , and  $BW_{EIR}=0$ ), simulation results show that case 3 (with DG at buses 9 and 10 and 0.8 pf lag) is the best for maximizing the overall benefits. With maximum importance given for environmental impact reduction ( $BW_{VPI}=0$ ,  $BW_{LLR}=0$ , and  $BW_{EIR}=1$ ), case 3 turns out to be the best. If all the benefit weighting factors are equally weighted ( $BW_{VPI}=0.33$ ,  $BW_{LLR}=0.33$ , and  $BW_{EIR}=0.33$ ), the results suggest that once again case 3 is the best to maximize the overall benefits. In practice, the benefit weighting factors can be set to emphasize the desired attributes.

The quantification approach proposed in this thesis can assist in identifying the best locations, ratings, and operating power factors of DG. Locations, ratings and operating power factors of DG have to be considered very carefully together to capture the maximum benefits of DG. In addition, the proposed approach is flexible enough to include as many factors and attributes as desired, including evaluation under varying load conditions.

## 7.2 Areas for Further Work

The approach to quantify some of the technical benefits of DG proposed in this work is useful and can help utility planners to identify the best locations and ratings to install DG in existing distribution networks to maximize the overall benefits. There are, however, a few limitations to this work. These limitations offer scope for further research. The areas for possible further research are listed below.

- Study potential operating conflicts that can arise with the inclusion of DG. Some utilities may not want to accept power from DGs. One area for further study is reverse power flow. DG can impact system reliability since it can change the power flow profile and equipment can misoperate or become overloaded and cause problems.
- Study the dispatch problem. In reality, a large number of DGs can be included in existing distribution networks. This can make the dispatch problem very complex. The decision will depend on several factors such as type of DG, availability of resources, and fuel cost. Further research is suggested to develop procedures and control strategies to decide which DG units will go on line and when.
- A twelve-bus test system has been used to simulate and quantify the technical benefits in this research. However, this is only a first step. Further work is recommended to study larger and realistic distribution networks.
- The goal of this research was to quantify only the technical benefits of DG. Even there, only three major benefits have been studied and quantified. Several other benefits of DG need further work. One significant area among

them is system reliability improvement. In general, DG can improve system reliability by reducing System Average Interruption Duration Index (SAIDI). Further work is needed to develop an appropriate procedure to quantify this benefit. Other possible areas include: improving power quality, improving overall energy efficiency, and reduction of transformer losses.

- Conduct a detailed economic analysis of DG. Generally, capital costs of most DG technologies are relatively high as compared to conventional technologies. Therefore, it is important to quantify and evaluate whether DG is worth its capital cost. This will involve assigning monetary values to all the benefits realized by the introduction of DG.
- This research has considered only a snapshot of load conditions and DG outputs. However, load and power output of DG vary continuously. Further work is necessary to study the overall impacts for daily and seasonal cases based on real-world data.

## REFERENCES

1. Bayegan, M., "A Vision of the Future Grid," IEEE Power Engineering Review, Vol. 21, Iss. 12, pp. 10-12, December 2001.
2. Brown, M., "Clean Energy opportunities-The Linkage of Renewable and Natural Gas in Distributed Generation Markets-An NREL Point of View," paper presented at the 31<sup>st</sup> Energy Information Dissemination Program, organized by The Engineering Energy Laboratory, Oklahoma State University, Stillwater, Oklahoma, April 2000.
3. Chiradeja, P., and Ramakumar, R., "A Review of Distributed Generation and Storage," Proceedings of the 31<sup>st</sup> Annual Frontiers of Power Conference, Stillwater, Oklahoma, pp. VIII-1 to VIII-11, October 1998.
4. Ramakumar, R., and Chiradeja, P., "Distributed Generation and Renewable Energy Systems," Proceedings of the 37<sup>th</sup> Intersociety Energy Conversion Engineering Conference, Washington, D. C., pp. IECEC-2002-20027-1-8, July 2002.
5. Sweet, W., "Networking Assets", IEEE Spectrum, Vol. 38, Iss. 1, pp. 84-88, January 2001.
6. Daly, P. A., "Understanding the Potential Benefits of Distributed Generation on Power Delivery Systems," paper presented at the Rural Electric Power Conference 2001, Little Rock, Arkansas, 2001.
7. Dugan, R. C., and Price, S. K., "Issues for Distributed Generations in the US," IEEE Power Engineering Society 2002 Winter Meeting, New York, New York, Vol.1, pp. 121-126, January 2002.
8. Chiradeja, P., and Ramakumar, R., "A Study of the Benefits of Distributed Generation," Proceedings of the 35<sup>th</sup> Annual Frontiers of Power Conference, Stillwater, Oklahoma, pp. VIII-1 to VIII-11, October 2002.
9. Brown, R. E., Pan, J., Feng, X., and Koutlev, K., "Siting Distributed Generation to Defer T&D Expansion," IEEE/PES Transmission and Distribution Conference and Exposition, Raleigh, NC, Vol. 2, pp. 622-627, October 2001.

10. Spera, D. A., Wind Turbine Technology. New York, NY: ASME Press, 1994.
11. Koepl, W. G., Putnam's Power from Wind. New York, NY: Van Nostrand Reinhold, 1981.
12. Johnson, G. L., Wind Energy Systems. Englewood Cliffs, NJ: Prentice-Hall, 1985.
13. Scott, W. G., "Micro-Turbine Generators for Distribution Systems," IEEE Industry Applications Magazine, pp. 57-62, May/June 1998.
14. Friedman, R., "Microturbine Power Generation: Technology Development Needs and Challenges," paper presented at the Vision-21, Environmental Electric Energy Opportunities for the next century, organized by IEEE and EPRI, Washington DC, April 1998.
15. Price, D. L., "Distributed Generation in General and Micro Turbines," paper presented at the 33<sup>rd</sup> Energy Information Dissemination Program, organized by The Engineering Energy Laboratory, Oklahoma State University, Stillwater, Oklahoma, April 2002.
16. Bube, R. H., and Fahrenbruch, A. L., Fundamental of Solar Cells. New York, NY: Academic Press, 1983.
17. Rauschenbach, H. S., Solar Cell Array Design Handbook: The Principle and Technology of Photovoltaic Energy Conversion. New York, NY: Van Nostrand Reinhold, 1980.
18. Ramakumar, R., and Bigger J. E., "Photovoltaic Systems," Proceedings of the IEEE, Vol. 81, No.3, pp. 365-377, March 1993.
19. Del Monaco, J. L., "Current Status of Distributed Generation Technologies," paper presented at the 31<sup>st</sup> Energy Information Dissemination Program, organized by The Engineering Energy Laboratory, Oklahoma State University, Stillwater, Oklahoma, April 2000.
20. Boes, E., "Renewable Power Outlook," paper presented at the Vision-21, Environmental Electric Energy Opportunities for the next century, organized by IEEE and EPRI, Washington DC, April 1998.
21. Blomen, L. J. M. J., and Mugerwa, M. N., Fuel Cell Systems. New York, NY: Plenum Press, 1993.
22. Oman, H., "Fuel Cells for Personal Electricity," IEEE AES Systems Magazine, pp. 43-45, September 2000.

23. Anahara, R., Yokokawa, S., and Sakurai, M., "Present Status and Future Prospects for Fuel Cell Power Systems," Proceedings of the IEEE, Vol. 81, No. 3, pp. 399-408, March 1993.
24. Sawyer, T. R., The Modern Gas Turbine. New York, NY: Prentice-Hall, 1947.
25. Bathie, W. W., Fundamentals of Gas Turbines. New York, NY: John Wiley & Sons, 1984.
26. Constant, H., Gas Turbines and Their Problems. London, England: Todd Publishing Group Limited, 1953.
27. Welsh, R. J., and Waller, G., The Gas Turbine Manual. London, England: Temple Press Limited, 1951.
28. Ramakumar, R., "Technology and Economic Market Integration of DG," Proceedings of the 34<sup>th</sup> Annual Frontiers of Power Conference, Stillwater, Oklahoma, pp. X-1 to X-14, October 2001.
29. Badeer, G. H., "GE Aeroderivative Gas Turbines-Design and Operating Features," GE Power Systems, pp.1-15, October 2000.
30. Richardson, R. D., and Mcnerney, G. M., "Wind Energy Systems," Proceedings of the IEEE, Vol. 81, No. 3, pp. 378-389, March 1993.
31. Ramakumar, R., "Electricity from Renewable Energy-A Timely Option," Keynote Address at the National Seminar on Renewable Energy Sources-Electric Power Generation, Pune, Maharashtra, India, August 2001.
32. T-Raissi, A., "Current Technology of Fuel Cell Systems," Proceedings of the 32<sup>nd</sup> Intersociety Energy Conversion Engineering Conference, Honolulu, HI, Vol. 3, pp. 1953-1957, July 1997.
33. Rahman, S., "Fuel Cell as a Distributed Generation Technology," IEEE Power Engineering Society 2001 Summer Meeting, Vancouver, Canada, Vol.1, pp. 551-552, July 2001.
34. Wong, E., Chairman, "Collaborative Report and Action Agenda," Report prepared for CADER, California Alliance for Distributed Energy Resources, January 1998.
35. Dugan, R. C., and Mcdermott, T. E., "Distributed Generation," IEEE Industry Applications Magazine, pp. 19-25, March/April 2002.
36. Goodman, F., "Increasing the Benefits of Distributed Resources in Future Electricity Supply Infrastructure," paper presented at the 31<sup>st</sup> Energy



Information Dissemination Program, organized by The Engineering Energy Laboratory, Oklahoma State University, Stillwater, Oklahoma, April 2000.

37. Green, R., "The Electric Distribution Company's Role in Distributed Generation," paper presented at the 31<sup>st</sup> Energy Information Dissemination Program, organized by The Engineering Energy Laboratory, Oklahoma State University, Stillwater, Oklahoma, April 2000.
38. Dale, L., "Distributed Generation and Transmission," IEEE Power Engineering Society 2002 Winter Meeting, New York, New York, Vol.1, pp. 132-134, January 2002.
39. Barker, P. P., and De Mello, R. W., "Determining the Impact of Distributed Generation on Power Systems: Part I-Radial Distributed Systems," IEEE Power Engineering Society 2000 Summer Meeting, Seattle, Washington, Vol.3, pp. 1645-1656, July 2000.
40. Hadjsaid, N., Canard, J. F., and Dumas, F., "Dispersed Generation Impact on Distribution Networks," IEEE Applications in Power, Vol. 12, No. 2, pp. 22-28, April 1999.
41. Chou, K., and Corotis, R., "Simulation of Hourly Wind Speed And Array Wind Power," Solar Energy, Vol. 26, pp. 199-212, 1981.
42. Johnson, G., "Economic Design of Wind Electric Systems," IEEE Transactions on Power Apparatus and Systems, Vol. PAS 97, No.2, pp. 554-562, 1978.
43. Evtuhov, V., "Parametric Cost Analysis of Photovoltaic Systems," Solar Energy, Vol. 22, pp. 427-433, 1979.
44. Billinton, R., and Gan, L., "Wind Power Modeling and Application in Generating Adequacy Assessment," IEEE Conference Proceedings of Communications, Computers, and the Modern Environment, pp. 100-106, May 1993.
45. Watson, S. J., Landberg, L., and Halliday, J. A., "Application of Wind Speed Forecasting to the Integration of Wind Energy into a Large Scale Power System," IEE Proceedings of Generation, Transmission, and Distribution, Vol. 141, No. 4, pp. 357-362, July 1994.
46. Abouzahr, I., and Ramakumar, R., "Loss of Power Supply Probability of Stand-Alone Wind Electric Systems," IEEE Transaction on Energy Conversion, Vol. 5, No. 3, pp. 445-451, September 1990.

47. Karaki, S. H., Chedid, R. B., and Ramadan, R., "Probabilistic Performance Assessment of Wind Energy Conversion Systems," IEEE Transaction on Energy Conversions, Vol. 14, No. 2, pp. 217-224, June 1999.
48. Shuhui, Li, Wunsch, D.C., O'Hair, E. A., and Giesselmann, M. G., "Using Neural Networks to Estimate Wind Turbine Power Generation," IEEE Transaction on Energy Conversion, Vol. 16, No. 3, pp. 276-282, September 2001.
49. Xueguang, W., Weisheng, W., Huizhu, D., and Yunping, C., "Application of Models of the Wind Energy Conversion System to Wind Power Dynamic Analysis," International Conference on Power System Technology, organized by the IEEE, Beijing, China, Vol. 2, pp. 1406-1411, August 1998.
50. Usaola, J. and Ledesma, P., "Dynamic Incidence of Wind Turbines in Networks with High Wind Penetration," IEEE Power Engineering Society 2001 Summer Meeting, Vancouver, Canada, Vol.2, pp. 755-760, July 2001.
51. "Modeling New Forms of Generation and Storage," CIGRE Technical Brochure TF 38.01.10. Paris, France, June 2000.
52. Etezadi-Amoli, M., Choma, K., "Electrical Performance Characteristics of a New Micro-Turbine Generator," IEEE Power Engineering Society 2001 Winter Meeting, Columbus, Ohio, Vol. 2, pp. 736-740, January 2001.
53. Lasseter, R., "Dynamic Models for Micro-Turbines and Fuel Cells," IEEE Power Engineering Society 2001 Summer Meeting, Vancouver, Canada, Vol.2, pp. 761-766, July 2001.
54. Young, K. L., Woo, M., and Munro, D. S., "Simple Approaches to Modeling Solar Radiation in the Arctic," Solar Energy, Vol. 54, No.1, pp. 33-40, 1995.
55. Yaramanoglu, M., Brinsfield, R., and Muller, R., "Estimation of Solar Radiation Using Stochastically Generated Cloud Cover Data," Energy in Agriculture, No. 4, pp.227-242, 1985.
56. Abouzahr, I., and Ramakumar, R., "Loss of Power Supply Probability of Stand-Alone Photovoltaic Systems," IEEE Transaction on Energy Conversion, Vol. 6, No. 1, pp. 1-11, March 1991.
57. Jewell, W. and Ramakumar, R., "The Effects of Moving Clouds on Electric Utilities with Dispersed Photovoltaic Generation," IEEE Transaction on Energy Conversion, Vol. EC-2, No. 4, pp. 570-576, December 1987.

58. Ujiie, K., Izumi, T., Yokoyama, T., and Haneyoshi, T., "Study on Dynamic and Static Characteristics of Photovoltaic cell," Proceedings of the Power Conversion Conference 2002, Osaka, Japan, Vol. 2, pp. 810-815, April 2002.
59. Padulles, J., Ault, G. W., and McDonald, J. R., "An Approach to the Dynamic Modeling of Fuel Cell Characteristics for Distributed Generation Operation," IEEE Power Engineering Society 2000 Winter Meeting, Vol.1, pp. 134-138, January 2000.
60. Lukas, M. D., Lee, Y. K., and Ghezal-Ayagh, H., "Performance Implications of Rapid Load Changes in Carbonate Fuel Cell Systems," IEEE Power Engineering Society 2001 Winter Meeting, Columbus, Ohio, Vol. 3, pp. 979-984, January 2001.
61. Lukas, M. D., Lee, K. Y., and Ghezal-Ayagh, H., "Development of a Stack Simulation Model for Control Study on Direct Molten Carbonate Fuel Cell Power Plant," IEEE Transactions on Energy Conversion, Vol. 14, No. 4, pp. 1651-1657, December 1999.
62. Lukas, M. D., Lee, K. Y., and Ghezal-Ayagh, H., "Operation and Control of Direct Reforming Fuel Cell Power Plant," IEEE Power Engineering Society Winter Meeting, Vol. 1, pp. 523-527, 2000.
63. Lukas, M. D., Lee, K. Y., and Ghezal-Ayagh, H., "Reduced-Order Dynamic Model of Carbonate Fuel Cell Systems for Distributed Generation Control," IEEE Power Engineering Society Summer Meeting, Seattle, Washington, Vol. 4, pp. 1965-1969, 2000.
64. Lukas, M. D., Lee, K. Y., and Ghezal-Ayagh, H., "Experimental Transient Validation of a Direct Fuel Cell Stack Model," IEEE Power Engineering Society Summer Meeting, Vancouver, BC, Canada, Vol. 3, pp. 1363-1368, 2001.
65. Lukas, M. D., Lee, K. Y., and Ghezal-Ayagh, H., "An Explicit Dynamic Model for Direct Reforming Carbonate Fuel Cell Stack," IEEE Transaction on Energy Conversion, Vol. 16, No. 3, pp. 289-295, September 2001.
66. Hatziaioniu, C. J., Lobo, A. A., Pourboghrat, F., and Daneshdoost, M., "A Simplified Dynamic Model of Grid-Connected Fuel-Cell Generators," IEEE Transactions on Power Delivery, Vol. 17, No. 2, pp. 467-473, April 2002.
67. Hall, D. J. and Colclaser, R. G., "Transient Modeling and Simulation of a Tubular Solid Oxide Fuel Cell," IEEE Transaction on Energy Conversion, Vol. 14, No. 3, pp. 749-753, September 1999.

68. Correa, J. M., Farret, F. A., and Canha, L. N., "An Analysis of the Dynamic Performance of Proton Exchange Membrane Fuel Cells using an Electrochemical Model," The Annual Conference of the IEEE: Industrial Electronics Society 2001, Vol. 1, pp. 141-146, December 2001.
69. Turner, W., Parten, M., Vines, D., Jones, J., Maxwell, T., "Modeling a PEM Fuel Cell for Use in a Hybrid Electric Vehicle," IEEE 49<sup>th</sup> Vehicular Technology Conference, Vol. 2, pp.1385-1388, 1999.
70. Milligan, M. R., and Graham, M. S., "An Enumerated Probabilistic Simulation Technique and Case Study: Integrating Wind Power into Utility Production Cost Models," Report to National Renewable Energy Laboratory for Wind Energy Program, 1996.
71. Hoff, T., "The Value of Photovoltaics: A Utility Perspective," IEEE Conference Record of Photovoltaic Specialists Conference, New Orleans, Louisiana, pp.1145-1149, May 1987.
72. Shugar, D. S., "Photovoltaics in the Utility Distribution Systems: The evaluation of System and Distributed Benefits," IEEE Conference Record of Photovoltaic Specialists Conference, Vol. 2, pp. 836-843, 1990.
73. Chowdhury, B., and Sawab, A. W., "Evaluation the Value of Distributed Photovoltaic Generation in Radial Distributions Systems," IEEE Transactions on Energy Conversion, Vol. 11, No. 3, pp. 595-600, September 1996.
74. Hoff, T., and Shugar, D. S., "The Value of Grid-Support Photovoltaics in Reducing Distribution System losses," IEEE Transactions on Energy Conversion, Vol. 10, No. 3, pp. 569-576, September 1995.
75. Hoff, T., and Shugar, D. S., "The Value of Grid-Support Photovoltaics to Substation Transformers," paper presented at 13<sup>th</sup> IEEE Transmission and Distribution Conference, Chicago, IL, July 1994.
76. Ijumba, N. M., Jimoh, A. A., and Nkabinde, M., "Influence of Distribution Generation on Distribution Network Performance," IEEE Africon, Vol. 2, pp. 961-964, 1999.
77. Chiradeja, P., and Ramakumar, R., "Benefits of Distributed Generation: A Simple Case Study," Proceedings of the 32<sup>nd</sup> Annual Frontiers of Power Conference, Stillwater, Oklahoma, pp. X-1 to X-9, October 1999.
78. Chiradeja, P., and Ramakumar, R., "A Probabilistic Approach to the Analysis of Voltage Profile Improvement with Distributed Wind Electric Generation,"

Proceedings of the 34<sup>th</sup> Annual Frontiers of Power Conference, Stillwater, Oklahoma, pp. XII-1 to XII-10, October 2001.

79. Caire, R., Retiere, N., Martino, N., Andrieu, C., and Hadjsaid, N., "Impact Assessment of LV Distributed Generation on MV Distribution Network," IEEE Power Engineering Society Summer Meeting, Chicago, IL, July 2002.
80. Deshmukh, R. G., and Ramakumar, R., "Reliability Analysis of Combined Wind-Electric and Conventional Generation Systems," Solar Energy, Vol. 28, No. 4, pp. 345-352, 1982.
81. Billinton, R., and Chowdhury, A. A., "Incorporation of Wind Energy Conversion Systems in Conventional Generating Capacity Adequacy Assessment," IEE Proceeding-C, Vol. 139, No. 1, pp. 47-56, January 1992.
82. Billinton, R., Chen H., and Ghajar, R., "A Sequential Simulation Technique for Adequacy Evaluation of Generating Systems Including Wind Energy," IEEE Transactions on Energy Conversion, Vol. 11, No. 4, pp. 728-734, December 1996.
83. Ubeda, J. R., and Rodriguez Garcia, M. A. R., "Reliability and Production Assessment of Wind Energy Production Connected to the Electric Network Supply," IEE Proceedings of Generation, Transmission, and Distribution, Vol. 146, No. 2, pp. 169-175, March 1999.
84. Brown, R. E., and Freeman, L. A. A., "Analyzing the Reliability Impact of Distributed Generation," IEEE Power Engineering Summer Meeting, Vancouver, BC, Canada, Vol. 2, pp. 1013-1018, July 2001.
85. Billinton, R., and Wang P., "Distribution System Reliability Cost/Worth Analysis Using Analytical and Sequential Simulation Techniques," IEEE Transactions on Power System, Vol. 13, No. 4, pp. 1245-1250, November 1998.
86. Karki, R., and Billinton, R., "Reliability/Cost Implication of PV and Wind Energy Utilization in Small Isolated Power Systems," IEEE Transactions on Energy Conversion, Vol. 16, No. 4, pp. 368-373, December 2001.
87. Karagiannis, F. E., "Wind Energy Investments in Greece- An Economic Approach," Electrotechnical Conference 2000: Melcon 2000, Mediterranean, 2000.
88. Ramakumar, R., Butler, N. G., Rodriguez, A. P., and Venkata, S. S., "Economic Aspects of Advanced Energy Technologies," Proceedings of the IEEE, Vol. 81, No. 3, pp. 318-332, March 1993.

89. Lamberth, R., and Lepley T., "Distributed Photovoltaic System Evaluation by Arizona Public Service Company," IEEE Conference Record of Photovoltaic Specialists Conference, pp. 14-20,
90. Patel, M. R., Wind and Solar Power Systems. New York, N.Y.: CRC Press, 1999.
91. Erich, H., Wind Turbines: Fundamentals, Technologies, Application, and Economics. New York, NY: Springer, 2000.
92. Ramakumar, R., Engineering Reliability: Fundamentals and Applications. Englewood Cliffs, NJ: Prentice-Hall, 1993.
93. Cheremisinoff, N. P., Fundamentals of Wind Energy. Ann Arbor, MI: Ann Arbor Science Publishes, 1978.
94. Ohta, T., Energy Technology: Sources, Systems, and Frontier Conversion. London England: Pergamon, 1994.
95. Shanmugan, K. S., and Breipohl, A. M., Random Signals: Detection, Estimation and Data Analysis. New York, NY: John Wiley&Sons, 1988.
96. Papoulis, A., Probability, Random Variables, and Stochastic Processes. New York, NY: McGraw-Hill, 1965.
97. Turner, W. C., et. al., Energy Management Handbook. Lilburn, GA: The Fairmont Press, 1992.
98. Schwartz, R. J., "Photovoltaic Power Generation," Proceedings of the IEEE, Vol. 81, No. 3, pp355-364, March 1993.
99. Rosenburg, P., The Alternatives Energy Handbook. Lilburn, GA: The Fairmont Press, 1992.
100. Abouzahr, I., and Ramakumar, R., "An Approach Assess the Performance of Utility-Interactive Photovoltaic Systems," IEEE Transactions on Energy Conversion, Vol. 8, No. 2, pp. 145-153, June 1993.
101. Hassmann, K., "Electric Power Generation," Proceedings of the IEEE, Vol. 81, No.3, pp. 346-354, March 1993.
102. "Fuel Cell Handbook," Publication by National Energy Technology Laboratory, U.S. Department of Energy, October 2000.
103. Laughton, A. M., "Fuel Cells," Power Engineering Journal, pp. 37-47, February 2002.

104. Ellis, M. W., Von Spakovsky, M. R., and Nelson, D. J., "Fuel Cell Systems: Efficient, Flexible Energy Conversion for 21<sup>st</sup> Century," Proceedings of the IEEE, Vol. 89, No. 2, pp. 1808-1818, December 2001.
105. Farooque, M., and Maru, H. C., "Fuel Cells-The Clean and Efficient Power Generators," Proceedings of the IEEE, Vol. 89, No. 2, pp. 1819-1829, December 2001.
106. Williams, K. R., An Introduction to Fuel Cells. New York, NY: Elsevier Publishing, 1966.
107. Bockris, J. O'M., Srinivasan, S, Fuel Cells: Their Electrochemistry. New York, NY: Mcgraw-Hill Book, 1969.
108. "Distributed Power Generation in a Deregulated Market Environment, Part I: Electricity Market and their Impact on Distributed Power Generation," Publication by Royal Institute of Technology: Electric Power System, June 1999.
109. "IEEE Reliability Test System," reported by the Reliability Test System Task Force of the Application of Probability Methods Subcommittee, IEEE Transaction on Power Apparatus and Systems, Vol. PAS-98, No. 6, pp. 2047-2054, November/December 1979.
110. "IEEE Reliability Test System - 1996," reported by the Reliability Test System Task Force of the Application of Probability Methods Subcommittee, IEEE Transaction on Power Systems, Vol. 14, No. 3, pp. 1010-1020, August 1999.
111. Faulkenberry, L. M., and Coffey, W., Electrical Power Distribution and Transmission. Englewood Cliffs, NJ: Prentice-Hall, 1996.
112. Elgerd, O. I., Electric Energy Systems Theory: An Introduction. New York, NY: Mcgraw-hill, Inc, 1982.
113. Glover, J. D., and Sarma, M., Power System Analysis & Design. Boston, MA: PWS Publishing Company, 1993.
114. Bergen, A. R., Power Systems Analysis. Englewood Cliffs, NJ: Prentice-Hall, 1986.
115. El-Hawary, M. E., Electrical Power Systems. New York, NY: The Institute of Electrical and Electronics Engineers, Inc., 1983.
116. Seidman, A. H., Mahrous, H., and Hicks, T. G., Handbook of Electric Power Calculations. New York, NY: Mcgraw-Hill Book Company, 1984.

117. Del Toro, V., Electric Power Systems. Englewood Cliffs, NJ: Prentice-Hall, 1992.



APPENDIXES

## APPENDIX A

TABLE 17

THERMODYNAMIC CHARACTERISTICS AND IDEAL  
VOLTAGES OF FUEL CELL REACTIONS AT 650 °C  
[SEE REFERENCE 107]

Reaction	$\Delta G^\circ$ (Kj.mol <sup>-1</sup> )	$E^\circ$ (V)
$\text{H}_2 + \frac{1}{2} \text{O}_2 \rightarrow \text{H}_2\text{O}$	-196.92	1.020
$\text{CO} + \frac{1}{2} \text{O}_2 \rightarrow \text{CO}_2$	-202.51	1.049
$\text{CH}_4 + 2\text{O}_2 \rightarrow \text{CO}_2 + 2\text{H}_2\text{O}$	-800.89	1.038
$\text{CH}_4 + \text{H}_2\text{O} \rightarrow \text{CO} + 3\text{H}_2$	-7.62	0.010
$\text{CH}_4 + \text{CO}_2 \rightarrow 2\text{CO} + 2\text{H}_2$	-2.04	0.003
$\text{CO} + \text{H}_2\text{O} \rightarrow \text{CO}_2 + \text{H}_2$	-5.58	0.029
$2\text{CO} \rightarrow \text{CO} + \text{CO}_2$	-14.62	0.076

## APPENDIX B

## SOLUTION FOR EQUATION (4.3.1.5)

$$E = 2XB$$

$$G = 9V_s^2 + 6v_L^2 B^2 - 6Xv_L \sqrt{V_s^2 + v_L^2 (B^2 - 1)}$$

$$K = 9V_s^4 + 36v_L^2 V_s^2 (B^2 - 1) + 36v_L^4 (1 + 2B^4 - 3B^2) + 72Bv_L^3 (1 - B^2) \sqrt{B^2 v_L^2 - v_L^2 + V_s^2}$$

$$Q = 24XBv_L^2 (1 - B^2) - 12XBV_s^2 + 24Xv_L (B^2 - 1) \sqrt{B^2 v_L^2 - v_L^2 + V_s^2}$$

## APPENDIX C

## CLOSED FORM SOLUTION FOR PROBABILITY DENSITY FUNCTION OF C

$$f_c(c) = f_{P_w}(p_w) * f_L(l)$$

where  $f_c(c)$  is given by:

$$\text{Case i) } P_R \geq \left( \frac{L_{\max} - L_{\min}}{a PF_L} \right)$$

$$\text{a) } \frac{L_{\min}}{PF_L} - a P_R \leq c \leq \frac{L_{\max}}{PF_L} - a P_R$$

$$\frac{PF_L}{L_{\max} - L_{\min}} \left[ \exp \left[ - \left( \frac{U_C^{2.28} + \left( \frac{U_R^{2.28} - U_C^{2.28}}{a P_R} \right) \left( \frac{L_{\min}}{PF_L} - c \right)}{\alpha_w} \right)^{\frac{1}{2.28}} \right]^{\beta_w} \right] \\ - \exp \left[ - \left( \frac{U_O}{\alpha_w} \right)^{\beta_w} \right]$$

$$\text{b) } \frac{L_{\max}}{PF_L} - a P_R < c < \frac{L_{\min}}{PF_L}$$

$$\text{Subcase b1: } L_{\max} < L_{\min} + a P_R \left( \frac{PF_L}{2} \right)$$

$$\frac{PF_L}{L_{\max} - L_{\min}} \left[ \begin{array}{l} \exp \left[ - \left( \frac{U_C^{2.28} + \left( \frac{U_R^{2.28} - U_C^{2.28}}{a P_R} \right) \left( \frac{L_{\min} - c}{PF_L} \right)}{\alpha_w} \right)^{\frac{1}{2.28}} \beta_w \right] \\ - \exp \left[ - \left( \frac{U_C^{2.28} + \left( \frac{U_R^{2.28} - U_C^{2.28}}{a P_R} \right) \left( \frac{L_{\max} - c}{PF_L} \right)}{\alpha_w} \right)^{\frac{1}{2.28}} \beta_w \right] \end{array} \right]$$

$$\text{Subcase b2: } L_{\max} \geq L_{\min} + a P_R \left( \frac{PF_L}{2} \right)$$

$$\frac{PF_L}{L_{\max} - L_{\min}} \left[ \begin{array}{l} 1 + \exp \left( - \left( \frac{U_R}{\alpha_w} \right)^{\alpha_w} \right) + \exp \left( - \left( \frac{U_o}{\alpha_w} \right)^{\beta_w} \right) \\ - 2 \exp \left( - \left( \frac{U_C}{\alpha_w} \right)^{\beta_w} \right) \end{array} \right]$$

$$c) \quad \frac{L_{\min}}{PF_L} \leq c \leq \frac{L_{\max}}{PF_L}$$

$$\frac{PF_L}{L_{\max} - L_{\min}} \left[ \begin{array}{l} 1 + \exp\left(-\left(\frac{U_o}{\alpha_w}\right)^{\beta_w}\right) \\ - \exp\left(-\left\{ \frac{U_C^{2.28} + \left(\frac{U_R^{2.28} - U_C^{2.28}}{a P_R}\right) \left(\frac{L_{\max} - c}{PF_L}\right)^{\frac{1}{2.28}}}{\alpha_w} \right\}^{\beta_w}\right) \end{array} \right]$$

$$\text{Case ii) } P_R < \left( \frac{L_{\max} - L_{\min}}{a PF_L} \right)$$

$$a) \quad \frac{L_{\min}}{PF_L} - a P_R \leq c \leq \frac{L_{\min}}{PF_L}$$

$$\frac{PF_L}{L_{\max} - L_{\min}} \left[ \begin{array}{l} \exp\left(-\left\{ \frac{U_C^{2.28} + \left(\frac{U_R^{2.28} - U_C^{2.28}}{a P_R}\right) \left(\frac{L_{\min} - c}{PF_L}\right)^{\frac{1}{2.28}}}{\alpha_w} \right\}^{\beta_w}\right) \\ - \exp\left(-\left(\frac{U_o}{\alpha_w}\right)^{\beta_w}\right) \end{array} \right]$$

$$\text{b) } \frac{L_{\min}}{PF_L} < c < \frac{L_{\max}}{PF_L} - a P_R$$

$$\frac{PF_L}{L_{\max} - L_{\min}}$$

$$\text{c) } \frac{L_{\max}}{PF_L} - a P_R \leq c \leq \frac{L_{\max}}{PF_L}$$

$$\frac{PF_L}{L_{\max} - L_{\min}} \left[ \begin{array}{l} 1 + \exp \left( - \left( \frac{U_o}{\alpha_w} \right)^{\beta_w} \right) \\ - \exp \left( - \left( \frac{U_C^{2.28} + \left( \frac{U_R^{2.28} - V_C^{2.28}}{a P_R} \right) \left( \frac{L_{\max}}{PF_L} - c \right)}{\alpha_w} \right)^{\frac{1}{2.28}} \right)^{\beta_w} \end{array} \right]$$

## APPENDIX D

### LOAD FLOW CALCULATION BY NEWTON-RAPHSON METHOD

Two methods have been used to solve load flow equation over the years. They are: Gauss-Seidel method and Newton-Raphson method. The Gauss-Seidel method is simpler and less demanding of computer calculation time but it does suffer from relatively slow convergence as the system size grows. As a result, the more powerful Newton-Raphson method is dominating the power flow solution field because of its fast-converging feature. The basic idea of solving load flow problem with Newton-Raphson method is presented next.

#### D.1 Iterative Solutions to Newton-Raphson Method [112-117]

The Newton-Raphson method is based on making a good initial guess of the unknown variable in the non-linear equation. Let  $f(x)$  be a non-linear function and we want to solve for  $x$  where

$$f(x) = 0$$

An initial guess is made on  $x$ ; call it  $x^{(0)}$ . After testing how close  $x^{(0)}$  is to actual solution, we have to find a way to improve on this guess in the next try at the solution. One method to achieve this goal is to apply a Taylor series expansion around the guessed value.



The result leads to:

$$f(x) = f(x^{(0)}) + \Delta x^{(0)} \left( \frac{df}{dx} \right)^{(0)} + \frac{1}{2} (\Delta x^{(0)})^2 \left( \frac{d^2 f}{dx^2} \right)^{(0)} + h.o.t = 0$$

where “h.o.t” stands for high-order terms. All derivatives are computed at  $x=x^{(0)}$ .

Assuming that the error is relatively small, all the high-order terms can be dropped and

the result leads to:

$$f(x) = f(x^{(0)}) + \Delta x^{(0)} \left( \frac{df}{dx} \right)^{(0)} = 0$$

and

$$\Delta x^{(0)} = - \frac{f(x)^{(0)}}{\left( \frac{df}{dx} \right)^{(0)}}$$

The error ( $\Delta x^{(0)}$ ) is added to the original guess to obtain an improved value  $x^{(1)}$  as

follows:

$$x^{(1)} = x^{(0)} + \Delta x^{(0)} = x^{(0)} - \frac{f(x)^{(0)}}{\left( \frac{df}{dx} \right)^{(0)}}$$

A general form of the last expression for the  $\nu$  th iteration can be expressed as:

$$x^{(\nu+1)} = x^{(\nu)} - \frac{f(x)^{(\nu)}}{\left(\frac{df}{dx}\right)^{(\nu)}}$$

The solution for the n-dimensional equation can be expressed by expanding each equation in a Taylor series around the initial guess.

$$\mathbf{x}^{(0)} = \begin{bmatrix} x_1^{(0)} \\ x_2^{(0)} \\ x_3^{(0)} \\ \vdots \\ x_n^{(0)} \end{bmatrix}$$

By neglecting the high order terms, Taylor series expansion with only the first derivative terms can be expressed as:

$$\begin{bmatrix} f_1(\mathbf{x}^{(0)}) \\ f_2(\mathbf{x}^{(0)}) \\ \vdots \\ f_n(\mathbf{x}^{(0)}) \end{bmatrix} + \begin{bmatrix} \frac{\partial f_1}{\partial x_1} & \frac{\partial f_1}{\partial x_2} & \dots & \frac{\partial f_1}{\partial x_n} \\ \frac{\partial f_2}{\partial x_1} & \frac{\partial f_2}{\partial x_2} & \dots & \frac{\partial f_2}{\partial x_n} \\ \vdots & \vdots & \dots & \vdots \\ \frac{\partial f_n}{\partial x_1} & \frac{\partial f_n}{\partial x_2} & \dots & \frac{\partial f_n}{\partial x_n} \end{bmatrix} \begin{bmatrix} \Delta x_1 \\ \Delta x_2 \\ \vdots \\ \Delta x_n \end{bmatrix} = \begin{bmatrix} 0 \\ 0 \\ \vdots \\ 0 \end{bmatrix}$$

Let  $\mathbf{J}$  is Jacobian matrix and expressed as:

$$\mathbf{J} = \begin{bmatrix} \frac{\partial f_1}{\partial x_1} & \frac{\partial f_1}{\partial x_2} & \dots & \frac{\partial f_1}{\partial x_n} \\ \frac{\partial f_2}{\partial x_1} & \frac{\partial f_2}{\partial x_2} & \dots & \frac{\partial f_2}{\partial x_n} \\ \vdots & \vdots & \dots & \vdots \\ \frac{\partial f_n}{\partial x_1} & \frac{\partial f_n}{\partial x_2} & \dots & \frac{\partial f_n}{\partial x_n} \end{bmatrix}$$

Using matrix notation, the result leads to:

$$\mathbf{f}(\mathbf{x}^{(0)}) = \mathbf{J}^{(0)} \Delta \mathbf{x}^{(0)} = \mathbf{0}$$

and

$$\Delta \mathbf{x}^{(0)} = -[\mathbf{J}^{(0)}]^{-1} \mathbf{f}(\mathbf{x}^{(0)})$$

By adding error vector ( $\Delta \mathbf{x}^{(0)}$ ) to the original guess, the Newton-Raphson algorithm can be expressed as:

$$\mathbf{x}^{(\nu+1)} = \mathbf{x}^{(\nu)} - [\mathbf{J}^{(\nu)}]^{-1} \mathbf{f}(\mathbf{x}^{\nu})$$

The process continues until the following criterion is satisfied:

$$\left| \frac{x_i^{(\nu+1)} - x_i^\nu}{x_i^\nu} \right| < \varepsilon$$

where  $\varepsilon$  is a specified tolerance level.

## D.2 Application of the Newton-Raphson Method to the Power Flow Problem

In an electric power system, most of the buses are load buses. Generally, bus 1 is assumed to be slack bus. Therefore, for a system with  $n$  buses, unknown variables consist of  $n-1$  voltage magnitudes ( $|V_2|, |V_3|, \dots, |V_n|$ ) and  $n-1$  angles ( $\delta_2, \delta_3, \dots, \delta_n$ ). The general bus  $i$  of a power system as shown in Figure 59 is used to formulate the power flow equations in the general case.

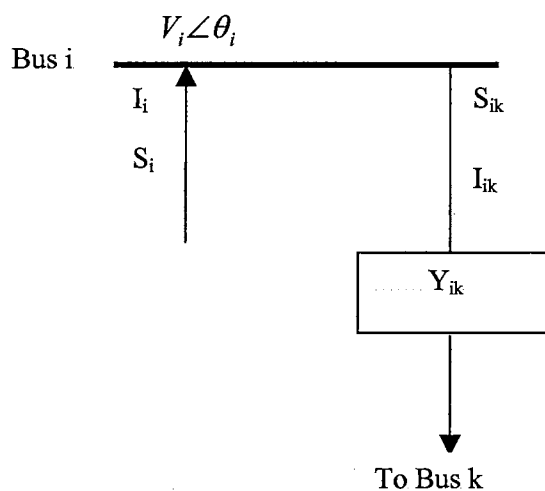


Figure 59. A General Power System Bus [See Reference 112]

Using  $\mathbf{Y}_{bus}$ , the nodal equations for a general power system can be expressed as:

$$\mathbf{I} = \mathbf{Y}_{bus} \mathbf{V}$$

where  $\mathbf{I}$  and  $\mathbf{V}$  is the n-dimensional bus current and bus voltage vectors and  $\mathbf{Y}_{bus}$  is the  $n \times n$  dimensional bus admittance.

For bus  $i$ , the expression for  $I_i$  can be expressed as:

$$\bar{I}_i = \sum_{k=1}^n \bar{Y}_{ik} \bar{V}_k$$

Complex power can be expressed as:

$$\bar{S}_i = \bar{V}_i \bar{I}_i^*$$

By substituting  $\bar{I}_i$  into the complex power, power flow equations can be expressed as:

$$\bar{S}_i = \bar{V}_i \sum_{k=1}^n \bar{Y}_{ik}^* \bar{V}_k^*$$

with:

$$\bar{V}_k = V_k e^{j\delta_k}$$

$$\bar{Y}_{ik} = Y_{ik} e^{j\theta_{ik}}$$

By substituting  $V_k$  and  $Y_{ik}$  into the power flow equation, the result leads to:

$$\bar{S}_i = V_i \sum_{k=1}^n Y_{ik} V_k e^{j(\delta_i - \delta_k - \theta_{ik})}$$

By equating real and imaginary parts of power flow equation, real and reactive power delivered to bus  $i$  can be expressed as:

$$P_i = V_i \sum_{k=1}^n Y_{ik} V_k \cos(\delta_i - \delta_k - \theta_{ik})$$

$$Q_i = V_i \sum_{k=1}^n Y_{ik} V_k \sin(\delta_i - \delta_k - \theta_{ik})$$

To solve power flow problem, vectors  $x$ ,  $y$ , and  $f$  are defined as follows:

$$\mathbf{x} = \begin{bmatrix} \delta \\ \mathbf{V} \end{bmatrix} = \begin{bmatrix} \delta_2 \\ \delta_3 \\ \vdots \\ \delta_n \\ V_2 \\ V_3 \\ \vdots \\ V_n \end{bmatrix}$$

$$\mathbf{y} = \begin{bmatrix} \mathbf{P} \\ \mathbf{Q} \end{bmatrix} = \begin{bmatrix} P_2 \\ P_3 \\ \vdots \\ P_n \\ Q_1 \\ Q_2 \\ \vdots \\ Q_n \end{bmatrix}$$

$$\mathbf{f}(\mathbf{x}) = \begin{bmatrix} \mathbf{P}(\mathbf{x}) \\ \mathbf{Q}(\mathbf{x}) \end{bmatrix} = \begin{bmatrix} P_2(x) \\ P_3(x) \\ \vdots \\ P_n(x) \\ Q_1(x) \\ Q_2(x) \\ \vdots \\ Q_n(x) \end{bmatrix}$$

where  $\delta_1$  and  $V_1$  are the input data at reference bus and are omitted from the equations since they are already known.

The Jacobian matrix can be formed and calculated as follows:

$$\mathbf{J} = \begin{bmatrix} \frac{\partial P_2}{\partial \delta_2} & \dots & \frac{\partial P_2}{\partial \delta_n} & \frac{\partial P_2}{\partial V_2} & \dots & \frac{\partial P_2}{\partial V_n} \\ \vdots & & \vdots & \vdots & & \vdots \\ \frac{\partial P_n}{\partial \delta_2} & \dots & \frac{\partial P_n}{\partial \delta_n} & \frac{\partial P_n}{\partial V_2} & \dots & \frac{\partial P_n}{\partial V_n} \\ \frac{\partial Q_2}{\partial \delta_2} & \dots & \frac{\partial Q_2}{\partial \delta_n} & \frac{\partial Q_2}{\partial V_2} & \dots & \frac{\partial Q_2}{\partial V_n} \\ \vdots & & \vdots & \vdots & & \vdots \\ \frac{\partial Q_n}{\partial \delta_2} & \dots & \frac{\partial Q_n}{\partial \delta_n} & \frac{\partial Q_n}{\partial V_2} & \dots & \frac{\partial Q_n}{\partial V_n} \end{bmatrix}$$

The power flow problem can be solved as follows:

- i) Guess at an initial value  $\mathbf{x}^{(0)}$
- ii) Calculate the bus power mismatches  $\Delta\mathbf{y}^{(v)}$  as follows:

$$\Delta\mathbf{y}^{(v)} = \begin{bmatrix} \Delta\mathbf{P}^{(v)} \\ \Delta\mathbf{Q}^{(v)} \end{bmatrix} = \begin{bmatrix} \mathbf{P} - \mathbf{P}[\mathbf{x}^{(v)}] \\ \mathbf{Q} - \mathbf{Q}[\mathbf{x}^{(v)}] \end{bmatrix}$$

- iii) Calculate the Jacobian matrix
- iv) Solve phase angle and voltage magnitude mismatches  $\Delta\mathbf{x}^{(v)}$  as follows:

$$\Delta\mathbf{x}^{(v)} = \mathbf{J}^{-1}(\mathbf{x}^{(v)}) * \Delta\mathbf{y}^{(v)}$$

- v) Compute the new  $\mathbf{x}$  as follows:

$$\mathbf{x}^{(v+1)} = \begin{bmatrix} \delta^{(v+1)} \\ \mathbf{V}^{(v+1)} \end{bmatrix} = \begin{bmatrix} \delta^{(v)} \\ \mathbf{V}^{(v)} \end{bmatrix} + \begin{bmatrix} \Delta\delta^{(v)} \\ \Delta\mathbf{V}^{(v)} \end{bmatrix}$$

- vi) Repeat the above steps until convergence is obtained or until the number of iterations exceeds a specified maximum value.

### D.3 An Example of Load Flow Calculation

In this section, a five-bus test system is constructed and used to study load flow problem. The Newton-Raphson method is used to solve phase angle and voltage



magnitude at each bus. The system under study is illustrated in Figure 60. This system is obtained by modifying Example 7.9 of reference 113. The bus, transformer, and line data are shown in Tables 18, 19, and 20 respectively. The computer source code used in this analysis is also presented.

TABLE 18

BUS DATA

BUS	TYPE	V (pu)	$\delta$ (degrees)	$P_G$ (pu)	$Q_G$ (pu)	$P_L$ (pu)	$Q_L$ (pu)	$Q_{Gmax}$ (pu)	$Q_{Gmin}$ (pu)
1	Swing	1.0	0	-	-	0	0	-	-
2	Load	-	-	0	0	1.0	0.5	-	-
3	Constant Voltage	1.05	-	1.5	-	0.75	0.25	1.0	-0.7
4	Load	-	-	0	0	0.5	0.2	-	-
5	Load	-	-	0	0	0.25	0.1	-	-

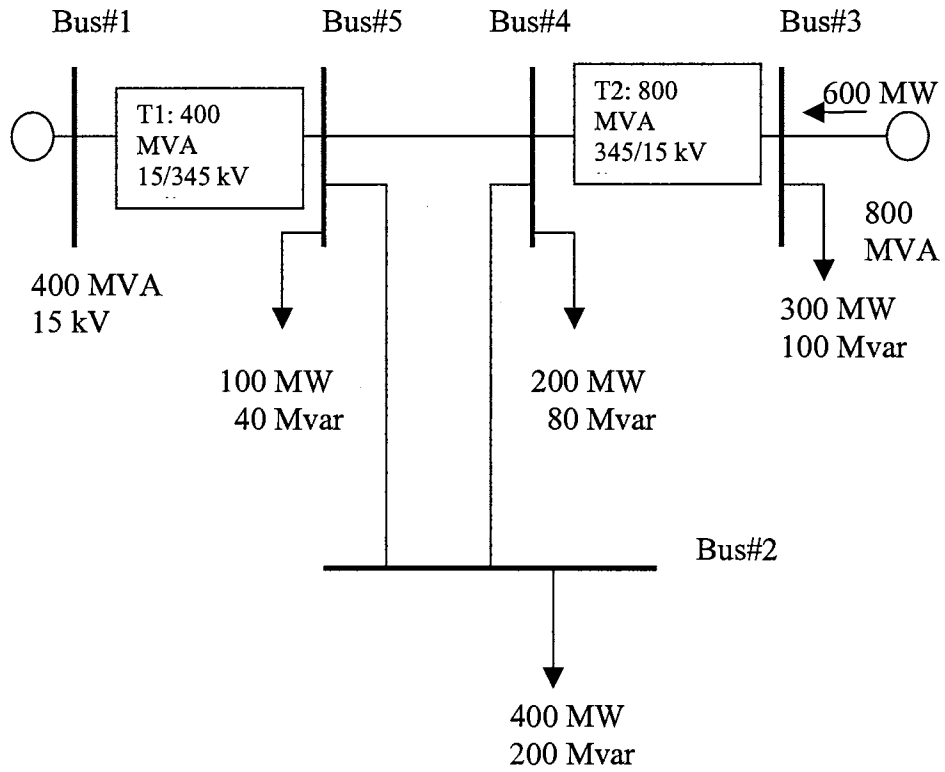


Figure 60. A Single Line Diagram of Test System [See Reference 113]

TABLE 19  
TRANSFORMER DATA

Bus to Bus	R (pu)	X (pu)	$G_c$ (pu)	$B_m$ (pu)	Maximum MVA (pu)
1 to 5	0.010	0.10	0	0	1.5
3 to 4	0.005	0.05	0	0	2.5

TABLE 20  
LINE DATA

Bus to Bus	R (pu)	X (pu)	$G_c$ (pu)	$B_m$ (pu)	Maximum MVA (pu)
2 to 4	0.03	0.3	0	0.43	3.0
2 to 5	0.05	0.5	0	0.22	3.0
4 to 5	0.02	0.2	0	0.11	3.0

$S_{\text{base}}=400$  MVA,  $V_{\text{base}}=15$  kV at busses 1 and 3, and 345 kV at busses 2, 4, and 5

### D.3.1 Load Flow Program

The calculation of load flow program is coded by Matlab Version 5.3.1 (Release 11.1).

```

% Load flow programming by Newton Raphson method
%Load ybus function
[angleY,magnitudeY]=ybus;
% Angle delta1(known); initial guess for delta2=delta3=delta4=delta5=0
delta = [0;0;0;0;0];
% Voltage V1 and V3(known); initial guess for V2=V4=V5=1
V = [1;1;1.05;1;1];
%Form matrix to use in x (V2,V4,V5) (V1&V3known)
Vx=[V(2,1);V(4:5,1)];
%Bulid x matrix; x=[delta V] 7x1
%d (delta) in x runs from row 1 to 4(delta2-delta5) (delta1known)
x=[delta(2:5,1);Vx];
%Set starting Iteration numbers
I=0;
fprintf(I,'Initial Guess::\n\n\n delta2(%0.0f)=%0.0f\n delta3(%0.0f)=%0.0f\n
delta4(%0.0f)=%0.0f\n delta5(%0.0f)=%0.0f\n V2(%0.0f)=%0.0f\n
V4(%0.0f)=%0.0f\n V5(%0.0f)=%0.0f\n\n\n',
I,x(1,1),I,x(2,1),I,x(3,1),I,x(4,1),I,x(5,1),I,x(6,1),I,x(7,1));
%Build y(P,Q) matrix 7x1
%known P2,P3,P4,P5,Q2,Q4,Q5
%P2,P3,P4,P5 run from row 1-4; Q2,Q4,Q5 run from row 5-7
y = [ -1 ; 0.75 ; -0.5 ; -0.25 ; -0.5 ; -0.2 ; -0.1 ];
% Set total numbers of iteration
for I=1:10
% Calculate P1-P5 & Q1-Q5
for n=1:5
Pcal(n,1)=0;
Qcal(n,1)=0;
for i = 1:5
Pcal(n,1)=Pcal(n,1)+(V(n,1)*magnitudeY(n,i)*V(i,1)*cos(delta(n,1)-delta(i,1)-
angleY(n,i)));
Qcal(n,1)=Qcal(n,1)+(V(n,1)*magnitudeY(n,i)*V(i,1)*sin(delta(n,1)-delta(i,1)-
angleY(n,i)));
end
end
%Form Q matrix 3x1
Qx=[Qcal(2,1);Qcal(4:5,1)];
%Form f matrix 7x1
%P runs from row 1-4
%Q runs from row 5-7
f = [Pcal(2:5,1);Qx]

```

```

%Find and form dy matrix
dy = y-f;
%Calculate Jacobian matrix 7x7
%Calculate J11 4x4
for n=2:5
for m=2:5
if n==m
J1(n,m)=0
for k=1:5
if k~=n
J1(n,m)=J1(n,m)+(-V(n,1)*magnitudeY(n,k)*V(k,1)*sin(delta(n,1)-delta(k,1)-
angleY(n,k)));
end
end
else
J1(n,m)=(V(n,1)*magnitudeY(n,m)*V(m,1)*sin(delta(n,1)-delta(m,1)-angleY(n,m)));
end
end
end
%Build J11 matrix
J11=J1(2:5,2:5);
%Calculate J12 4x3
for n=1:5
for m=1:5
if n==m
J2(n,m)=0;
for k=1:5
J2(n,m)=J2(n,m)+(magnitudeY(n,k)*V(k,1)*cos(delta(n,1)-delta(k,1)-angleY(n,k)));
if n==k
J2(n,m)=J2(n,m)+(magnitudeY(n,k)*V(k,1)*cos(delta(n,1)-delta(k,1)-angleY(n,k)));
end
end
else
J2(n,m)=(V(n,1)*magnitudeY(n,m)*cos(delta(n,1)-delta(m,1)-angleY(n,m)));
end
end
end
%Build J12 matrix
J12(1:4,1)=J2(2:5,2);
J12(1:4,2:3)=J2(2:5,4:5);
%Calculate J21 3x4
for n=1:5
for m=1:5
if n==m
J3(n,m)=0;
for k=1:5

```

```

if k~=n
J3(n,m)=J3(n,m)+(V(n,1)*magnitudeY(n,k)*V(k,1)*cos(delta(n,1)-delta(k,1)-
angleY(n,k)));
end
end
else
J3(n,m)=(-V(n,1)*magnitudeY(n,m)*V(m,1)*cos(delta(n,1)-delta(m,1)-angleY(n,m)));
end
end
end
%Build J21 matrix
J21(1,1:4)=J3(2,2:5);
J21(2:3,1:4)=J3(4:5,2:5);
%Calculate J22
for n=1:5
for m=1:5
if n==m
J4(n,m)=0;
for k=1:5
J4(n,m)=J4(n,m)+(magnitudeY(n,k)*V(k,1)*sin(delta(n,1)-delta(k,1)-angleY(n,k)));
if n==k
J4(n,m)=J4(n,m)+(magnitudeY(n,k)*V(k,1)*sin(delta(n,1)-delta(k,1)-angleY(n,k)));
end
end
else
J4(n,m)=(V(n,1)*magnitudeY(n,m)*sin(delta(n,1)-delta(m,1)-angleY(n,m)));
end
end
end
%Build J22 matrix
J22(1,1)=J4(2,2);
J22(2:3,1)=J4(4:5,2);
J22(1,2:3)=J4(2,4:5);
J22(2:3,2:3)=J4(4:5,4:5);
%Set up J matrix 7x7
J=[J11 J12 ; J21 J22];
%Calculate dx (new value)
dx=inv(J)*dy
% To find new guess
x_new=dx+x;
%To check error
error=abs((x_new-x)/(x))
%Assign new value
x=x_new
delta(2:5,1)=x(1:4,1);
V(2,1)=x(5,1);

```

```

V(4:5,1)=x(6:7,1);
fprintf(1,'Iteration Number=%0.0f,\n\n',I);
Voltage_Phase=delta*180/pi
Voltage_Magnitude=V
I = I+1;
end
%Sub program for Ybus function
function [angleY,magnitudeY]=ybus
%Zseries line impedances=zi; line admittance=adm
%Line impedance input data
zi(1,5) = (0.01+j*0.1);
zi(2,4) = (0.03+j*0.3);
zi(2,5) = (0.05+j*0.5);
zi(3,4) = (0.005+j*0.05);
zi(4,5) = (0.02+j*0.2);
[x,y,z] = find(zi);
%Convert impedances into admittances
invim = -1./z;
%Create Non-diagonal elements
adm=zeros(5,5);
adm(1,5)= invim (3,1);
adm(5,1)= invim (3,1);
adm(4,5)= invim (5,1);
adm(5,4)= invim (5,1);
adm(3,4)= invim (2,1);
adm(4,3)= invim (2,1);
adm(2,5)= invim (4,1);
adm(5,2)= invim (4,1);
adm(2,4)= invim (1,1);
adm(4,2)= invim (1,1) ;
%Shunt admittances input data
Bshunt= [ 0; (j*0.325); 0; (j*0.27) ; (j*0.165)] ;
%Create diagonal elements without shunt admittance
dbus1=-[adm(1,5);adm(2,4)+adm(2,5);adm(3,4);adm(4,5)+adm(2,4)+adm(3,4);
adm(4,5)+adm(2,5)+adm(1,5)] ;
%Calculate diagonal elements
dbus = Bshunt + dbus1 ;
ybus = adm + diag(dbus);
Y = ybus
for n = 1:5;
m = 1:5;
magnitudeY(n,m)=sqrt((real(Y(n,m)).^2)+(imag(Y(n,m)).^2));
angleY(n,m)=angle(Y(n,m));
end

```

### D.3.2 Simulation Results

Simulations results of magnitude and angle of voltage at each bus of the test system using Newton-Raphson method are presented in Table 21.

TABLE 21  
BUS OUTPUT DATA

Bus	V(pu)	$\delta$ (degree)
1	1.0000	0
2	0.9286	-19.7115
3	1.0500	-8.0257
4	1.0246	-9.8981
5	0.9940	-6.0035



## VITA 2

Pathomthat Chiradeja

Candidate for the Degree of

Doctor of Philosophy

Thesis: AN APPROACH TO THE QUANTIFICATION OF THE BENEFITS OF  
DISTRIBUTED GENERATION

Major Field: Electrical Engineering

Biographical:

Personal Data: Born in Bangkok, Thailand, February 20, 1969, the son of Pravit and Paitoontong Chiradeja.

Education: Graduated from Bodin Decha School, Bangkok, Thailand in March 1987; received Bachelor of Engineering Degree in Electrical Engineering from Kasetsart University, Bangkok, Thailand in May 1991; received Master of Science Degree in Electrical Engineering from Oklahoma State University in 1994; completed requirements for the Doctor of Philosophy Degree at Oklahoma State University in Electrical Engineering in May 2003.

Professional Experience: System Planning Engineer, Metropolitan Electricity Authority (MEA), Bangkok, Thailand 1991-1992.

Professional Memberships: Institute of Electrical and Electronics Engineers.